

Harnessing single amino acid catalysis : development of the enantioselective intramolecular Morita-Baylis-Hillman and Rauhut-Currier reactions and studies toward the synthesis of (+)-SCH 642305

Author: Carrie Elizabeth Aroyan

Persistent link: <http://hdl.handle.net/2345/959>

This work is posted on [eScholarship@BC](#),
Boston College University Libraries.

Boston College Electronic Thesis or Dissertation, 2008

Copyright is held by the author, with all rights reserved, unless otherwise noted.

Boston College
The Graduate School of Arts and Sciences
Department of Chemistry

HARNESSING SINGLE AMINO ACID CATALYSIS:
DEVELOPMENT OF THE ENANTIOSELECTIVE INTRAMOLECULAR
MORITA-BAYLIS-HILLMAN AND RAUHUT-CURRIER REACTIONS
AND
STUDIES TOWARD THE SYNTHESIS OF (+)-SCH 642305

a dissertation

by

CARRIE ELIZABETH AROYAN

submitted in partial fulfillment of the requirements

for the degree of

Doctor of Philosophy

May 2008

© copyright by CARRIE ELIZABETH AROYAN

2008

**Harnessing Single Amino Acid Catalysis: Development of the Enantioselective
Intramolecular Morita-Baylis-Hillman and Rauhut-Currier Reactions and Studies
Toward the Synthesis of (+)-Sch 642305**

Carrie Elizabeth Aroyan

Thesis Advisor: Scott J. Miller

Abstract

The development of two catalytic asymmetric synthetic methods is presented and culminates with studies of their application to the synthesis of a natural product. The intramolecular variant of the Morita-Baylis-Hillman (MBH) reaction has remained almost untouched by asymmetric catalysis. A significant advance in the field is demonstrated with the development of a highly enantioselective intramolecular MBH reaction employing a co-catalytic system of *N*-methylimidazole (NMI) and pipercolinic acid (Pip). The optimization of various reaction parameters and the use of protic conditions (THF-H₂O, 3:1) afforded the desired products in up to 82% yield and 80% ee. The extension of this methodology to include the use of vinylogous reaction partners in the Rauhut-Currier (RC) reaction has been achieved, establishing the first highly enantioselective RC reaction. A single amino acid derivative of cysteine, in the presence of potassium *tert*-butoxide and a critical concentration of water in acetonitrile, was demonstrated to function as a highly selective catalyst providing products in up to 95% ee. Finally, the application of the MBH and RC reactions to the synthesis of complex

molecules presents highly useful methodology for the formation of a new C–C bond in the generation of densely functionalized enantiopure products. Preliminary studies toward the application of this methodology to the stereoselective synthesis of (+)-Sch 642305 are described. Examination of the catalyst's ability to dictate the stereoselectivity of the key step (*catalyst control*) and allow the synthesis of both the natural product, and difficult-to-obtain unnatural stereoisomeric analogs, will be the subject of on-going studies.

Acknowledgments

I have had the great fortune of encountering many amazing people, all of whom have influenced my life in a variety of ways. My graduate career would not have been possible if I had not been exposed to remarkable teachers along the way. I would like to begin by thanking my advisor, Scott J. Miller, who has been an inspiration with his vast knowledge of science and constant enthusiasm and optimism. I am grateful that he has created an environment in which we can develop as independent scientists, while at the same time providing the right amount of encouragement and support. From my eighth-grade science teacher, Mrs. Moss, and continuing with my undergraduate advisor, Professor Andrew J. McCammon, and many people at GNF and Cytokinetics, I have had many positive experiences which helped lead the way to graduate school.

I would like to thank all the members of the Miller group, past and present, who have contributed to the positive intellectual environment. Specifically, Melissa Vasbinder, who not only did a wonderful job with all the MBH chemistry before me, she was my mentor in the lab and has become a great friend of mine over the years. I am only disappointed that we were not able to overlap for more time in the group and in Boston. In addition, it was nice to join the lab with Bianca Sculimbrene and Cathy Evans, as they were both always willing to help me draw transition states and work through mechanisms, while at the same time making me laugh with all their banter. Bryan Cowen has been my labmate for four years, and I will really miss our chemistry conversations and his great attitude. Elizabeth Colby Davie was here for such little time,

but I will always value the time she spent in the group and our chance to become friends. I am also very thankful to my labmates, Bryan Cowen, Angela Puchlopek, Kristin Fiori, and Gorka Peris, who graciously spent the time to proof read my thesis.

As sad as it was to leave Boston College, I am fortunate to have been a part of the chemistry department at two great institutions of science and learning, BC and Yale University. Furthermore, I would like to express my appreciation to my orals and defense committees as well as all the professors at Boston College who I had the opportunity to interact with through courses and teaching.

Finally, my family and friends have been the center of my peace and happiness, which has made me who I am today. My mom and dad, both in different ways, however equally so, have always been such a support and source of strength. My brother, Branden, has always reminded me not to take myself too seriously – always convincing me in times of stress to jump up and touch my toes and refusing to let me go without a laugh. I would not have made it through graduate school, nor would have I wanted to, if I had not met Juliet Znovena, my classmate at BC, fellow Californian, and dearest friend. I am thankful for all my friends from home, from growing up and through college, and the new friends I have made during my time in graduate school. And finally, all the love and support from Adam Tomasi, who I have the greatest respect for as a person and as a scientist, and has been my best friend and clear voice through all of this. He was nothing but supportive of my decision to move far away for graduate school and has been extremely patient and understand through it all. I could not imagine a day without his love.

To my family

Table of Contents

List of Schemes.....	vi
List of Tables	ix
List of Figures.....	x

Chapter 1

1	Development of the Enantioselective Morita-Baylis-Hillman Reaction	1
1.1	Introduction	1
1.2	Overview of Catalytic Intramolecular Morita-Baylis-Hillman Reactions	2
1.3	Mechanistic Details	9
1.4	Dual Catalyst Control in the Enantioselective MBH Reaction	11
1.4.1	Prior Studies of Metal-Free Peptide-Based Catalysis	11
1.4.2	Intramolecular MBH: Distinct from Intermolecular MBH.....	14
1.4.3	Development of the Co-Catalytic System: Pipecolinic acid/NMI.....	19
1.4.4	Optimization of Reaction Conditions: Solvent.....	21
1.4.5	Re-Examination of Peptide Catalysts	24
1.4.6	Optimization: Catalyst Loading and Stoichiometry	28
1.4.7	Extension of Proline Surrogates: Ring Size.....	31
1.4.8	Determination of Absolute Stereochemistry.....	34
1.4.9	Mechanism.....	35

1.4.10	Substrate Scope.....	41
1.5	Enhancement of Enantioselectivity: Kinetic Resolution.....	43
1.6	Conclusion.....	47
1.7	Experimental	49
1.7.1	NMR Spectra and HPLC Data.....	60

Chapter 2

2	The Rauhut-Currier Reaction: A History and Its Synthetic Application.....	70
2.1	Introduction	70
2.2	Overview of the Intermolecular Rauhut-Currier Reaction.....	72
2.3	Intramolecular Rauhut-Currier Reaction.....	82
2.4	Enantioselective RC Reactions	91
2.5	Extension to Include Alternative Electrophilic Partners	95
2.6	Application in Total Synthesis.....	102
2.7	Conclusion.....	109

Chapter 3

3	Development of the Enantioselective Rauhut-Currier Reaction.....	111
3.1	Introduction	111
3.2	Development of the Enantioselective Intramolecular RC Reaction.....	114
3.2.1	Nitrogen-Based Nucleophiles	114
3.2.2	Phosphorous-Based Nucleophiles.....	116
3.3	Chalcogenides	120
3.3.1	Overview of Chalcogenides in MBH-Type Reactions	120
3.3.2	Examination of Cysteine-Based Catalysis	123
3.3.3	Cystine Catalysis.....	128
3.3.4	Development of Cysteine Derivatives	129
3.3.5	Protic Additives in the RC Reaction.....	130
3.3.6	Optimization of Cysteine-Based Catalysis	134
3.3.7	Determination of Absolute Stereochemistry.....	138
3.4	Mechanistic Studies.....	139
3.5	Reaction Scope.....	144
3.6	Conclusion.....	149
3.7	Experimental	152
3.7.1	NMR Spectra	168
3.7.2	Appendix: Crystallographic Data for Compound 25	186

Chapter 4

4	Synthetic Studies Toward the Synthesis of (+)-Sch 642305 via Selective Transannular Rauhut-Currier Reaction.....	202
4.1	Introduction.....	202
4.2	Biological Significance: Anti-bacterial and Anti-HIV.....	204
4.3	Previous Synthesis of (+)-Sch 642305.....	205
4.4	Retrosynthetic Analysis.....	211
4.5	Synthesis of (+)-Sch 642305: <i>Route A</i>	213
4.5.1	Synthesis of Divergent Intermediate 11.....	213
4.5.2	Preliminary Studies of the RC Reaction in <i>Route A</i>	217
4.5.3	Thioenoates as Reactive Rauhut-Currier Substrates.....	220
4.5.4	Phosphine Catalysis.....	222
4.5.5	Examination of Sterics: Synthesis of 11-OMe.....	224
4.5.6	Preliminary Rauhut-Currier Studies in <i>Route A</i> : 11-OMe.....	225
4.5.7	Synthesis in <i>Route A</i>	227
4.6	Synthesis of (+)-Sch 642305: <i>Route B</i>	228
4.6.1	Synthetic Plan for <i>Route B</i>	228
4.6.2	Synthesis with TBDPS Protecting Group.....	230
4.6.3	Synthesis with Me Ether Protecting Group.....	233
4.6.4	1,3-Dioxolane.....	234
4.6.5	1,3-Dioxolane with OAc Protecting Group.....	236

4.6.6	Masked α,β -Unsaturated Carbonyl	238
4.6.7	Initial Yamaguchi Cyclization	240
4.6.8	Carbonyl Reduction/Protection.....	241
4.6.9	Preliminary Studies of the Rauhut-Currier Reaction in <i>Route B</i>	244
4.7	Conclusion.....	245
4.8	Experimental	247
4.8.1	NMR Spectra	280

List of Schemes

Chapter 1

Scheme 1.1: First intramolecular MBH reaction.....	3
Scheme 1.2: Mechanistic support provided by Drewes and co-workers.....	4
Scheme 1.3: Amine-catalyzed intramolecular MBH cyclization.	4
Scheme 1.4: Intramolecular MBH of thioenoates.	5
Scheme 1.5: Lewis acid catalyzed MBH reaction.....	6
Scheme 1.6: Extension of reaction scope to include seven-membered ring formation.....	6
Scheme 1.7: First diastereoselective intramolecular MBH reaction.	7
Scheme 1.8: Proline and proline/imidazole catalyzed enantioselective intramolecular MBH reaction.....	8
Scheme 1.9: Enantioselective MBH reaction presented by Gladysz and co-workers.....	8
Scheme 1.10: Optimized conditions for the intermolecular MBH reaction.....	14
Scheme 1.11: Intramolecular MBH reaction.....	14
Scheme 1.12: Catalysis of the MBH reaction with pip/NMI under protic reaction conditions.....	23
Scheme 1.13: Synthesis of proline derivatives 46 and 47	33
Scheme 1.14: Mosher analysis of intramolecular MBH product 9	34
Scheme 1.15: Theoretical kinetic resolution of MBH products.	45
Scheme 1.16: Enantioselective acylation of racemic MBH product 9	45
Scheme 1.17: Tandem one-pot MBH-kinetic resolution.....	47

Chapter 2

Scheme 2.1: Dimerization of acrylonitrile by Baizer and Anderson.....	73
Scheme 2.2: Tricyclohexylphosphine-catalyzed coupling reported by Morita and Kobayashi.	73
Scheme 2.3: Cross-Coupling in the RC reaction.....	74
Scheme 2.4: Selective formation of cross-coupled product 4	75
Scheme 2.5: Amine-catalyzed RC reaction.....	76
Scheme 2.6: DABCO-catalyzed dimerization of acrylate esters.....	76
Scheme 2.7: Tris(dimethylamino)phosphine (TDAP) catalyzed RC reaction in the synthesis of (\pm) sarkomycin esters.	77
Scheme 2.8: α -Alkylation of α,β -unsaturated enones catalyzed by DBU.....	78
Scheme 2.9: (5) Dimerization of various activated alkenes with DABCO or DBU. (6) In situ RC reaction with MBH product 26	81
Scheme 2.10: Intramolecular RC reaction.....	83
Scheme 2.11: Cycloisomerization of 5- and 6-membered symmetrical bis(enones) by Roush (7) and Krische (8).....	84

Scheme 2.12: Electronic control of product distribution in the RC reaction of unsymmetric substrates by Krische and co-workers.....	85
Scheme 2.13: Kinetic control of product distribution.....	86
Scheme 2.14: Steric effects in the RC cyclization.....	87
Scheme 2.15: Diastereoselectivity in the RC cycloisomerization reaction.....	88
Scheme 2.16: Tandem Michael/Michael reaction reported by Murphy and co-workers.....	89
Scheme 2.17: Thiol-catalyzed RC transformation by Murphy and co-workers.....	90
Scheme 2.18: Tandem intramolecular RC/aldol reaction.....	90
Scheme 2.19: RC cyclization under optimized conditions with 18-C-6.....	93
Scheme 2.20: Elimination of Cys-based catalyst under irreversible conditions.....	93
Scheme 2.21: Rhenium-containing phosphine-catalyzed enantioselective intramolecular RC reaction.....	94
Scheme 2.22: Extension of the RC reaction to include allyl halides as electrophilic partners.....	95
Scheme 2.23: Synthesis of 2,4-functionalized 1,4-pentadienes.....	96
Scheme 2.24: Extension of the RC reaction to include vinylsulfone coupling partners.....	97
Scheme 2.25: Intramolecular RC cycloisomerization of enones and allylic leaving groups.....	98
Scheme 2.26: Direct intramolecular α -alkylation of enones.....	99
Scheme 2.27: Synthesis of azepines from allenolate-enone coupling products.....	102
Scheme 2.28: Synthesis of the tetraquinane ring system of waihoensene.....	103
Scheme 2.29: Synthesis of tetraquinane ring system without elimination of the catalyst.....	103
Scheme 2.30: Synthesis of (\pm)-ricciocarpin A by Krische and co-workers.....	104
Scheme 2.31: Synthesis of (-)-spinosyn A by Roush and co-workers.....	105
Scheme 2.32: Advanced model system in the synthetic studies of FR182877.....	107

Chapter 3

Scheme 3.1: Intramolecular Rauhut-Currier reaction.....	114
Scheme 3.2: Phosphine- and nitrogen-based catalysis of the RC reaction.....	115
Scheme 3.3: Chiral phosphine catalyst to promote an enantioselective RC reaction?.....	117
Scheme 3.4: Chiral phosphine-containing amino acid (Pps) preparation.....	118
Scheme 3.5: Chalcogenide catalysis of MBH-type reactions.....	121
Scheme 3.6: Formation of hydrazone 25 for crystallization.....	139
Scheme 3.7: RC reaction under optimized reaction conditions with 18-crown-6.....	140
Scheme 3.8: Use of sodium <i>tert</i> -butoxide versus potassium <i>tert</i> -butoxide in the RC cyclization.....	140
Scheme 3.9: Isolation of intermediate 27 and subjection to irreversible elimination.....	142
Scheme 3.10: Possible base promoted cyclization to provide racemic product.....	143
Scheme 3.11: Synthesis of symmetrical and unsymmetrical RC substrates.....	147

Chapter 4

Scheme 4.1: Application of our developed enantioselective Rauhut-Currier reaction to the synthesis of (+)-Sch 642305 (1).....	204
Scheme 4.2: Proposed biomimetic synthesis of 1 by Snider and co-workers.....	208
Scheme 4.3: Transannular Michael reaction leading to the opposite epimer at C6.....	208
Scheme 4.4: Catalyst-controlled diastereoselective TADA of a biased macrocycle.....	210
Scheme 4.5: Retrosynthetic analysis displaying two alternative routes, A and B	212
Scheme 4.6: Retrosynthetic analysis of common intermediate 11	213
Scheme 4.7: In-situ aminooxylation/ HWE/ N-O Cleavage:.....	214
Scheme 4.8: Resubjection of alcohol 20 to reaction conditions with copper(II) species.	215
Scheme 4.9: Synthesis of common intermediate 11	216
Scheme 4.10: Synthesis of aldehyde fragment 14	217
Scheme 4.11: Initial study of the key RC reaction in route A with an achiral catalyst..	218
Scheme 4.12: Phosphine catalysis in Route A	223
Scheme 4.13: Synthesis of analog 11 -OMe <i>cis/trans</i>	225
Scheme 4.14: Initial study of the RC reaction of 11 -OMe in route A with an achiral phosphine-based catalyst.....	226
Scheme 4.15: Preliminary experiments in the Rauhut-Currier reaction of 11 -OMe catalyzed by protected cysteine catalyst 29	226
Scheme 4.16: Synthesis of (+)-Sch 642305 in route A	228
Scheme 4.17: Synthesis of (+)-Sch 642305 in route B	230
Scheme 4.18: Hydrolysis of divergent intermediate 4	231
Scheme 4.19: Successful hydrolysis of methyl ester 11	231
Scheme 4.20: Selective silyl deprotection.....	232
Scheme 4.21: Hydrolysis of 11 -OMe <i>cis</i> and 11 -OMe <i>trans</i>	233
Scheme 4.22: Silyl deprotection of 58 - <i>cis</i> and 58 - <i>trans</i>	234
Scheme 4.23: Synthetic plan for (+)-Sch 642305 in route B with a ketal protected α,β -unsaturated ketone.....	235
Scheme 4.24: Attempted ketalization of 11 -OMe.....	236
Scheme 4.25: Synthetic plan incorporating a modified protecting group scheme.....	237
Scheme 4.26: Synthesis of masked α,β -unsaturated ketone 69	240
Scheme 4.27: Initial attempt at the Yamaguchi macrolactonization with substrate 59 ..	241
Scheme 4.28: Synthetic plan employing a reduction/protection sequence.....	242
Scheme 4.29: Synthesis employing carbonyl reduction and macrolactonization on fully deprotected intermediate 75	242
Scheme 4.30: Synthesis employing carbonyl reduction/protection.....	244
Scheme 4.31: Rauhut-Currier reaction in route B	245

List of Tables

Chapter 1

Table 1.1: Alanine scan of peptide 30 in combination with proline.	18
Table 1.2: Solvent effects in the intramolecular cyclization of 7 to 9 catalyzed by Pro/NMI.	22
Table 1.3: Solvent effects in the cyclization of 7 to 9 catalyzed by peptide 36 /proline... ..	25
Table 1.4: Effect of catalyst loading and stoichiometry	30
Table 1.5: Screen of co-catalyst combinations	40

Chapter 2

Table 2.1: RC cyclization with (<i>Z</i>)- and (<i>E</i>)-enoates.	106
Table 2.2: Studies of the intramolecular RC reaction in the synthesis of FR182877.	107

Chapter 3

Table 3.1: Base screen in the RC reaction.....	125
Table 3.2: Solvent screen in the RC cyclization of 1 to 2 promoted by 15	126
Table 3.3: Effects of base stoichiometry and reaction concentration.....	128
Table 3.4: Effect of various additives in the RC reaction catalyzed by 20	133
Table 3.5: Effects of water additive in the RC reaction catalyzed by 20	134
Table 3.6: Optimization of reaction conditions in the RC cyclization reaction.	138
Table 3.7: Effect of catalyst loading on the RC reaction of 1 to 2 promoted by 20	145
Table 3.8: Substrate scope in the enantioselective Rauhut-Currier reaction promoted by catalyst 20	149

Chapter 4

Table 4.1: N-O cleavage experiments.	215
Table 4.2: Preliminary experiments in the Rauhut-Currier reaction in route A catalyzed by protected cysteine catalyst 29	219
Table 4.3: Ketalization conditions tested in the protection of α,β -unsaturated ketone 64	238

List of Figures

Chapter 1

Figure 1.1: Intramolecular Morita-Baylis-Hillman reaction.....	2
Figure 1.2: Proposed mechanism of the MBH reaction.....	9
Figure 1.3: Revision of the mechanism proposed by McQuade and co-workers.....	10
Figure 1.4: Transition state proposed by Aggarwal and co-workers.....	11
Figure 1.5: Synthetic tool box of nucleophile-embedded peptide-based catalysts.....	12
Figure 1.6: Essential co-catalysis of NMI and proline in the intermolecular MBH reaction.....	13
Figure 1.7: Catalysis of the intramolecular MBH reaction with (a) NMI, (b) proline, (c) co-catalysts NMI and proline.....	15
Figure 1.8: Co-catalysis of the intramolecular MBH reaction: (a) peptide/proline versus (b) NMI/proline.....	16
Figure 1.9: Alanine scan of peptide 30 in the kinetic resolution of secondary alcohols.	17
Figure 1.10: Proline derivatives tested as co-catalysts with NMI in the intramolecular MBH reaction.....	20
Figure 1.11: Aldol dimerization by-product 40	21
Figure 1.12: Catalysis of the intramolecular MBH under protic conditions with various peptides/proline.....	25
Figure 1.13: Alternative peptides tested under protic reaction conditions.....	26
Figure 1.14: Catalysis of the MBH reaction with peptide 39	27
Figure 1.15: Cross-comparison of the co-catalytic systems.....	28
Figure 1.16: Comparison of proline and pipercolinic acid in CDCl ₃ and THF-H ₂ O.....	29
Figure 1.17: Investigation of pipercolinic acid derivatives of varying ring size.....	32
Figure 1.18: Comparison of H _b in Mosher esters 55 and 56	35
Figure 1.19: Mechanism of the intermolecular MVK-MBH reaction proposed by Shi and co-workers.....	36
Figure 1.20: Potential mechanism A.....	37
Figure 1.21: Potential mechanism B.....	38
Figure 1.22: Substrate scope in the pipercolinic acid/NMI catalyzed MBH reaction.....	43
Figure 1.23: Kinetic resolution of secondary alcohols catalyzed by peptide 30	44

Chapter 2

Figure 2.1: Comparison of the MBH and RC reactions.....	71
Figure 2.2: Proposed mechanism of the Rauhut-Currier reaction.....	72
Figure 2.3: Mechanistic study by Hwu and co-workers.....	79
Figure 2.4: Phosphine-catalyzed dimerization of acrylic compounds.....	80
Figure 2.5: Divergent reactivity in phosphine-promoted RC reactions.....	82
Figure 2.6: RC cyclization of various unsymmetric substrates by Roush and co-workers.....	86

Figure 2.7: Substrate scope in the enantioselective RC cyclization.	92
Figure 2.8: Proposed transition state to explain the obtained enantioselectivity.	94
Figure 2.9: Cycloallylation of enones using the two-component catalyst system of phosphine and palladium.	97
Figure 2.10: Intramolecular RC cyclization via epoxide ring opening.	100
Figure 2.11: Coupling of allenic esters and various α,β -unsaturated carbonyl compounds.	101
Figure 2.12: Synthesis of (+)-harziphilone by Sorensen and co-workers.	109

Chapter 3

Figure 3.1: Morita-Baylis-Hillman and Rauhut-Currier Reactions.	112
Figure 3.2: Opportunities for advancement in the MBH and RC reactions.	113
Figure 3.3: Investigation of co-catalysis in the RC cyclization.	116
Figure 3.4: Catalysis of 1 to 2 with achiral MePh ₂ P.	119
Figure 3.5: Catalysis of the RC reaction with catalysts 7 and 8	120
Figure 3.6: Catalysis of the RC reaction with thiophenol and thiophenolate.	122
Figure 3.7: Catalysis of the RC reaction with catalyst 15	124
Figure 3.8: Catalysis of the RC reaction with cystine derivatives.	129
Figure 3.9: Simple SAR of the nitrogen protecting group of catalyst 15	130
Figure 3.10: Effects of a protic additive in the cyclization of 1 to 2 promoted by various Cys-protected derivatives.	132
Figure 3.11: Effects of various amide protecting groups on cysteine in the RC cyclization.	135
Figure 3.12: Solvent effects with water additive in the RC cyclization of 1 to 2 promoted by 20	136
Figure 3.13: Proposed mechanism of the Cys-catalyzed RC reaction.	143
Figure 3.14: Transition state models to explain formation of the observed enantiomer.	144

Chapter 4

Figure 4.1: Use of macrocyclic control of the Rauhut-Currier Reaction in the synthesis of Spinosyn A by Roush and co-workers.	203
Figure 4.2: Synthesis of compound 1 by the groups of (1) Mehta, (2) Watanabe, and (3) Trauner.	206
Figure 4.3: Synthesis of compound 1 by the groups of (4) Carda and (5) Fujioka.	207
Figure 4.4: Catalyst-controlled diastereoselective TADA of unbiased macrocycle 8	210
Figure 4.5: Possible substrates for the Rauhut-Currier reaction in Route A	220
Figure 4.6: Heightened thioenoate reactivity in the RC reaction.	221
Figure 4.7: Model system employing a thiol ester electrophilic partner.	221
Figure 4.8: Phosphine catalysis in the Rauhut-Currier reaction.	223
Figure 4.9: Application of the Rauhut-Currier reaction in route B	229

Figure 4.10: Rapid 6-exo-trig cyclization leading to undesired cyclic by-product.	233
Figure 4.11: Potential side reactivity in macrolactonization of the fully deprotected intermediate.....	243

1 Development of the Enantioselective Morita-Baylis-Hillman Reaction

1.1 Introduction

The formation of carbon-carbon bonds in an efficient manner is an important challenge in synthetic organic chemistry. Moreover, the ability to catalyze the formation of new C-C bonds in a highly enantioselective and chemoselective fashion is critical to the effective synthesis of natural products and biologically and medicinally interesting molecules.¹ Research efforts to control these processes have driven the development of many synthetically useful methods and continue to fuel advancements in synthetic chemistry.

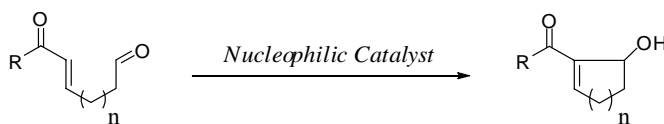
The Morita-Baylis-Hillman (MBH) reaction is a powerful transformation that has attracted the attention of many research groups for over five decades.² This C-C bond forming reaction involves the selective coupling of an activated alkene with an aldehyde through nucleophilic catalysis to produce an α -methylene- β -hydroxycarbonyl. Although catalysis of the reaction has traditionally suffered from slow reaction rates as well as low chemo- and enantioselectivity, the last decade has seen much progress in the way of catalyst design leading to heightened reactivity, stereinduction, and ultimately the

¹ (a) Hong, B.-C.; Nimje, R. Y. *Curr. Org. Chem.* **2006**, *10*, 2191-2225. (b) Taylor, M. S.; Jacobsen, E. N. *Proc. Natl. Acad. Sci. U.S.A.* **2004**, *101*, 5368-5373. (c) Douglas, C. J.; Overman, L. E. *Proc. Natl. Acad. Sci. U.S.A.* **2004**, *101*, 5363-5367.

² For selected reviews, please see: (a) Drewes, S. E.; Roos, G. H. P. *Tetrahedron* **1988**, *44*, 4653-4670. (b) Basavaiah, D.; Rao, P. D.; Hyma, R, S. *Tetrahedron* **1996**, *52*, 8001-8062. (c) Basavaiah, D.; Rao, A. J.; Satyanarayana, T. *Chem. Rev.* **2003**, *103*, 811-891. (d) Lee, K. Y.; Gowrisankar, S.; Kim, J. N. *Bull. Kor. Chem. Soc.* **2005**, *26*, 1481-1490. (e) Masson, G.; Housseman, C.; Zhu, J. *Angew. Chem., Int. Ed.* **2007**, *46*, 4614-4628.

expansion of reaction scope. While success in the *intermolecular* MBH has been substantial, a parallel success in the *intramolecular* variant (Figure 1.1), which would provide access to densely functionalized cyclic products in one step, has been slower. Herein, we present a significant advance in the field through the development of an enantioselective *intramolecular* Morita-Baylis-Hillman reaction with high levels of stereoselection (84% ee) using a co-catalyst system of pipercolinic acid (Pip) and *N*-methylimidazole (NMI).³

Figure 1.1: Intramolecular Morita-Baylis-Hillman reaction.



1.2 Overview of Catalytic Intramolecular Morita-Baylis-Hillman Reactions

The MBH reaction was first discovered in 1968 by Morita and co-workers,⁴ followed by a report in 1972 in a German patent by Baylis and Hillman.⁵ The *intermolecular* variant of the MBH reaction has received much attention in the literature, benefitting from countless studies, thus becoming a synthetically useful reaction.⁶ Several extensive reviews have been written on the *intermolecular* variant and will not be covered here.⁷ Furthermore, another derivative known as the aza-Baylis-Hillman

³ Aroyan, C. E.; Vasbinder, M. M.; Miller, S. J. *Org. Lett.* **2005**, *7*, 3849-3851.

⁴ Morita, K.; Suzuki, Z.; Hirose, H. *Bull. Chem. Soc. Jpn.* **1968**, *41*, 2815.

⁵ Baylis, A. B.; Hillman, M. E. D. German Patent 2155113, 1972; *Chem. Abstr.* **1972**, *77*, 34174q.

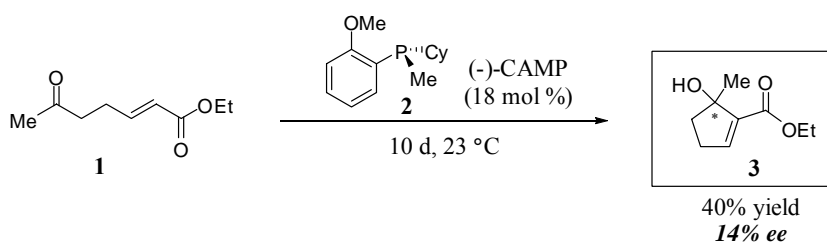
⁶ (a) Lee, K. Y.; Gowrisankar, S.; Kim, J. N. *Bull. Korean Chem. Soc.* **2005**, *26*, 1481-1490. (b) Reddy, L. R.; Saravanan, P.; Corey, E. J. *J. Am. Chem. Soc.* **2004**, *126*, 6230-6231.

⁷ (a) Basavaiah, D.; Kalapala, V. R.; Reddy, R. J. *Chem. Soc. Rev.* **2007**, *36*, 1581-1588. (b) Krishna, P. R.; Sharma, G. V. M. *Mini-Rev. Org. Chem.* **2006**, *3*, 137-153 and references therein.

reaction, has been investigated by multiple research groups and has been discussed elsewhere.⁸

The study of the *intramolecular* reaction, on the other hand, which would lead to highly versatile cyclization products, has remained essentially undeveloped. For example, the first account of an intramolecular variant, and the only enantioselective variant (until our report in 2005), was documented by Fráter and co-workers⁹ in 1992, twenty-four years after the initial discovery of Morita.¹⁰ Cyclization of substrate **1** in the presence of chiral phosphine (-)-CAMP (**2**, 18 mol %) provided cyclopentenol **3** (40% yield) with 14% enantiomeric excess after a reaction time of ten days (Scheme 1.1).

Scheme 1.1: First intramolecular MBH reaction.



One year later, Drewes and co-workers¹¹ documented the cyclization of substrate **4** leading to crystalline coumarin salt **5** (Scheme 1.2). The structure of **5** was confirmed by X-ray crystallography and lent credence to the proposed mechanism and understanding that the MBH product was the outcome of an addition-elimination sequence involving a nucleophilic catalyst, activated alkene, and electrophile.

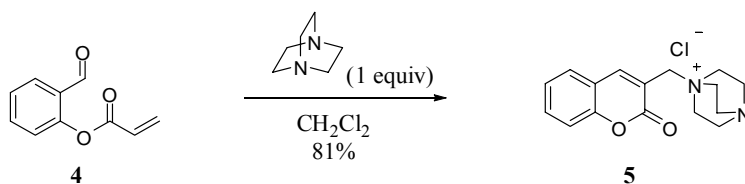
⁸ Shi, Y.-L.; Shi, M. *Eur. J. Org. Chem.* **2007**, 2905-2916.

⁹ Roth, F.; Gygax, P.; Fráter, G. *Tetrahedron Lett.* **1992**, 33, 1045-1048.

¹⁰ Masson, G.; Housseman, C.; Zhu, J. *Angew. Chem., Int. Ed.* **2007**, 46, 4614-4628.

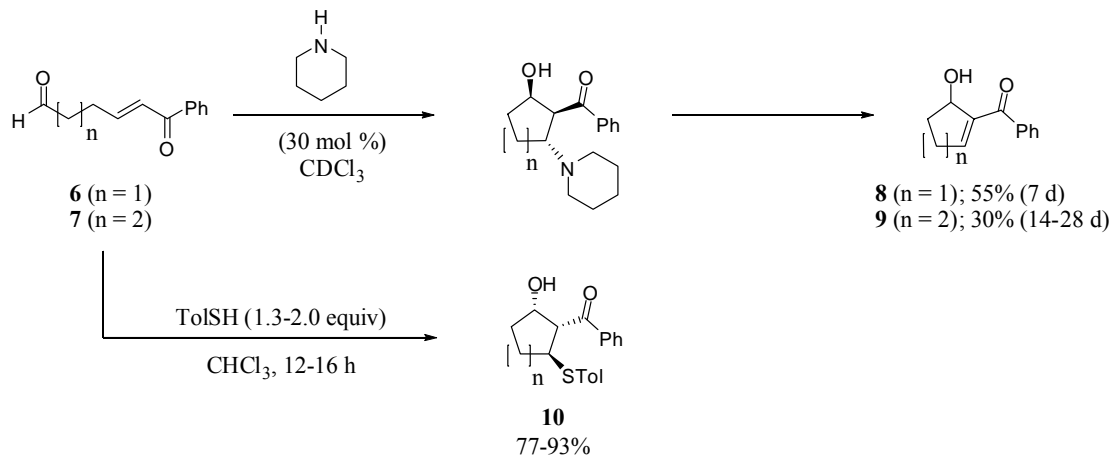
¹¹ Drewes, S. E.; Njamela, O. L.; Emslie, N. D.; Ramesar, N.; Field, J. S. *Synth. Commun.* **1993**, 23, 2807-2815.

Scheme 1.2: Mechanistic support provided by Drewes and co-workers.



Murphy and co-workers have also reported on the intramolecular cyclization of both five- and six-membered enone-aldehydes.¹² Piperidine (30 mol %) was found to be the best nitrogen-based catalyst, leading to the desired cyclization products **8** and **9** in moderate yield after long reaction times ($n=1$, 55% yield, 7 days; $n=2$, 30% yield, 14-28 days). Phosphines and thiols were reported to catalyze the reaction as well; however, phosphine catalysis led to variable yields, and thiol catalysis led to the single aldol addition by-product (**10**) in lieu of the desired MBH products (Scheme 1.3).

Scheme 1.3: Amine-catalyzed intramolecular MBH cyclization.

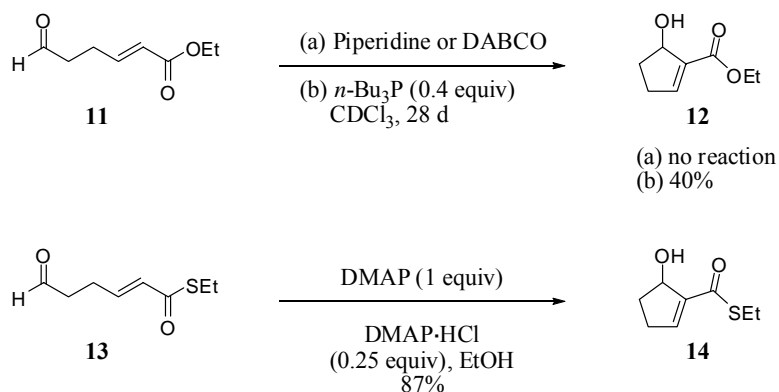


Although it has been demonstrated that enoates are much less reactive towards conjugate addition than their enone counterparts, and thus difficult substrates for the

¹² Richards, E. L.; Murphy, P. J.; Dinon, F.; Fratucello, S.; Brown, P. M.; Gelbrich, T.; Hursthouse, M. B. *Tetrahedron* **2001**, *57*, 7771-7784.

intramolecular MBH reaction, thioenates have been shown to have heightened reactivity; their reactivity lies closer to that of enones.¹³ For example, Murphy and co-workers demonstrated that cyclization of enoate-aldehyde **11** under nitrogen-based catalysis (piperidine or DABCO) did not provide the desired MBH product and under phosphine-based catalysis (*n*-Bu₃P) provided product **12** in moderate yield (40%, Scheme 1.4).¹² On the other hand, Keck and co-workers demonstrated that cyclization of thioenoate **13** in the presence of the mixed catalyst system of DMAP (1 equiv) and DMAP·HCl (0.25 equiv) provided the MBH product, **14**, in 82% yield.

Scheme 1.4: Intramolecular MBH of thioenates.

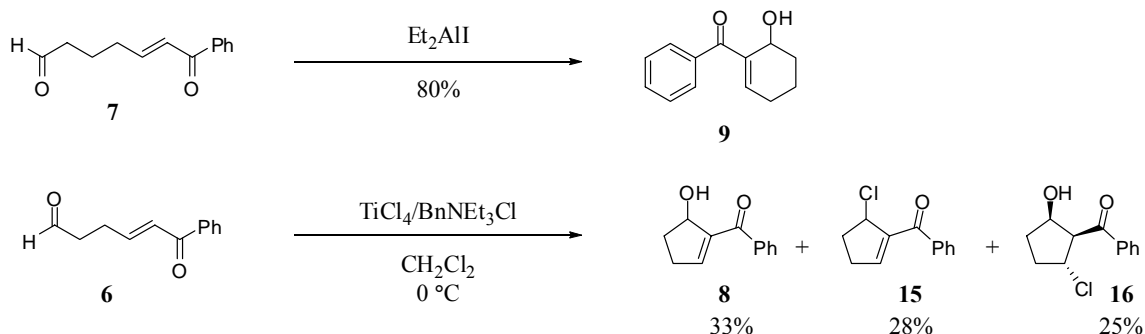


Oshima and co-workers demonstrated the use of Lewis acids (Et₂AlI and TiCl₄) in the intramolecular MBH cyclization (Scheme 1.5). Employing diethylaluminum iodide, they were able to catalyze the Michael aldol cyclization of α,β -unsaturated enone **7** to provide the six-membered ring MBH product **9** in 80% yield. Using titanium tetrachloride and benzylammonium chloride (BnNEt₃Cl) they were able to access the

¹³ Keck, G. E.; Welch, D. S. *Org. Lett.* **2002**, *4*, 3687-3690.

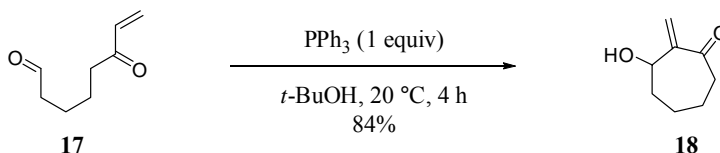
five-membered ring product, **8**, however in low yield (33%) in addition to the corresponding elimination product **15** (28%) and hydroxyl ketone **16** (25%).¹⁴

Scheme 1.5: Lewis acid catalyzed MBH reaction.



Koo and co-workers were able to extend the substrate scope to include enone-aldehyde **17** providing a seven-membered ring MBH product, **18** (Scheme 1.6). Catalysis with a stoichiometric amount of triphenylphosphine in *t*-BuOH led to the desired product in 84% yield.¹⁵

Scheme 1.6: Extension of reaction scope to include seven-membered ring formation.



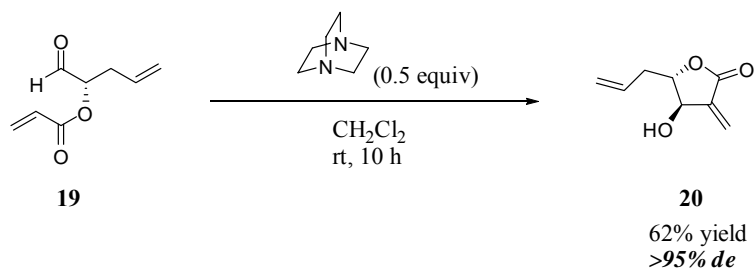
In 2005, Krishna and co-workers reported exquisite control over diastereoselectivity in the development of the first diastereoselective intramolecular MBH reaction (Scheme 1.7).¹⁶ Chiral enone-aldehyde **19** underwent DABCO-catalyzed (0.5 equiv) MBH cyclization to provide product **20** as a single isomer (>95%) in 62% yield.

¹⁴ Yagi, K.; Turitani, T.; Shinokubo, H.; Oshima, K. *Org. Lett.* **2002**, *4*, 3111-3114.

¹⁵ Yeo, J. E.; Yang, X.; Kim, H. J.; Koo, S. *Chem. Commun.* **2004**, 236-237.

¹⁶ Krishna, P. R.; Kannan, V.; Sharma, G. M. *J. Org. Chem.* **2004**, *69*, 6467-6469.

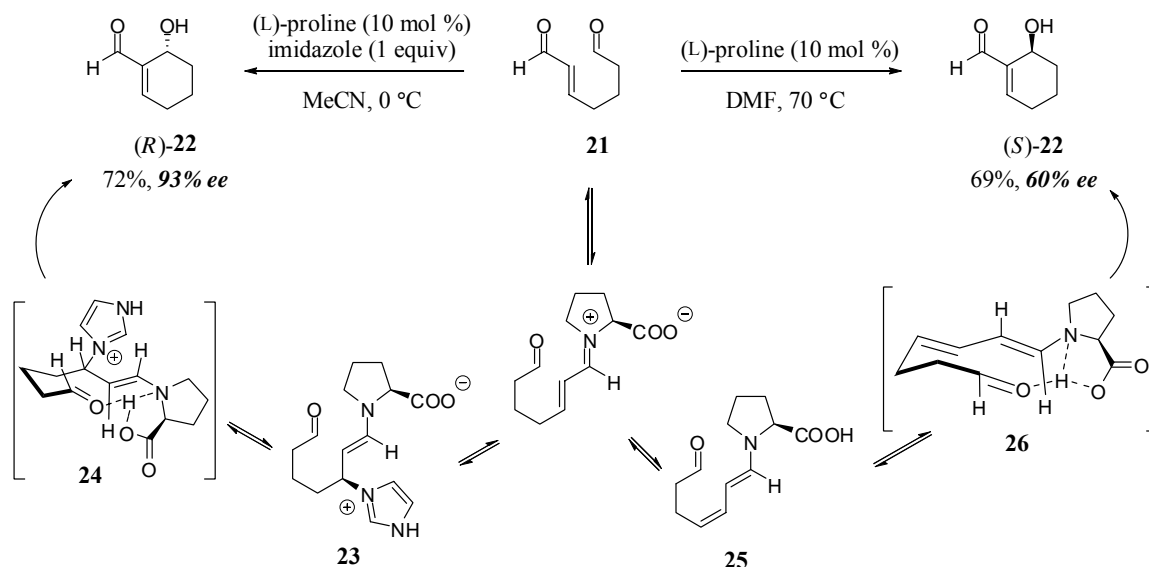
Scheme 1.7: First diastereoselective intramolecular MBH reaction.



Shortly after our report on the enantioselective intramolecular MBH reaction in 2005,³ Hong and co-workers reported a nitrogen-catalyzed enantioselective variant as well (Scheme 1.8).¹⁷ Interestingly, it was determined that proline, in combination with imidazole, catalyzed the transformation of enedial **21** to (*R*)-**22** with 93% ee in 72% yield, while proline in combination with DMF led to the opposite enantiomer, (*S*)-**22**, with 60% ee in 69% yield. Mechanistically, in the imidazole-catalyzed reaction, it was proposed that initial conjugate addition was directed by a hydrogen bond with the carboxylate to afford enamine **23**. An unfavorable 1,3-diaxial interaction was minimized in intermediate **24**, leading to *R*-enriched allylic alcohol **22**. Alternatively, the iminium species could undergo tautomerization to enamine **25** which would then proceed through a Zimmerman-Traxler transition state (**26**) to furnish (*S*)-**22**. These mechanistic issues will be discussed in more detail below.

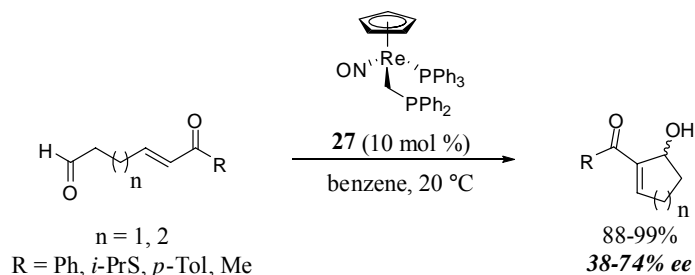
¹⁷ Chen, S.-H.; Hong, B.-C.; Su, C.-F. Sarshar, S. *Tetrahedron Lett.* **2005**, *46*, 8899-8903.

Scheme 1.8: Proline and proline/imidazole catalyzed enantioselective intramolecular MBH reaction.



Finally, Gladysz and co-workers presented a phosphine-catalyzed enantioselective intramolecular MBH reaction in 2007 (Scheme 1.9).¹⁸ Using catalyst **27** (10 mol %), the cycloisomerization of various enone-enals provided the corresponding substituted cyclopentene and cyclohexene products in good yield (88-99%) and with modest to good enantioselectivity (38-74%). It was proposed that the basicity and nucleophilicity of the donor atom (CH₂D:) in the active catalyst ($\eta^5\text{-C}_5\text{H}_5\text{Re}(\text{NO})(\text{PPh}_3)(\text{CH}_2\text{PPh}_2)$) was enhanced due to the incorporation of the 18-electron rhenium fragment.

Scheme 1.9: Enantioselective MBH reaction presented by Gladysz and co-workers.

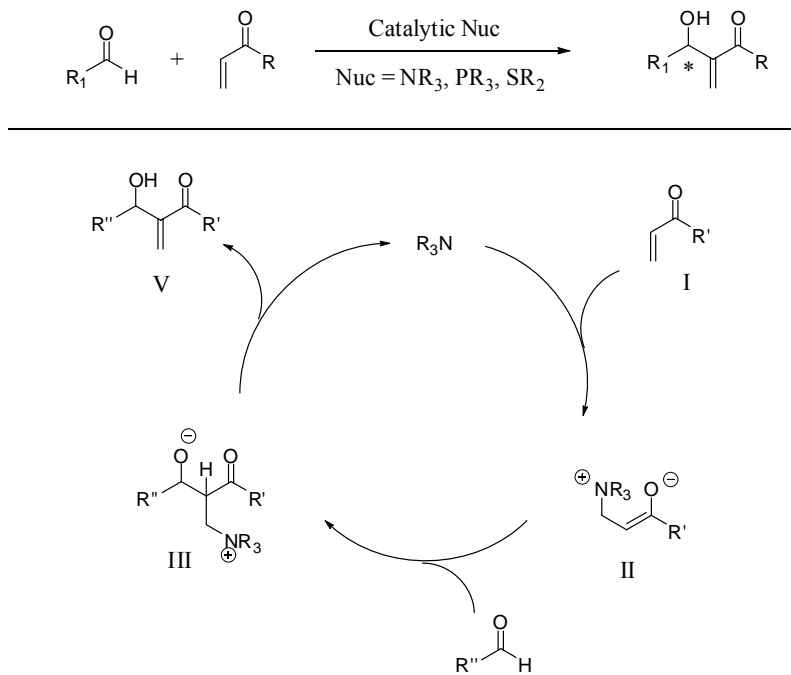


¹⁸ Seidel, F.; Gladysz, J. A. *Synlett* **2007**, 6, 986-988.

1.3 Mechanistic Details

Formally, the Morita-Baylis-Hillman reaction involves a one-pot combination of three consecutive transformations: Michael addition, aldol reaction, and β -elimination. The most widely accepted mechanism of the reaction is presented in Figure 1.2.^{2c} The reaction is believed to proceed via initial conjugate addition of a nitrogen-, phosphorous-, or sulfur-based nucleophile to the activated alkene (**I**) to generate zwitterionic intermediate **II**. This latent enolate then undergoes nucleophilic attack on the aldehyde, generating a second zwitterionic species, **III**, followed by subsequent proton transfer and extrusion of the catalyst to generate MBH adduct **V**.

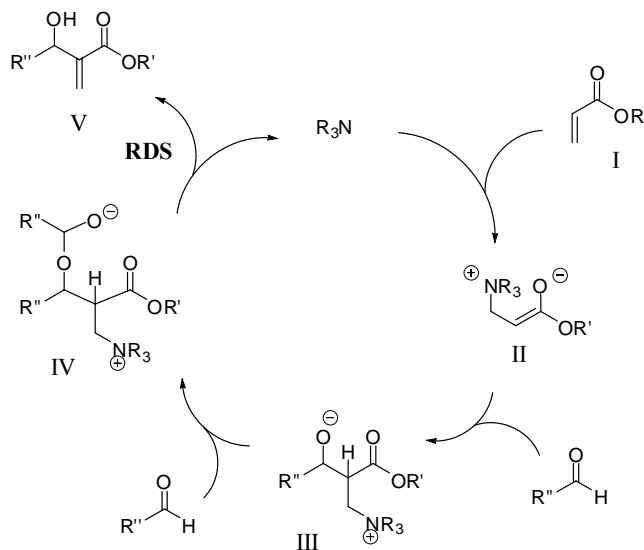
Figure 1.2: Proposed mechanism of the MBH reaction.



It was long believed that the rate-determining step (RDS) was carbon-carbon bond formation in the aldol reaction of intermediate **II** with the aldehyde.² However,

there have been several revisions of the mechanism recently by the research groups of Aggarwal and McQuade suggesting that the RDS is not yet fully understood.¹⁹ In studying isotopic-labeling and kinetic experiments in the acrylate-based MBH reaction, McQuade and co-workers have proposed that the reaction was second order in aldehyde and that the RDS involved proton transfer in the cleavage of the α -position C-H bond. This modification of the mechanism involves analogous steps to provide zwitterionic intermediate **III**, at which point the generated alkoxide undergoes nucleophilic attack on a second equivalent of aldehyde, providing hemi-acetal intermediate **IV** which is poised for facile proton transfer (Figure 1.3).

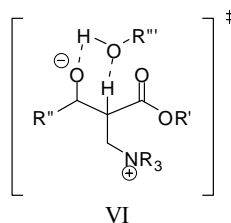
Figure 1.3: Revision of the mechanism proposed by McQuade and co-workers.



¹⁹ For mechanistic studies regarding the MBH reaction, see: (a) Aggarwal, V. K.; Fulford, S.; Lloyd-Jones, G. C. *Angew. Chem., Int. Ed.* **2005**, *44*, 1706-1708. (b) Price, K. E.; Broadwater, S. J.; Walker, B. J.; McQuade, D. T. *J. Org. Chem.* **2005**, *70*, 3980-3987. (c) Price, K. E.; Broadwater, S. J.; Jung, H. M.; McQuade, D. T. *Org. Lett.* **2005**, *7*, 147-150. For mechanistic studies regarding the related aza-MBH reaction, please see: (d) Buskens, P.; Klankermayer, J.; Leitner, W. *J. Am. Chem. Soc.* **2005**, *127*, 16762-16763. (e) Raheem, I. T.; Jacobsen, E. N. *Adv. Synth. Catal.* **2005**, *347*, 1701-1708.

In the presence of a protic additive, Aggarwal and co-workers also proposed that abstraction the α -H atom of intermediate **III** was rate-limiting and suggested intermediate **VI** to explain the proton shift (Figure 1.4).

Figure 1.4: Transition state proposed by Aggarwal and co-workers.



1.4 Dual Catalyst Control in the Enantioselective MBH Reaction

1.4.1 Prior Studies of Metal-Free Peptide-Based Catalysis

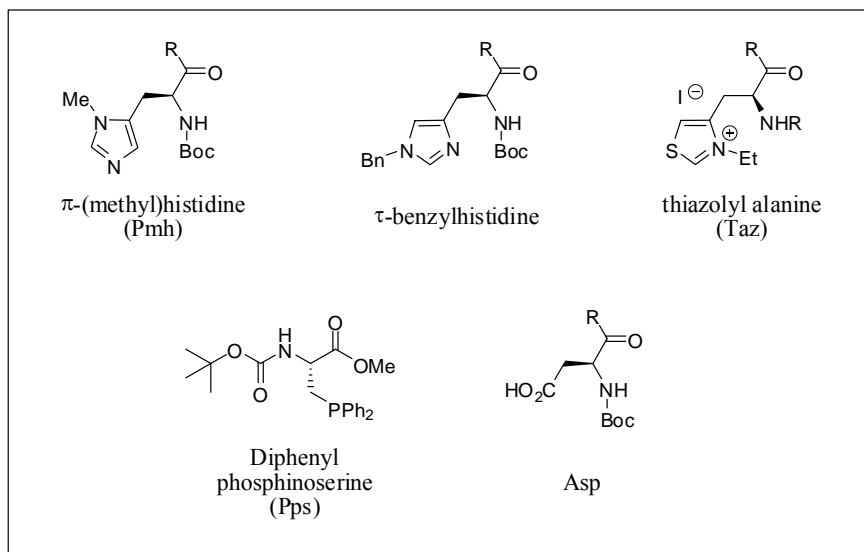
It is known that nature has the ability to catalyze various transformations with exquisite levels of chemo-, regio-, and stereoselectivity.²⁰ Enzyme conformation, hydrogen bonding, proton transfer, and nucleophilic addition are several factors that control enzymatic activity and the ability to confer high levels of selectivity in a desired process. The question we were interested in pursuing regarded what fraction of an enzyme is critical for selective catalysis. Translating this quest into an on-going study, we set out to build synthetic mimics of biosynthetic tools by creating powerful small peptide-based catalysts for synthetic organic transformations.²¹ With this goal in mind, our laboratory has studied nucleophile-embedded peptides that can serve as highly efficient catalysts for a variety of transformations: π -(methyl)histidine (Pmh)-based

²⁰ For the use of enzymes as catalysts in organic synthesis, see: Wong, C.-H.; Whitesides, G. M. *Enzymes in Synthetic Organic Chemistry*; Elsevier Science Ltd.; Oxford, **1994**.

²¹ For a review of peptides as asymmetric catalysts, see: (a) Davie, E. A. C.; Mennen, S. M.; Xu, Y.; Miller, S. J. *Chem. Rev.* **2007**, *107*, 5759-5812. (b) Revell, J. D.; Wennemers, H. *Curr. Opin. Chem. Biol.* **2007**, *11*, 269-278. (c) Miller, S. J. *Acc. Chem. Res.* **2004**, *37*, 601-610 and references therein.

peptides for asymmetric group transfer reactions (acylation,²² phosphorylation,²³ sulfinylation,²⁴ thionoformylation²⁵), τ -benzyl histidine for azide conjugate addition,²⁶ thiazolyl alanine (Taz) for intermolecular aldehyde-imine cross-coupling,²⁷ diphenylphosphinoserine (Pps) for [3+2]-cycloadditions,²⁸ and finally aspartate-embedded peptides for enantioselective epoxidation (Figure 1.5).²⁹

Figure 1.5: Synthetic tool box of nucleophile-embedded peptide-based catalysts.



When the work described in this thesis was initiated, the ability to catalyze carbon–carbon bond-forming reactions employing peptide-based catalysis was not well developed. Thus, with the goal of extending our group methodology to transformations involving the formation of a new C–C bond, exploration of the Morita-Baylis-Hillman

²² Copeland, G. T.; Miller, S. J. *J. Am. Chem. Soc.* **2001**, *123*, 6496-6502.

²³ Sculimbrene, B. R.; Miller, S. J. *J. Am. Chem. Soc.* **2001**, *123*, 10125-10126.

²⁴ Evans, J. W.; Fierman, M. B.; Miller, S. J.; Ellman, J. A. *J. Am. Chem. Soc.* **2004**, *126*, 8134-8135.

²⁵ Sánchez-Roselló, M.; Puchlopek, A. L. A.; Morgan, A. J.; Miller, S. J. *J. Org. Chem.* **2008**, *73*, 1774-1782.

²⁶ Guerin, D. J.; Miller, S. J. *J. Am. Chem. Soc.* **2002**, *124*, 2134-2136.

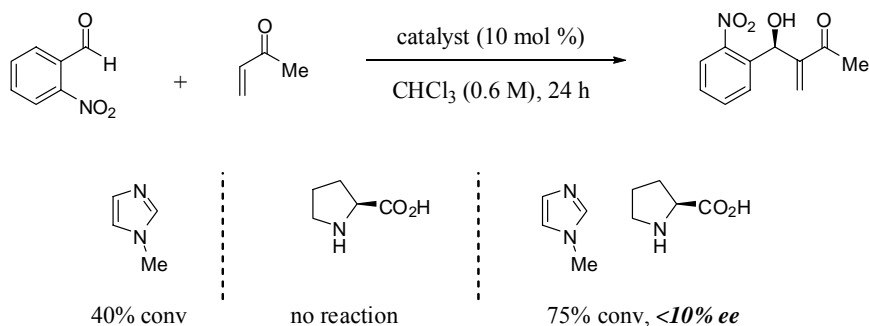
²⁷ Mennen, S. M.; Gipson, J. D.; Kim, Y. R.; Miller, S. J. *J. Am. Chem. Soc.* **2005**, *127*, 1654-1655.

²⁸ Cowen, B. J.; Miller, S. J. *J. Am. Chem. Soc.* **2007**, *129*, 10988-10989.

²⁹ Peris, G.; Jakobsche, C. E.; Miller, S. J. *J. Am. Chem. Soc.* **2007**, *129*, 8710-8711.

reaction began. Initial studies of the MBH reaction began with an investigation of the *intermolecular* variant. As illustrated in Figure 1.6, it was determined that co-catalysis (*N*-methylimidazole (NMI) and proline) was essential in the methyl vinyl ketone (MVK)-based MBH reaction with *o*-nitrobenzaldehyde to achieve efficient conversion to the desired products.³⁰

Figure 1.6: Essential co-catalysis of NMI and proline in the intermolecular MBH reaction.

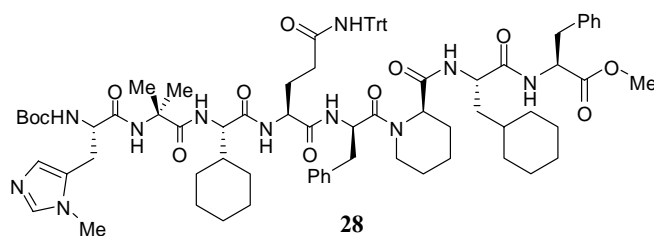
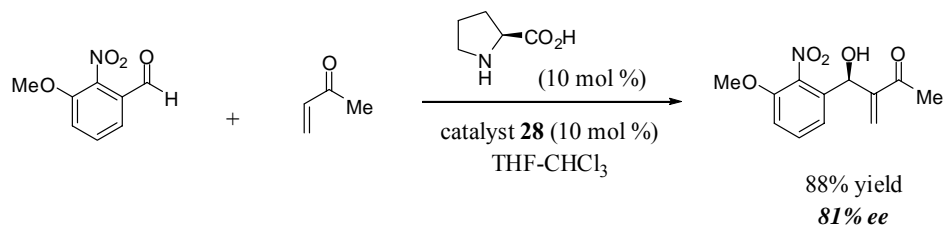


Once sufficient reactivity was established with *N*-methylimidazole and proline, the possibility of rendering the reaction enantioselective was explored. Therefore, NMI was incorporated into peptide-based catalysts in the form of an *N*-terminal π -(methyl)histidine residue, and screened in combination with L-proline (Scheme 1.10). Ultimately, through the optimization of multiple parameters of the reaction and co-catalytic system, peptide catalyst **28** was found to be highly efficient in the catalysis of the intermolecular MVK-based MBH reaction with various activated aromatic aldehydes providing the coupled products in 52-95% yield and with 63-81% enantiomeric excess.

³⁰ (a) Imbriglio, J. E.; Vasbinder, M. M.; Miller, S. J. *Org. Lett.* **2003**, *5*, 3741-3743. (b) Vasbinder, M. M.; Imbriglio, J. E.; Miller, S. J. *Tetrahedron* **2006**, *62*, 11450-11459. This finding was in analogy to observations by Shi and Jiang in their studies employing a cinchona alkaloid catalyst: Shi, M.; Jiang, J.-K. *Tetrahedron: Asymmetry* **2002**, *13*, 1941-1947.

At the time of this study, these results represented the highest enantioselectivities reported to date for the ketone-based MBH reaction.

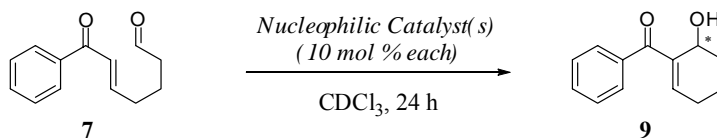
Scheme 1.10: Optimized conditions for the intermolecular MBH reaction.



1.4.2 Intramolecular MBH: Distinct from Intermolecular MBH

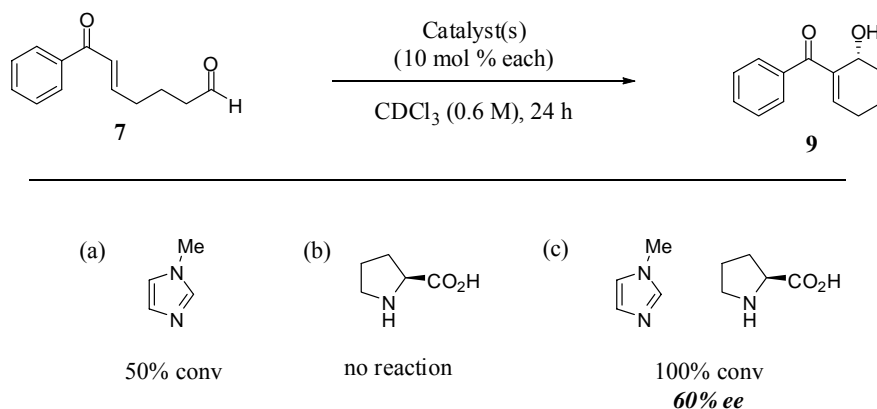
Our study of the *intramolecular* Morita-Baylis-Hillman reaction commenced with the investigation of the cyclization shown in Scheme 1.11. In analogy to work that had been on-going in our laboratory in both the *intermolecular* MBH reaction as well as other peptide-catalyzed processes, we began our study with the catalytic system of *N*-methylimidazole (NMI) and proline. We were optimistic that upon demonstration of sufficient co-catalysis and reactivity, the *N*-methylimidazole moiety could subsequently be embedded into a peptide catalyst and used in combination with proline in order to achieve substantial enantioselectivity.

Scheme 1.11: Intramolecular MBH reaction.



Similar to our findings in the *intermolecular* MBH reaction,³⁰ co-catalysis was essential to achieve conversion to the desired products (Figure 1.7). In the cyclization of enone-aldehyde **7** to provide cyclized product **9**, the use of *N*-methylimidazole as the sole catalyst resulted in low reactivity (50% conv, 24 h), whereas no reaction occurred with proline alone. However, in the presence of *both* NMI and proline we observed significant rate acceleration (100 % conv, 24 h). Excitingly, instead of producing a racemic product (as in the *intermolecular* reaction) these conditions provided product **9** with moderate enantioselectivity (60% ee).

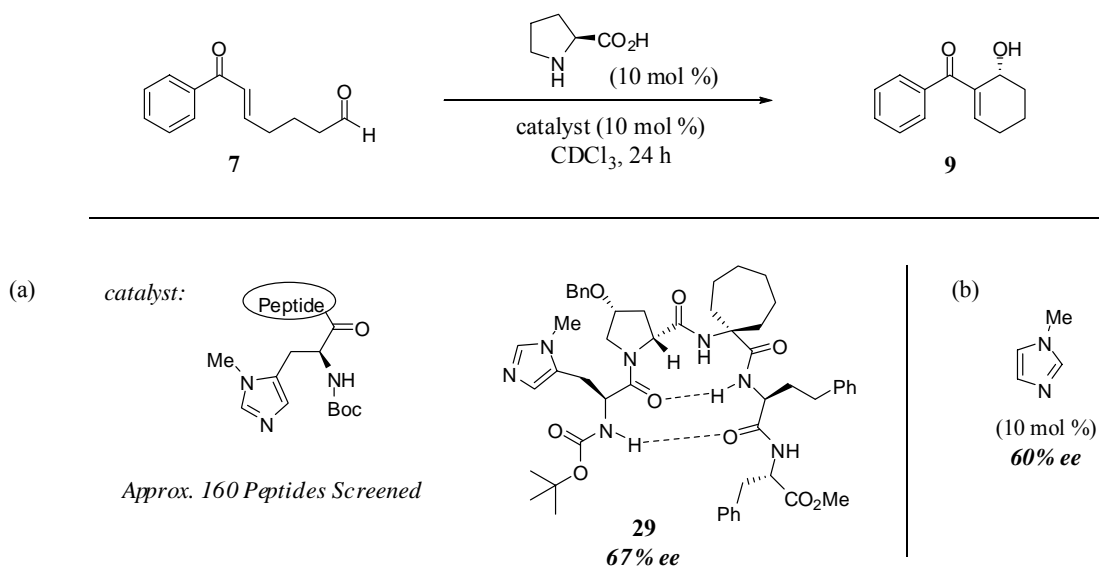
Figure 1.7: Catalysis of the intramolecular MBH reaction with (a) NMI, (b) proline, (c) co-catalysts NMI and proline.



Once sufficient reactivity was established under co-catalysis, we explored the possibility of enhancing the enantioselectivity of the reaction. Thus, NMI was incorporated into small nucleophilic oligopeptides in the form of π -methyl(histidine) (Pmh). As demonstrated in the *intermolecular* case, as well as in previous methodology within our group, we believed that the chiral environment provided by the peptide secondary structure would confer high enantioselectivity in the reaction. In stark contrast to this precedence in the *intermolecular* MBH reaction, a screen of approximately 160

peptides in combination with L-proline did not lead to a significant improvement of enantioselectivity. Peptides varying in chain length, ranging from the single amino acid up to a decapeptide, as well as variations in secondary structure (random and discrete β -turn peptides) were tested. Peptide catalyst **29** was found to provide the highest level of stereoinduction, producing cyclized product **9** in 67% ee (Figure 1.8).³¹ Notably, this was not an appreciable increase in stereoinduction when compared to employing just NMI and proline alone, which led to desired product **9** in 60% ee.

Figure 1.8: Co-catalysis of the intramolecular MBH reaction: (a) peptide/proline versus (b) NMI/proline.

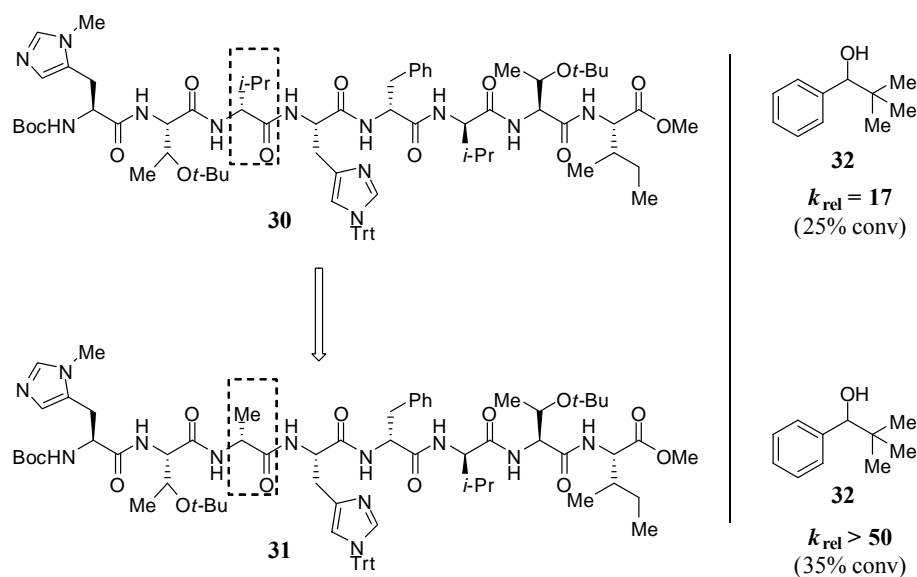


In addition to screening the aforementioned peptides, we also looked more closely at known peptide catalyst **30**, which was found to be a moderately selective catalyst in combination with L-proline (42% ee). This peptide was previously discovered in our laboratory through a combinatorial screen as an excellent catalyst in the kinetic resolution

³¹ Vasbinder, M. M. Ph.D. Thesis, Boston College, 2004.

of various secondary alcohols.²² Interestingly, it was found that an alanine scan³² of peptide **30**, where each amino acid was sequentially substituted with alanine using the original stereochemistry, elucidated new derivatives that were substantially more selective (Figure 1.9).³³ For example, while peptide **30** was able to resolve alcohol **32** with observed $k_{\text{rel}} = 17$, peptide **31** (alanine substitution at the *i*+2 position) afforded $k_{\text{rel}} > 50$.

Figure 1.9: Alanine scan of peptide **30** in the kinetic resolution of secondary alcohols.



We investigated the possibility of a similar boost in stereoselectivity in the MBH reaction by screening an alanine scan of peptide **30** in combination with L-proline (Table 1.1). As expected, elimination of the terminal nucleophilic π -methyl histidine residue (peptide **33**) rendered the catalyst inactive and resulted in <5% conversion of **7** to **9**. On the other hand, several peptides were found to provide a modest enhancement in

³² Morrison, K. L.; Weiss, G. A. *Curr. Opin. Chem. Biol.* **2001**, *5*, 302-307.

³³ Fierman, M. B.; O'Leary, D. J.; Steinmetz, W. E.; Miller, S. J. *J. Am. Chem. Soc.* **2004**, *126*, 6967-6971.

enantioselectivity, with substitution at the $i + 3$ position providing 52% ee (catalyst **35**) and at the $i + 5$ position (catalyst **37**) providing 55% ee. In order to investigate the proline-peptide catalyst interaction, D-proline and racemic proline were also examined in conjunction with each alanine scan peptide. It can be seen that there were matched and mismatched pairs of co-catalysts, such that D-proline/peptide led to a slight preference for the formation of the opposite enantiomer of product **9** while D/L-proline/peptide led to non-selective transformations.

Table 1.1: Alanine scan of peptide **30** in combination with proline.

Reaction scheme: Aldehyde **7** reacts with proline (10 mol %) and peptide catalyst (10 mol %) in CDCl_3 at 0.1 M for 24 h to yield alcohol **9**.

Chemical structure of peptide **30**, an alanine scan peptide with various side chains including BocHN, Me, Ot-Bu, i-Pr, Ph, Me, Ot-Bu, Me, and Trt.

Peptide	30	33	34	31	35	36	37	38	39
(aa replaced)	-	(i) PMH	(i + 1) Thr(<i>t</i>-Bu)	(i + 2) D-Val	(i + 3) His(Trt)	(i + 4) D-Phe	(i + 5) D-Val	(i + 6) Thr(<i>t</i>-Bu)	(i + 7) Ile
(L)-Proline	+42	n.r.	+42	+37	+52	+50	+55	+46	+46
(D)-Proline	-3	n.r.	-21	-15	-15	-15	-17	-12	-17
(D/L)-Proline	-4	n.r.	-3	+2	-2	-5	-5	-1	+2

(reported as % ee)

In light of the fact that the examined peptide catalysts used co-catalytically with proline maintained similar reactivity to that of NMI with proline, in addition to the understanding that the *inter*- and the *intramolecular* MBH reactions were dramatically

distinct processes,³⁴ we embarked on a new optimization study that addressed each component in the reaction.

1.4.3 Development of the Co-Catalytic System: Pipecolinic acid/NMI

Having explored the chiral space around the NMI moiety of our co-catalytic system by way of peptide screening, we determined that the modifications were not significantly beneficial and could be deleterious to stereoselectivity in the mismatched cases. Alternatively, we were intrigued with the possibility of altering the chiral space around proline in an attempt to surpass the moderate selectivity achieved with NMI/proline (60% ee).

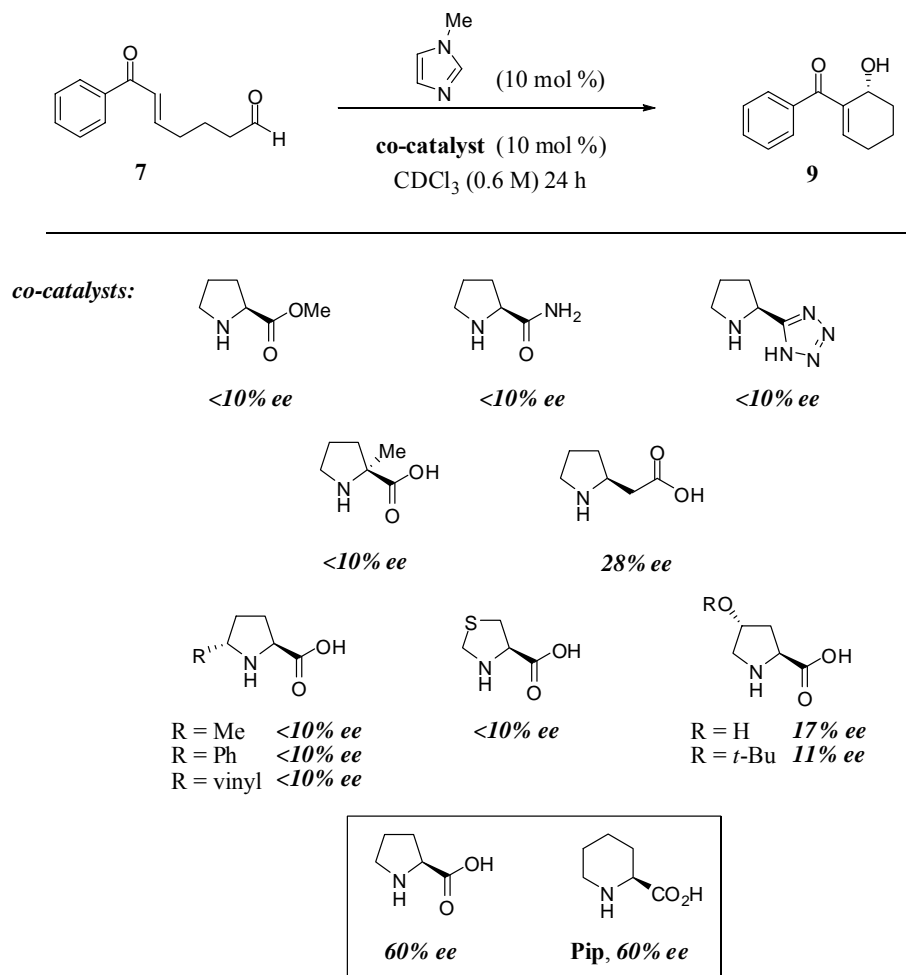
With this in mind, we began our optimization studies by exploring the role of the proline component in the co-catalytic system. As shown in Figure 1.10, we examined the cyclization of **7** to **9** catalyzed by multiple proline analogs in combination with NMI. The free carboxylic acid was found to be critical, as masking of the acid moiety with a methyl ester or replacement with an amide or tetrazole³⁵ led to negligible levels of stereoselection (<10% ee). α -Methyl substitution³⁶ as well as acid homologation were also unsuccessful, providing <10% ee and modest enantioselectivity (28% ee), respectively. Finally, substitution in and around the ring was deleterious, with only hydroxy-substitution leading to detectable levels of enantioselectivity (<20% ee).

³⁴ This idea is reflected in the literature as well, with very few successful reports of the intramolecular MBH while numerous reports on the intermolecular reaction continue to be published. See; Basavaiah, D.; Rao, A. J.; Satyanarayana, T. *Chem. Rev.* **2003**, *103*, 811-891.

³⁵ (a) Torii, H.; Nakadai, M.; Ishihara, K.; Saito, S.; Yamamoto, H. *Angew. Chem., Int. Ed.* **2004**, *43*, 1983-1986. (b) Cobb, A. J. A.; Shaw, D. M.; Ley, S. V. *Synlett* **2004**, 558-560. (c) List, B. *Tetrahedron* **2002**, *58*, 5573-5590.

³⁶ Vignola, N.; List, B. *J. Am. Chem. Soc.* **2004**, *126*, 450-451.

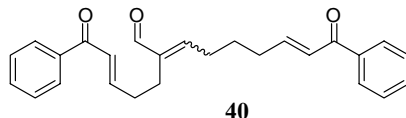
Figure 1.10: Proline derivatives tested as co-catalysts with NMI in the intramolecular MBH reaction.



With the exception of pipecolic acid (Pip), the proline surrogates examined led to diminished enantioselectivity, low reactivity, or the formation of intermolecular aldol dimerization by-product **40** (Figure 1.11). Interestingly, homologation of the five-membered ring of proline to the six-membered ring derivative, L-pipecolic acid, in combination with NMI, led to catalysis of the cyclization with indistinguishable results from that catalyzed using L-proline/NMI. Due to the unique ability of proline and pipecolic acid to catalyze the reaction with significant enantioselectivity, we elected to

proceed with both co-catalytic systems, NMI/proline and NMI/pipecolinic acid, in our further optimization studies.

Figure 1.11: Aldol dimerization by-product **40**.



1.4.4 Optimization of Reaction Conditions: Solvent

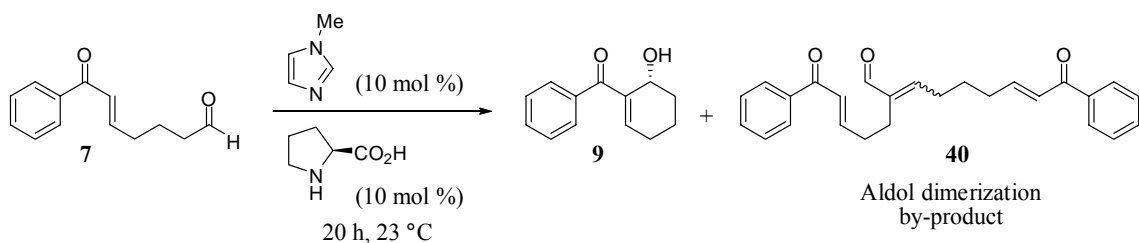
One method employed in the Morita-Baylis-Hillman reaction to overcome slow reaction rates is the fine-tuning of solvent. Protic solvents have been shown to accelerate the reaction, presumably through hydrogen bonding to either stabilize the formed enolate or activate the aldehyde.³⁷ In our studies, we found that the choice of solvent had a dramatic effect not only on the reaction rate, but also on product distribution and the enantioselectivity of the desired product.

Beginning with the NMI/proline co-catalytic system, we were able to obtain complete control over product distribution by simply changing our solvent system (Table 1.2). The cyclization of phenyl ketone-based substrate **7** in the presence of NMI and proline (10 mol % each) in a non-polar solvent, toluene, was unreactive and we recovered only starting material (entry 1). Alternatively, in a highly polar solvent, DMF, under the same reaction conditions, we observed full conversion to the intermolecular aldol dimerization by-product (**40**) instead of desired product **9** (entry 7). Examining various solvents with dielectric constants ranging between toluene (2.0) and DMF (38.3) led to

³⁷ (a) Methot, J. L.; Roush, W. R. *Org. Lett.* **2003**, *5*, 4223-4226. (b) Aggarwal, V. K.; Dean, D. K.; Mereu, A.; Williams, R. *J. Org. Chem.* **2002**, *67*, 510-514. (c) Keck, G. E.; Welch, D. S. *Org. Lett.* **2002**, *4*, 3687-3690 and references therein.

mixed results. The rate of this reaction in Et₂O and THF was sluggish, with 25% conversion to by-product **40** in 20 h with little or no detectable cyclized product **9** (entries 2 and 4). Chloroform, CH₂Cl₂, and acetonitrile all led to moderate levels of enantioselectivity (53%, 73%, and 67%, respectively) with varying degrees of conversion and product distribution (entries 3, 5, and 6). Although methylene chloride looked promising from the standpoint of stereoinduction (73% ee, entry 5), it suffered from poor product distribution. It is important to note that the conversion of the MBH reaction in CDCl₃ was substantially lower than that previously reported (30% versus full conversion) due to the change in reaction concentration (0.6M to 0.3M). Although we later found that more concentrated reaction conditions were optimal (0.6M), the solvent screen at 0.3M was a highly informative comparison of reaction efficiency in varying solvents.

Table 1.2: Solvent effects in the intramolecular cyclization of **7** to **9** catalyzed by Pro/NMI.

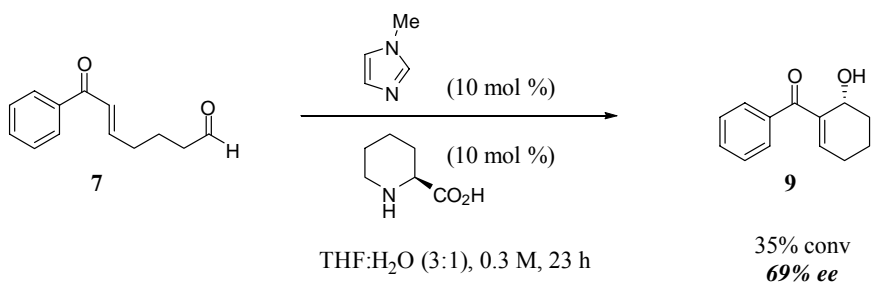


entry	solvent (0.3 M)	dielectric constant (ϵ)	% ee	7 : 9 : 40
1	Toluene	2.4	-	100 : 0 : 0
2	Et ₂ O	4.3	-	75 : 0 : 25
3	CDCl ₃	4.8	53	70 : 30 : 0
4	THF	7.6	-	65 : 10 : 25
5	CH ₂ Cl ₂	9.1	73	20 : 65 : 15
6	MeCN	37.5	67	0 : 30 : 70
7	DMF	36.7	-	0 : 0 :100
8	THF:H ₂ O (3:1)	-	33	0 : 100 : 0

In accord with the literature, it appeared that more polar solvents correlated to higher levels of conversion, however, there was not an obvious correlation to reaction outcome; formation of by-product **40** was an important factor that reduced efficiency in the intramolecular MBH reaction. A critical discovery was the impact of protic reaction conditions, THF-H₂O (3:1). Ultimately using this solvent system, we were able to completely suppress the formation of **40** and obtain full conversion to desired product **9**. Although the enantioselectivity of this reaction was relatively low (33% ee), we were optimistic that with the heightened reactivity and chemoselectivity we would be able to further optimize the reaction to restore stereoselectivity.

Eager to test the new protic solvent conditions with our alternative co-catalyst system, we next investigated the cyclization of **7** to **9** with NMI and pipercolinic acid (Scheme 1.12). Excitingly, in THF-H₂O we were now able to obtain the desired product with 69% enantiomeric excess, a modest increase in enantioselectivity compared to catalysis in CDCl₃ (60% ee, Figure 1.10), yet a bold increase in enantioselectivity when compared with NMI/proline (33% ee) in THF-H₂O. Unfortunately, with the increase in enantioselectivity obtained by using NMI/pipercolinic acid, we saw a decrease in reactivity (35% conversion).

Scheme 1.12: Catalysis of the MBH reaction with pip/NMI under protic reaction conditions.



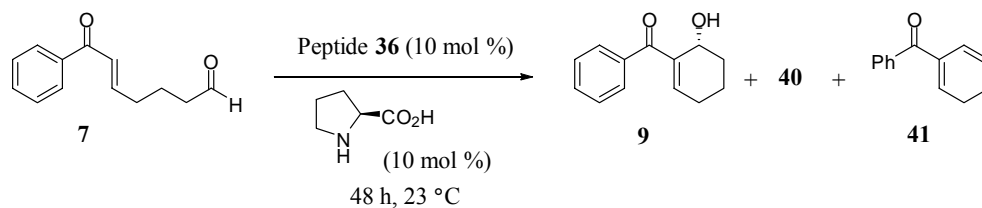
1.4.5 Re-Examination of Peptide Catalysts

Our initial investigations into the intramolecular MBH reaction demonstrated that enriching the chiral information around the nucleophilic NMI moiety, in as many as 160 peptides, did not provide a noticeable improvement from simply employing NMI as the sole nucleophilic catalyst. However, having been able to demonstrate the dramatic effects of solvent on this reaction leading to the identification of optimal protic conditions, as well as a new co-catalyst (pipercolinic acid), we turned to reinvestigate the possibility of using of a peptide-based catalyst.

An examination of solvent effects in the cyclization of **7** to **9** catalyzed by alanine scan peptide **36** in combination with proline revealed similar results to those previously disclosed in the case of NMI/proline; the choice of solvent directly affected reactivity, stereoselectivity, and chemoselectivity. In addition to intermolecular aldol dimerization by-product **40**, peptide catalysis also led to dehydrated by-product **41**. Notably, catalysis of this cyclization in toluene/CDCl₃ (0.3M) provided the desired product with 60% enantiomeric excess and 80% conversion.³⁸ Under protic conditions (THF-H₂O), we obtained 60% conversion to product **9** with 46% ee (Table 1.3). Once again the levels of stereoinduction observed did not surpass those obtained when using the more simple catalyst NMI. Additionally, we were intrigued about the prospect of catalyzing the MBH reaction under aqueous conditions and, therefore, decided to continue our optimization study in THF-H₂O.

³⁸ A concentration screen was run for the cyclization reaction using peptide **39**/proline in which it was determined that a reaction concentration of 0.3M was ideal. All the following peptide work was conducted at this concentration, in contrast to 0.1M from the previous screen of the alanine scan peptides.

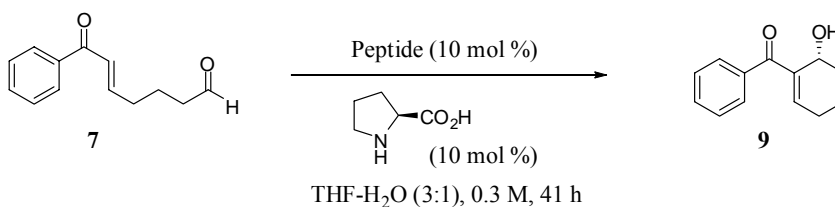
Table 1.3: Solvent effects in the cyclization of **7** to **9** catalyzed by peptide **36**/proline.



entry	solvent (0.3 M)	% ee	7 : 9 : 40 : 41
1	CH ₂ Cl ₂	56	0 : 50 : 35 : 15
2	CCl ₄	-	70 : 0 : 30 : 0
3	CDCl ₃	31	10 : 45 : 35 : 10
4	Tol/CDCl ₃	60	10 : 80 : 10 : 0
5	THF/CDCl ₃	54	0 : 50 : 50 : 0
6	MeCN	55	0 : 40 : 50 : 10
7	THF:H ₂ O (3:1)	46	0 : 60 : 30 : 0

Having adopted aqueous reaction conditions, we proceeded to test a small sampling of the best peptides in combination with each co-catalyst, proline and pipercolinic acid. As illustrated in Figure 1.12, we determined that the optimal peptide-based catalyst in combination with proline was alanine scan peptide **39**, affording product **9** with 40% enantiomeric excess.

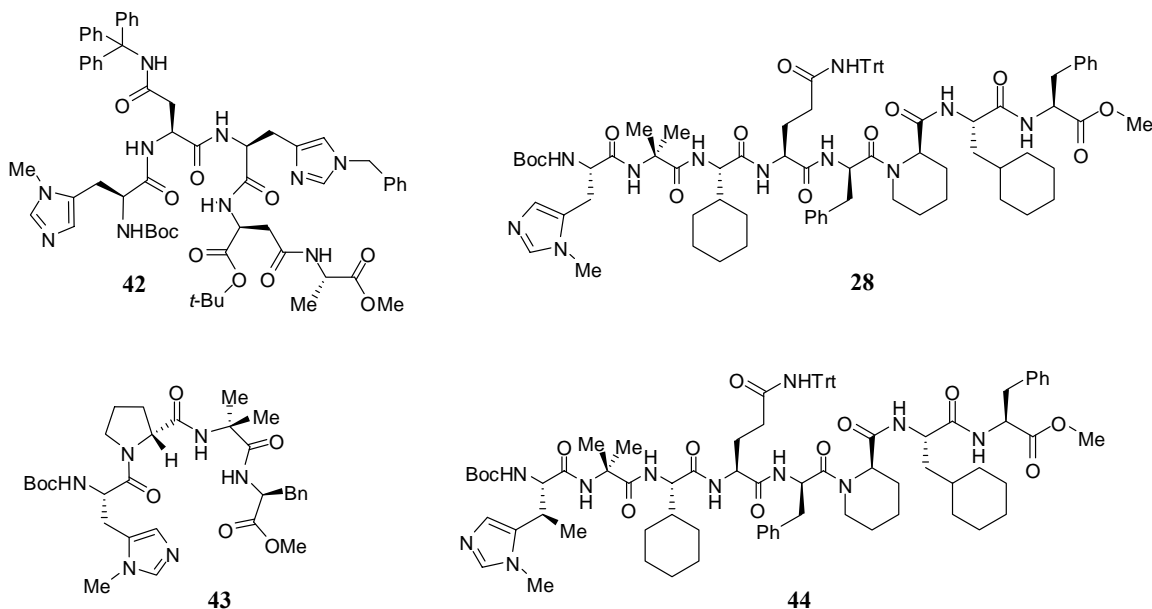
Figure 1.12: Catalysis of the intramolecular MBH under protic conditions with various peptides/proline.



peptide	30	31	35	36	37	38	39	42	43	28	44
% ee	34	28	27	29	33	33	40	29	26	31	33

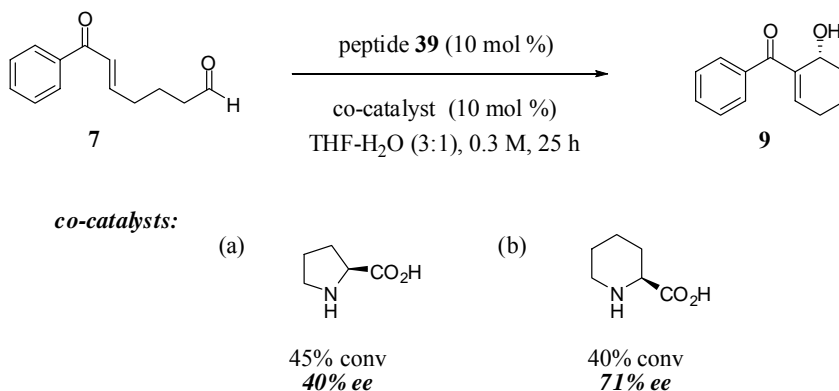
Several peptides (**28**, **42**, **43**, and **44**, Figure 1.13) that were known to be successful catalysts for other transformations in our laboratory (asymmetric phosphorylation,²³ acylation,²² and intermolecular MBH)³⁰ were included in the screen; however, they were found to be less efficient (Figure 1.12).

Figure 1.13: Alternative peptides tested under protic reaction conditions.



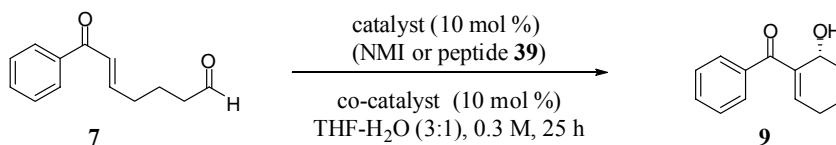
As illustrated in Figure 1.14, the best alanine scan peptide, **39**, was then employed in the cyclization of enone-aldehyde **7** to **9** with the alternative co-catalyst, pipercolinic acid. Under the optimized solvent conditions (THF-H₂O, 3:1) peptide **39**/proline provided 45% conversion to **9** with 40% enantioselectivity, while peptide **39**/pipercolinic acid provided similar reactivity (40% conv) but now with higher stereinduction (71% ee).

Figure 1.14: Catalysis of the MBH reaction with peptide **39**.



Although the enantioselectivity provided by the co-catalysis of peptide **39** with pipercolinic acid was substantial, it was instructive to perform a direct comparison of the nucleophilic catalysts, NMI and peptide, with each co-catalyst, proline and pipercolinic acid (Figure 1.15). Considering peptide **39** first, it was clear that catalysis with pipercolinic acid led to much higher levels of enantioselectivity than with proline (68% ee versus 40% ee), with both co-catalysts providing similar levels of conversion (40-45%). Analysis of NMI with each co-catalyst showed that conversion of **7** to **9** was low with pipercolinic acid (35% conversion) while very high (>90%) with proline. On the other hand, enantioselectivity was high (69%) when NMI/pipercolinic acid was used and low with NMI/proline (33%). Importantly, we noticed that the levels of stereinduction obtained when using either NMI or peptide **39** were very similar. This analysis reiterated our previous conclusion which suggested that altering the chiral space around the *N*-methylimidazole moiety did not provide enhanced selectivity, and that we should maintain our focus on optimization of the proline component as well as reaction parameters.

Figure 1.15: Cross-comparison of the co-catalytic systems.

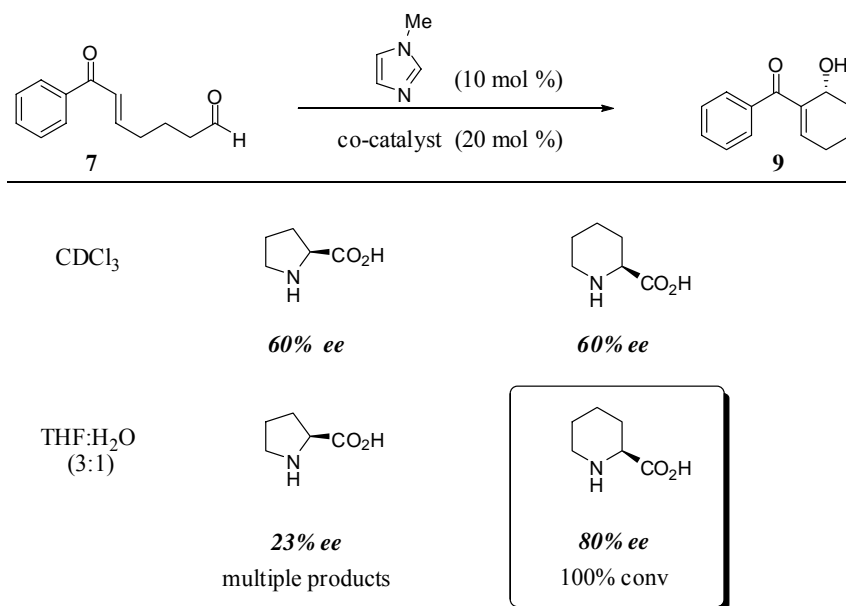


	(L)-pipecolinic acid	(L)-proline
peptide 39	40% conv, 71% ee	45% conv, 40% ee
NMI	35% conv, 69% ee	>90% conv, 33% ee

1.4.6 Optimization: Catalyst Loading and Stoichiometry

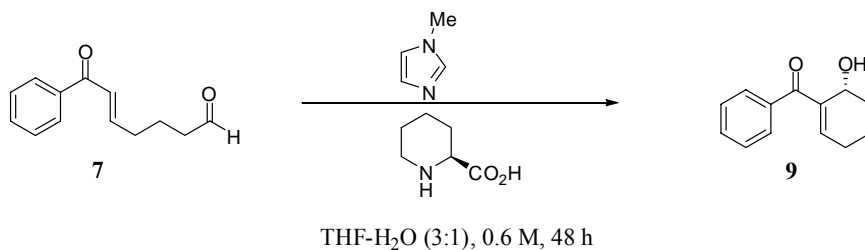
In the continued optimization of reaction parameters, a critical discovery was the impact of optimal catalyst loading under protic conditions (THF-H₂O, 3:1), which both accelerated the reaction rate and increased enantioselectivity. As illustrated in Figure 1.16, a dramatic distinction between the two co-catalytic systems was revealed in both CDCl₃ and under protic conditions with increased loading of the co-catalyst to 20 mol %. Importantly, the combination of pipecolinic acid and NMI now proved to be an excellent co-catalytic system in the cyclization of **7** to **9**, leading to 80% enantiomeric excess with 100% conversion. Proline, on the other hand, in combination with NMI, was an inferior catalyst, providing only 23% ee with the formation of multiple by-products.

Figure 1.16: Comparison of proline and pipercolinic acid in CDCl_3 and $\text{THF-H}_2\text{O}$.



This dramatic improvement in stereoselection and reactivity was demonstrated more extensively using the co-catalytic system pipercolinic acid/NMI. As shown in Table 1.4 (entry 1), low conversion was observed (45%) when the Morita-Baylis-Hillman reaction was carried out at 0.6 M with NMI/pipercolinic acid, 10 mol % each, while good enantioselectivity was maintained (64% ee). However, a stark change was observed when the cyclization was run under the same reaction conditions with increased co-catalyst loading (NMI/pipercolinic acid, 20 mol % each, entry 2). Within the same time frame, the reaction underwent full conversion to product **9** with increased enantioselectivity (76% ee).

Table 1.4: Effect of catalyst loading and stoichiometry.



entry	NMI (mol %)	pipecolinic acid (mol %)	% ee
1 ^a	10	10	64
2	20	20	76
3	10	20	80
4	10	30	76
5	10	40	75
6	20	10	50
7	30	10	30

^a 45% conv

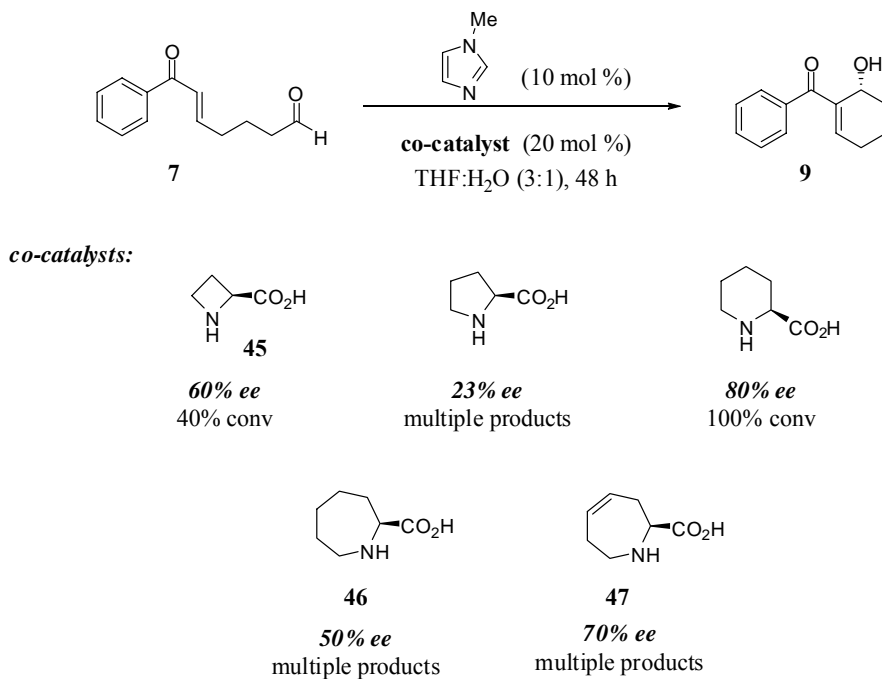
Furthermore, a subtle change in catalyst loading displayed another modest boost in enantioselectivity; NMI (10 mol %)/pipecolinic acid (20 mol %) led to 80% ee with full conversion (entry 3). No significant improvement occurred by increasing the ratio further from 2:1 pipecolinic acid/NMI to 3:1 (76% ee) and 4:1 (75% ee) (entries 4 and 5). Importantly, pipecolinic acid was required in equal or greater quantity than NMI for a productive reaction (1:1 or greater, pipecolinic acid/NMI). When the cyclization was performed with greater equivalents of NMI than pipecolinic acid, lower enantioselectivity was observed. For example, 1:2 pipecolinic acid/NMI produced 50% ee (entry 6) and 1:3 pipecolinic acid/NMI led to 30% enantiomeric excess. Additionally, these reactions were less chemoselective, leading to the formation of by-products. Excess NMI in the reaction

was found to catalyze an unselective reaction, exemplified in the decreased enantioselectivity. This will be discussed further in our mechanistic studies.

1.4.7 Extension of Proline Surrogates: Ring Size

Having demonstrated the dramatic difference between proline and its six-membered ring derivative as co-catalysts in the MBH reaction, we sought to explore this further by looking at various ring contraction or ring expansion derivatives. For example, catalysis with the four-membered ring azetidine derivative (**45**) provided moderate enantioselectivity (60% ee) with low conversion (40%) (Figure 1.17). The seven-membered ring azepines, both saturated (**46**) and unsaturated (**47**), were also inferior to pipercolinic acid, providing product **9** as a complex mixture in 50% ee and 70% ee, respectively. Pipercolinic acid proved to be unique and unequivocally outperformed any of the other co-catalysts in both its efficiency for the transformation of **7** to **9** and its ability to induce high stereoselectivity in combination with NMI.

Figure 1.17: Investigation of pipercolinic acid derivatives of varying ring size.



As illustrated in Scheme 1.13, the seven-membered ring pipercolinic acid derivatives, **46** and **47**, were synthesized from the methyl ester (**48**) of (*S*)-*C*-allylglycine. Mono-alkylation of the primary amine was achieved by protection of the primary amine as *o*-nitrobenzenesulfonamide (nosyl-amide) as described by Fukuyama and co-workers (82% yield),³⁹ followed by Mitsunobu⁴⁰ *N*-alkylation via treatment with diethylazodicarboxylate and triphenylphosphine (DEAD-PPh₃) and homoallyl alcohol to provide **50** in 95% yield. Compound **50** was then subjected to ring-closing metathesis⁴¹ (RCM) conditions using Grubbs' second-generation catalyst (92% yield) and subsequent deprotection of the Ns group by treatment with thiophenol to produce secondary amine

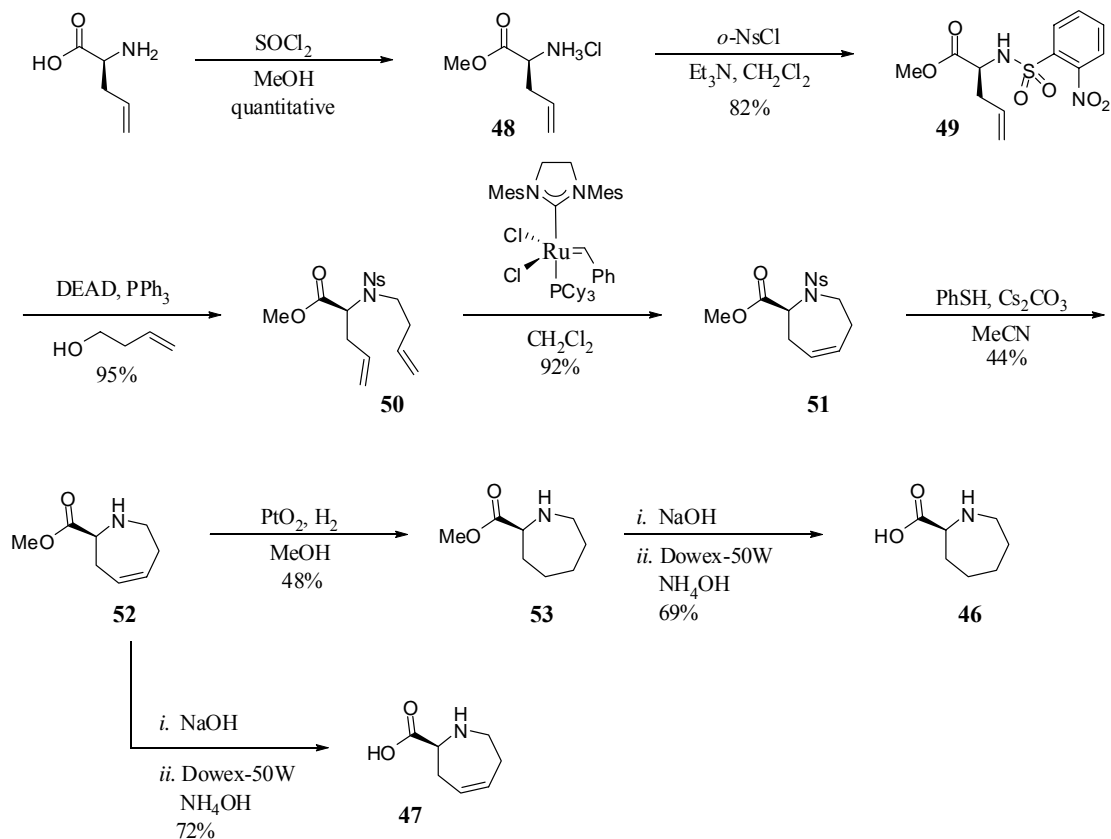
³⁹ (a) Kan, T.; Fukuyama, T. *Chem. Commun.* **2004**, 353-359. (b) Fukuyama, T.; Jow, C.-K.; Cheung, M. *Tetrahedron Lett.* **1995**, *36*, 6373-6374.

⁴⁰ Mitsunobu, O. *Synthesis* **1981**, 1-28.

⁴¹ Miller, S. J.; Blackwell, H. E.; Grubbs, R. H. *J. Am. Chem. Soc.* **1996**, *118*, 9606-9614.

52 (44% yield). Hydrogenation of **52** using Adam's catalyst (PtO_2) followed by hydrolysis and filtration through an acidic ion-exchange resin generated the saturated seven-membered ring pipecolic acid derivative, **46**. Alternatively, direct hydrolysis of compound **52** and conversion to the zwitterion generated unsaturated analog **47**.

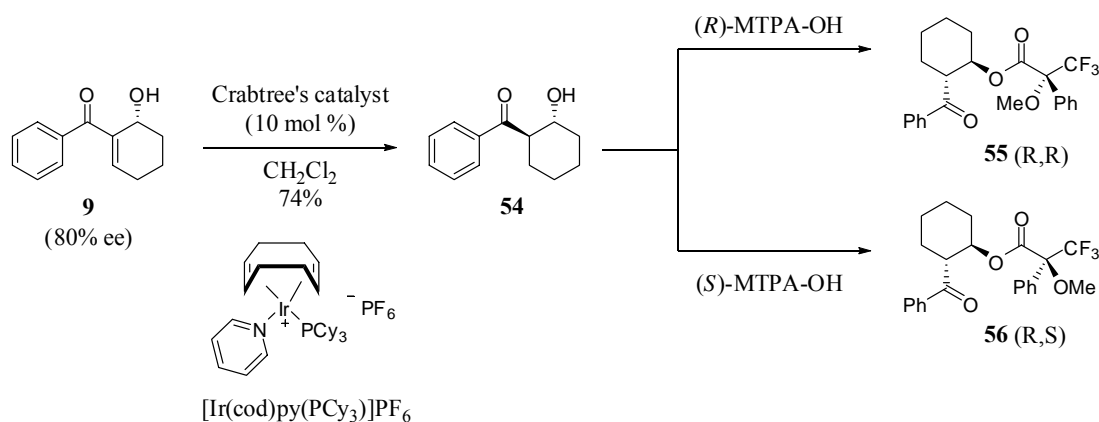
Scheme 1.13: Synthesis of proline derivatives **46** and **47**.



1.4.8 Determination of Absolute Stereochemistry

The method of Mosher analysis⁴² was used in order to determine the absolute stereochemistry of the cyclization products from the intramolecular MBH reaction. As illustrated in Scheme 1.14, optically enriched product **9** (80% ee) was first diastereoselectively hydrogenated using Crabtree's catalyst ($[\text{Ir}(\text{cod})\text{py}(\text{PCy}_3)]\text{PF}_6$)⁴³ to provide compound **54**, which served as the substrate for Mosher analysis. Both the (*R*)- and (*S*)-methoxy trifluoromethylphenyl acetate (MTPA) esters of **54** were prepared (**55** and **56**) and subjected to ¹H NMR analysis.

Scheme 1.14: Mosher analysis of intramolecular MBH product **9**.

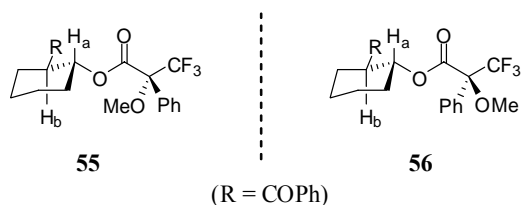


The different chemical shifts of resonances corresponding to diagnostic proton H_b from both diastereomers, **55** and **56**, were then compared (Figure 1.18). Due to the anisotropic magnetic shielding induced from the phenyl ring, H_b was shifted upfield in compound **56** compared to the shift seen in compound **55**, determining the products to be optically enriched with the (*R*) configuration.

⁴² (a) Dale, J. A.; Dull, D. L.; Mosher, H. S. *J. Org. Chem.* **1969**, *34*, 2543-2549. (b) Dale, J. A.; Mosher, H. S. *J. Am. Chem. Soc.* **1973**, *95*, 512-519. (c) Ward, D. E.; Rhee, C. K. *Tetrahedron Lett.*, **1991**, *32*, 7165-7166. (d) Ohtani, I.; Kusumi, T.; Kashman, Y.; Kakisawa, H. *J. Org. Chem.* **1991**, *56*, 1296-1298.

⁴³ Crabtree, R. H.; Davis, M. W. *J. Org. Chem.* **1986**, *51*, 2655.

Figure 1.18: Comparison of H_b in Mosher esters **55** and **56**.

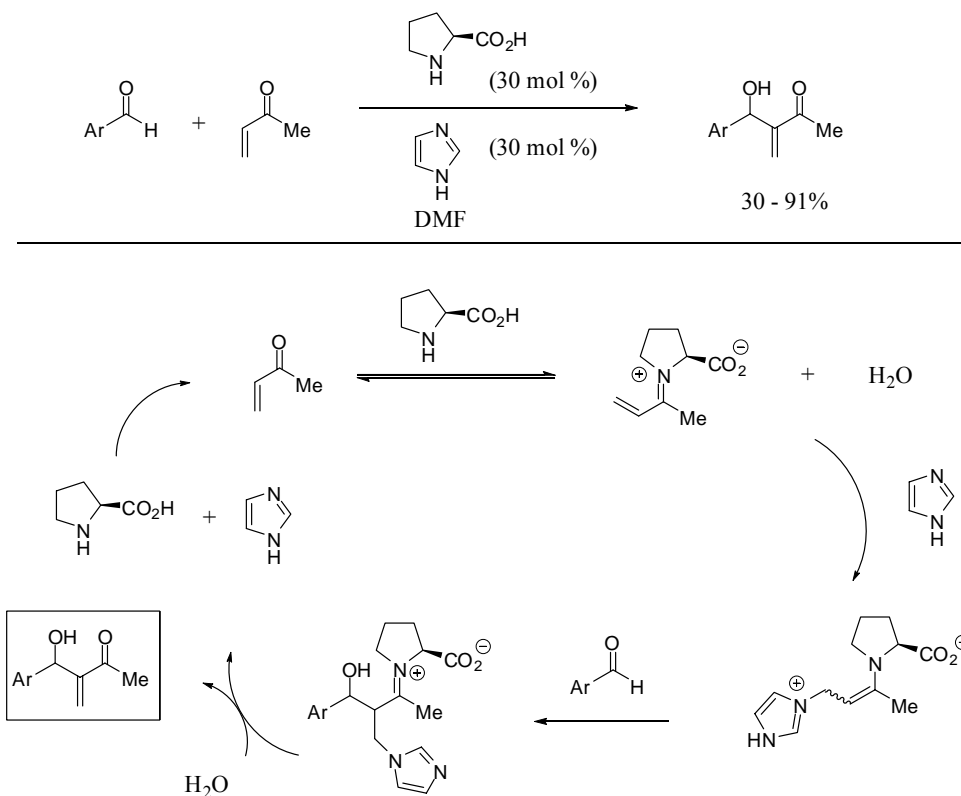


1.4.9 Mechanism

The exact mechanism of the MBH reaction has been elusive and is of debate in the current literature.¹⁹ Although there is a generally accepted mechanism of the reaction, involving conjugate addition followed by aldol reaction and β -elimination, it appears to vary with each system and has been difficult to generalize. Shi and co-workers⁴⁴ reported an intermolecular version of the MBH reaction catalyzed by imidazole in the presence of proline as a co-catalyst (30 mol % each), affording yields from 30% to 90% for various activated aldehydes. The proposed mechanism involved generation of an iminium species from activation of methyl vinyl ketone (MVK) by proline, followed by the accepted MBH catalytic cycle (Figure 1.19).

⁴⁴ Shi, M.; Jiang, J. K.; Li, C. Q. *Tetrahedron Lett.* **2002**, *43*, 127-130.

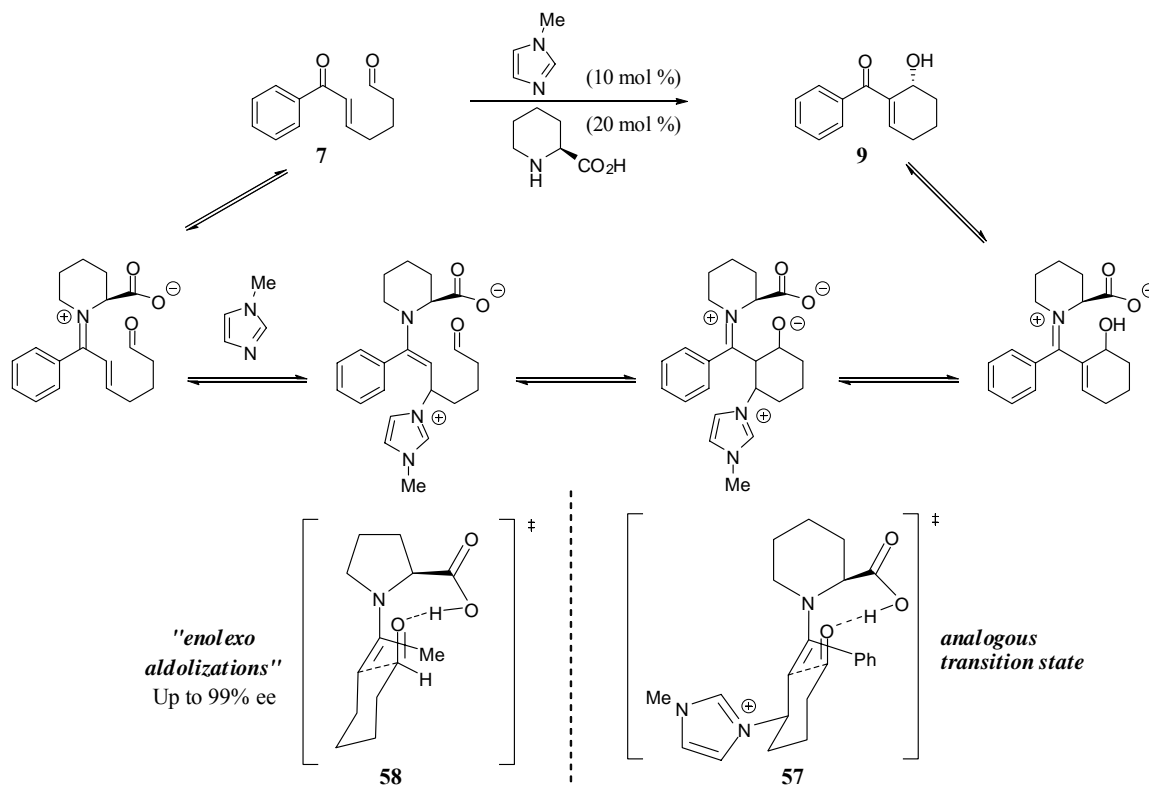
Figure 1.19: Mechanism of the intermolecular MVK-MBH reaction proposed by Shi and co-workers.



Herein, we suggest two possible mechanisms for the enantioselective intramolecular MBH reaction of enone-aldehyde **7** to **9**, as just described, under the co-catalytic system of pipecolinic acid/NMI. Mechanism A, in analogy to that reported by Shi and co-workers, would involve activation of the enone by pipecolinic acid to form an iminium species (Figure 1.20). This intermediate would then undergo nucleophilic attack by *N*-methylimidazole followed by enamine cyclization, proton shift and elimination of the catalyst, and finally hydrolysis to generate the desired product. An analogous transition state structure can be drawn, **57**, that closely compares to that presented by List and co-workers, **58**, in the highly enantioselective proline catalyzed

enolexo aldolizations where they achieved up to 99% ee.⁴⁵ This analysis of the mechanism would be supportive of the formation of an iminium species followed by enamine cyclization.

Figure 1.20: Potential mechanism A.

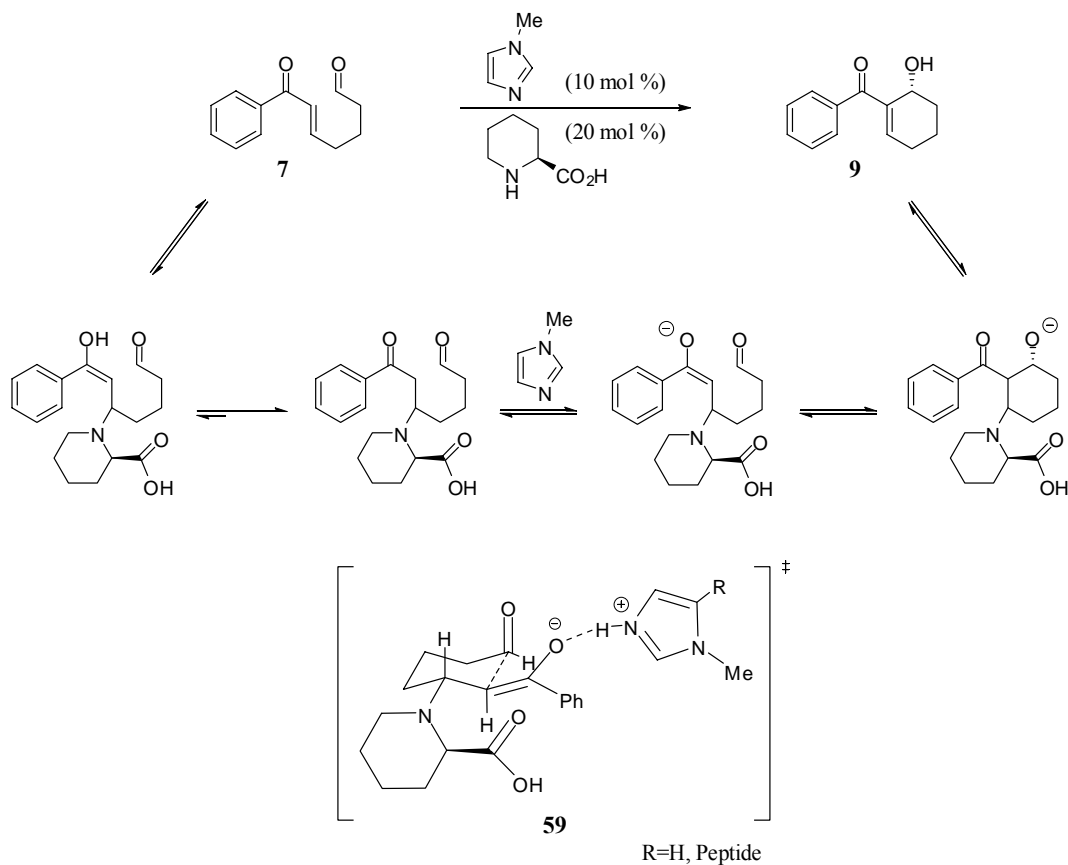


Alternatively, mechanism B may be operative in the enantioselective cyclization reaction where enone-aldehyde **7** would first undergo direct nucleophilic conjugate addition of pipercolinic acid, followed by attack of the ensuing enolate on the internal aldehyde. *N*-methylimidazole in this case would act as a base to maintain the enolate during the reaction (Figure 1.21). As described previously, the chiral space around NMI does not drive the stereoselectivity of the reaction, as could be reasoned by model B and

⁴⁵ (a) Pidathala, C.; Hoang, L.; Vignola, N.; List, B. *Angew. Chem. Int. Ed.* **2003**, *42*, 2785-2788. (b) Bahmanyar, S.; Houk, K. N. *J. Am. Chem. Soc.* **2001**, *123*, 12911-12912.

transition state **59**; the R group (where R = H or peptide) would not necessarily affect the formation of the stereogenic center, and could be inconsequential or deleterious to enantioselectivity.

Figure 1.21: Potential mechanism B.



Furthermore, studies by Stork and co-workers⁴⁶ suggest that mechanism A may not be operative for this specific catalytic system. Their study showed that the rate of formation of enamines,⁴⁷ in addition to the efficiency of alkylation of the formed enamines, was greater with pyrrolidine than with piperidine. Since the basicity and steric environment of the secondary amino group as well as the nature of the carbonyl were

⁴⁶ Stork, G. A.; Landesman, B. H.; Szmuszkovicz, J.; Terrell, R. *J. Am. Chem. Soc.* **1963**, 85, 207-222.

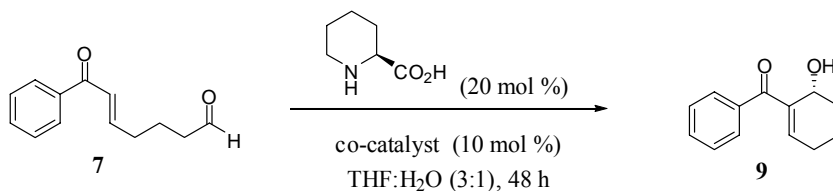
⁴⁷ Brown, H. C. *J. Chem. Soc.* **1956**, 1248-1268.

similar, this difference was attributed to the greater ease of formation of a trigonal carbon in a five-membered ring than in a six-membered ring. With the understanding that enamine formation/alkylation is not as facile with piperidine, it would suggest that transition structure **57** may not actually resemble **58** with regard to reactivity.

Although we have not performed an extensive study of the reaction mechanism, we have begun an initial investigation to clarify the role of NMI in the cyclization of **7** to **9**, in the hopes of eventually deciphering the true mechanism. Therefore, pipercolinic acid was held constant, while other possible Lewis bases/co-catalysts were screened. As illustrated in Table 1.5, catalysis of the cyclization with pipercolinic acid and 2,6-lutidine (entry 1) led to no reaction. This could support either mechanism, as it is possible that lutidine was too hindered to act as a nucleophile or too weak to be a general base. Catalysis with pipercolinic acid and 1,4-diazabicyclo[2.2.2]octane (DABCO) (entry 3), on the other hand, provided full conversion to the desired cyclic product, however with dramatically reduced enantioselectivity. In this case, it is possible that DABCO reacted faster as the nucleophilic catalyst than pipercolinic acid, and therefore catalyzed a non-selective MBH cyclization, represented in the diminished enantioselectivity, supporting the second mechanism. Additionally, triethylamine, 1,2,2,6,6-pentamethyl piperidine (PEMP), and Hünig's base were examined in combination with pipercolinic acid. All three co-catalysts provided the desired product in slightly depressed enantioselectivity (approximately 70% ee), with varying levels of efficiency that appeared to reflect the steric hindrance of the base. Triethyl amine and Hünig's base led to similar results, 60% (entry 4) and 55% conversion (entry 6), while low conversion was achieved with PEMP

(35%, entry 5). The slight depression of stereoselectivity could be ascribed to “leakage” in catalysis where triethyl amine or Hünig’s base served as the nucleophile, whereby out-competing pipercolinic acid and catalyzing a non-selective MBH cyclization.

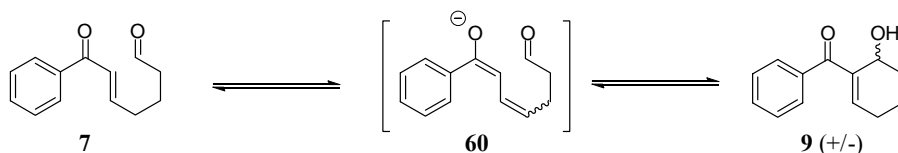
Table 1.5: Screen of co-catalyst combinations.



entry	co-catalyst	% conv	% ee
1		0	-
2		100	80
3		100	19
4		60	68
5		35	71
6		55	70

In the case of PEMP, it is not believed that this severely hindered tertiary amine could act as a nucleophile. In this case, a third possible mechanism may account for the

10% decrease in enantioselectivity; γ -deprotonation would lead to intermediate **60** which, in turn, could undergo cyclization and olefin isomerization to provide **9** (+/-).



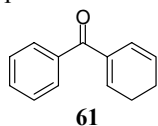
Considering the presented data, it is possible that the mechanism may indeed change with each co-catalytic system, such that catalysis with proline/NMI may proceed by mechanism A, while pipercolinic acid/NMI through mechanism B. A kinetics study and isotopic-labeling experiments would be required in future studies to determine the rate determining step and lend further credence to one of the aforementioned mechanisms, or possibly a new mechanism.

1.4.10 Substrate Scope

With a set of optimized reaction parameters in hand for the intramolecular MBH reaction, we were interested in exploring the scope of our newly developed methodology. Ultimately, using the co-catalytic system of pipercolinic acid/NMI (20 mol %/10 mol %) under protic conditions (THF-H₂O, 3:1), we were able to catalyze the cyclization of several activated aromatic enones with good enantioselectivities and yields. As illustrated in Figure 1.22, product **9** could be isolated with 80% ee in 82% yield after extractive work up, and in 51% yield after silica gel chromatography. Although the MBH products were not stable to various purification methods (which led to

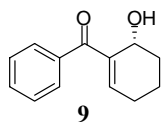
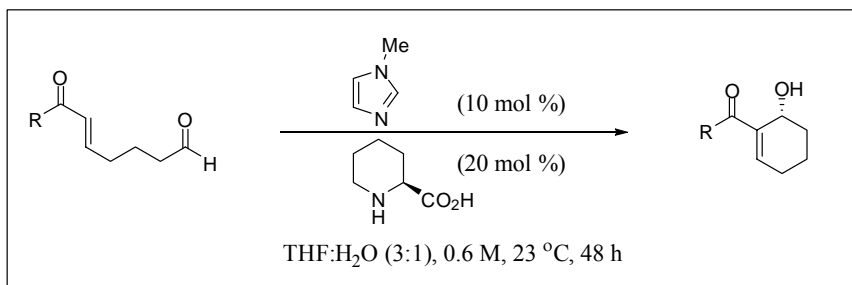
corresponding diene **61** as a result of dehydration),⁴⁸ it was determined that the purity of the cyclized products was very high (>90%)⁴⁹ prior to chromatography. Lowering the reaction temperature had a nominal effect on enantioselectivity, providing 50% conversion to **9** at 4 °C with a slight increase in enantioselectivity to 84% ee. Preliminary investigation of scope showed that substitution around the aromatic ring was moderately tolerated, providing both *p*-Br-substituted **62** and *p*-Cl-substituted **63** with 79% ee in 88% yield and 92% yield, respectively. A marked decrease in selectivity was seen in the case of *ortho*-substitution; MBH product **64** was obtained with 51% ee, although high yield was maintained (94% yield). Heteroaromatic substitution was tolerated as well, with the MBH reaction providing thiophene analog **65** in 83% yield and with 74% ee.³

⁴⁸ The products were not stable to silica gel chromatography as well as several other methods of purification such as fluorosil, neutral alumina, and basic alumina, all leading to the dehydrated product, **61**.

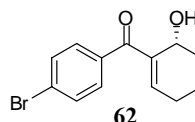


⁴⁹ As determined by TLC and ¹H NMR analysis.

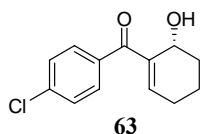
Figure 1.22: Substrate scope in the pipercolinic acid/NMI catalyzed MBH reaction.



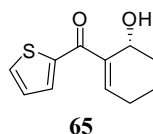
82% (51%), **80% ee**
4 °C: 50% conv, **84% ee**



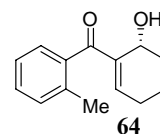
88% (68%)
79% ee



92% (56%)
79% ee



83% (50%)
74% ee



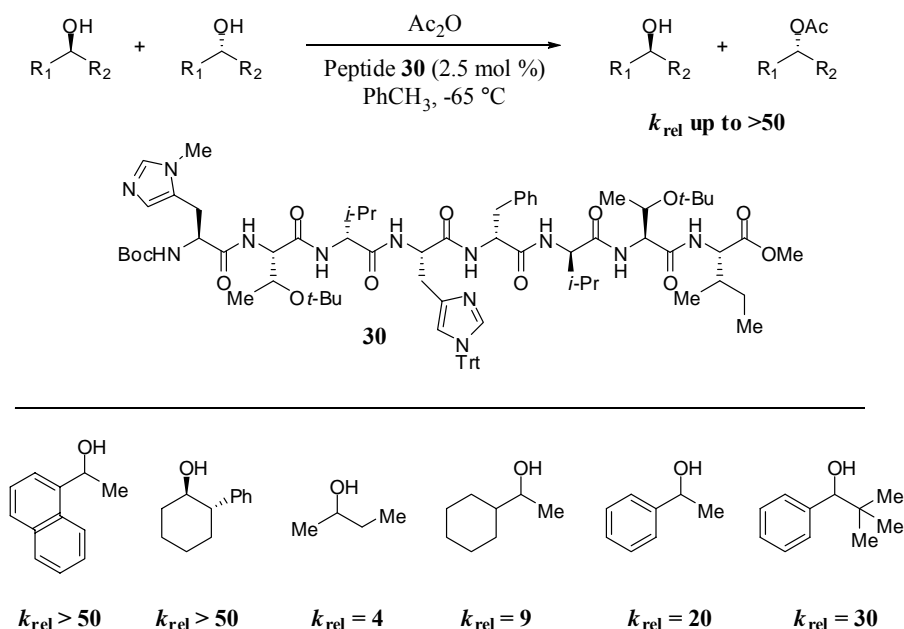
94% (46%)
51% ee

yield after extraction (after silica gel chromatography)

1.5 Enhancement of Enantioselectivity: Kinetic Resolution

As mentioned earlier, previous work from the Miller laboratory had uncovered a class of octapeptide catalysts that was highly effective for the kinetic resolution of secondary alcohols (Figure 1.23).²² Because the products from the intramolecular MBH reaction were indeed secondary alcohols, and possible substrates for asymmetric acylation, we were eager to determine if we could couple these two processes and effectively enhance the enantioselectivity of our MBH reaction.

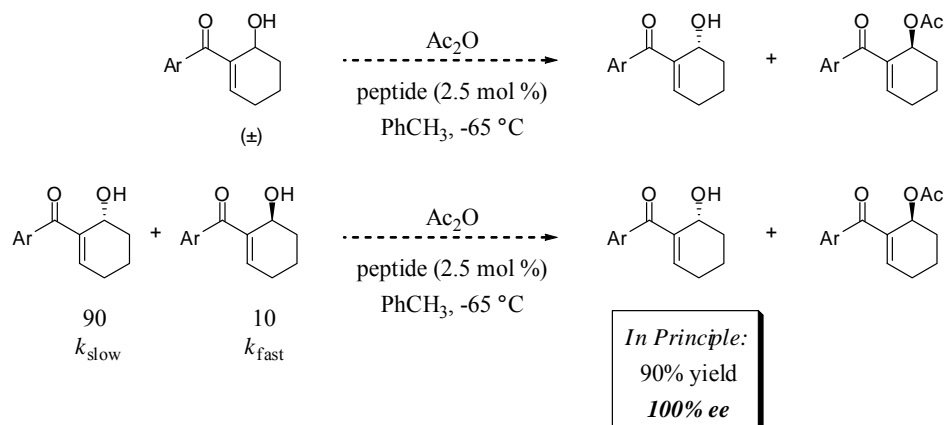
Figure 1.23: Kinetic resolution of secondary alcohols catalyzed by peptide **30**.



A variety of secondary alcohols had been demonstrated to undergo enantioselective acylation using peptide **30** with moderate to excellent levels of selectivity ($k_{rel} = 4$ to >50).⁵⁰ The first question we had to answer was whether the products of the MBH reaction could be viable substrates for a similar kinetic resolution (Scheme 1.15). Secondly, if we were able to efficiently catalyze the enantioselective acylation of racemic products, the analogous kinetic resolution with enantioenriched products from the MBH reaction could, in theory, provide enantiopure products in high yield. For example, if the rate of acylation of the major enantiomer was slow while acylation of the minor enantiomer was fast, we could hypothetically obtain 90% yield and 100% ee of the desired product when beginning with 80% enantiopure material.

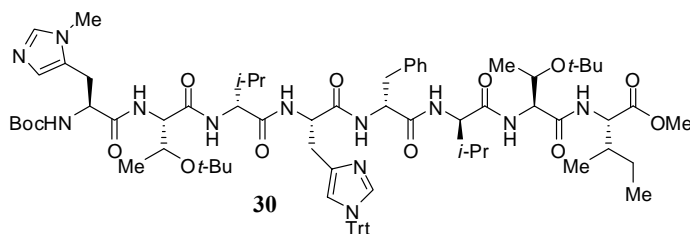
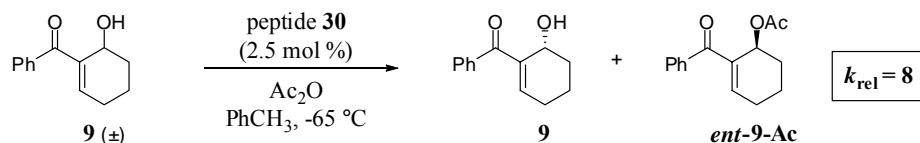
⁵⁰ $k_{rel} = k_{fast}/k_{slow}$

Scheme 1.15: Theoretical kinetic resolution of MBH products.



Accordingly, initial examination of the kinetic resolution of MBH product **9** was promising; the racemic alcohol could be resolved with a k_{rel} of 8 using acylation catalyst peptide **30** (Scheme 1.16). It was further demonstrated that the application of peptide **30** to various MBH adducts afforded the desired products with up to 95% ee in moderate yields (<50%).³¹

Scheme 1.16: Enantioselective acylation of racemic MBH product **9**.



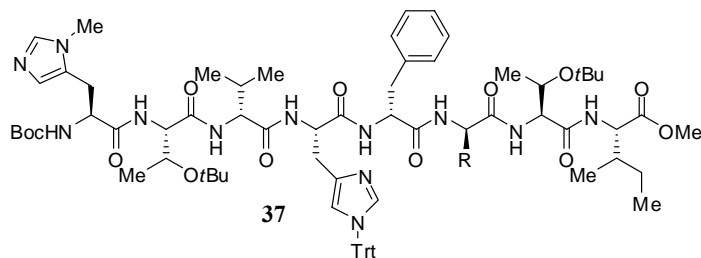
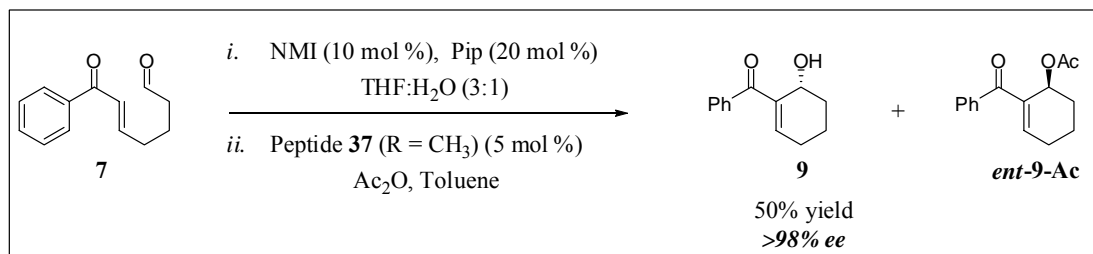
As previously discussed, we were once again interested in the possibility of obtaining a boost in enantioselectivity by way of an alanine scan of peptide **30**. After

testing peptides **33–39** for their efficiency in the kinetic resolution of MBH product **9** (80% ee), it was determined that alanine scan peptide **37** was superior. Peptide **30** afforded **9** with 92% ee while peptide **37** afforded **9** with greater than 98% ee (under identical reaction conditions).

Once we had determined that the MBH products were viable substrates for asymmetric acylation using a peptide catalyst, and that peptide **37** was a highly efficient catalyst for this process, we were interested in pursuing a one-pot tandem sequence of the enantioselective MBH followed by an asymmetric acylation. Excitingly, this was accomplished via quench of the MBH reaction mixture with acetic anhydride and the addition of peptide-based asymmetric acylation catalyst **37**.⁵¹ We found the initial MBH reaction could be carried out using pipercolinic acid/NMI (presumably affording product **9** with 80% ee), which was then followed by the addition of acetic anhydride with peptide **37**, providing the desired product with >98% enantiomeric excess and in 50% isolated yield (after silica gel chromatography). Thus we were able to effect an asymmetric MBH reaction coupled to a kinetic resolution of the nonracemic reaction mixture (Scheme 1.17).

⁵¹ Jarvo, E. R.; Miller, S. J. Asymmetric Acylation. In *Comprehensive Asymmetric Catalysis, Supplement 1*; Jacobsen, E. N., Pfaltz, A., Yamamoto, H., Eds.; Springer-Verlag: Berlin Heidelberg, 2004; Chapter 43.

Scheme 1.17: Tandem one-pot MBH-kinetic resolution.



1.6 Conclusion

The Morita-Baylis-Hillman reaction holds great promise of becoming a highly useful reaction. Both the *inter*- and *intramolecular* variants have traditionally suffered from problems with reactivity and chemoselectivity, in addition to low stereoselectivity. However, with each successful advance in the reaction, it is possible that one day this reaction will be highly predictable and programmable. Multiple parameters of the intramolecular MBH reaction were investigated and found to be crucial to reaction outcome (catalyst, co-catalyst, solvent, reaction concentration, and catalyst/co-catalyst loading and stoichiometry) and the fine-tuning of these parameters led to a set of optimized conditions that were amenable to the catalysis of several activated aromatic enone-aldehydes. Moreover, building from previous work accomplished in our laboratory, we have been able to extend our peptide-catalyzed processes to include the most simplified variant, enantioselective catalysis using a single amino acid. By coupling

the enantioselective MBH reaction with a secondary kinetic resolution, we were able to successfully combine the simple catalytic system with a peptide-based catalyst to afford enantiopure products.

Moving forward, we are excited to extend the reaction scope to include a more expansive range of substrates as well as increase the enantioselectivity of the reaction even further. Additionally, further investigation into the mechanism, through a kinetics study and isotopic labeling experiments, could shed light on the mechanism and enable the development of a superior catalytic system. Importantly, our work has established that the enantioselective intramolecular MBH reaction *can* be performed rapidly and catalytically with high levels of stereinduction in synthetically useful yields using a simple co-catalyst system and reaction conditions.

1.7 Experimental

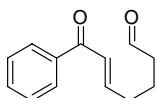
General Procedures. Proton NMR spectra were recorded on a Varian 400 MHz spectrometer. Proton chemical shifts are reported in ppm (δ) relative to internal tetramethylsilane (TMS, δ 0.0 ppm) or with the solvent reference relative to TMS employed as the internal standard (CDCl_3 , δ 7.26 ppm; d_6 -DMSO, δ 2.50 ppm; CD_3OD , δ 3.31 ppm; D_2O , δ 4.79 ppm). Data are reported as follows: chemical shift (multiplicity [singlet (s), doublet (d), triplet (t), quartet (q), and multiplet (m)], coupling constants [Hz], integration). Carbon NMR spectra were recorded on a Varian 400 (100 MHz) spectrometer with complete proton decoupling. Carbon chemical shifts are reported in ppm (δ) relative to TMS with the respective solvent resonance as the internal standard (CDCl_3 , δ 77.0 ppm). Infrared spectra were obtained on a Perkin-Elmer Spectrum 1000 spectrometer. Analytical thin-layer chromatography (TLC) was performed using Silica Gel 60 Å F254 precoated plates (0.25 mm thickness). TLC R_f values are reported. Visualization was accomplished by irradiation with a UV lamp and/or staining with KMnO_4 or cerium ammonium molybdenate (CAM) solutions. Flash column chromatography was performed using Silica Gel 60A (32-63 μm).⁵² Optical rotations were recorded on a Rudolf Research Analytical Autopol IV Automatic polarimeter at the sodium D line (path length 50 mm). High resolution mass spectra were obtained at the Mass Spectrometry Facility of either Boston College (Chestnut Hill, MA) or the University of Illinois (Urbana-Champaign, IL). The method of ionization is given in parentheses.

⁵² Still, W.C.; Kahn, M.; Mitra, J. *J. Org. Chem.* **1978**, *43*, 2923.

Analytical normal phase HPLC was performed on a Hewlett-Packard 1100 Series chromatograph equipped with a diode array detector (214 nm and 254 nm). All reactions were carried out under an argon or nitrogen atmosphere employing oven- and flame-dried glassware. All solvents were distilled from appropriate drying agents prior to use. *N*-methyl imidazole and acetic anhydride were distilled and stored in a Schlenk flask for no more than two weeks prior to use. Intramolecular Baylis-Hillman substrate **7** was prepared as reported previously in the literature⁵³ as well as by the general procedure described.

Experimental Procedures

Representative procedure for the preparation of intramolecular Morita-Baylis-Hillman substrates (7, 63b, 62b, 64b and 65b).



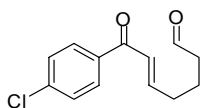
(E)-7-oxo-7-phenylhept-5-enal (7). 2-(triphenylphosphanylidene)acetophenone⁵⁴ (9.1 g, 24 mmol) was added to a solution of 5,5-dimethoxypentanal⁵⁵ (2.5 g, 17 mmol) in CH₂Cl₂ (43 mL). After stirring for 24 h at ambient temperature, the reaction was

⁵³ (a) Montgomery, J; Savchenko, A. V.; Zhao, Y. *J. Org. Chem.* **1995**, *60*, 5699-5701. (b) Richards, E. L.; Murphy, P. J.; Dinon, F.; Fratucello, S.; Brown, P. M.; Gelbrich, T.; Hursthouse, M. B. *Tetrahedron* **2001**, *57*, 7771-7784.

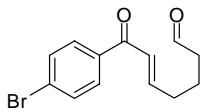
⁵⁴ (a) Ramirez, F.; Dershowitz, S. *J. Org. Chem.* **1957**, *22*, 41-45. (b) Denney, D. B.; Smith, L. C.; Song, J.; Rossi, C. J. *J. Org. Chem.* **1963**, *28*, 778-780.

⁵⁵ Schreiber, S. L.; Claus, R. E.; Reagan, J. *Tetrahedron Lett.* **1982**, *23*, 3867-3870.

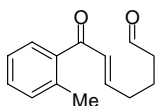
concentrated under reduced pressure and purified via silica gel chromatography (hexane-EtOAc, 5:1) to afford the (*E*) Wittig product. This material was then dissolved in THF (60 mL) and 1N HCl (20 mL) and stirred at 23 °C. After 2 h, THF was removed in vacuo from the yellow solution and the resultant residue was diluted with Et₂O (100 mL) and washed with water (50 mL), saturated aqueous NaHCO₃ (50 ml), and saturated aqueous NaCl (50 mL). The aqueous layers were extracted with ether (2 x 50 mL) and the combined organic layers were then dried over Na₂SO₄ and concentrated under reduced pressure. Flash chromatography (toluene-EtOAc, 5:1) provided **7** as a pale yellow oil (960 mg, 4.7 mmol, 28%). Compound **7**, prepared in this manner, is identical to that prepared previously.⁵³ Compounds **63b**, **62b**, **64b** and **65b** were prepared by analogous methodology.



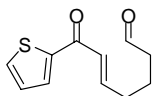
Compound 63b. ¹H NMR (CDCl₃, 400 MHz) δ 9.83 (s, 1H), 7.92 (d, *J* = 8.8 Hz, 2H), 7.49 (d, *J* = 8.8 Hz, 2H), 7.08 (m, 1H), 6.92 (d, *J* = 15.6 Hz, 1H), 2.58 (t, *J* = 7.2 Hz, 2H), 2.42 (q, *J* = 7.2 Hz, 2H), 1.92 (quintet, *J* = 7.6 Hz, 2H); ¹³C NMR (CDCl₃, 100 MHz) δ 201.6, 189.3, 148.7, 139.3, 136.2, 130.1, 129.0, 126.2, 43.1, 32.0, 20.6; IR (film, cm⁻¹) 2942, 2823, 2722, 1727, 1671, 1621, 1583, 1401, 1293, 1224, 1092, 1016; TLC R_f 0.31 (3:1 toluene-EtOAc); HRMS (ESI) *m/z* 237.0693 (237.0682 calcd for C₁₃H₁₄O₂Cl [M+H]⁺).



Compound 62b. ^1H NMR (CDCl_3 , 400 MHz) δ 9.83 (s, 1H), 7.83 (d, $J = 8.8$ Hz, 2H), 7.64 (d, $J = 8.8$ Hz, 2H), 7.06 (dt, $J = 15.2, 6.8$ Hz, 1H), 6.89 (d, $J = 15.2$ Hz, 1H), 2.56 (dt, $J = 7.2$ Hz, 1.2 Hz, 2H), 2.40 (q, $J = 6.8$ Hz, 2H), 1.91 (quintet, $J = 7.2$ Hz, 2H); ^{13}C NMR (CDCl_3 , 100 MHz) δ 200.8, 188.7, 148.1, 136.0, 131.4, 129.6, 127.4, 125.6, 42.8, 31.7, 20.2; IR (film, cm^{-1}) 2949, 2886, 2829, 2722, 1721, 1671, 1620, 1583, 1400, 1073, 1010; TLC R_f 0.36 (3:1 toluene-EtOAc); HRMS (ESI) m/z 281.0188 (281.0177 calcd for $\text{C}_{13}\text{H}_{14}\text{O}_2\text{Br}$ $[\text{M}+\text{H}]^+$).

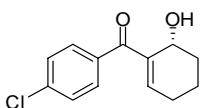


Compound 64b. ^1H NMR (CDCl_3 , 400 MHz) δ 9.80 (s, 1H), 7.42-7.35 (m, 2H), 7.30-7.24 (m, 2H), 6.71 (dt, $J = 15.6, 6.8$ Hz, 1H), 6.53 (d, $J = 16.0$ Hz, 1H), 2.55-2.53 (dt, $J = 7.2, 1.2$ Hz, 2H), 2.42 (bs, 3H), 2.34 (q, $J = 7.2$ Hz, 2H), 1.85 (quintet, $J = 7.6$ Hz, 2H); ^{13}C NMR (CDCl_3 , 100 MHz) δ 201.1, 196.1, 149.2, 138.5, 136.6, 131.0, 130.2, 127.8, 125.1, 43.0, 31.8, 20.4, 20.2; IR (film, cm^{-1}) 2930, 2829, 2728, 1728, 1652, 1627; TLC R_f 0.53 (3:1 toluene-EtOAc); HRMS (ESI) m/z 217.1238 (217.1229 calcd for $\text{C}_{14}\text{H}_{17}\text{O}_2$ $[\text{M}+\text{H}]^+$).



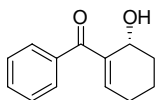
Compound 65b. ^1H NMR (CDCl_3 , 400 MHz) δ 9.82 (s, 1H), 7.77 (dd, $J = 3.6, 0.8$ Hz, 1H), 7.66 (dd, $J = 4.8, 0.8$ Hz, 1H), 7.16 (dd, $J = 4.8, 4.0$ Hz, 1H), 7.07 (dt, $J = 15.2, 7.2$ Hz, 1H), 6.83 (d, $J = 15.2$ Hz, 1H), 2.53 (dt, $J = 7.2, 1.2$ Hz, 2H), 2.37 (q, $J = 6.8$ Hz, 2H), 1.88 (quintet, $J = 7.2$ Hz, 2H); ^{13}C NMR (CDCl_3 , 100 MHz) δ 201.2, 181.7, 146.9, 144.7, 133.6, 131.7, 128.0, 126.0, 43.0, 31.7, 20.5; IR (film, cm^{-1}) 3094, 2936, 2829, 2722, 1728, 1659, 1614, 1520, 1420; TLC R_f 0.46 (3:1 toluene-EtOAc); HRMS (ESI) m/z 209.0634 (209.0636 calcd for $\text{C}_{11}\text{H}_{13}\text{O}_2\text{S}$ $[\text{M}+\text{H}]^+$).

Representative procedure for the catalytic intramolecular Morita-Baylis-Hillman reactions.



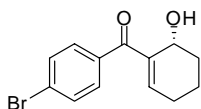
Compound 63. Pipecolinic acid (14.2 mg, 0.11 mmol), water (233 μL), THF (659 μL), and NMI (1.37 M solution in THF, 41 μL) were added sequentially to a vessel containing aldehyde **63b** (132 mg, 0.56 mmol). The reaction was allowed to stir at room temperature for 48 h, whereupon the yellow solution was added to 30 mL of EtOAc and washed with saturated aqueous NH_4Cl (20 mL), saturated aqueous NaHCO_3 (20 mL), and

saturated aqueous NaCl (20 mL). The organic layer was dried over Na₂SO₄, filtered, and concentrated under reduced pressure to afford **63** as a pale yellow oil (121 mg, 92%). The product isolated in this manner appears as a single compound with slight impurities manifested by low intensity peaks in the baseline of the ¹H NMR spectrum (see figure A). This material may be purified further by silica gel chromatography using a gradient eluent (toluene-ethyl acetate 10:1 to 1:10) affording **63** (74 mg) as a clear oil in 56% isolated yield. ¹H NMR (CDCl₃, 400 MHz) δ 7.62 (d, *J* = 8.4 Hz, 2H), 7.42 (d, *J* = 8.8 Hz, 2H), 6.70 (t, *J* = 4.4 Hz, 1H), 4.73 (br s, 1H), 3.38 (s, 1H), 2.39-2.27 (m, 2H), 1.97-1.85 (m, 3H), 1.68-1.64 (m, 1H); ¹³C NMR (CDCl₃, 100 MHz) δ 197.6, 146.7, 139.9, 138.2, 135.9, 130.6, 128.4, 63.9, 29.9, 26.5, 17.5; IR (film, cm⁻¹) 3440, 2936, 2867, 1646, 1583; TLC R_f 0.37 (3:1 toluene-EtOAc); [α]_D +18 (*c* 1.0, CHCl₃, 79% ee); HRMS (ESI) *m/z* 259.0503 (259.0502 calcd for C₁₃H₁₃O₂ClNa [M+Na]⁺); Assay of enantiomeric purity: Enantiomers of product were separated by chiral HPLC employing a Chiralcel OJ column (Daicel). Conditions: 98:2 hexanes-ethanol; Flow rate 0.60 mL/min; 28.3 min (major ent), 32.7 min (minor ent).



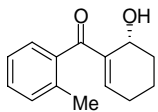
2-benzoyl-1-hydroxycyclohex-2-ene (9). The characterization data for this compound matched that which has previously been reported.⁵³ [α]_D +30 (*c* 1.0, CHCl₃, 80% ee); Assay of enantiomeric purity: Enantiomers of product were separated by chiral HPLC

employing a Chiralcel OD column (Daicel). Conditions: 98:2 hexanes-ethanol; Flow rate 0.75 mL/min; 18.8 min (major ent), 22.2 min (minor ent). The absolute stereochemistry was assigned by Mosher analysis.⁵⁶

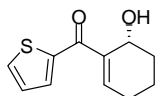


Compound 62. ¹H NMR (CDCl₃, 400 MHz) δ 7.59 (d, *J* = 8.8 Hz, 2H), 7.53 (d, *J* = 8.8 Hz, 2H), 6.70 (t, *J* = 4.4 Hz, 1H), 4.73 (br s, 1H), 3.38 (s, 1H), 2.39-2.22 (m, 2H), 1.96-1.83 (m, 3H), 1.69-1.62 (m, 1H); ¹³C NMR (CDCl₃, 100 MHz) δ 197.7, 146.8, 139.9, 136.4, 131.4, 130.7, 126.8, 63.9, 29.8, 26.5, 17.5; IR (film, cm⁻¹) 3414, 2936, 2867, 1634; TLC R_f 0.36 (3:1 toluene-EtOAc); [α]_D +15.4 (*c* 1.0, CHCl₃, 79% ee); HRMS (ESI) *m/z* 302.9996 (302.9997 calcd for C₁₃H₁₃O₂BrNa [M+Na]⁺); Assay of enantiomeric purity: Enantiomers of product were separated by chiral HPLC employing a Chiralcel OJ column (Daicel). Conditions: 98:2 hexanes-ethanol; Flow rate 0.60 mL/min; 30.8 min (major ent), 35.4 min (minor ent).

⁵⁶ (a) Dale, J. A.; Dull, D. L.; Mosher, H. S *J. Org. Chem.* **1969**, *34*, 2543-2549. (b) Dale, J. A.; Mosher, H. S. *J. Am. Chem. Soc.* **1973**, *95*, 512-519. (c) Ward, D. E.; Rhee, C. K. *Tetrahedron Lett.* **1991**, *32*, 7165-7166. (d) Ohtani, I.; Kusumi, T.; Kashman, Y.; Kakisawa, H. *J. Org. Chem.* **1991**, *56*, 1296-1298.



Compound 64. ^1H NMR (CDCl_3 , 400 MHz) δ 7.32 (m, 1H), 7.21 (m, 3H), 6.65 (t, J = 4.0 Hz, 1H), 4.78 (br s, 1H), 3.52 (br s, 1H), 2.30 (s, 3H), 2.34-2.15 (m, 2H), 1.93-1.78 (m, 3H), 1.66-1.58 (m, 1H); ^{13}C NMR (CDCl_3 , 100 MHz) δ 201.3, 148.8, 141.4, 138.2, 135.8, 130.6, 129.6, 127.6, 124.9, 63.5, 29.9, 26.7, 19.7, 17.8; IR (film, cm^{-1}) 3478, 2943, 2867, 1633; TLC R_f 0.38 (3:1 toluene-EtOAc); $[\alpha]_D +4.2$ (c 1.0, CHCl_3 , 51% ee); HRMS (ESI) m/z 239.1045 (239.1048 calcd for $\text{C}_{14}\text{H}_{16}\text{O}_2\text{Na}$ $[\text{M}+\text{Na}]^+$); Assay of enantiomeric purity: Enantiomers of product were separated by chiral HPLC employing a Chiralcel OD column (Daicel). Conditions: 98:2 hexanes-ethanol; Flow rate 0.75 mL/min; 14.2 min (major ent), 27.6 min (minor ent).

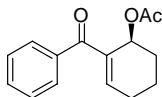


Compound 65. ^1H NMR (CDCl_3 , 400 MHz) δ 7.66 (dd, J = 4.8 Hz, 1.1 Hz, 1H), 7.62 (dd, J = 4.0 Hz, 1.1 Hz, 1H), 7.12 (m, 1H), 6.95 (m, 1H), 4.68 (br s, 1H), 3.46 (br s, 1H), 2.42-2.35 (m, 1H), 2.32-2.23 (m, 1H), 1.96-1.81 (m, 3H), 1.70-1.65 (m, 1H); ^{13}C NMR (CDCl_3 , 100 MHz) δ 189.8, 143.2, 142.6, 139.9, 133.4, 133.3, 127.6, 64.1, 29.9, 26.2, 17.4; IR (film, cm^{-1}) 3440, 2936, 2867, 1621; TLC R_f 0.32 (3:1 toluene-EtOAc); $[\alpha]_D +37$ (c 1.0, CHCl_3 , 74% ee); HRMS (ESI) m/z 231.0459 (231.0456 calcd for $\text{C}_{11}\text{H}_{12}\text{O}_2\text{NaS}$ $[\text{M}+\text{Na}]^+$); Assay of enantiomeric purity: Enantiomers of product were

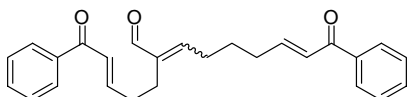
separated by chiral HPLC employing a Chiralcel OD column (Daicel). Conditions: 95:5 hexanes-ethanol; Flow rate 0.60 mL/min; 25.7 min (major ent), 23.2 min (minor ent).

**Procedure for the tandem enantioselective intramolecular MBH reaction-
asymmetric acylation reaction**

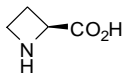
Pipecolinic acid (2.6 mg, 0.02 mmol), water (41 μ L), THF (94 μ L), and NMI (30 μ L of a 0.33 M solution in THF) were added sequentially to a vessel containing aldehyde **7** (20 mg, 0.1 mmol). The reaction was stirred at room temperature for 48 hours, whereupon the yellow solution was concentrated, transferred to a round bottom flask, and azeotroped with toluene (5 x 10 mL). The residue was then dissolved in toluene (16.8 mL) and peptide **30** (7 mg, 0.005 mmol) and acetic anhydride (37.4 μ L, 0.4 mmol) were added. The solution was maintained at 23 °C for 24 h and then quenched with methanol (2 mL). After concentration under reduced pressure, the residue was dissolved in EtOAc (30 mL), washed with saturated aqueous NH_4Cl (20 mL), saturated aqueous NaHCO_3 (20 mL), and saturated aqueous NaCl (20 mL), and dried (Na_2SO_4). Purification via silica gel chromatography (toluene-ethyl acetate, 7:1) afforded **9** (9.9 mg, 50% yield, >98% ee) as a clear oil.



Compound *ent*-9-Ac. ^1H NMR (CDCl_3 , 400 MHz) δ 7.70 (d, $J = 7.0$ Hz, 2H), 7.53 (t, $J = 7.3$ Hz, 1H), 7.43 (t, $J = 7.3$ Hz, 2H), 6.72 (m, 1H), 5.99 (m, 1H), 2.46-2.39 (m, 1H), 2.24-2.15 (m, 1H), 2.05-1.98 (overlapping s and m, 4H), 1.86-1.70 (m, 3H); ^{13}C NMR (CDCl_3 , 100 MHz) δ 195.3, 169.8, 146.0, 137.8, 136.7, 131.7, 129.0, 127.9, 65.0, 28.0, 25.8, 21.3, 17.3; IR (film, cm^{-1}) 2942, 2867, 1733, 1652; TLC R_f 0.51 (2:1 hexanes-EtOAc); HRMS (ESI) m/z 267.0988 (267.0997 calcd for $\text{C}_{15}\text{H}_{16}\text{O}_3\text{Na}$ $[\text{M}+\text{Na}]^+$); Assay of enantiomeric purity: Enantiomers of product were separated by chiral HPLC employing a Chiralcel OD column (Daicel). Conditions: 98:2 hexanes-ethanol; Flow rate 0.75 mL/min; 15.3 min (major *ent*), 16.6 min (minor *ent*).



Aldol dimerization by-product (40). ^1H NMR (CDCl_3 , 400 MHz) δ 9.42 (s, 1H), 7.92 (t, $J = 7.6$ Hz, 4H), 7.58-7.52 (m, 2H), 7.49-7.43 (m, 4H), 7.08-6.84 (m, 4H), 6.54 (t, $J = 7.6$ Hz, 1H), 2.51-2.34 (m, 8H), 1.75 (quintet, $J = 7.6$ Hz, 2H); ^{13}C NMR (CDCl_3 , 100 MHz) δ 194.3, 190.2, 154.4, 147.8, 147.6, 142.2, 137.6, 132.6, 128.4, 126.4, 32.4, 31.5, 28.7, 27.3, 23.2; IR (film, cm^{-1}) 3056, 2936, 2861, 2722, 1671, 1647, 1620, 1596, 1451, 1287, 1224; TLC R_f 0.59 (3:1 toluene-EtOAc); HRMS (ESI) m/z 387.1943 (387.1960 calcd for $\text{C}_{26}\text{H}_{27}\text{O}_3$ $[\text{M}+\text{H}]^+$).

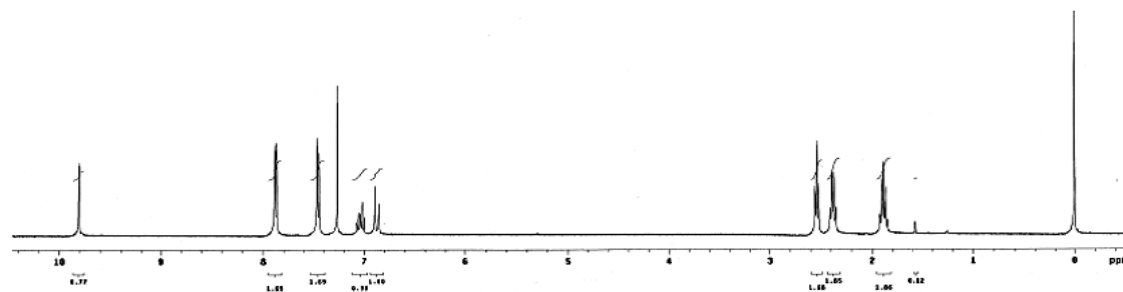
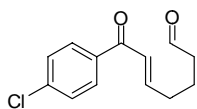


Compound 45. Boc-L-azetidine-2-carboxylic acid (440 mg, 2.20 mmol) was added to a solution of 10% H₂SO₄ (10 mL) and dioxane (10 mL). The solution was allowed to stir for 12 h and then concentrated under reduced pressure. The resulting residue was dissolved in aqueous H₂SO₄ (0.25 N, 10 mL) and DOWEX 50-2-200 cation exchange resin (2.0 g) was added.⁵⁷ This mixture was allowed to stir for 12 h, then transferred to a column and washed with water (100 mL). The desired product was then eluted with 5% NH₄OH (200 mL) and concentrated under reduced pressure to afford **1** as a white solid. The characterization data for this compound matched that which has previously been reported. ¹H NMR (CDCl₃, 400 MHz) δ 4.64 (dd, *J* = 7.6 Hz, 9.6 Hz, 1H), 4.05-3.98 (m, 1H), 3.90-3.85 (m, 1H), 2.80-2.71 (m, 1H), 2.57-2.47 (m, 1H); ¹³C NMR (CDCl₃, 100 MHz) δ 174.2, 60.7, 43.9, 25.1.

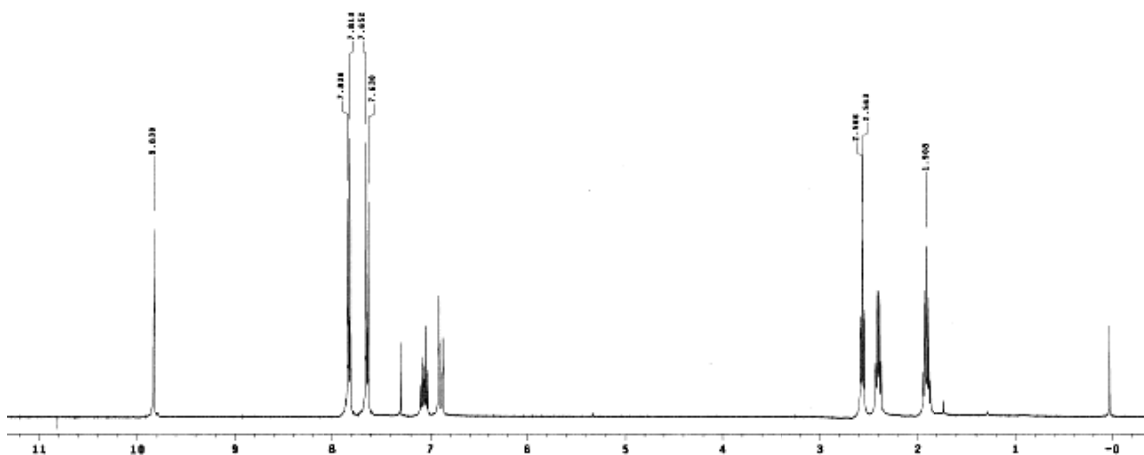
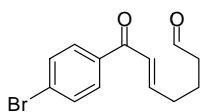
⁵⁷ Kazlauskas, R. J. *J. Org. Chem.* **1994**, *59*, 2075-2078.

1.7.1 NMR Spectra and HPLC Data

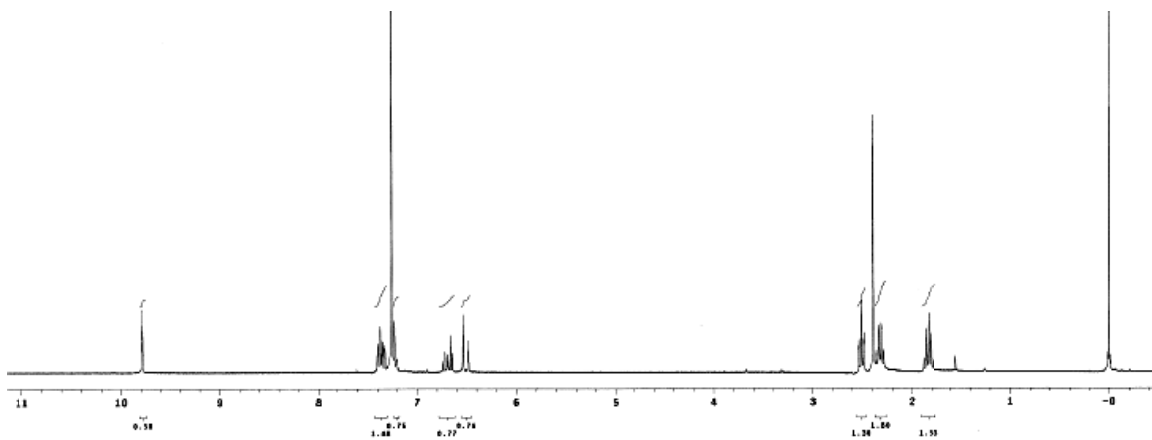
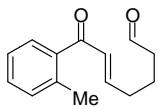
Compound 63b.



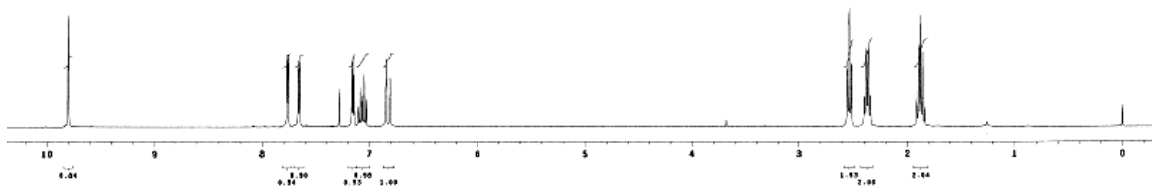
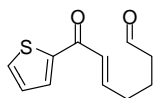
Compound 62b.



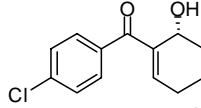
Compound 64b.



Compound 65b.



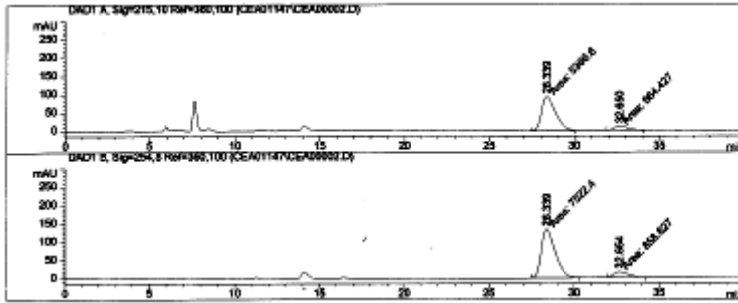
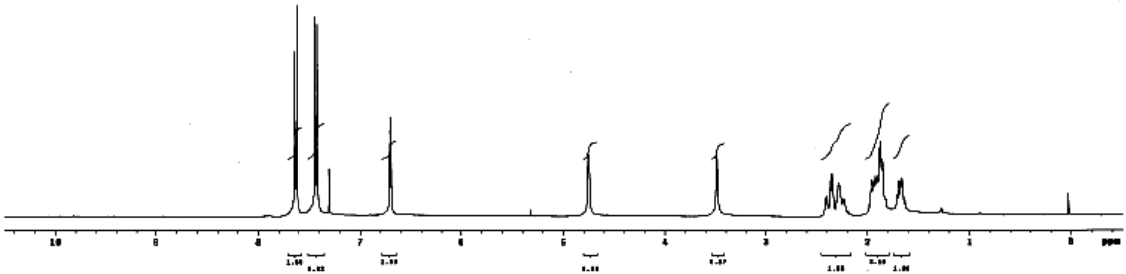
Compound 63.



```

C000001
NAME: 63
EXP: 01001
DATE: 01/13/00
TIME: 14:00
INSTR: 400
PROG: 1
P1: 10.00
P2: 10.00
P3: 10.00
P4: 10.00
P5: 10.00
P6: 10.00
P7: 10.00
P8: 10.00
P9: 10.00
P10: 10.00
P11: 10.00
P12: 10.00
P13: 10.00
P14: 10.00
P15: 10.00
P16: 10.00
P17: 10.00
P18: 10.00
P19: 10.00
P20: 10.00
P21: 10.00
P22: 10.00
P23: 10.00
P24: 10.00
P25: 10.00
P26: 10.00
P27: 10.00
P28: 10.00
P29: 10.00
P30: 10.00
P31: 10.00
P32: 10.00
P33: 10.00
P34: 10.00
P35: 10.00
P36: 10.00
P37: 10.00
P38: 10.00
P39: 10.00
P40: 10.00
P41: 10.00
P42: 10.00
P43: 10.00
P44: 10.00
P45: 10.00
P46: 10.00
P47: 10.00
P48: 10.00
P49: 10.00
P50: 10.00
P51: 10.00
P52: 10.00
P53: 10.00
P54: 10.00
P55: 10.00
P56: 10.00
P57: 10.00
P58: 10.00
P59: 10.00
P60: 10.00
P61: 10.00
P62: 10.00
P63: 10.00
P64: 10.00
P65: 10.00
P66: 10.00
P67: 10.00
P68: 10.00
P69: 10.00
P70: 10.00
P71: 10.00
P72: 10.00
P73: 10.00
P74: 10.00
P75: 10.00
P76: 10.00
P77: 10.00
P78: 10.00
P79: 10.00
P80: 10.00
P81: 10.00
P82: 10.00
P83: 10.00
P84: 10.00
P85: 10.00
P86: 10.00
P87: 10.00
P88: 10.00
P89: 10.00
P90: 10.00
P91: 10.00
P92: 10.00
P93: 10.00
P94: 10.00
P95: 10.00
P96: 10.00
P97: 10.00
P98: 10.00
P99: 10.00
P100: 10.00

```



Signal 1: DAD1 A, Sig=215,10 Ref=360,100

Peak #	RetTime [min]	Type	Width [min]	Area [mAU*s]	Height [mAU]	Area %
1	28.339	PK	0.9551	5366.59717	93.64401	90.4835
2	32.650	PK	0.9106	564.42731	10.33063	9.5165

Totals : 5931.02448 103.97464

Results obtained with enhanced integrator!

Signal 2: DAD1 B, Sig=254,8 Ref=360,100

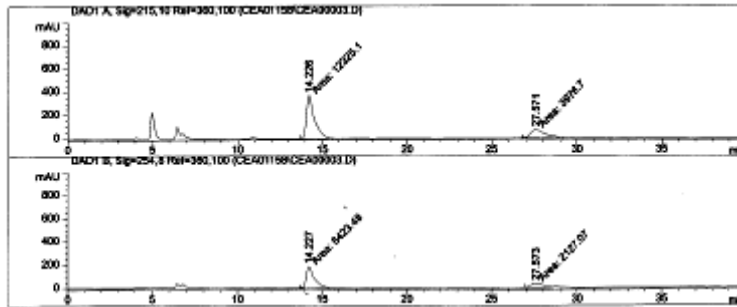
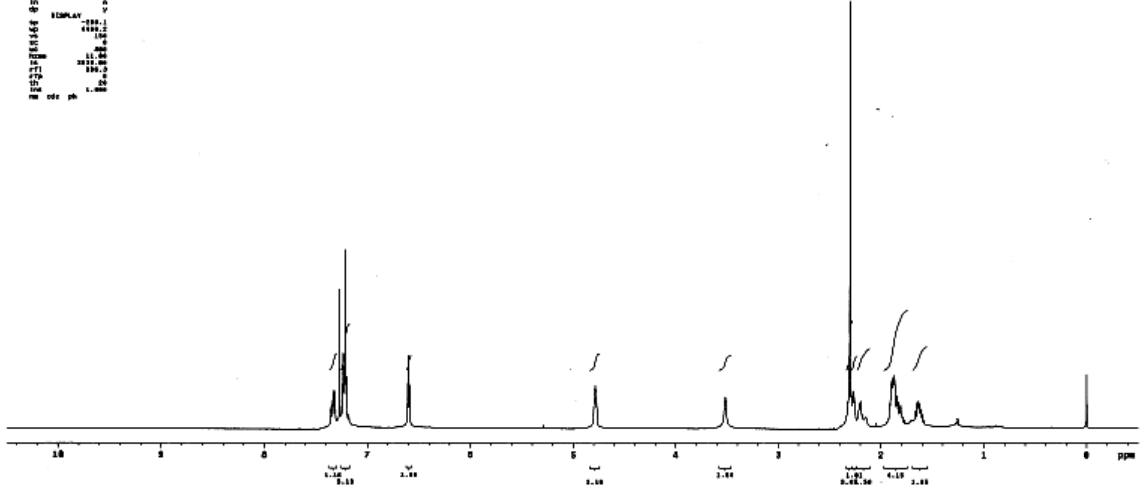
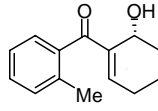
Peak #	RetTime [min]	Type	Width [min]	Area [mAU*s]	Height [mAU]	Area %
1	28.339	PK	0.9440	7522.39697	132.80659	89.7551
2	32.654	PK	0.9459	858.62701	15.12957	10.2449

Compound 64.

```

NAME: 64
EXPNO: 1
PROCNO: 1
PROCAMT: 1
PROCBS: 1
PROBHD: 5mm QNP 1H/13
PROBHD2:
PROBHD3:
PULPROG: zgpg30
PCPDPRG2:
PCPDPRG3:
TD: 65536
SOLVENT: DMSO
AQ: 0.10000000
RG: 327.50000000
RG2: 327.50000000
RG3: 327.50000000
AQ2: 0.10000000
AQ3: 0.10000000
F2: 125.76000000
F3: 125.76000000
F4: 125.76000000
WDW: EM
SSB: 0
LB: 3.00000000
GB: 0
PC: 1
GC: 0
MC: 0
MD: 0
ME: 0
MPC: 0
MPR: 0
DQ: 0
RDECOR: 0
WALTZ16: 0
GAMMA: 0
GAMMA2: 0
GAMMA3: 0
TE: 300.2
DELTA: 0
DELTA2: 0
DELTA3: 0
TD0: 1
TD1: 1
TD2: 1
TD3: 1
NUC1: 13C
NUC2: 13C
NUC3: 13C
NUC4: 13C
NUC5: 13C
NUC6: 13C
NUC7: 13C
NUC8: 13C
NUC9: 13C
NUC10: 13C
NUC11: 13C
NUC12: 13C
NUC13: 13C
NUC14: 13C
NUC15: 13C
NUC16: 13C
NUC17: 13C
NUC18: 13C
NUC19: 13C
NUC20: 13C
NUC21: 13C
NUC22: 13C
NUC23: 13C
NUC24: 13C
NUC25: 13C
NUC26: 13C
NUC27: 13C
NUC28: 13C
NUC29: 13C
NUC30: 13C
NUC31: 13C
NUC32: 13C
NUC33: 13C
NUC34: 13C
NUC35: 13C
NUC36: 13C
NUC37: 13C
NUC38: 13C
NUC39: 13C
NUC40: 13C
NUC41: 13C
NUC42: 13C
NUC43: 13C
NUC44: 13C
NUC45: 13C
NUC46: 13C
NUC47: 13C
NUC48: 13C
NUC49: 13C
NUC50: 13C
NUC51: 13C
NUC52: 13C
NUC53: 13C
NUC54: 13C
NUC55: 13C
NUC56: 13C
NUC57: 13C
NUC58: 13C
NUC59: 13C
NUC60: 13C
NUC61: 13C
NUC62: 13C
NUC63: 13C
NUC64: 13C
NUC65: 13C
NUC66: 13C
NUC67: 13C
NUC68: 13C
NUC69: 13C
NUC70: 13C
NUC71: 13C
NUC72: 13C
NUC73: 13C
NUC74: 13C
NUC75: 13C
NUC76: 13C
NUC77: 13C
NUC78: 13C
NUC79: 13C
NUC80: 13C
NUC81: 13C
NUC82: 13C
NUC83: 13C
NUC84: 13C
NUC85: 13C
NUC86: 13C
NUC87: 13C
NUC88: 13C
NUC89: 13C
NUC90: 13C
NUC91: 13C
NUC92: 13C
NUC93: 13C
NUC94: 13C
NUC95: 13C
NUC96: 13C
NUC97: 13C
NUC98: 13C
NUC99: 13C
NUC100: 13C

```



Signal 1: DAD1 A, Sig=215,10 Ref=360,100

Peak #	RetTime [min]	Type	Width [min]	Area [nAU*s]	Height [nAU]	Area %
1	14.226	HM	0.5523	1.23251e4	371.93393	75.6058
2	27.571	HM	0.9235	3976.69873	71.76760	24.3942

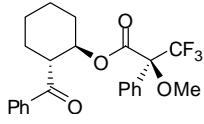
Totals : 1.63018e4 443.70153

Results obtained with enhanced integrator!

Signal 2: DAD1 B, Sig=254,8 Ref=360,100

Peak #	RetTime [min]	Type	Width [min]	Area [nAU*s]	Height [nAU]	Area %
1	14.227	HM	0.5698	6423.48047	187.90344	75.1236
2	27.573	HM	0.9629	2127.06934	36.81874	24.8764

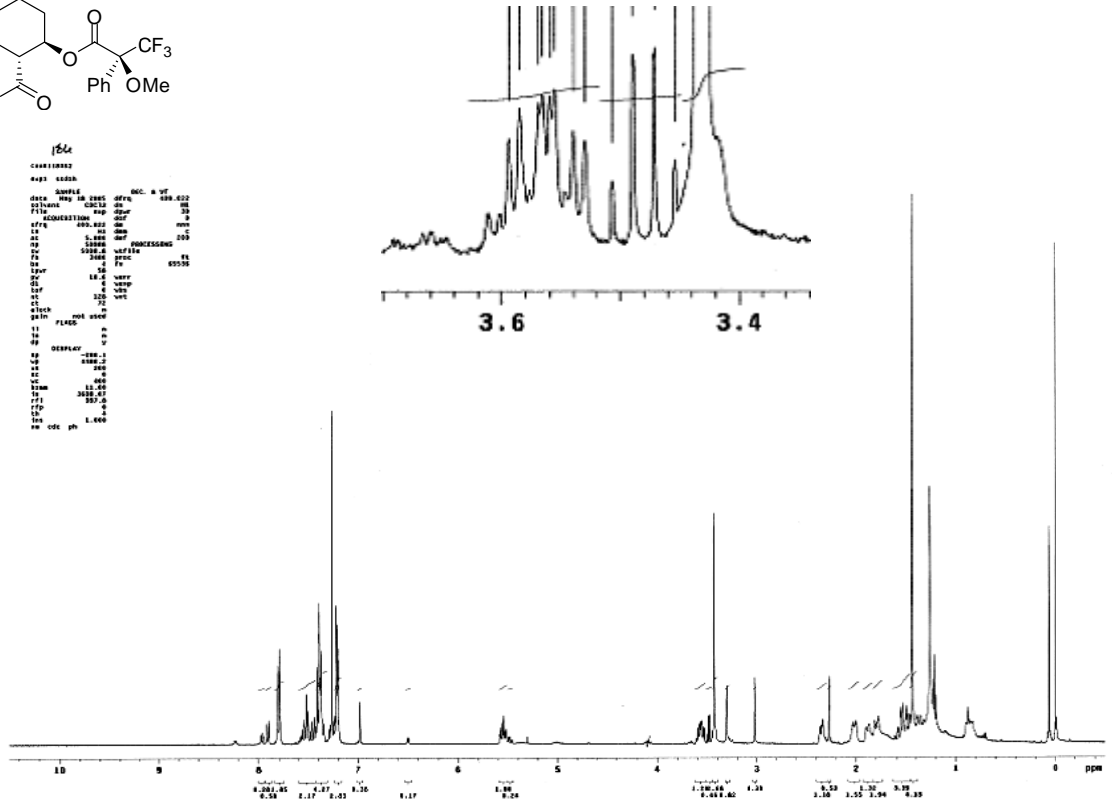
Compound 56.



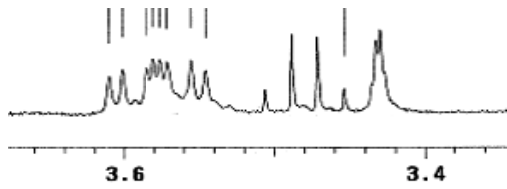
```

156x
=====
NAME          156x
EXPNO         1
PROCNO        1
PROCRES       1
DATE_         20080825
TIME          09.55
INSTRUM       spect
PROBHD        zgpg30
PULPROG       zgpg30
AQ            0.02000000
RG            327.50000000
SF            400.14640000
WDW            EM
SSB            GB
LB            3.00000000
GB            0.00000000
PC            1.00000000
DC            0.00000000
SC            0.00000000
RC            0.00000000
IC            0.00000000
EC            0.00000000
PC1           0.00000000
PC2           0.00000000
PC3           0.00000000
PC4           0.00000000
PC5           0.00000000
PC6           0.00000000
PC7           0.00000000
PC8           0.00000000
PC9           0.00000000
PC10          0.00000000
PC11          0.00000000
PC12          0.00000000
PC13          0.00000000
PC14          0.00000000
PC15          0.00000000
PC16          0.00000000
PC17          0.00000000
PC18          0.00000000
PC19          0.00000000
PC20          0.00000000
PC21          0.00000000
PC22          0.00000000
PC23          0.00000000
PC24          0.00000000
PC25          0.00000000
PC26          0.00000000
PC27          0.00000000
PC28          0.00000000
PC29          0.00000000
PC30          0.00000000
PC31          0.00000000
PC32          0.00000000
PC33          0.00000000
PC34          0.00000000
PC35          0.00000000
PC36          0.00000000
PC37          0.00000000
PC38          0.00000000
PC39          0.00000000
PC40          0.00000000
PC41          0.00000000
PC42          0.00000000
PC43          0.00000000
PC44          0.00000000
PC45          0.00000000
PC46          0.00000000
PC47          0.00000000
PC48          0.00000000
PC49          0.00000000
PC50          0.00000000
PC51          0.00000000
PC52          0.00000000
PC53          0.00000000
PC54          0.00000000
PC55          0.00000000
PC56          0.00000000
PC57          0.00000000
PC58          0.00000000
PC59          0.00000000
PC60          0.00000000
PC61          0.00000000
PC62          0.00000000
PC63          0.00000000
PC64          0.00000000
PC65          0.00000000
PC66          0.00000000
PC67          0.00000000
PC68          0.00000000
PC69          0.00000000
PC70          0.00000000
PC71          0.00000000
PC72          0.00000000
PC73          0.00000000
PC74          0.00000000
PC75          0.00000000
PC76          0.00000000
PC77          0.00000000
PC78          0.00000000
PC79          0.00000000
PC80          0.00000000
PC81          0.00000000
PC82          0.00000000
PC83          0.00000000
PC84          0.00000000
PC85          0.00000000
PC86          0.00000000
PC87          0.00000000
PC88          0.00000000
PC89          0.00000000
PC90          0.00000000
PC91          0.00000000
PC92          0.00000000
PC93          0.00000000
PC94          0.00000000
PC95          0.00000000
PC96          0.00000000
PC97          0.00000000
PC98          0.00000000
PC99          0.00000000
PC100         0.00000000
=====

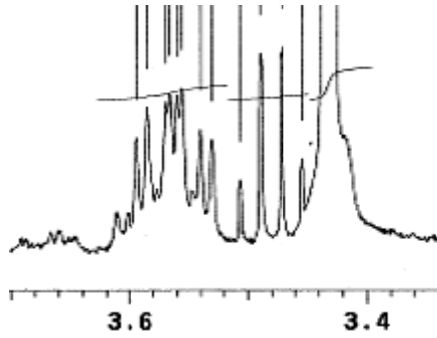
```



Compound 55.



Compound 56.



2 The Rauhut-Currier Reaction: A History and Its Synthetic Application

2.1 Introduction

Carbon–carbon bond formation is of fundamental importance in organic synthesis, with much attention directed towards controlling reaction efficiency, stereoselectivity, and chemoselectivity.⁵⁸ Among the many methods established for the formation of a new C–C bond, carbon-based nucleophilic conjugate addition reactions constitute a significant and synthetically useful method, with the ability to build rings, set multiple stereocenters, and engage a wide variety of substrates.⁵⁹ Furthermore, for almost half a century, the use of enones as latent enolates has provided a successful method for the regioselective alkylation of carbonyl compounds.⁶⁰

The Morita-Baylis-Hillman (MBH) and Rauhut-Currier (RC) reactions comprise a class of transformations that encompass the ability to generate a new C–C bond in an atom economical manner by combining the power of nucleophilic catalysis with the use of enones as latent enolates. While the MBH reaction involves the coupling of an activated alkene with an aldehyde, the Rauhut-Currier reaction involves the reaction of two activated alkenes, creating a new C–C bond between the α -position of one activated

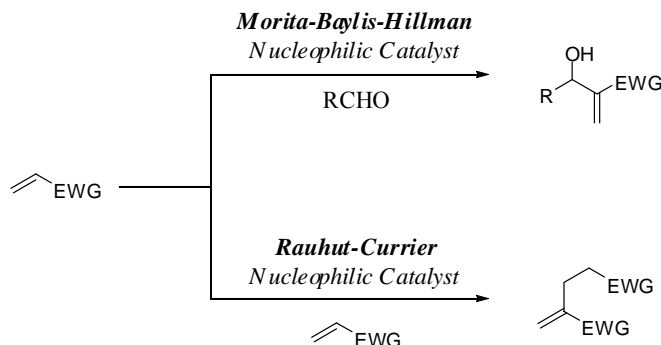
⁵⁸ (a) Dalko, P. I.; Moisan, L. *Angew. Chem., Int. Ed.* **2004**, *43*, 5138-5175. (b) Dalko, P. I.; Moisan, L. *Angew. Chem., Int. Ed.* **2001**, *40*, 3726-3748.

⁵⁹ For selected reviews, please see: (a) Almaši, D.; Alonso, D. A.; Nájera, C. *Tetrahedron: Asymmetry* **2007**, *18*, 299-365. (b) Vicario, J. L.; Badía, D.; Carrillo, L. *Synthesis* **2007**, *14*, 2065-2092. (c) Krause, N.; Hoffmann-Röder, A. *Synthesis* **2001**, *2*, 171-196. (d) Sibi, M. P.; Manyem, S. *Tetrahedron* **2000**, *56*, 8033-8061.

⁶⁰ Stork, G.; Rosen, P.; Goldman, N. L. *J. Am. Chem. Soc.* **1961**, *83*, 2965-2966.

alkene and the β -position of a second alkene under the influence of a nucleophilic catalyst (Figure 2.1).

Figure 2.1: Comparison of the MBH and RC reactions.



A vast array of literature has been established regarding the MBH reaction, reflecting its impact on organic synthesis by providing densely functionalized products with a new stereogenic center that serve as substrates for a multitude of subsequent transformations.⁶¹ The Rauhut-Currier reaction, on the other hand, has received much less attention due, in part, to low reactivity and great difficulty in controlling the selectivity of the cross-coupling reaction. While the development of the reaction has not been rapid, great advancement has been made in recent years, providing the synthetic community with new prospects for efficient C–C bond formation.⁶² Herein, the state-of-the-art of the Rauhut-Currier reaction will be presented, from its inception to the present day. Derivatives of this coupling reaction, such as alternative electrophilic and nucleophilic partners, will be discussed. Finally, its application in the synthesis of

⁶¹ For selected reviews, please see: (a) Drewes, S. E.; Roos, G. H. P. *Tetrahedron* **1988**, *44*, 4653-4670. (b) Basavaiah, D.; Rao, P. D.; Hyma, R, S. *Tetrahedron* **1996**, *52*, 8001-8062. (c) Basavaiah, D.; Rao, A. J.; Satyanarayana, T. *Chem. Rev.* **2003**, *103*, 811-891.

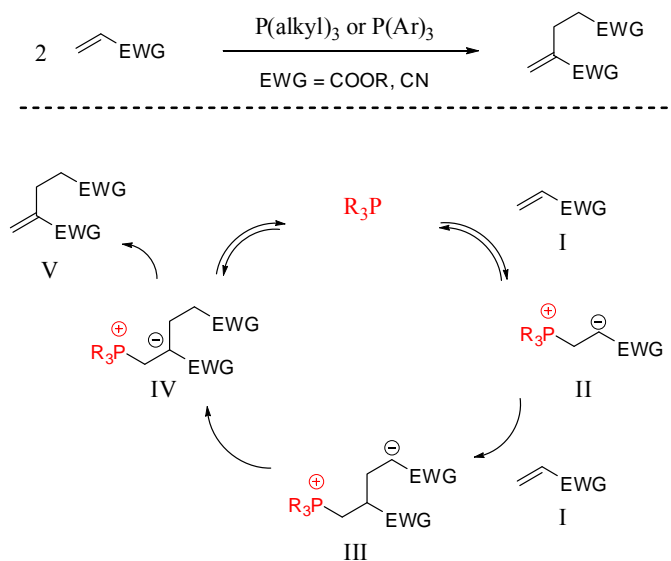
⁶² (a) Lee, K. Y.; Gowrisankar, S.; Kim, J. N. *Bull. Kor. Chem. Soc.* **2005**, *26*, 1481-1490. (b) Masson, G.; Housseman, C.; Zhu, J. *Angew. Chem., Int. Ed.* **2007**, *46*, 4614-4628.

representative natural products will be described, as this transformation has recently begun to impact complex molecule synthesis.

2.2 Overview of the Intermolecular Rauhut-Currier Reaction

In 1963, Rauhut and Currier⁶³ reported the phosphine-catalyzed dimerization of electron-deficient alkenes, acrylonitrile and ethyl acrylate, in what has become known as the Rauhut-Currier reaction (RC) (Figure 2.2). The transformation is believed to proceed via reversible conjugate addition of either trialkylphosphine or triarylphosphine to activated alkene **I** to generate zwitterionic species **II**. A Michael reaction of the enolate with a second equivalent of activated alkene **I** generates zwitterionic intermediate **III**, which then undergoes a prototropic shift followed by extrusion of the phosphine catalyst to generate the RC coupling product (**V**).

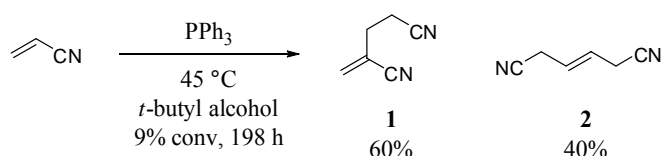
Figure 2.2: Proposed mechanism of the Rauhut-Currier reaction.



⁶³ Rauhut, M. M.; Currier, H. (American Cyanamid Co.), U.S. Patent 3074999/19630122, 1963; *Chem. Abstr.* **1963**, 58, 11224a.

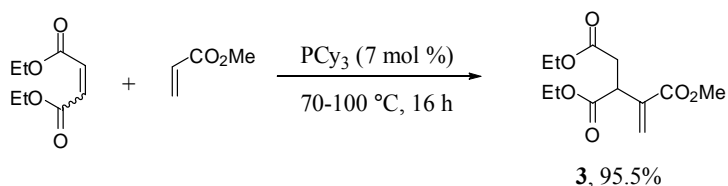
Two years later, McClure⁶⁴ and Baizer and Anderson⁶⁵ similarly described the successful dimerization of acrylonitrile in the presence of tributylphosphine. The analogous triphenylphosphine-catalyzed dimerization was reported to be less efficient, producing a low yield of α -methylene-glutaronitrile (**1**, 60%) in addition to 1,4-dicyano-1-butene (**2**, 40%), based on 9% conversion of acrylonitrile (Scheme 2.1). The reaction was performed at 45 °C in the presence of *t*-butyl alcohol for 198 h.

Scheme 2.1: Dimerization of acrylonitrile by Baizer and Anderson.



In 1969 Morita and Kobayashi⁶⁶ reported the first cross-coupling reaction of activated alkenes (methyl acrylate and acrylonitrile) with fumaric/maleic esters (diethyl and dibutyl) in the presence of tricyclohexylphosphine (Scheme 2.2). They achieved high yield (95.5%) in the coupling of methyl acrylate and diethyl fumarate, to provide addition product 3-butene-1,2,3-tricarboxylic acid 1,2-diethyl-3-methyl ester, **3**. The analogous reactions affording dibutyl (1-cyanovinyl)succinate and dibutyl (1-cyanoethylidene)succinate were presented without yields.

Scheme 2.2: Tricyclohexylphosphine-catalyzed coupling reported by Morita and Kobayashi.



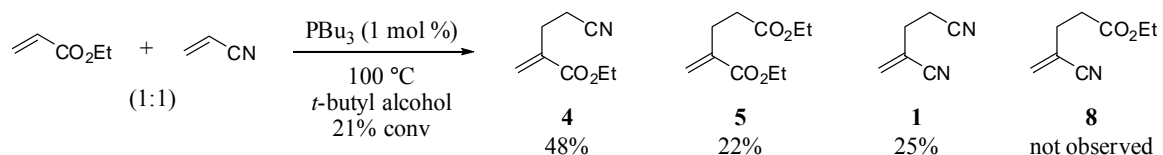
⁶⁴ McClure, J. D., *U. S. Patent* 3225083, **1965**.

⁶⁵ Baizer, M. M., Anderson, J. D. *J. Org. Chem.* **1965**, 30, 1357-1360.

⁶⁶ Morita, K.; Kobayashi, T. *Bull. Chem. Soc. Jpn.* **1969**, 42, 2732.

McClure⁶⁷ presented a similar cross-coupling reaction of ethyl acrylate and acrylonitrile catalyzed by tributylphosphine in 1970 (Scheme 2.3). In the presence of *t*-BuOH at 100 °C, only one of two possible cross-coupled products was obtained, 2-ethoxycarbonyl-4-cyano-1-butene (**4**, 48%), in addition to the products corresponding to homodimerization of both reactants (**5**, 22%; **1**, 25%).

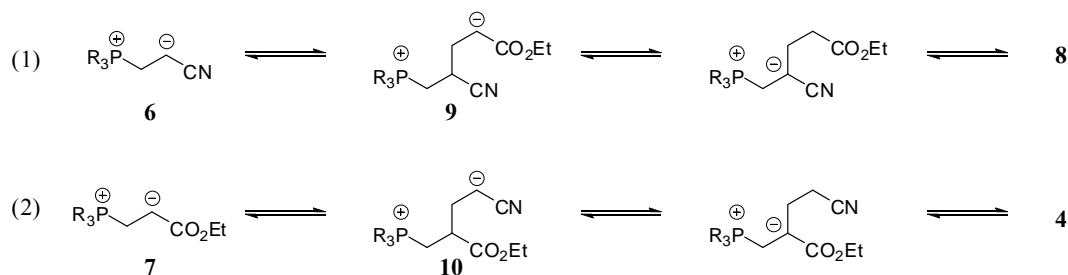
Scheme 2.3: Cross-Coupling in the RC reaction.



Homodimerization by-products **5** and **1** were isolated in similar amounts, suggesting that both intermediates, **6** and **7**, were formed during the reaction (Scheme 2.4). The absence of product **8** was thus rationalized by assuming that the subsequent reaction of the phosphonium zwitterions with ethyl acrylate (eq 1) was less favorable than reaction with acrylonitrile (eq 2). The subsequent proton transfer step was also implicated in the selective product formation, with proton transfer being less favored in the case of intermediate **9** than **10**. Ultimate product formation was therefore dependent not on the relative ease of the initial conjugate addition (forming intermediates **6** and **7**), but rather the ensuing steps in the transformation.

⁶⁷ McClure, J. D. *J. Org. Chem.* **1970**, 35, 3045-3048.

Scheme 2.4: Selective formation of cross-coupled product **4**.



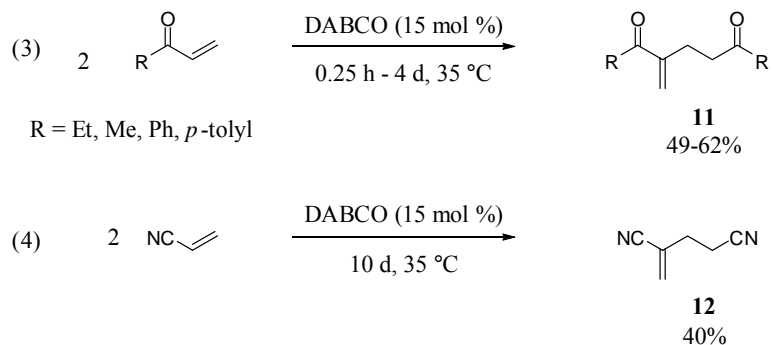
More than 15 years later, various reports of similar processes were established under the influence of amine-based catalysts. In 1986 Amri and Villieras presented an amine-catalyzed variant of the Rauhut-Currier transformation.⁶⁸ In an investigation of the related MBH reaction, researchers discovered that methyl vinyl ketone (MVK) underwent slow dimerization (7 days) in the presence of 1,4-diazabicyclo[2.2.2]octane (DABCO) to provide 3-methylene-2,6-heptadione.

The DABCO-catalyzed dimerization was extended further by Basavaiah and co-workers to include various α,β -unsaturated ketones and acrylonitrile (Scheme 2.5).⁶⁹ A range of reaction times (0.25 h, phenyl vinyl ketone; 4 d, methyl vinyl ketone; 10 d, acrylonitrile) were reported with 15 mol % catalyst loading at 35 °C to provide the corresponding 2-methylene-1,5-diketones (**11**) and acrylonitrile dimer (**12**) in moderate to good yields (eq 3 and 4, Scheme 2.5).

⁶⁸ Amri, H.; Villieras, J. *Tetrahedron Lett.* **1986**, 27, 4307-4308.

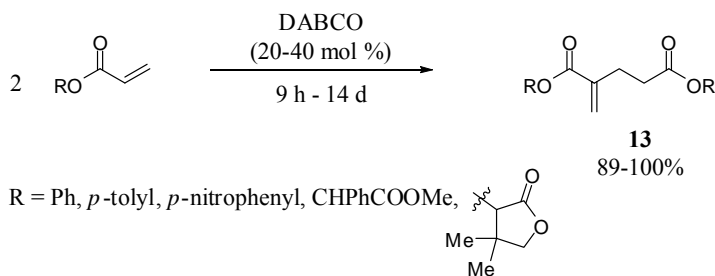
⁶⁹ Basavaiah, D.; Gowriswari, V. V. L.; Bharathi, T. K. *Tetrahedron Lett.* **1987**, 28, 4591-4592.

Scheme 2.5: Amine-catalyzed RC reaction.



Drewes and co-workers demonstrated that in the absence of an aldehyde coupling partner in the Morita-Baylis-Hillman reaction, acrylate esters will undergo self condensation under the Rauhut-Currier reaction to afford the corresponding dimers in nearly quantitative yield (89-100%, Scheme 2.6).⁷⁰ The dimerization of a variety of aryl and alkyl functionalized acrylates was promoted by DABCO (20-40 mol %) to provide the homoesters of α -methylene-glutaric acid (**13**). Under these conditions, methyl acrylate was unreactive, even after 30 days.

Scheme 2.6: DABCO-catalyzed dimerization of acrylate esters.

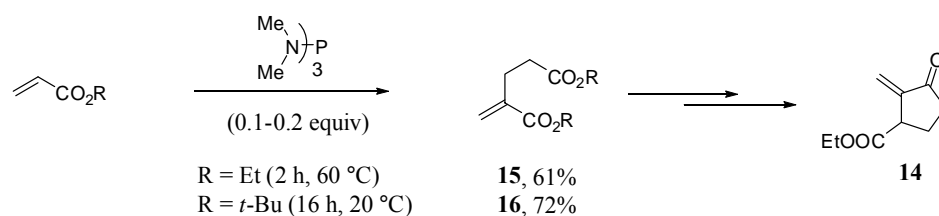


The utility of the dimerization of acrylates was highlighted in the efficient (4 step) synthesis of (\pm) sarkomycin ester **14** from ethyl acrylate by Amri and coworkers (Scheme

⁷⁰ Drewes, S. E.; Emslie, N. D.; Karodia, N. *Syn. Commun.* **1990**, *20*, 1915-1921.

2.7).⁷¹ This large scale application of the RC reaction was performed under the influence of a phosphine-based catalyst, tris(dimethylamino)phosphine (TDAP), which promoted the dimerization of ethyl and *tert*-butyl acrylates in good yields (**15**, 61%; **16**, 72%).

Scheme 2.7: Tris(dimethylamino)phosphine (TDAP) catalyzed RC reaction in the synthesis of (\pm) sarkomycin esters.

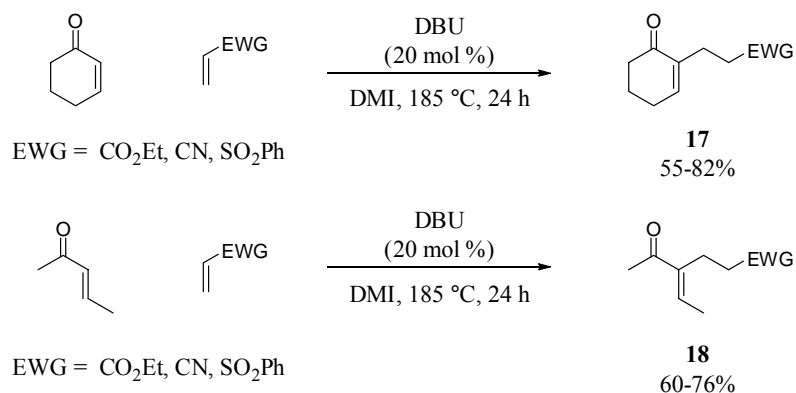


Hwu and co-workers introduced a related method for the α -alkylation of α,β -unsaturated enones using the tertiary amine 1,8-diazabicyclo[5.4.0]undec-7-ene (DBU) with 1,3-dimethyl-2-imidazolidinone (DMI) as the solvent (Scheme 2.8).⁷² Michael acceptors ethyl acrylate, acrylonitrile, and phenyl vinyl sulfone were employed in the cross-coupling reactions with 2-cyclohexen-1-one and 3-pentene-2-one, providing the corresponding α -substituted enones in good yields (**17**, 55-82%; **18**, 60-76%). This extension of the RC reaction to include β -substituted enones required elevated temperatures of 185 °C for 24 h. In the absence of alternative Michael acceptors, the dimerization of 2-cyclohexen-1-one was also possible, providing the corresponding product in 85% yield under identical conditions.

⁷¹ Amri, H.; Rambaud, M.; Villieras, J. *Tetrahedron Lett.* **1989**, *30*, 7381-7382.

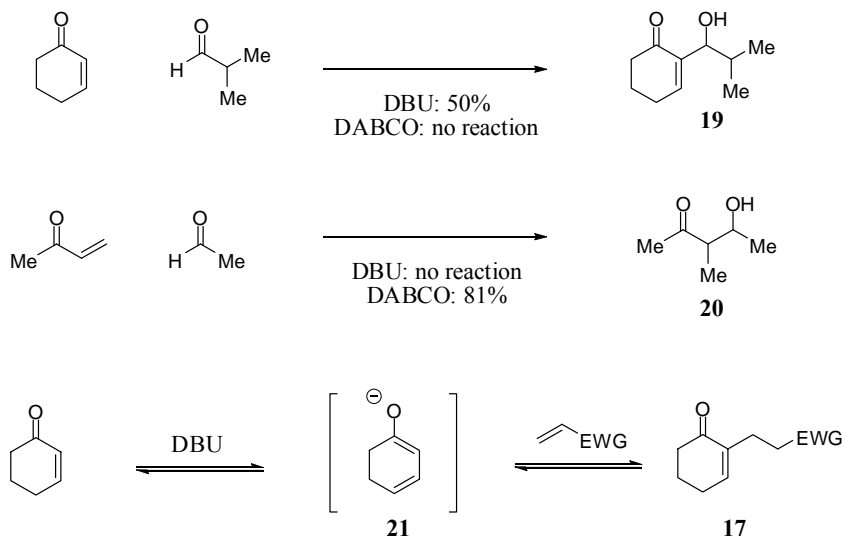
⁷² Hwu, J. R.; Hakimelahi, G. H.; Chou, C.-T. *Tetrahedron Lett.* **1992**, *33*, 6469-6472.

Scheme 2.8: α -Alkylation of α,β -unsaturated enones catalyzed by DBU.



Mechanistic work by Hwu and co-workers prompted them to propose that the DBU-catalyzed transformation proceeded via a different pathway than that previously presented for analogous MBH and RC reactions (Figure 2.3). The reaction of 2-cyclohexen-1-one with isobutyraldehyde in the presence of DBU generated the desired aldol adduct **19** in 50% yield, where as no reaction was detected in the presence of DABCO. Additionally, while DABCO was reported by Amri and co-workers to catalyze the MBH reaction of methyl vinyl ketone and acetaldehyde to provide **20** (81% yield),⁶⁸ the analogous DBU-catalyzed reaction in the Hwu laboratory led only to the recovery of starting material. It was therefore concluded that 2-cyclohexen-1-one, possessing acidic γ -protons, underwent deprotonation by DBU (vs. conjugate addition) to provide dienolate intermediate **21**. Subsequent Michael reaction with the desired activated alkene, and finally olefin migration, provided the observed α,β -unsaturated enones (**17**).

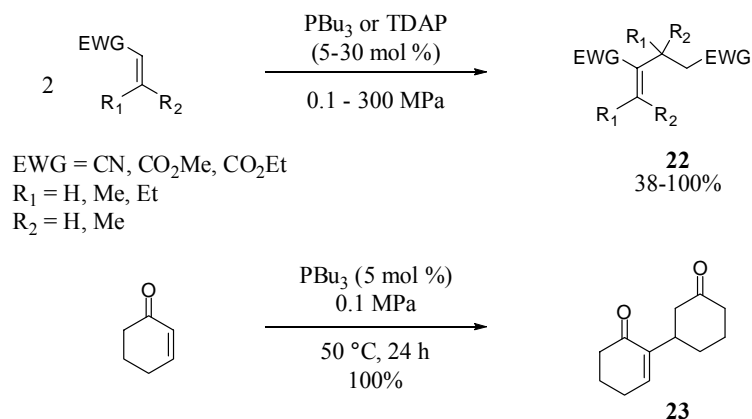
Figure 2.3: Mechanistic study by Hwu and co-workers.



Jenner and others presented the dimerization of acrylic esters, nitriles, and ketones under phosphine catalysis.⁷³ In an early report, it was demonstrated that the dimerization of acrylonitrile and methyl acrylate could be promoted with DABCO (10 mol %) at elevated pressure (300 MPa). Attempts to extend this methodology to include sluggish β -substituted analogs, such as hindered crotonitrile, were unsuccessful with traditional tertiary amine-based catalysts used in the MBH reaction (DABCO and 3-quinuclidinol) at ambient or elevated pressure. On the other hand, quantitative yield of the dimer was achieved using tri-*n*-butylphosphine at high pressure (300 MPa) or in slightly lower yield (87%) when using tris(dimethylamino)phosphine (TDAP) at ambient pressure (Figure 2.4). While the dimerization of β -substituted derivatives typically required higher pressures, cyclohex-2-en-1-one underwent quantitative dimerization using tri-*n*-butylphosphine at ambient pressure (**23**).

⁷³ (a) Jenner, G. *High Press. Res.* **1999**, *16*, 243-252. (b) Jenner, G. *Tetrahedron Lett.* **2000**, *41*, 3091-3094. (c) Su, W.; Mcleod, D.; Verkade, J. G. *J. Org. Chem.* **2003**, *68*, 9499-9501. (d) Hall, C. D.; Lowther, N.; Tweedy, B. R.; Hall, A. C.; Shaw, G. *J. Chem. Soc., Perkin Trans. 2* **1998**, 2047-2054.

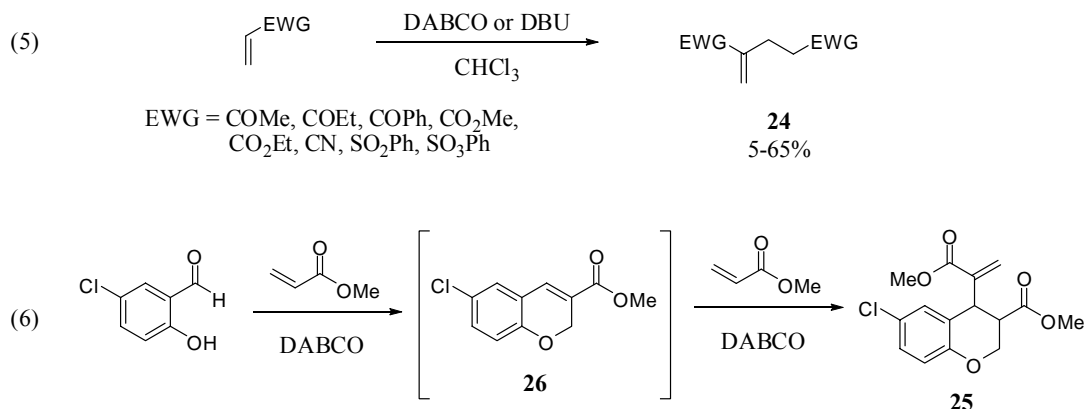
Figure 2.4: Phosphine-catalyzed dimerization of acrylic compounds.



In their study of the Morita-Baylis-Hillman reaction, Kaye and co-workers observed a competitive RC transformation leading to alkene dimerization products.⁷⁴ Accordingly, they presented a study of the direct dimerization reaction in the absence of an aldehyde coupling partner. Various activated alkenes were examined in the presence of DABCO and DBU and shown to undergo coupling to the corresponding dimers (**24**) in low to moderate yield (5-65%; eq 5, Scheme 2.9). They also reported the isolation of chromane **25** in the Morita-Baylis-Hillman reaction of salicylaldehyde and methyl acrylate. Researchers proposed that **25** was the product of an in situ RC transformation of MBH product **26** and a second equivalent of methyl acrylate (eq 6).

⁷⁴ (a) Kaye, P. T.; Nocanda, X. W. *J. Chem. Soc., Perkin Trans. 1* **2002**, 1318-1323. (b) Kaye, P. T.; Robinson, R. S. *Syn. Commun.* **1996**, 26, 2085-2097.

Scheme 2.9: (5) Dimerization of various activated alkenes with DABCO or DBU. (6) In situ RC reaction with MBH product **26**.

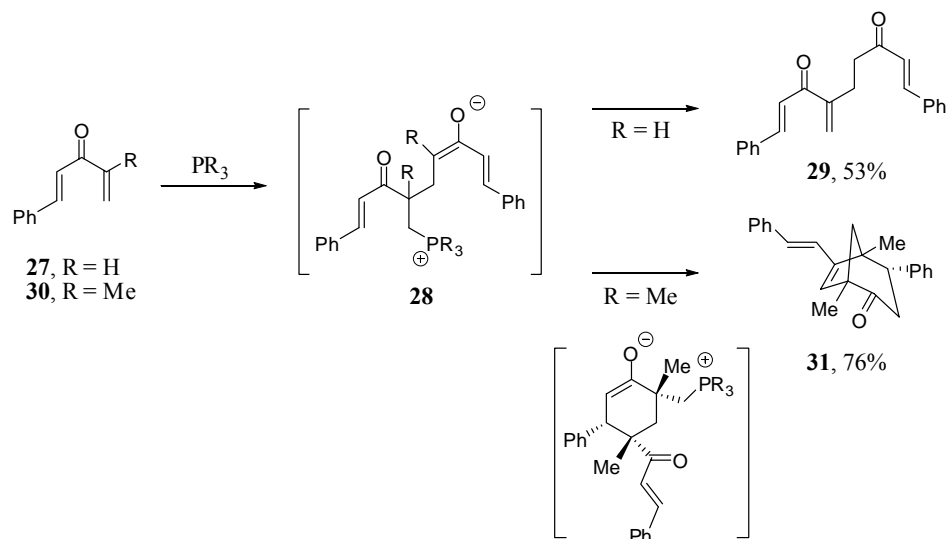


The RC transformation has also been employed in the generation of bicyclic systems when followed by a subsequent enolization and aldol reaction.⁷⁵ In the case of divinyl ketones, Schaus and co-workers have demonstrated divergent reactivity with differing α -substituted substrates to produce either traditional RC products or bicyclo[3.2.1]octenones with two bridgehead quaternary carbon centers (Figure 2.5).⁷⁶ When 1,4-diene-3-one **27** was employed in the cyclization reaction in the presence of triphenylphosphine (100 mol %), facile α -deprotonation of intermediate **28** (R = H) afforded RC product **29** in 53% yield. Alternatively, in the absence of the requisite α -proton (**30**, R = Me), the in situ generated enolate underwent intramolecular Michael addition followed by intramolecular Wittig olefination with the α,β -unsaturated ketone to generate bicycle **31** in good yield (76%).

⁷⁵ Couturier, M.; Ménard, F.; Ragan, J. A.; Riou, M.; Dauphin, E.; Andersen, B. M.; Ghosh, A.; Dupont-Gaudet, K.; Girardin, M. *Org. Lett.* **2004**, *6*, 1857-1860.

⁷⁶ McDougal, S. E.; Schaus, S. E. *Angew. Chem., Int. Ed.* **2006**, *45*, 3117-3119.

Figure 2.5: Divergent reactivity in phosphine-promoted RC reactions.



2.3 Intramolecular Rauhut-Currier Reaction

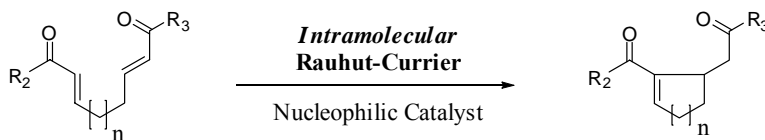
Although the Rauhut-Currier transformation was first disclosed in 1963, the reaction remained relatively undeveloped due to lack of selectivity in cross-coupling reactions involving different activated alkenes. In 1999, Moore and co-workers revealed a unique example of an intramolecular transannular RC reaction in the synthesis of natural product waihoensene (Section 2.6).⁷⁷ Then, in 2002 the groups of Roush⁷⁸ and Krische⁷⁹ presented methodology studies where they resolved the issue of selectivity by tethering coupling partners of differing electrophilicity, thereby creating an *intramolecular* Rauhut-Currier (RC) reaction (Scheme 2.10).

⁷⁷ Erguden, J. K.; Moore, H. W. *Org Lett.* **1999**, *1*, 375-377.

⁷⁸ Frank, S. A.; Mergott, D. J.; Roush, W. R. *J. Am. Chem. Soc.* **2002**, *124*, 2404-2405.

⁷⁹ Wang, L.-C.; Luis, A. L.; Agapiou, K.; Jang, H.-Y.; Krische, M. J. *J. Am. Chem. Soc.* **2002**, *124*, 2402-2403.

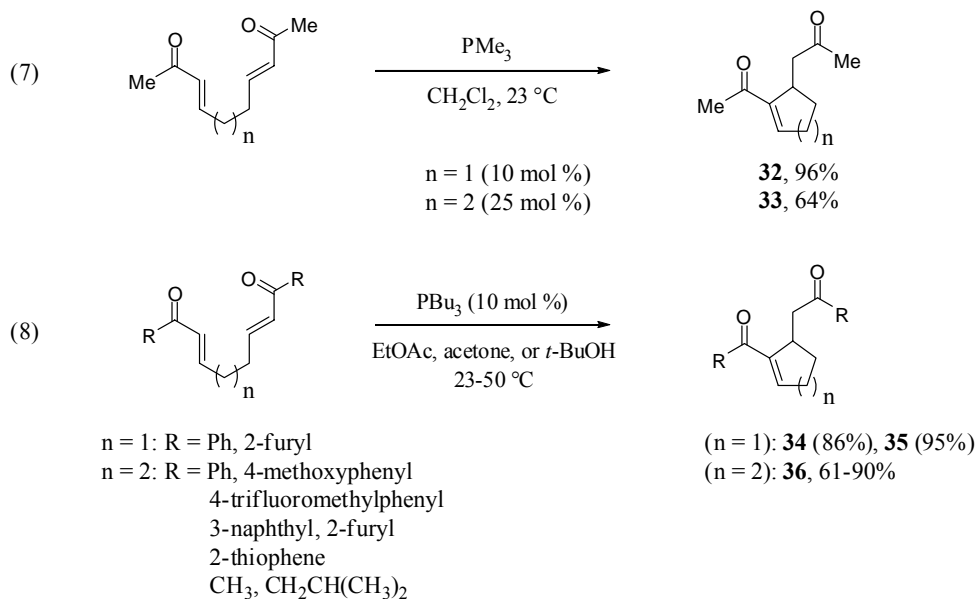
Scheme 2.10: Intramolecular RC reaction.



Both groups demonstrated that trialkylphosphines were able to catalyze the cycloisomerization of five- and six-membered symmetrical and unsymmetrical bis(enones) with high efficiency. Amine-based nucleophiles commonly employed in the Morita-Baylis-Hillman reaction of activated alkenes and aldehydes, such as DABCO, DBU, Et₂NH, and DMAP, were demonstrated to be much less efficient than phosphine-based nucleophiles in the intramolecular RC reaction. It was proposed that the lack of reactivity of amine-based nucleophiles was due to the softer character of phosphines being more suited to soft activated alkene substrates. In addition, while trialkylphosphines (10 mol %) were sufficiently reactive to catalyze the transformation, triphenylphosphine (100 mol %) demonstrated inferior reactivity. The relative order of reactivity of phosphine-based catalysts for the intramolecular RC reaction was empirically determined: Me₃P > Bu₃P >> Cy₃P >>> PPh₃. Solvent effects were examined by both research groups, leading to similar conclusions; undesired by-product formation (oligomerization and aldol cyclization) could be minimized or eliminated by varying solvents, generally with polar protic solvents providing optimal results and the fastest reaction rates. It is noteworthy that a single set of reaction conditions was not applicable to different substrate classes, and modifications were required for optimal results in each independent case.

The cyclization reaction of symmetrical bis(enones) was facile in the case of 5-membered ring formation leading to the production of various substituted cyclopentenes (Scheme 2.11). Cyclohexene formation was more difficult, providing slightly lower yields and requiring increased catalyst loading in some cases (25 mol %) to maintain useful reaction rates. Roush and co-workers employed trimethylphosphine (eq 7) in methylene chloride at ambient temperature to provide products such as **32** (96%) and **33** (64%). Krische and co-workers used tributylphosphine in various solvents at ambient and elevated temperatures (23-50 °C) in the analogous cyclization providing aromatic cyclopentene products (**34**, 86% and **35**, 95%, eq 8) as well as a variety of aromatic and aliphatic cyclohexene products (**36**, 61-90%).

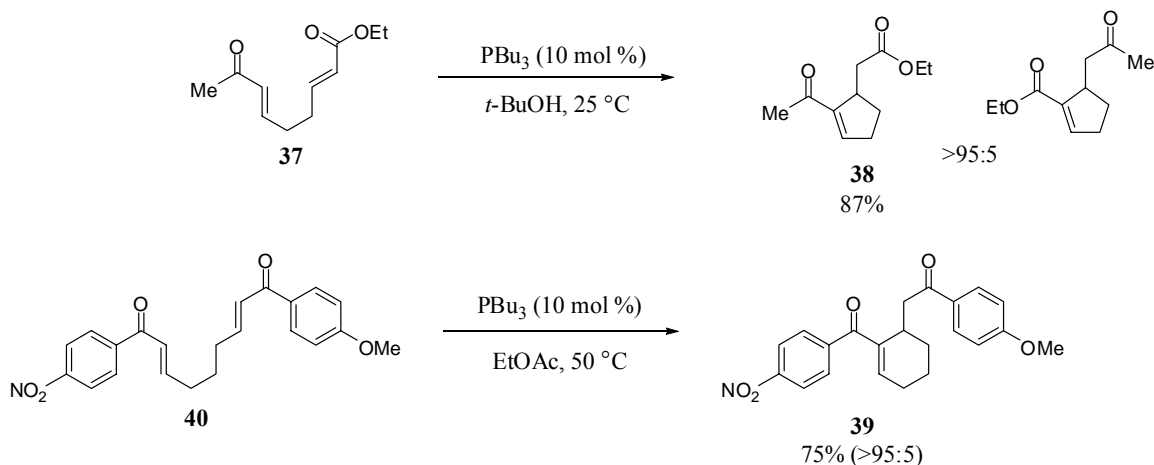
Scheme 2.11: Cycloisomerization of 5- and 6-membered symmetrical bis(enones) by Roush (7) and Krische (8).



The regioselectivity of the RC cycloisomerization of unsymmetric substrates was controlled through both electronic and steric differentiation. For example, Krische and

co-workers demonstrated high regioselectivity in 5- and 6-membered ring formation with ratios of >95:5 for single isomeric cyclization products (Scheme 2.12). In the case of enone-enoate **37**, regioisomeric product **38** was isolated as the sole product in 87% yield. Cyclization to provide unsymmetric product **39** from **40** was catalyzed by tributylphosphine at elevated temperature (50 °C) in EtOAc in good yield (75%) as a single regioisomeric product as well.

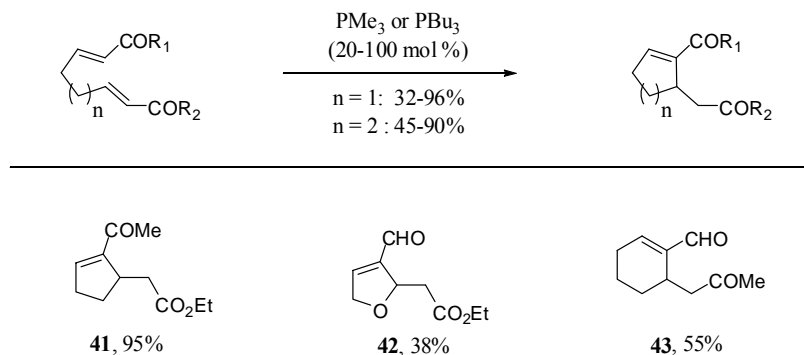
Scheme 2.12: Electronic control of product distribution in the RC reaction of unsymmetric substrates by Krische and co-workers.



Roush and co-workers reported similar electronic effects, with the major product of cyclization reflecting chemoselective nucleophilic addition of the phosphine catalyst to the more electrophilic enone, followed by cyclization on the less reactive Michael acceptor (Figure 2.6). Various substituted cyclopentenes and cyclohexenes were generated using either trimethylphosphine or tributylphosphine (20-100 mol %) in moderate to excellent yield (32-96%). For example, facile conversion to compound **41** was achieved in 95% yield, whereas enal-enoate **42** was more difficult (38%). Enal-

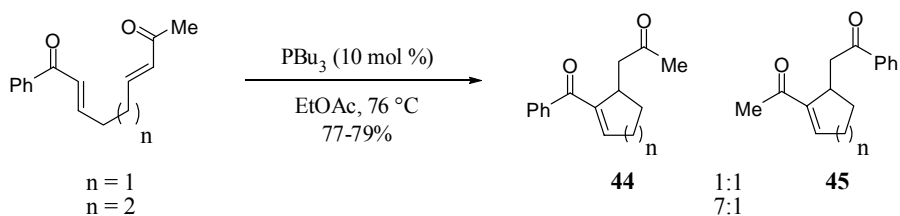
enone cyclization to afford cyclohexene product **43** was slightly more efficient (55% yield).

Figure 2.6: RC cyclization of various unsymmetric substrates by Roush and co-workers.



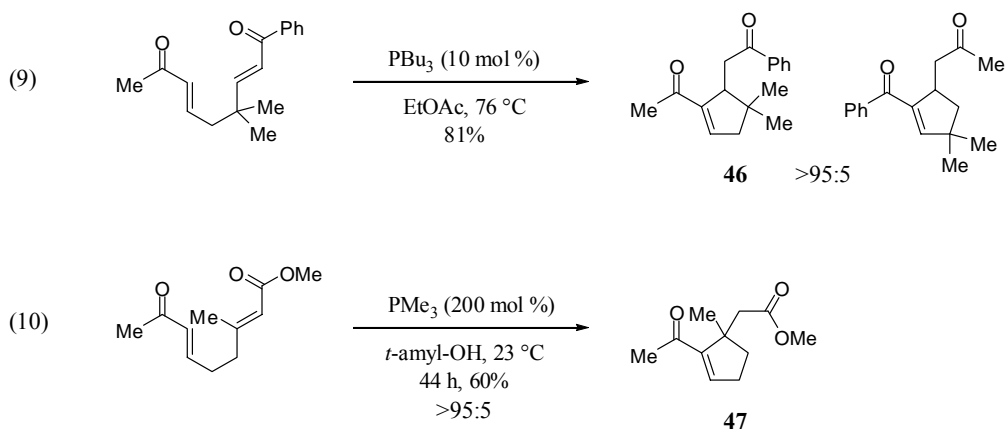
In the comparison of five- and six-membered ring formation of unsymmetric aromatic-aliphatic bis(enones) **44** and **45**, higher chemoselectivity was achieved in the case of cyclohexene formation (7:1 vs. 1:1, Scheme 2.13). It was proposed that trapping of the kinetic phosphine Michael adducts in the rapid five-membered ring formation led to indiscriminate product formation (1:1). Alternatively, the attenuated rate in homologous six-membered ring formation enabled the electronic effects of the different substituents to be reflected in the product distribution (7:1), with cyclization being the product- and rate-determining step.

Scheme 2.13: Kinetic control of product distribution.



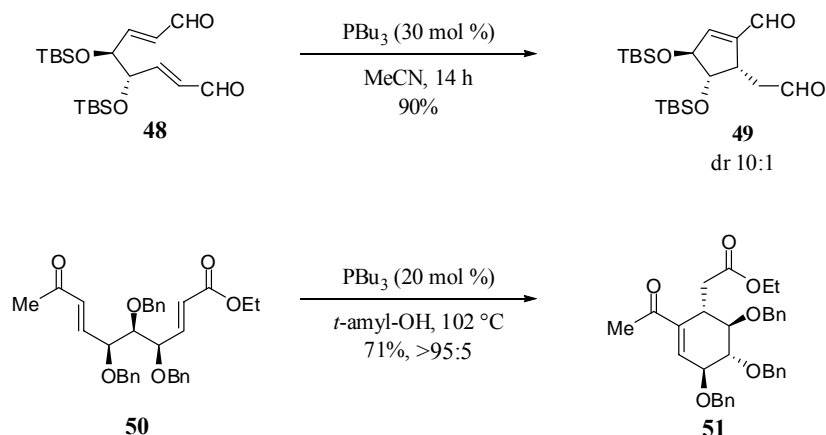
Furthermore, steric effects were demonstrated in the synthesis geminal dimethyl cyclohexene **46** by Krische and co-workers (eq 9, Scheme 2.14) and β,β -disubstituted enoate **47**, establishing a quaternary center, by Roush and co-workers (eq 10). In both cases, RC transformation proceeded through initial addition to the less hindered enone, with the more hindered site serving as the Michael acceptor in the ring-closing step.

Scheme 2.14: Steric effects in the RC cyclization.



Finally, good diastereoselectivity was achieved (10:1) in the cyclization reaction of bis(enal) **48**, providing desired cyclized product **49** in excellent yield (90%). Optically pure xylose-derived substrate **50** underwent cyclization to provide pentasubstituted **51** as a single diastereomer (Scheme 2.15).

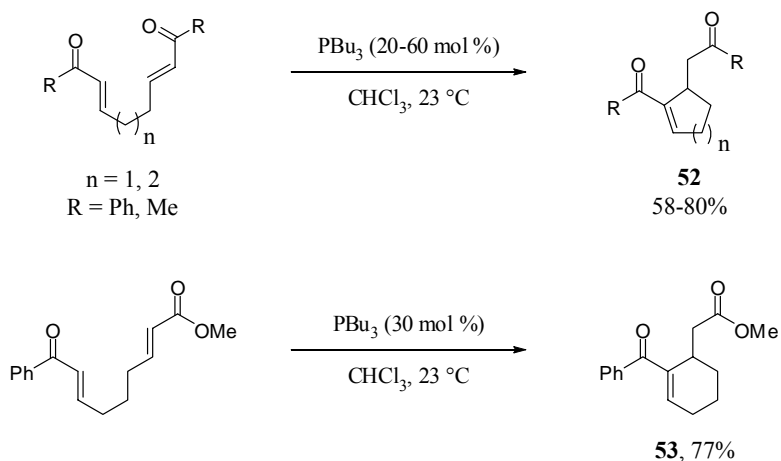
Scheme 2.15: Diastereoselectivity in the RC cyclisomerization reaction.



Following the work of the Roush and Krische laboratories, Murphy and co-workers demonstrated a similar tandem Michael/Michael cyclization reaction.⁸⁰ Symmetrical phenyl and methyl bis(enones) underwent cyclization catalyzed by *n*-Bu₃P (20-60 mol %) at ambient temperature to provide the corresponding cyclopentene and cyclohexene derivatives in good yields (58-80%, Scheme 2.16). The homologous bis(enone) that would generate a seven-membered ring was resistant to cyclization. Additionally, as was observed in the work of Roush⁷⁸ and Krische,⁷⁹ bis(enoates) were demonstrated to be unreactive under these reaction conditions, while a crossed enone-enoate substrate was successfully cyclized to provide cyclohexene derivative **53** as the only product in good yield (77%).

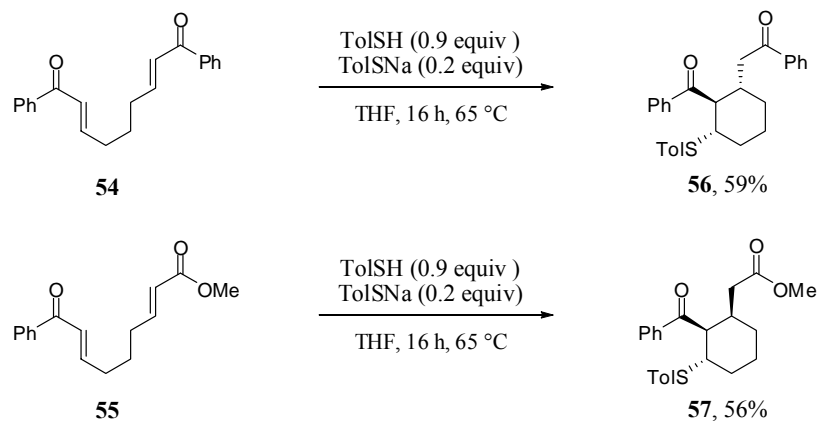
⁸⁰ (a) Brown, P. M.; Käppel, N.; Murphy, P. J. *Tetrahedron Lett.* **2002**, *43*, 8707-8710. (b) Brown, P. M.; Käppel, N.; Murphy, P. J.; Coles, S. J.; Hursthouse, M. B. *Tetrahedron* **2007**, *63*, 1100-1106.

Scheme 2.16: Tandem Michael/Michael reaction reported by Murphy and co-workers.



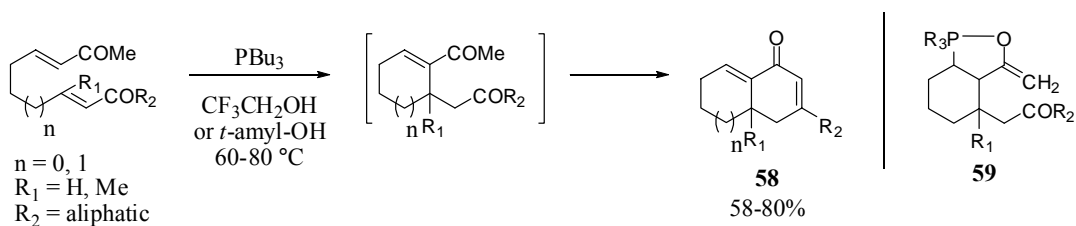
Murphy and co-workers also examined thiol-mediated catalysis of the identical transformations and discovered that upon exposure to both *p*-TolSH and *p*-TolSNa in refluxing THF, symmetrical bis(phenyl) enone **54** and unsymmetrical enone-enoate **55** underwent cyclization (Scheme 2.17). Although the reaction conditions did not enable the final catalyst elimination step in the RC reaction, affording products with the thiolate promoter covalently incorporated, they uncovered interesting stereochemical information regarding the corresponding intermediates in the transformation. Substrate **54** afforded cyclized product **56** as a single stereoisomer, with an all-*trans* relationship of the three contiguous stereocenters. Enone-enoate **55**, on the other hand, provided the analogous product **57** with a *syn-anti* relationship of the ring substituents. It was suggested that cyclization may be reversible in the case of the symmetrical bis(enone) and non-reversible in the case of the enone-enoate substrate due to the lower acidity of the α -protons of the resultant ester.

Scheme 2.17: Thiol-catalyzed RC transformation by Murphy and co-workers.



In 2005, Roush and co-workers presented a tandem intramolecular RC/aldolization reaction.⁸¹ The secondary aldol reaction was observed as a by-product in their initial study of the RC transformation and was further optimized in this study to provide products **58** in good yield (Scheme 2.18). The high regioselectivity in the aldol reaction was attributed to an interaction between the phosphonium moiety and the adjacent carbonyl, increasing the acidity of the β -phosphonium-substituted methyl ketone leading to intermediate **59** and therefore regioselective deprotonation.

Scheme 2.18: Tandem intramolecular RC/aldol reaction.



⁸¹ Thalji, R. K.; Roush, W. R. *J. Am. Chem. Soc.* **2005**, *127*, 16778-16779.

2.4 Enantioselective RC Reactions

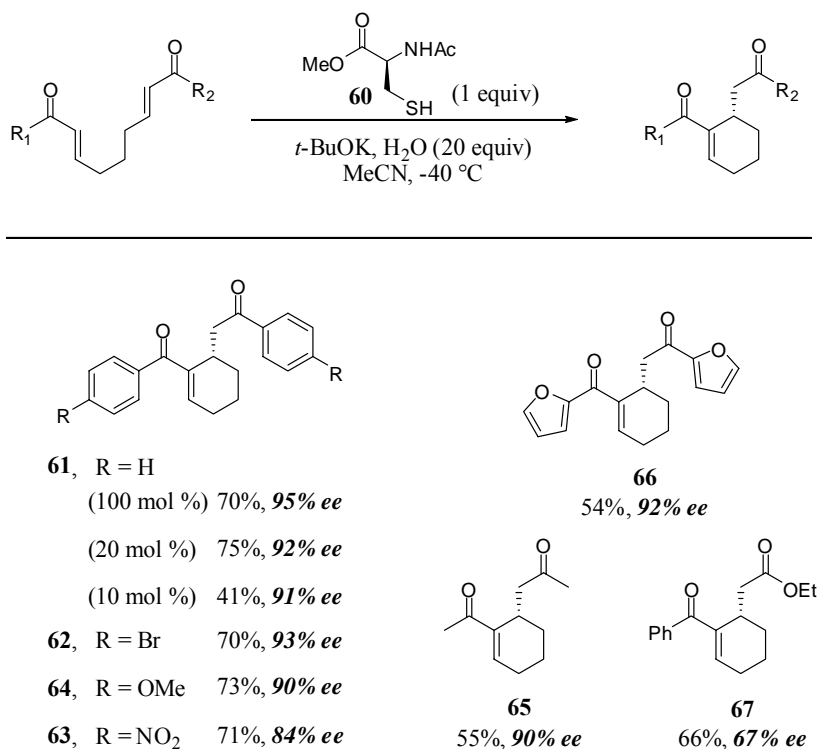
Although progress in the development of this forty-five year old reaction has been slow due to difficulties in controlling reactivity, it has recently become a potentially more useful reaction with the advent of an intramolecular variant. In 2007, Miller and co-workers⁸² were able to contribute to the further advancement of this transformation by establishing a method to perform an enantioselective Rauhut-Currier reaction in high yield and enantioselectivity using convenient reagents and conditions. This report also documented the first use of a simple cysteine (Cys) derivative as an asymmetric catalyst.

Aroyan and Miller discovered that Cys-based amino acid **60** was able to catalyze the cycloisomerization of symmetrical and unsymmetrical bis(enones) in the presence of potassium *t*-butoxide in acetonitrile with synthetically useful enantioselectivities and yields within 24 h (Figure 2.7). Notably, the incorporation of a precise quantity of water (20 equiv) had a dramatic effect on enantioselectivity. Systematic optimization of various reaction parameters, including solvent, concentration, base, and temperature, led to the optimal conditions which afforded cyclized product **61** in 95% ee and 70% yield. The cycloisomerization was extended to include electron-deficient (**62**, 70%, 93% ee; **63**, 71%, 84% ee) and electron-rich (**64**, 73%, 90% ee) aryl symmetrical bis(enones), as well as aliphatic (**65**, 55%, 90% ee) and heteroaromatic (**66**, 54%, 92% ee) bis(enones) while maintaining high enantioselectivity and good efficiency. The reaction of unsymmetrical substrate **67** resulted in reduced enantioselectivity and yield. Additionally, the use of substoichiometric catalyst loading (20 mol %) provided comparable results, with

⁸² Aroyan, C. E.; Miller, S. J. *J. Am. Chem. Soc.* **2007**, *129*, 256-257.

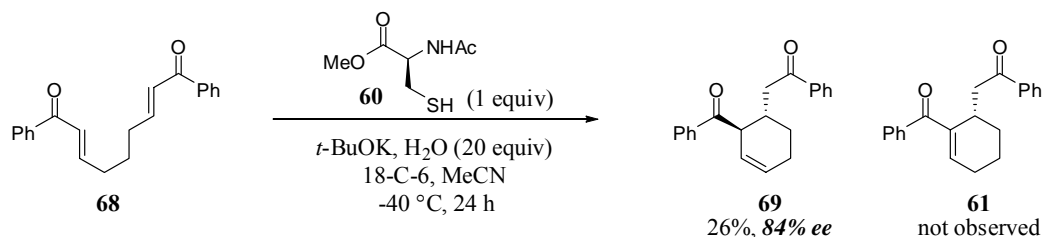
attenuated rate observed only when a further reduction in catalyst loading was utilized (10 mol %).

Figure 2.7: Substrate scope in the enantioselective RC cyclization.



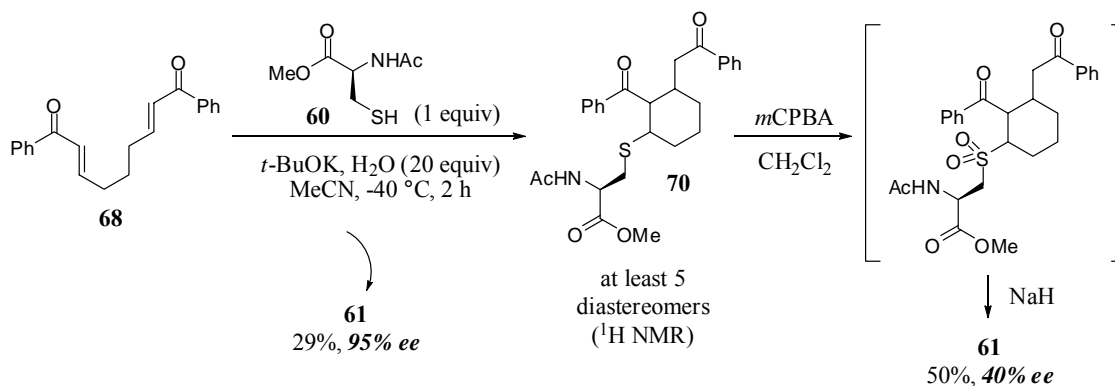
In order to provide a plausible mechanism of stereinduction, two experiments were performed to guide in the formation of a transition state model. First, when the cycloisomerization of bis(enone) **68** was run under optimized conditions in the presence of 18-crown-6, unconjugated by-product **69** (vs. **61**) was isolated as the predominant product (26% yield, 84% ee) suggesting that potassium ion chelation was essential in the formation of desired RC product (Scheme 2.19).

Scheme 2.19: RC cyclization under optimized conditions with 18-C-6.



In the second experiment, the optimized cycloisomerization reaction was interrupted after 2 h, providing desired product **61** (29% yield, 95% ee) in addition to a mixture of five diastereomers of intermediate **70** (Scheme 2.20). The mixture was then subjected to oxidation and elimination under irreversible conditions (*i.* $m\text{CPBA}$, *ii.* NaH), which afforded desired product **61** with reduced enantioselectivity of 40% ee. It is therefore possible that carbon–carbon bond formation is reversible and that abstraction of the $\alpha\text{-H}$ atom and extrusion of the catalyst may be the first irreversible and stereochemical-determining step.

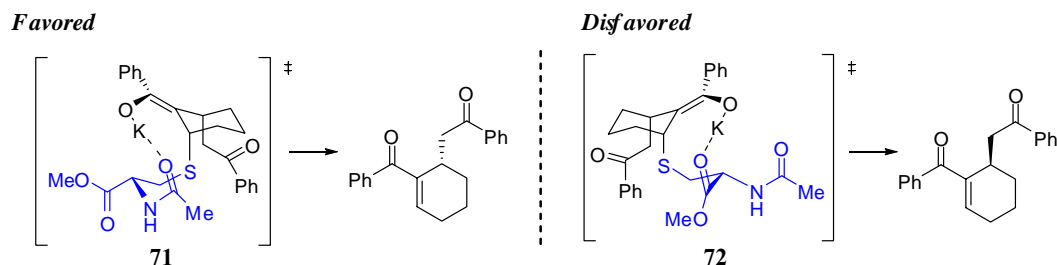
Scheme 2.20: Elimination of Cys-based catalyst under irreversible conditions.



Based on these experiments, it was suggested that favored transition state **71** benefits from a more stable potassium chelate between the enolate oxygen and the amide

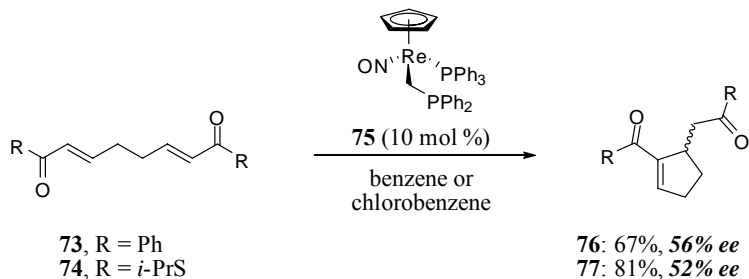
carbonyl of the catalyst, leading to a faster rate of elimination and subsequent formation of **61** with high enantiomeric excess (Figure 2.8).

Figure 2.8: Proposed transition state to explain the obtained enantioselectivity.



Later in the same year, Gladysz and co-workers presented a phosphine-catalyzed enantioselective intramolecular RC reaction of symmetrical bis(enone) **73** and **74** (Scheme 2.21).⁸³ It was proposed that the 18-electron rhenium fragment increased the Lewis basicity and nucleophilicity of the phosphorous donor atom (CH_2PPh_2) in the active catalyst ($\eta^5\text{-C}_5\text{H}_5$) $\text{Re}(\text{NO})(\text{PPh}_3)(\text{CH}_2\text{PPh}_2)$ (**75**). Using catalyst **75** (10 mol %), cycloisomerization of the bis(phenyl)ketone and bis(thioester) provided compounds **76** and **77**, respectively, in good yield (67% and 81%) and with enantioselectivities of 56% and 52% ee.

Scheme 2.21: Rhenium-containing phosphine-catalyzed enantioselective intramolecular RC reaction.

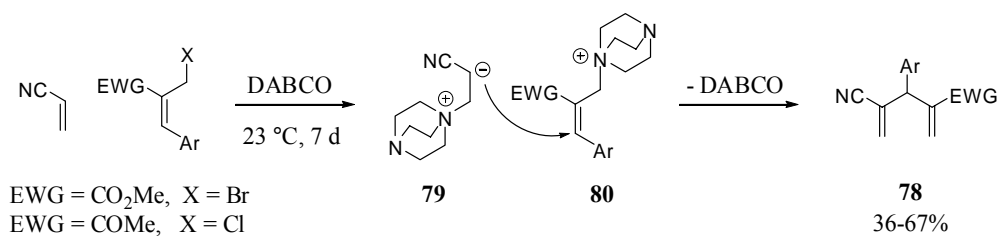


⁸³ Seidel, F.; Gladysz, J. A. *Synlett* **2007**, 6, 986-988.

2.5 Extension to Include Alternative Electrophilic Partners

Exciting advances have also been made in the extension of the traditional RC transformation to include alternative non-classical electrophilic partners. In 2001, Basavaiah and co-workers incorporated the use of (*Z*)-allyl halides (chlorides and bromides) as coupling partners in the synthesis of 3-substituted 2,4-functionalized 1,4-pentadienes (Scheme 2.22).⁸⁴ Researchers proposed generation of the desired products (**78**) via unique reactivity in the RC transformation. They suggested that DABCO underwent reaction with both acrylonitrile and the requisite allyl halide to provide intermediates **79** and **80**. Subsequently, **80** underwent S_N2' displacement of DABCO by zwitterionic species **79**. Finally, elimination of a second equivalent of DABCO provided the desired 1,4-pentadienes in moderate to good yields (**78**, 36-67%). Simple allyl bromides, such as 3-bromoprop-1-ene, were unreactive under analogous conditions (23 °C, 7 d). No further studies were presented in support of the proposed mechanism.

Scheme 2.22: Extension of the RC reaction to include allyl halides as electrophilic partners.



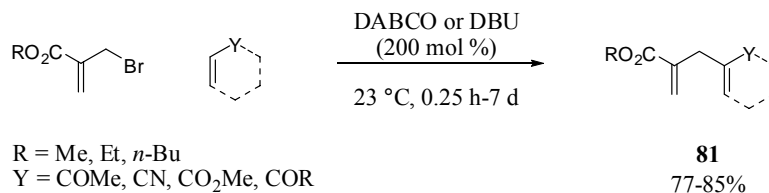
In another report, Basavaiah and co-workers expanded the scope to produce 2,4-functionalized 1,4-pentadienes without substitution at the 3-position (Scheme 2.23).⁸⁵ In the presence of a tertiary amine (DABCO or DBU), they illustrated the coupling alkyl 2-

⁸⁴ Basavaiah, D.; Kumaragurubaran, N.; Sharada, D. S. *Tetrahedron Lett.* **2001**, 42, 85-87.

⁸⁵ Basavaiah, D.; Sharada, D. S.; Kumaragurubaran, N.; Reddy, R. M. *J. Org. Chem.* **2002**, 67, 7135-7137.

(bromomethyl)prop-2-enoates with various activated alkenes, including methyl vinyl ketone, acrylonitrile, alkyl acrylates, and cyclohex-2-en-1-one. DABCO was also employed successfully by Lee and Lee in the coupling of dihalonaphthoquinones with methyl vinyl ketone and methyl acrylate to form α -vinylquinones.⁸⁶

Scheme 2.23: Synthesis of 2,4-functionalized 1,4-pentadienes.



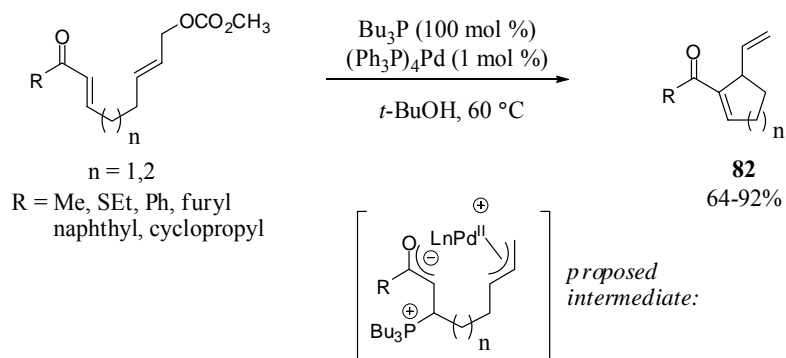
Krische and co-workers have presented a two-component catalyst system to combine the nucleophilic features of the MBH-type reaction with the electrophilic features of the Trost-Tsuji reaction to effect a catalytic enone cycloallylation (Figure 2.9).⁸⁷ In this derivative of the RC reaction, an allylic carbonate activated by palladium- π -allyl formation has been employed as a latent electrophilic partner, with an enone activated by phosphine addition as the latent nucleophilic partner. A variety of enone-allylic carbonates, including aromatic, heteroaromatic, and aliphatic enones, were subjected to stoichiometric tributylphosphine and catalytic quantities of $(\text{Ph}_3\text{P})_4\text{Pd}$ (1 mol %) to afford the corresponding five- or six-membered ring cycloallylated products in good to excellent yields (**82**, 64-92%). Although enoates were found to be unreactive in this system, the related thioenoates were viable substrates (73% yield).⁸⁸

⁸⁶ Lee, C. H.; Lee, K.-J. *Synthesis* **2004**, 12, 1941-1946.

⁸⁷ Jellerichs, B. G.; Kong, J.-R.; Krische, M. J. *J. Am. Chem. Soc.* **2003**, 125, 7758-7759.

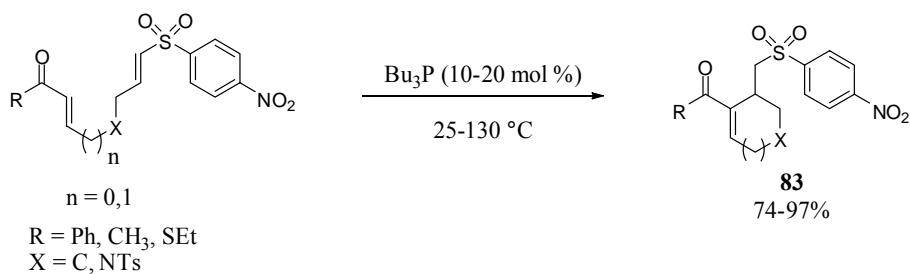
⁸⁸ Keck and co-workers pioneered the use of thioenoates in the MBH reaction, see: Keck, G. E.; Welch, D. *S. Org. Lett.* **2002**, 4, 3687-3690.

Figure 2.9: Cycloallylation of enones using the two-component catalyst system of phosphine and palladium.



Another interesting variant reported by Krische and co-workers involved the use of *p*-nitrophenyl substituted vinylsulfones as the electrophilic coupling partner with a variety of enones and thienoates (Scheme 2.24).⁸⁹ Cyclopentene and cyclohexene products **83** were afforded in good to excellent yield (74-97%) using 10-20 mol % tributylphosphine. Reaction temperature and solvent were substrate dependent and required individual optimization.

Scheme 2.24: Extension of the RC reaction to include vinylsulfone coupling partners.



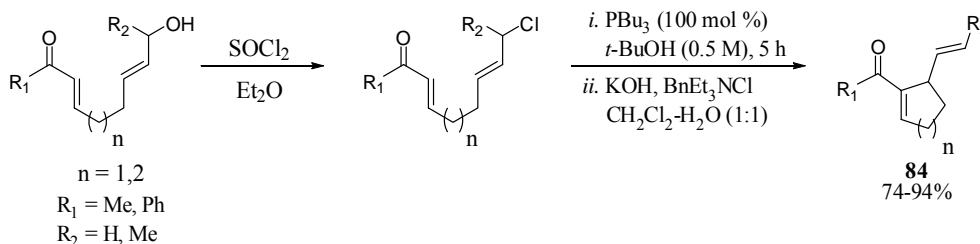
In work similar to Basavaiah's, Krafft and Haxell have demonstrated the direct use of allyl halides as electrophiles in the intramolecular RC reaction (Scheme 2.25).⁹⁰ Tributylphosphine (100 mol %) was used to promote the cyclization of various enones

⁸⁹ Luis, A. L.; Krische, M. J. *Synthesis* **2004**, 15, 2579-2585.

⁹⁰ Krafft, M. E.; Haxell, T. F. N. *J. Am. Chem. Soc.* **2005**, 127, 10168-10169.

with primary and secondary allylic chlorides in *t*-BuOH under phase transfer conditions (KOH, BnEt₃NCl) to afford both mono- and disubstituted alkenes **84** in good to excellent yields (74-94%). In analogy to the work presented by the groups of Roush and Krische in the intramolecular RC reaction, amine-based catalysts (DABCO, quinuclidine, DBU, and DMAP) were found to be inefficient catalysts. The use of allylic mesylates and tosylates was inferior to allylic chlorides, which were generated in situ from the corresponding enone-allylic alcohols using thionyl chloride.

Scheme 2.25: Intramolecular RC cycloisomerization of enones and allylic leaving groups.

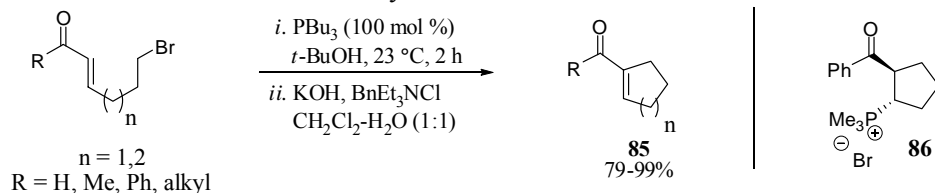


Thus far, the Morita-Baylis-Hillman and Rauhut-Currier transformations have involved the coupling of activated alkenes with highly reactive sp^2 hybridized carbon electrophiles, including aldehydes, α -keto esters, 1,2-diketones, enones, enoates, vinyl sulfones, allylic carbonates, and allylic halides. In 2005, Krafft and co-workers incorporated a new class of electrophiles into the expanding list of viable coupling partners;⁹¹ researchers successfully promoted the phosphine-catalyzed RC cycloisomerization reaction of activated alkenes with sp^3 hybridized electrophiles (Scheme 2.26). The formation of both five- and six-membered enone cycloalkylation products **85** was performed in a stepwise procedure in excellent yields (79-99%) using

⁹¹ Krafft, M. E.; Seibert, K. A.; Haxell, T. F. N.; Hirose, C. *Chem. Commun.* **2005**, 5772-5774.

stoichiometric tributylphosphine in *t*-BuOH followed by the addition of aqueous base under phase transfer conditions. In a related report, researchers were able to perform the reaction using substoichiometric phosphine (20 mol %) by demonstrating that all the required components of the transformation were compatible, enabling a one-step procedure under similar conditions (KOH, BnEt₃NCl, *t*-BuOH-CH₂Cl₂).⁹² Comparable results were obtained under lower catalyst loading, with PBu₃ as the optimal catalyst for five-membered ring formation and PMe₃ optimal for six-membered ring formation. The direct reaction of phosphine with the alkyl halide to generate a phosphonium salt was discounted through control experiments.

Scheme 2.26: Direct intramolecular α -alkylation of enones.



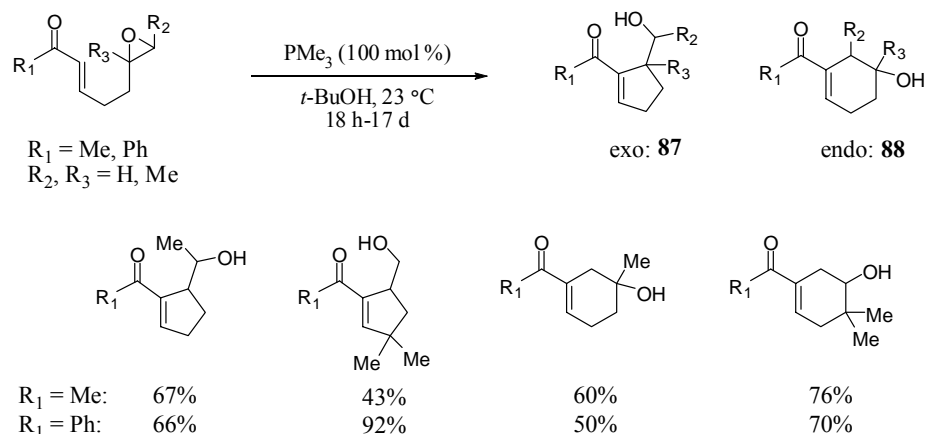
Intermediate ketophosphonium salt **86** was isolated in a later study by the same authors, lending credence to the proposed MBH/RC reaction mechanism.⁹³ Potential transition state conformations leading to the observed *trans*-configuration of the intermediate did not include the potentially beneficial oxygen-phosphorous electrostatic interaction. The authors suggested that this interaction, which has been involved in many MBH mechanistic discussions, may not be the overriding influence in defining the stereochemical outcome of the cyclization and may not be necessary for a successful transformation.

⁹² Krafft, M. E.; Seibert, K. A. *Synlett* **2006**, 3334-3336.

⁹³ Krafft, M. E.; Haxell, T. F. N.; Seibert, K. A.; Abboud, K. A. *J. Am. Chem. Soc.* **2006**, *128*, 4174-4175.

Expanding upon the use of sp^3 hybridized electrophiles, Krafft and Wright reported the incorporation of an epoxide as the electrophilic partner in the intramolecular RC transformation, giving rise to homologous aldol adducts.⁹⁴ As illustrated in Figure 2.10, RC cyclization of the epoxy enone could proceed to generate either alcohol **87** (from exo ring opening of the epoxide) or alcohol **88** (from endo ring opening). Investigation of several phenyl and methyl enones demonstrated that substitution on the epoxide or the tether was required for high endo/exo selectivity in the cyclization step, providing various cyclopentene and cyclohexene derivatives in good yield (43-92%). A control experiment confirmed that phosphine was not reacting directly with the epoxide and that the transformation proceeded through the traditional RC mechanistic pathway where conjugate addition of trimethylphosphine generated a zwitterionic enolate followed by epoxide opening. The final deprotonation/elimination of the catalyst was proposed to be promoted by the resultant alkoxide.

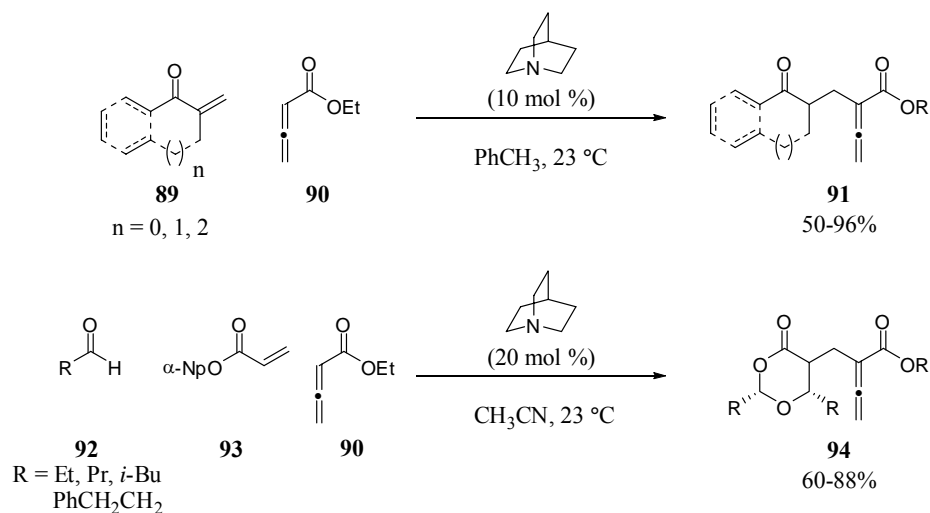
Figure 2.10: Intramolecular RC cyclization via epoxide ring opening



⁹⁴ Krafft, M. E.; Wright, J. A. *Chem. Commun.* **2006**, 2977-2979.

A further extension of the RC reaction to include an alternative latent nucleophile (vs. the original α,β -unsaturated enone) was presented by Miller and co-workers.⁹⁵ Divergent reactivity was demonstrated such that the phosphine-catalyzed reaction of enone **89** and allenic ester **90** afforded the corresponding [3+2]-cycloadduct.⁹⁶ Alternatively, the amine-catalyzed coupling (quinuclidine, 10 mol %) of various α,β -unsaturated carbonyls with allenolate **90** in toluene at ambient temperature underwent a traditional RC pathway, providing α,α' -disubstituted allenolates (**91**) in good to excellent yields (50-96%; Figure 2.11). A three-component coupling reaction was demonstrated with several aldehydes **92**, acrylate **93**, and allenolate **90**, affecting a MBH-RC tandem reaction sequence with good yields (**94**, 60-88%).

Figure 2.11: Coupling of allenic esters and various α,β -unsaturated carbonyl compounds.



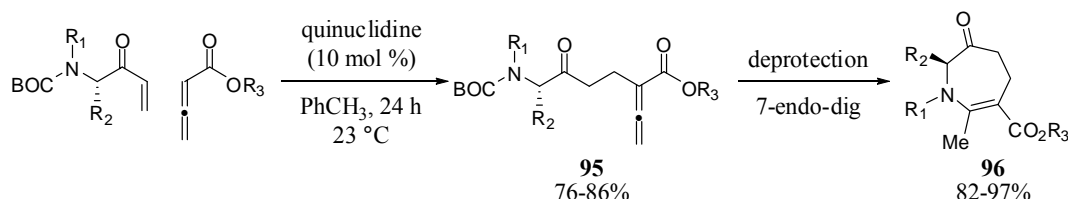
This methodology was expanded to include the coupling of α -amino acid derived vinyl ketones with allenic esters to provide a diverse range of α,α' -disubstituted allenolates

⁹⁵ Evans, C. A.; Miller, S. J. *J. Am. Chem. Soc.* **2003**, *125*, 12394-12395.

⁹⁶ Du, Y.; Lu, X.; Yu, Y. *J. Org. Chem.* **2002**, *67*, 8901-8905.

95 (76-86%, Scheme 2.27).⁹⁷ Allenic ester products were then elaborated to provide synthetically interesting chiral azacycles (**96**, 82-97%) through a deprotection/7-endo-dig cyclization-isomerization reaction sequence.

Scheme 2.27: Synthesis of azepines from allenolate-enone coupling products.



2.6 Application in Total Synthesis

The Rauhut-Currier reaction and its derivatives have the ability to establish complex ring systems with multiple stereogenic centers. While the development of this transformation has been slow due to highly substrate dependent yields and low reaction rates, the introduction of an intramolecular variant had a great affect on the utility of the reaction, as illustrated by its use in the synthesis of several natural products.

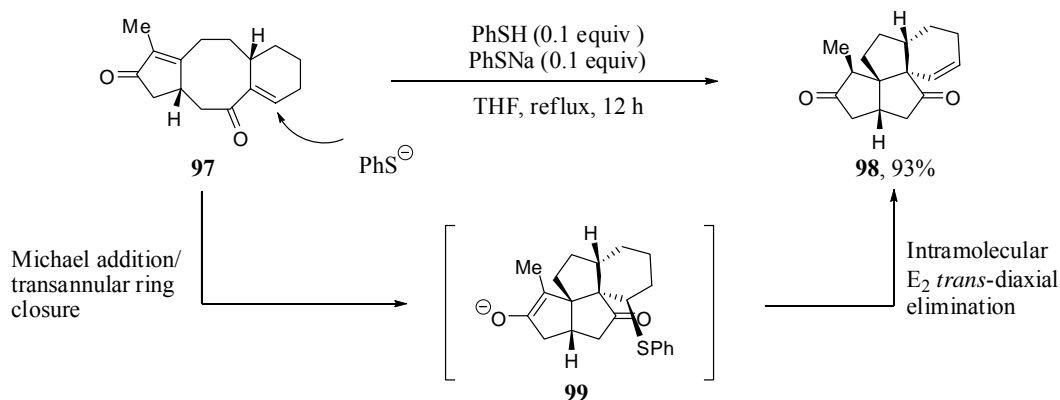
As noted above, in 1999, Moore and co-workers⁹⁸ demonstrated an interesting and unique application of the first intramolecular RC reaction in the synthesis of a fused tetraquinane ring system *en route* to the synthesis of natural product waihoensene (Scheme 2.28). The cycloisomerization of tricyclic bis(enone) **97** catalyzed by thiophenol and sodium thiophenolate provided angularly fused tetraquinane **98** was in excellent yield (93%**Scheme 2.28**). The transformation was believed to proceed through a tandem sequence of reactions, including initial conjugate addition of the thiolate

⁹⁷ Evans, C. A.; Cowen, B. J.; Miller, S. J. *Tetrahedron* **2005**, *61*, 6309-63.

⁹⁸ Erguden, J. K.; Moore, H. W. *Org Lett.* **1999**, *1*, 375-377.

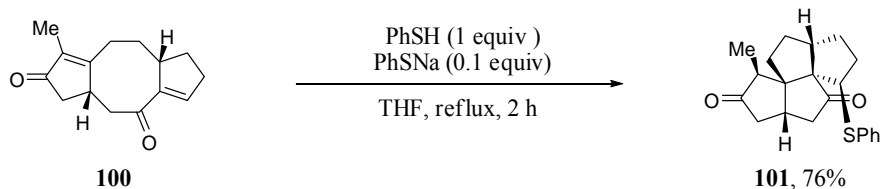
followed by transannular Michael reaction to provide intermediate **99**, and finally an intramolecular E_2 *trans*-diaxial elimination reaction to produce desired product **98** and regenerate the thiophenolate catalyst.

Scheme 2.28: Synthesis of the tetraquinane ring system of waihoensene.



Interestingly, in a very similar transformation involving homolog **100** (containing a five-membered ring versus a six-membered ring), the requisite intermediate was no longer in proper alignment for the elimination reaction and product **101** was isolated when a stoichiometric quantity of thiophenol was employed (Scheme 2.29). The covalent trapping of the catalyst is more representative of general thiol-based catalysis in MBH/RC-type transformations.⁹⁹

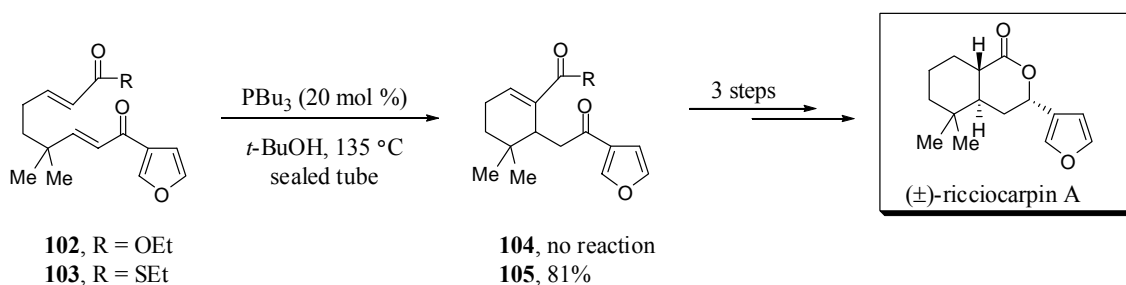
Scheme 2.29: Synthesis of tetraquinane ring system without elimination of the catalyst.



⁹⁹ Basavaiah, D.; Rao, A. J.; Satyanarayana, T. *Chem. Rev.* **2003**, *103*, 811-891.

Krische and Agapiou demonstrated the use of highly reactive and chemoselective thioenoates in the RC transformation in the synthesis of the furanosequiterpene lactone (±)-ricciocarpin A (Scheme 2.30).¹⁰⁰ While the phosphine-catalyzed cross Michael reaction of enoate-enone **102** was unreactive, the analogous thioenoate-enone substrate (**103**) demonstrated heightened reactivity, as well as exquisite chemoselectivity, to provide desired cyclized product **105** in 81% yield. Cyclohexene **105** was elaborated to the natural product in 3 steps.

Scheme 2.30: Synthesis of (±)-ricciocarpin A by Krische and co-workers.

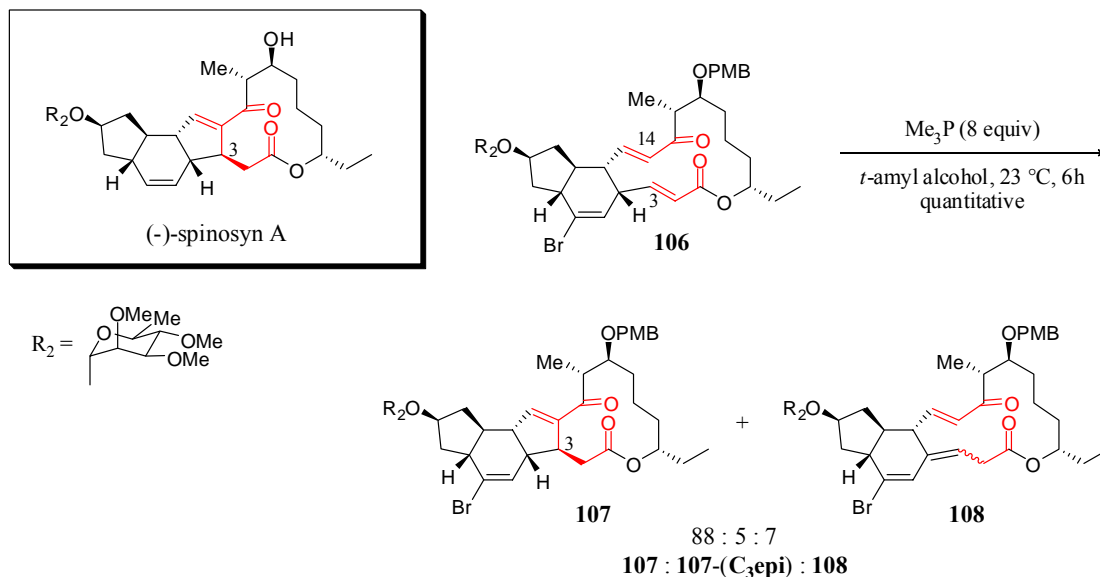


In 2004, Roush and co-workers reported the total synthesis of (-)-spinosyn A featuring a diastereoselective transannular Rauhut-Currier reaction (Scheme 2.31).¹⁰¹ An intramolecular Horner-Wadsworth-Emmons macrocyclization reaction followed by a transannular Diels-Alder reaction generated the RC substrate, **106**. The RC ring contraction was effected with trimethylphosphine (8 equiv) in *tert*-amyl-alcohol and proceeded with excellent diastereoselectivity in the generation of the C3-C14 carbon-carbon bond. Desired product **107** was provided with only minimal amounts of the C(3) epimer of **107** and olefin migration product **108** (88:5:7).

¹⁰⁰ Agapiou, K.; Krische, M. J. *Org. Lett.* **2003**, *5*, 1737-1740.

¹⁰¹ (a) Mergott, D. J.; Frank, S. A.; Roush, W. R. *Proc. Natl. Acad. Sci. U.S.A.* **2004**, *101*, 11955-11959. (b) Methot, J. L.; Roush, W. R. *Adv. Synth. Catal.* **2004**, *346*, 1035-1050.

Scheme 2.31: Synthesis of (-)-spinosyn A by Roush and co-workers.

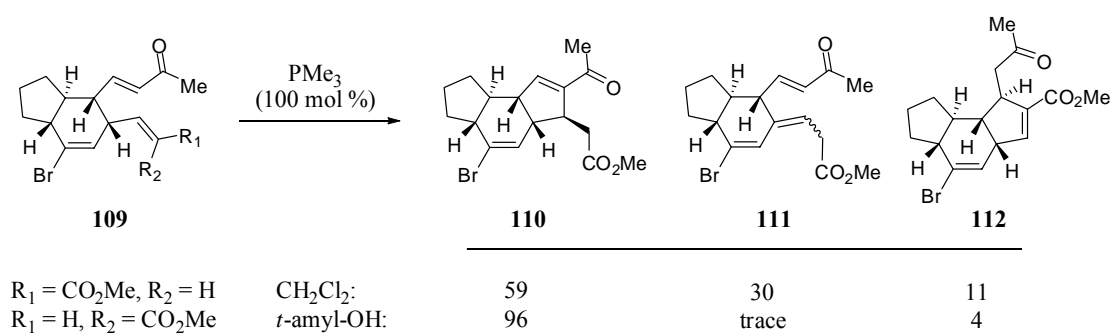


In studies leading up to the successful synthesis of (-)-spinosyn A, Roush and co-workers presented various studies of the transannular RC reaction in the generation of the *as*-indacene core.¹⁰² For example, olefin geometry had a critical effect on the product distribution in the phosphine-catalyzed cyclization of enone-enoate **109** (Table 2.1). Cyclization of the (*E*)-enoate bicyclic precursor in CH₂Cl₂ provided approximately a 2:1 mixture of desired tricycle **110** and olefin migration by-product **111**, in addition to regioisomeric tricycle **112**. Excitingly, when the alternative (*Z*)-enoate precursor was employed in the cyclization with trimethylphosphine in *tert*-amyl alcohol, researchers were able to obtain the desired cyclization product in good yield (86%) and excellent chemoselectivity (96:4), with only trace amounts of the olefin migration by-product. Cycloisomerization of the (*E*)-enoate was examined in various solvents, with CH₂Cl₂ providing the best results. It was proposed that the change in olefin geometry to the (*Z*)-

¹⁰² Mergott, D. J.; Frank, S. A.; Roush, W. R. *Org. Lett.* **2002**, *4*, 3157-3160.

enoate resulted in restricted orbital alignment, which suppressed γ -deprotonation and therefore minimized formation of the olefin migration by-product.

Table 2.1: RC cyclization with (*Z*)- and (*E*)-enoates.

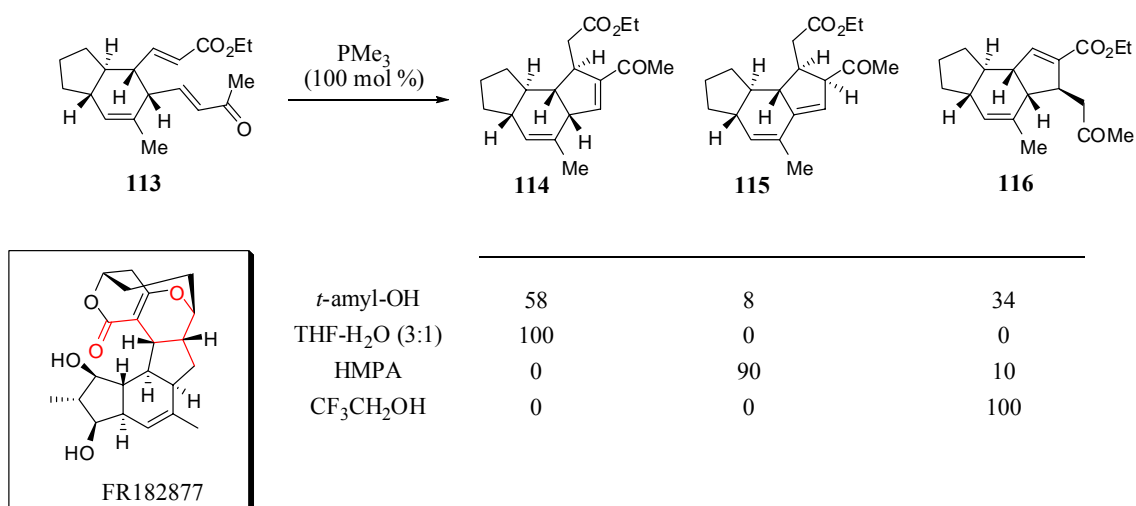


In an effort to synthesize antimitotic agent FR182877, Roush and co-workers illustrated the use of an intramolecular RC cycloisomerization to generate the *as*-indacene ring of this natural product.¹⁰³ RC cyclization of enone-enoate **113** under previously optimized conditions (*t*-amyl-OH) was unsuccessful and underscored the substrate dependence of this transformation (Table 2.2). Optimization of the reaction conditions revealed a dramatic solvent effect. Poor selectivity was obtained among the desired cyclization product (**114**), the olefin migration product (**115**), and regioisomeric product **116** when the reaction was performed in *t*-amyl alcohol (58:8:34). On the other hand, exquisite selectivity was obtained when the reaction was performed in THF-H₂O (3:1) with 2 equiv tributylphosphine providing exclusively desired product **114**. Interestingly, when the reaction was performed in 2,2,2-trifluoroethanol under otherwise identical reaction conditions, exclusive formation of regioisomeric product **116** was

¹⁰³ Methot, J. L.; Roush, W. R. *Org. Lett.* **2003**, *5*, 4223-4226.

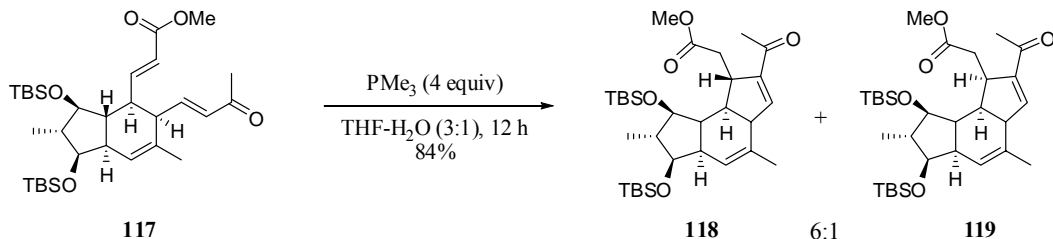
observed. Additionally, in hexamethylphosphoramide (HMPA) olefin migration product **115** was isolated as the major product.

Table 2.2: Studies of the intramolecular RC reaction in the synthesis of FR182877.



The optimal reaction conditions (THF-H₂O) were amenable to the more advanced model system, **117**, in the synthetic studies toward FR182877, providing desired cyclization product **118** in 84% yield with 6:1 diastereomeric ratio (**118:119**) (Scheme 2.32).

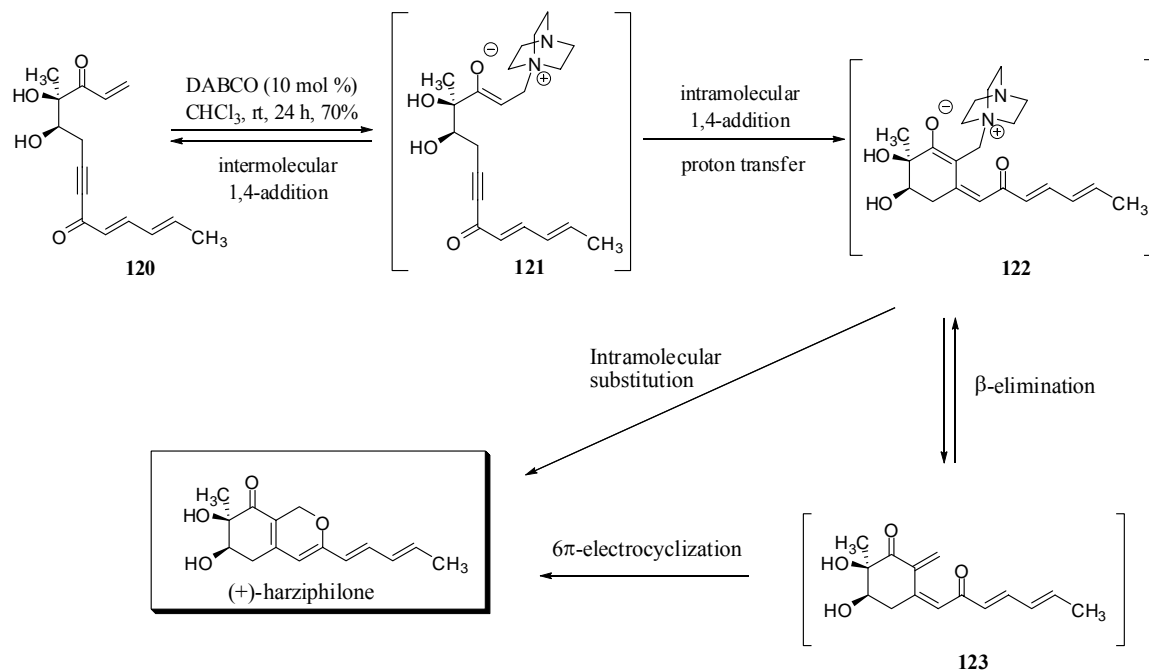
Scheme 2.32: Advanced model system in the synthetic studies of FR182877.



Sorensen and co-workers demonstrated the use of a tertiary amine-catalyzed RC transformation in the successful synthesis of (+)-harziphione (Figure 2.12).¹⁰⁴ Under mild catalysis with DABCO (10 mol %), they were able to promote the selective cyclization reaction to generate the bicyclic natural product. The mechanism of the bicycloisomerization was proposed to proceed via reversible conjugate addition of DABCO to the unsubstituted enone system of **120** followed by intramolecular Michael addition to afford zwitterion **122** after a proton transfer of the generated allenolate ion. The reaction could proceed through a traditional MBH-RC mechanism, such that β -elimination would provide **123** with regeneration of the catalyst, enabling a subsequent 6π -electrocyclization to provide the natural product. Alternatively, an intramolecular displacement of DABCO from intermediate **122** could be envisioned to lead directly to (+)-harziphione.

¹⁰⁴ Stark, L. M.; Pekari, K.; Sorensen, E. J. *Proc. Natl. Acad. Sci. U.S.A.* **2004**, *101*, 12064-12066.

Figure 2.12: Synthesis of (+)-harziphilone by Sorensen and co-workers.



2.7 Conclusion

The Rauhut-Currier reaction predates the Morita-Baylis-Hillman reaction by five years, however, with the great difficulty in controlling the selectivity of this reaction its widespread application has been limited. Successful dimerization of various enones and enoates has been achieved, yet with great potential to improve upon reactivity and breadth of viable substrates. The last five years has seen substantial growth in the RC methodology with the advent of the intramolecular variant, dramatically improving the utility of this transformation. Moreover, the development of an enantioselective variant has further enhanced the utility of this reaction and presented many possibilities in the realm of stereoselective carbon-carbon bond formation. Looking to the future, many opportunities persist for multidimensional growth in the development of an

enantioselective intermolecular version and continued expansion of substrate class in the enantioselective intramolecular version. Finally, the extended application of the RC reaction in complex molecule synthesis will remain the final frontier and serve as inspiration in the design of new substrate classes.

3 Development of the Enantioselective Rauhut-Currier Reaction

3.1 Introduction

Research efforts in our laboratory have taken place in the proverbial classroom of nature, as we glean inspiration from the ability of enzymes to exert exquisite control over a multitude of transformations critical to everyday function. As introduced in Chapter 1, we have been greatly interested in harnessing the power of biosynthetic tools in the form of small peptide-based nucleophilic catalysts for synthetic organic transformations.¹⁰⁵ Through the development of the enantioselective Morita-Baylis-Hillman reaction we were able to expand our synthetic tool box further to include not only a new co-catalytic system (pipercolinic acid/*N*-methylimidazole (NMI)), but a new class of transformations as well, namely the formation of a carbon-carbon bond.

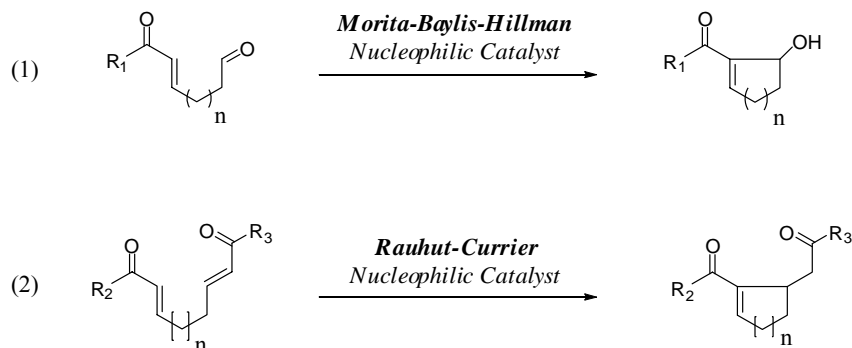
Although our progress in the intramolecular MBH reaction led to state-of-the-art levels of enantioselectivity, the reaction is still in its infancy. Inspired by our findings and our initial success, we sought to expand this methodology even further to aid in the development of this class of C-C bond forming reactions. Specifically, we sought to create an enantioselective variant of the Rauhut-Currier (RC) reaction with the goal of providing a method to access highly functionalized enantiopure ring systems.¹⁰⁶ The

¹⁰⁵ For a review of the use of peptides as asymmetric catalysts, see: (a) Davie, E. A. C.; Mennen, S. M.; Xu, Y.; Miller, S. J. *Chem. Rev.* **2007**, *107*, 5759-5812. (b) Miller, S. J. *Acc. Chem. Res.* **2004**, *37*, 601-610 and references therein.

¹⁰⁶ For selected reviews, please see: (a) Drewes, S. E.; Roos, G. H. P. *Tetrahedron* **1988**, *44*, 4653-4670. (b) Basavaiah, D.; Rao, P. D.; Hyma, R, S. *Tetrahedron* **1996**, *52*, 8001-8062. (c) Basavaiah, D.; Rao, A. J.; Satyanarayana, T. *Chem. Rev.* **2003**, *103*, 811-891.

Rauhut-Currier reaction, also known as the vinylogous MBH reaction,¹⁰⁷ involves the coupling of two activated alkenes compared to the coupling of an activated alkene and an aldehyde, as in the MBH reaction (Figure 3.1).

Figure 3.1: Morita-Baylis-Hillman and Rauhut-Currier Reactions.

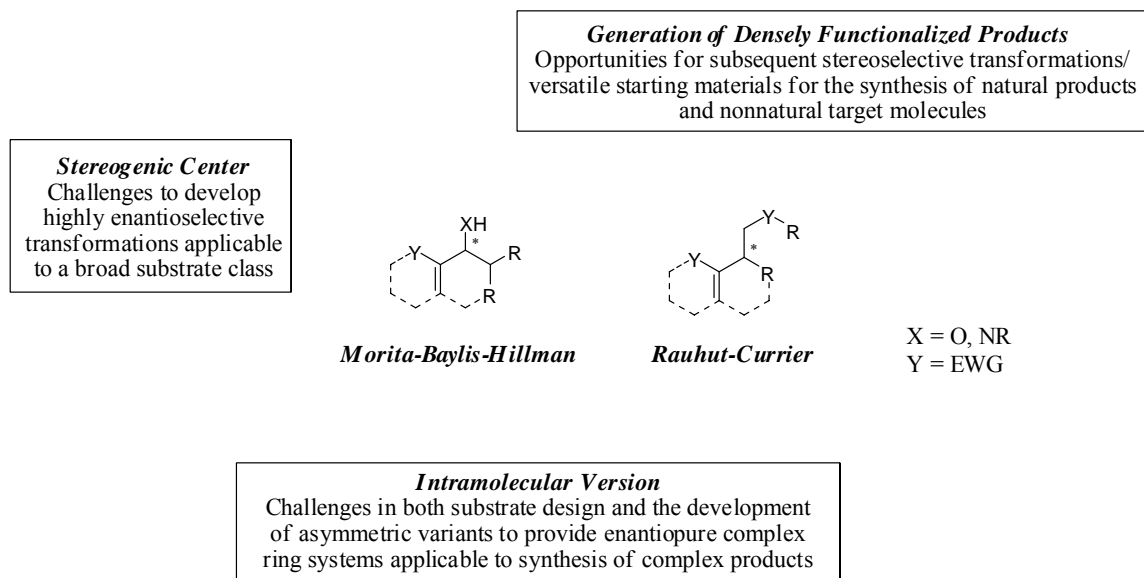


The development of methods for the formation of new carbon-carbon bonds as well as functional group transformations is central to the successful synthesis of target molecules. For this reason, both of these transformations hold great potential of becoming indispensable reactions in organic synthesis. Furthermore, the Morita-Baylis-Hillman and Rauhut-Currier reactions are of specific interest due to their ability to generate a new C-C bond in an atom economical manner, while generating a new stereogenic center and densely functionalized products that have served as substrates for

¹⁰⁷ Fuson, R. C. *Chem. Rev.* **1935**, *16*, 1-27. The definition of vinylogy is the transmission of stereoelectronic effects through conjugation. "The influence of a functional group may be felt at a distant point in the molecule when this position is connected by conjugated double bond linkages to the group...this concept allows the extension of the electrophilic or nucleophilic character of a functional group through the π -system of a carbon-carbon double bond." Although the term "vinylogous Morita-Baylis-Hillman" reaction has been used interchangeably with Rauhut-Currier in the literature, we have chosen to refer specifically to the coupling of two activated olefins through 1,4-addition as the Rauhut-Currier reaction, whereas the MBH reaction involves 1,2-addition. We make this distinction to emphasize the multidimensional differences between the two reactions

a multitude of subsequent transformations.¹⁰⁸ Although this class of reactions has been known in the scientific community for over four decades, these reactions still present many opportunities for multidimensional growth (Figure 3.2).¹⁰⁹ The development of a robust asymmetric version will require the design of highly efficient chiral catalysts, able to promote the coupling reaction of many diverse partners. Progress in the intramolecular (as well as asymmetric intramolecular) variant of both reactions will provide opportunities for the design of novel substrates leading to complex products with multiple stereogenic centers. Finally, the dense functionality present in the MBH and RC products offers many possibilities for further elaboration and the synthesis of natural products as well as nonnatural target molecules.

Figure 3.2: Opportunities for advancement in the MBH and RC reactions.



¹⁰⁸ (a) Lee, K. Y.; Gowrisankar, S.; Kim, J. N. *Bull. Kor. Chem. Soc.* **2005**, 26, 1481-1490. (b) Masson, G.; Housseman, C.; Zhu, J. *Angew. Chem., Int. Ed.* **2007**, 46, 4614-4628.

¹⁰⁹ Basavaiah, D.; Rao, K. V.; Reddy, R. J. *Chem. Soc. Rev.* **2007**, 36, 1581-1588.

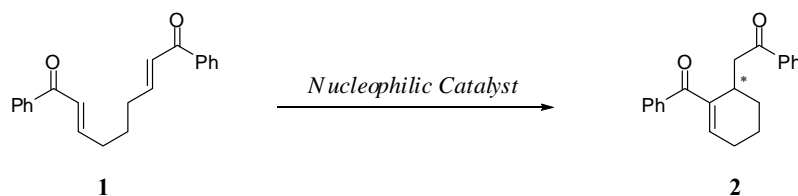
Importantly, until our report in 2007, the asymmetric Rauhut-Currier reaction was unknown.¹¹⁰ Herein, we present the natural extension of the intramolecular MBH reaction to allow the use of vinylogous reaction partners in the Rauhut-Currier reaction and demonstrate the use of a single amino acid derivative of cysteine as a highly selective catalyst to provide cyclized products in up to 70% yield and 95% ee.¹¹¹

3.2 Development of the Enantioselective Intramolecular RC Reaction

3.2.1 Nitrogen-Based Nucleophiles

Our study of the intramolecular Rauhut-Currier reaction commenced with the investigation of the cycloisomerization shown in Scheme 3.1. In analogy to our findings in the Morita-Baylis-Hillman reaction,¹¹² we were intrigued with the possibility of using our optimized co-catalytic system (pipercolinic acid/*N*-methylimidazole (NMI)) and protic reaction conditions (THF-H₂O) to extend the MBH methodology to include a vinylogous reaction partner.

Scheme 3.1: Intramolecular Rauhut-Currier reaction.



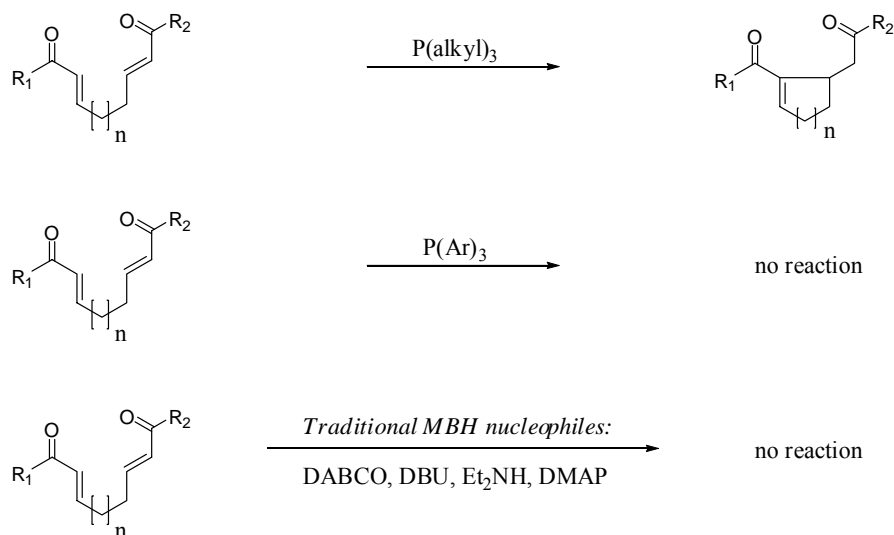
¹¹⁰ Gladysz and co-workers reported a moderately enantioselective intramolecular RC reaction later in the same year: Seidel, F.; Gladysz, J. A. *Synlett* **2007**, 6, 986-988. Please refer to Chapter 2 for a full discussion.

¹¹¹ Aroyan, C. E.; Miller, S. J. *J. Am. Chem. Soc.* **2007**, 129, 256-257.

¹¹² Please refer to Chapter 1 for a detailed discussion of our development of an enantioselective MBH reaction.

From previous reports in the literature, we began our investigation with the knowledge that the RC cycloisomerization differs in reactivity when compared to its MBH counterpart.¹⁰⁶ For example, trialkylphosphines were reported to be sufficiently reactive to catalyze the cycloisomerization of bis(enone) **1** to **2**. On the other hand, triarylphosphines were unreactive. Additionally, nitrogen-based nucleophiles, which were traditionally successful catalysts of the MBH reaction, were incapable of catalyzing the analogous RC cyclization reaction (Scheme 3.2).¹¹³

Scheme 3.2: Phosphine- and nitrogen-based catalysis of the RC reaction.

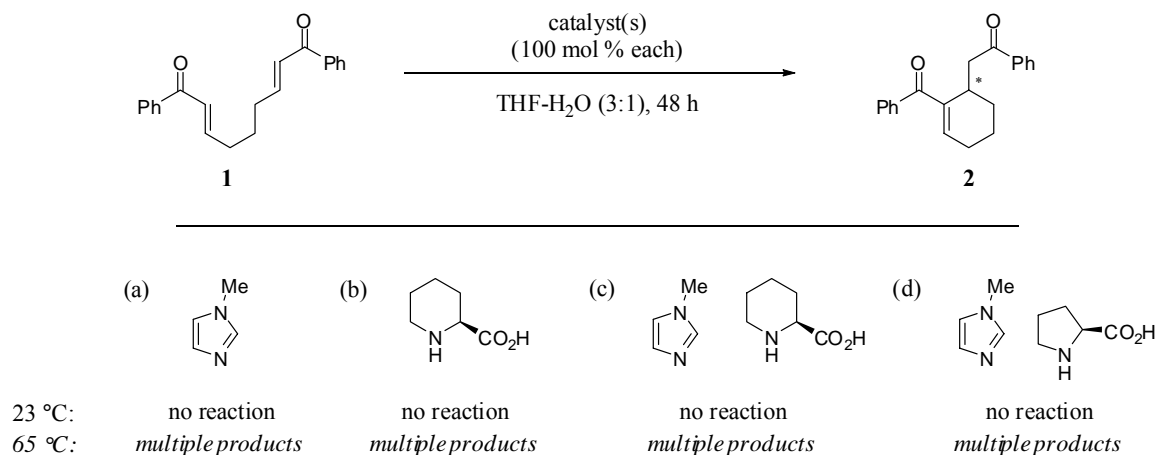


Despite reports that amine-based nucleophiles were ineffective at catalyzing this vinylogous reaction, we had previously displayed an impressive enhancement of reactivity in the MBH reaction by employing combination catalysis. Therefore, we were prompted to examine co-catalytic amines once again with the hope that the RC cyclization would benefit from a similar heightened reactivity. Accordingly, bis(enone) **1**

¹¹³ (a) Frank, S. A.; Mergott, D. J.; Roush, W. R. *J. Am. Chem. Soc.* **2002**, *124*, 2404-2405. (b) Wang, L.-C.; Luis, A. L.; Agapiou, K.; Jang, H.-Y.; Krische, M. J. *J. Am. Chem. Soc.* **2002**, *124*, 2402-2403.

was subjected to the previously optimized reaction conditions (THF-H₂O, 3:1) employing *N*-methylimidazole (NMI) (entry a, Figure 3.3), pipercolinic acid (entry b), and the co-catalytic combination of NMI/pipercolinic acid (entry c). Unfortunately, we were not able to successfully promote the cycloisomerization reaction employing these conditions, and under forcing conditions (65 °C, 48 h) we obtained significant decomposition of the starting material. The co-catalytic combination of NMI/proline¹¹⁴ was examined as well, however, it provided similar results with no reaction at room temperature and decomposition upon heating (entry d).

Figure 3.3: Investigation of co-catalysis in the RC cyclization.



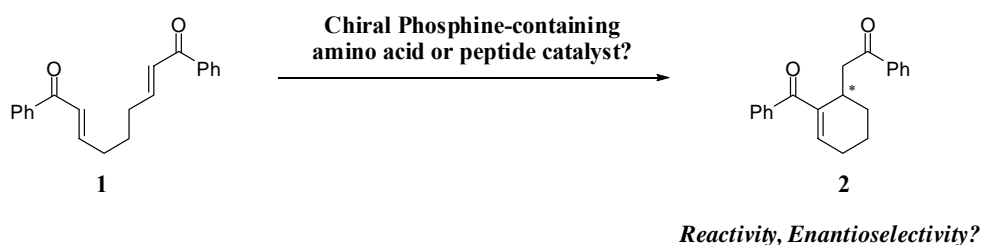
3.2.2 Phosphorous-Based Nucleophiles

Undaunted by the ineffectiveness of our amine-based catalysts, we turned to the more reactive phosphine-based catalysts, mindful that the steric and electronic environment would play a critical role in reactivity. In analogy to previous work in our laboratory, where a nucleophilic moiety (NMI) was incorporated into small peptide-based

¹¹⁴ For the use of NMI/proline in the MBH reaction, please refer to Chapter 1 and the references therein.

catalysts (as a modified histidine residue) to confer high levels of enantioselectivity,¹⁰⁵ we were intrigued with the possibility of employing a similar chiral phosphine-based catalyst in the RC reaction. In this sense, we were interested in determining if we could use a phosphine-containing amino acid or peptide catalyst to promote an enantioselective variant of the Rauhut-Currier reaction by taking advantage of the chiral environment provided by the amino acid or peptide secondary structure (Scheme 3.3).

Scheme 3.3: Chiral phosphine catalyst to promote an enantioselective RC reaction?

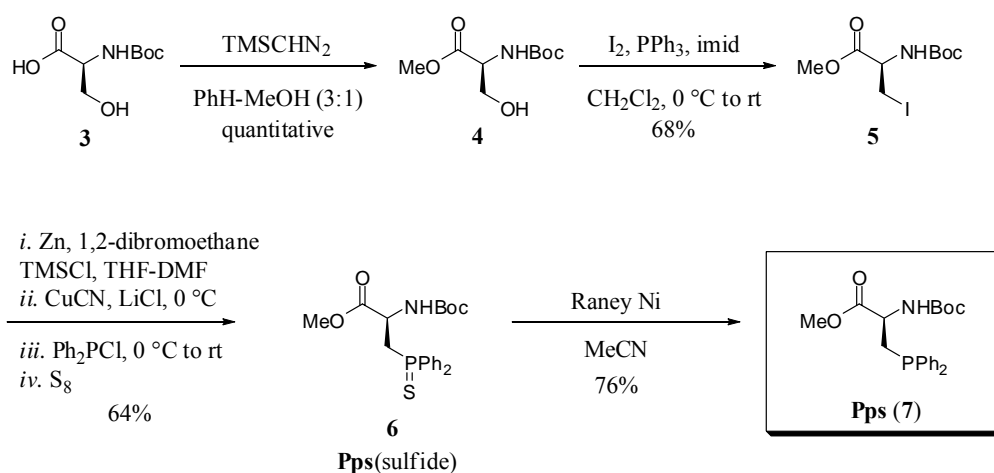


We began our study by focusing on diaryl phosphine-containing peptides due to their relative stability (compared with trialkylphosphines). Specifically, we were interested in using the known chiral phosphine-based amino acid diphenylphosphinoserine (Pps, **7**) which contains a β -stereogenic center. Gilbertson and co-workers have pioneered the use of Pps by incorporating the amino acid into peptides used as phosphorous-based metal ligands for various transformations such as hydrogenation and alkylation.¹¹⁵ Following Gilbertson's work, Pps was synthesized in four steps from commercially available Boc-Ser. Protection of the amino acid as the corresponding methyl ester (**4**, quantitative), was followed by conversion to Boc-

¹¹⁵ (a) Gilbertson, S. R.; Chen, G.; McLoughlin, M. *J. Am. Chem. Soc.* **1994**, *116*, 4481-4482. (b) Greenfield, S. J.; Gibertson, S. R. *Synthesis* **2001**, *15*, 2337-2340. (c) Agarkov, A.; Greenfield, S. J.; Xie, D.; Pawlick, R.; Starkey, G.; Gilbertson, S. R. *Biopolymers: Pept. Sci.* **2006**, *84*, 48-73.

protected 3-iodo-alanine methyl ester **5** (68%). Subsequently, **5** was converted to the zinc iodide with activated zinc and then treated with a stoichiometric amount of CuCN·2LiCl to create a reactive zinc/copper species. Addition of chlorodiphenylphosphine and protection of the phosphine as the sulfide provided enantiomerically pure Pps(sulfide) **6** in 64% yield. The less stable, desired Pps amino acid (**7**) was liberated prior to use by reaction with Raney nickel (Scheme 3.4).¹¹⁶

Scheme 3.4: Chiral phosphine-containing amino acid (Pps) preparation.

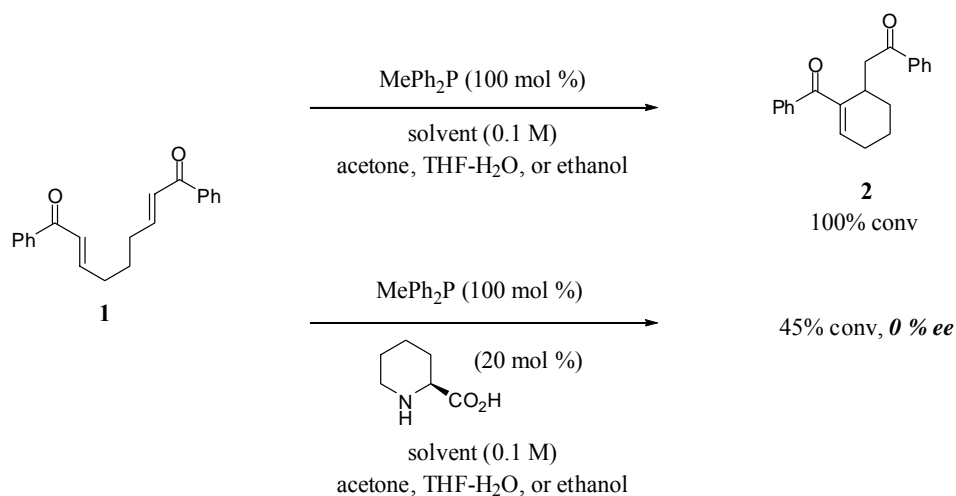


Prior to testing the chiral amino acid (**7**), it was imperative to establish the level of reactivity of phosphines in the RC reaction. As previously described, trialkylphosphines have been reported to catalyze the cycloisomerization of bis(enone) **1** to **2**, while triarylphosphines were not reactive enough and provided only recovered starting material (Scheme 3.2). Therefore, methyldiphenylphosphine (MePh₂P), the achiral counterpart to Pps, was tested as a model catalyst to provide insight into the relative reactivity of various substituted phosphines. Bis(enone) **1** was thus subjected to MePh₂P

¹¹⁶ Pps is not as air-sensitive as trialkylphosphines, however, it was found that Pps will oxidize completely to the corresponding diphenylphosphinoserine-oxide within 24 h when exposed to air.

(100 mol %), providing promising results in various solvents (acetone, THF-H₂O, or ethanol); the RC reaction underwent full conversion to the desired product within 12 hours (Figure 3.4). Encouraged by this initial data, we briefly investigated the possibility of employing combination catalysis with this new phosphine-based nucleophilic moiety. Therefore, bis(enone) **1** was subjected to MePh₂P in combination with pipercolinic acid (as in the MBH reaction), however preliminary experimentation suggested the presence of pipercolinic acid was deleterious to the phosphine-promoted RC reaction and resulted in less than 50% conversion to **2**.

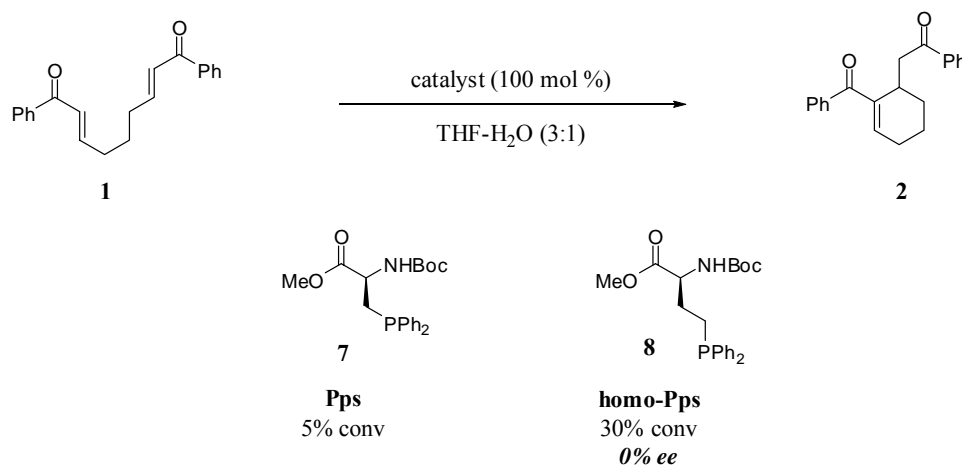
Figure 3.4: Catalysis of **1** to **2** with achiral MePh₂P.



Having established sufficient catalysis of the desired cyclization reaction with the model catalyst, methyldiphenylphosphine, we next examined catalysis employing the chiral variant, amino acid **7** (Figure 3.5). Unfortunately, the reactivity of MePh₂P did not translate to the amino acid and upon exposure of bis(enone) **1** to Pps at room temperature, only 5% conversion to **2** was obtained. We hypothesized that steric demand near the phosphorous center, and the inductive electron-withdrawing affect of the amino acid

functionality, interfered with productive enone addition. Thus, the less hindered and electronically more reactive homo-Pps (**8**) was synthesized and tested.¹¹⁷ However, this single amino acid catalyst was only modestly more reactive (30% conversion) and, not surprisingly, did not induce enantioselectivity. Consequently, we determined the relative order of reactivity of phosphine nucleophiles in this RC cyclization to increase with the number of aliphatic substituents, with the amino acid of interest being unreactive in the Rauhut-Currier reaction: $\text{Bu}_3\text{P} > \text{MePh}_2\text{P} \gg \gg \text{homo-Pps} \gg \text{Pps} > \text{Ph}_3\text{P}$.

Figure 3.5: Catalysis of the RC reaction with catalysts **7** and **8**.



3.3 Chalcogenides

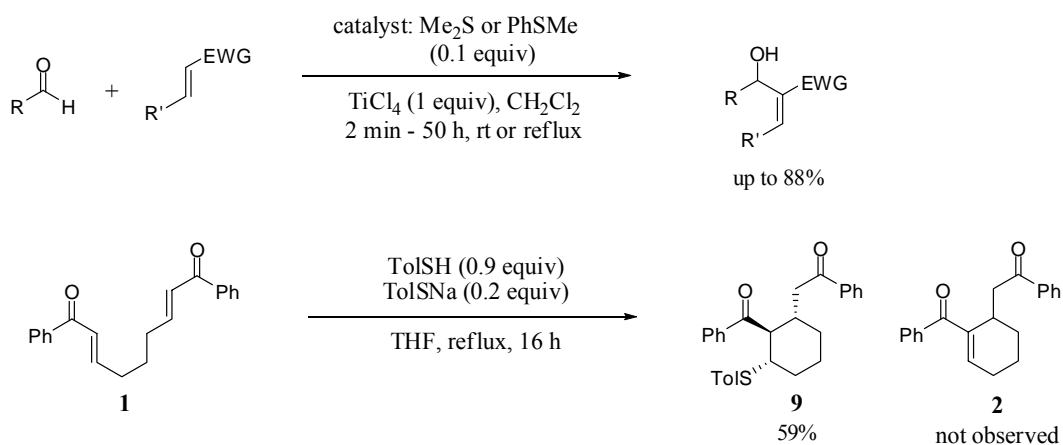
3.3.1 Overview of Chalcogenides in MBH-Type Reactions

During our initial investigation into the RC reaction, it became clear that the development of a powerful catalyst would require an entirely new methodology, and that our previous work in the Morita-Baylis-Hillman reaction would not be applicable here. Hence, during the study of nitrogen and phosphorous-based catalysts, we simultaneously

¹¹⁷ homo-Pps **8** was synthesized in analogy to Pps (**7**) from commercially available Boc-L-homoserine.

investigated the possibility of a thiolate-promoted cycloisomerization. Various chalcogenides have been reported as catalysts in MBH-type reactions; however, dialkyl chalcogenides require Lewis acid activation to overcome their low reactivity¹⁰⁶ and reactions catalyzed by monoalkyl chalcogenides terminate without elimination of the catalyst (Scheme 3.5).¹¹⁸ For example, the intermolecular MBH reaction can be promoted with catalytic dimethyl sulfide or thioanisole by employing stoichiometric amounts of titanium tetrachloride to provide the desired products in up to 88% yield. Additionally, Murphy and co-workers demonstrated the cyclization of bis(enone) **1** catalyzed by thiophenol and sodium thiophenolate, however they obtained cyclized addition product **9** instead of the desired Rauhut-Currier product, **2**.

Scheme 3.5: Chalcogenide catalysis of MBH-type reactions.



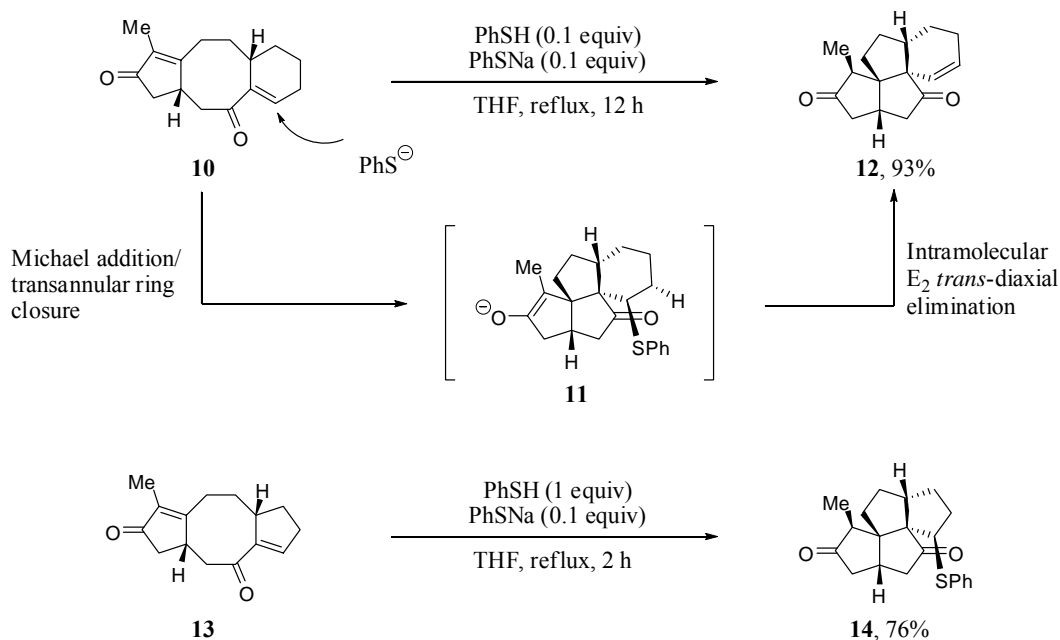
In a unique example by Moore and co-workers,¹¹⁹ they demonstrated the cycloisomerization of tricyclic bis(enone) **10** catalyzed by thiophenol and sodium

¹¹⁸ (a) Dinon, F.; Richards, E.; Murphy, P. J.; Hibbs, D. E.; Hursthouse, M. B.; Malik, K. M. A. *Tetrahedron Lett.* **1999**, *40*, 3279-3282. (b) Brown, P. M.; Käppel, N.; Murphy, P. J. *Tetrahedron Lett.* **2002**, *43*, 8707-8710.

¹¹⁹ Erguden, J. K.; Moore, H. W. *Org Lett.* **1999**, *1*, 375-377.

thiophenolate (Figure 3.6). This unusual transformation was believed to proceed through the conjugate addition of thiolate to substrate **10** which then underwent a transannular Michael reaction to provide intermediate **11**. From molecular modeling, these authors determined that the three-dimensional conformation of the molecule placed the generated enolate in close proximity to the β -proton of the thiophenolate leaving group. Thus, the enolate was able to induce an intramolecular E_2 *trans*-diaxial elimination to produce desired product **12** and regenerate the thiophenolate catalyst. Interestingly, and more representative of general thiol catalysis, in a very similar transformation involving homolog **13** (containing a five-membered ring versus a six-membered ring), the requisite intermediate was no longer in proper alignment for the elimination reaction and product **14** was isolated when a stoichiometric quantity of thiophenol was employed.

Figure 3.6: Catalysis of the RC reaction with thiophenol and thiophenolate.



3.3.2 Examination of Cysteine-Based Catalysis

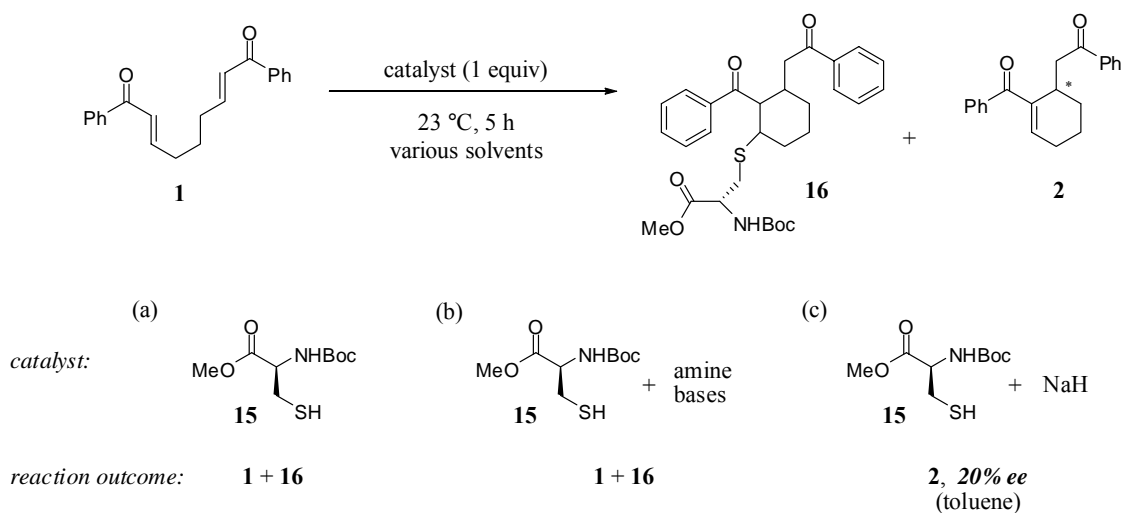
We began our study of the thiolate-promoted RC cycloisomerization with derivatives of cysteine (Cys) in the hope that upon demonstration of sufficient reactivity, the amino acid could be embedded into a peptide in order to achieve substantial enantioselectivity. However, unlike catalysis with nitrogen- or phosphorous-based catalysts, our new study began with many basic questions. Would cysteine be reactive enough to catalyze the desired RC transformation without the use of a Lewis acid? If we could catalyze the initial conjugate addition and cyclization steps, would our system be capable of promoting the final elimination step to regenerate the catalyst and deliver the desired cyclization products? And finally, would we be able to catalyze the transformation with discernable levels of stereoinduction using a cysteine nucleophile embedded into a peptide, effectively adding a new nucleophile to our catalytic tool box?¹²⁰

Beginning with the cyclization illustrated in Figure 3.7 (entry a), we were encouraged to find that the simple protected amino acid, **15**, was able to catalyze the reaction. However, as anticipated, catalyst elimination was a problem and intermediate **16** was isolated in addition to recovered starting material. Furthermore, Boc-Cys-OMe (**15**) in combination with various amine bases (such as triethyl amine, Hünig's base, diaza(1,3)bicyclo[5.4.0]undecane (DBU), and 2,6-lutidine) was not able to promote the elimination reaction in order to generate desired product **2** (entry b, Figure 3.7). Excitingly, we determined that by incorporating a stronger base, NaH, in combination

¹²⁰ Please refer to Chapter 1 for a discussion of alternative nucleophilic moieties embedded in small peptide-based catalysts to promote various selective processes.

with the Cys-based catalyst, we were able to promote the full transformation of bis(enone) **1** to provide **2**. Most importantly, not only were we able to catalyze the cyclization, we determined that this simple protected amino acid was able to promote the desired transformation with stereinduction, 20% ee. Although the enantioselectivity was modest, we were nonetheless surprised to find that *a more elaborate secondary structure was not needed to separate the energetics of diastereomeric transition states*. Thus, we decided to proceed in our study with the investigation of diverse reaction parameters using a single amino acid derivative as the catalyst.

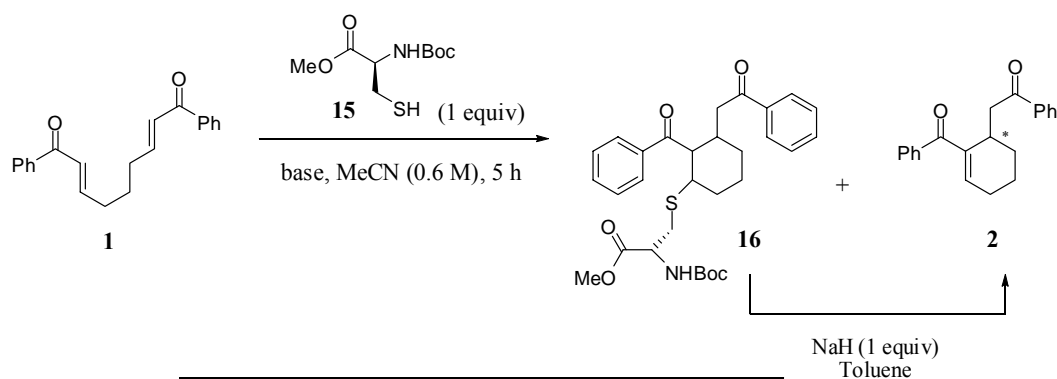
Figure 3.7: Catalysis of the RC reaction with catalyst **15**.



Realizing that the choice of base was critical to product distribution, we first performed a base screen in the RC reaction promoted by the Boc-protected Cys-based catalyst (**15**). In addition to the amine bases already tested in combination with **15**, sodium carbonate and sodium hydroxide were examined in the cyclization of bis(enone) **1** (Table 3.1). The results were similar to those obtained when using amine bases, such that we obtained a mixture of starting material and cyclized addition product **16**, without

production of the desired product. Importantly, NaH, KH, and *t*-BuOK provided the cleanest transformation while the stronger bases, LDA and *n*-BuLi (thiolate was preformed to avoid conjugate addition), led mainly to decomposition. It is interesting to note that **16** can be converted to **2** upon isolation and subjection to NaH, suggesting that it is indeed an intermediate en route to desired product **2**. This proved to be important in the following studies, as it required the fine-tuning of reaction conditions to promote the full reaction pathway of the cyclization followed by final elimination of the catalyst.

Table 3.1: Base screen in the RC reaction.

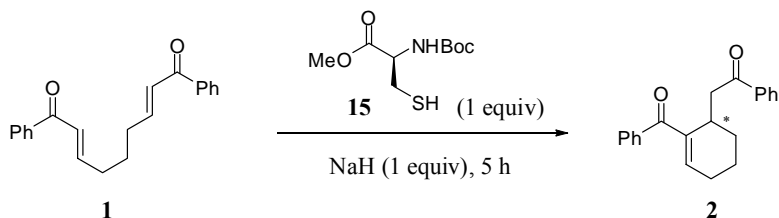


entry	base (1 equiv)	reaction outcome
1	Na ₂ CO ₃	1 + 16
2	NaOH	multiple products
3	<i>t</i> -BuONa	2 , by-products
4	<i>t</i> -BuOK	2 , by-products
5	KH	2 , by-products
6	LDA	multiple products
7	LHMDS (THF)	multiple products
8	<i>n</i> -BuLi (THF)	multiple products

As in the case of the intramolecular MBH reaction, solvent was found to affect the vinylogous reaction. Catalysis of the RC reaction with Cys derivative **15** (1 equiv)

and sodium hydride (1 equiv) in various solvents (THF, ether, acetonitrile, *N,N*-dimethylformamide, hexanes, toluene, CH₂Cl₂, and acetone) all produced the desired product with varying degrees of enantioselectivity and by-product formation. Notably, acetonitrile and acetone provided the cleanest reactions with the highest levels of stereoinduction (39% and 38% ee, respectively) (Table 3.2).

Table 3.2: Solvent screen in the RC cyclization of **1** to **2** promoted by **15**.

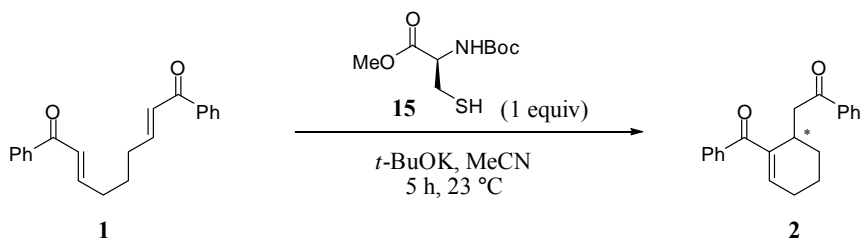


entry	solvent (0.6 M)	% ee (2)
1	THF	27
2	Et ₂ O	18
3	MeCN	39
4	DMF	29
5	hexanes	17
6	toluene	20
7	CH ₂ Cl ₂	26
8	acetone	38

Through careful optimization of solvent and base, we began to reveal a new catalytic system for the promotion of an enantioselective variant of the RC reaction. Due to inconsistencies in results when employing NaH, we decided to proceed in our optimization studies using *t*-BuOK, which provided indistinguishable results from those obtained when using NaH. Accordingly, further investigation of reaction conditions revealed that the stoichiometry of catalyst and base was extremely critical to product

distribution and levels of stereinduction in the cyclization. As illustrated in Table 3.3, the optimal ratio of catalyst/base was found to be 1:1.5. Under catalysis using fewer equivalents of base, the reaction terminated prematurely, leading to intermediate **16** as well as unidentifiable by-products. Alternatively, an excess in the amount of base employed furnished the desired product with varying degrees of decomposition. Additionally, greater dilution of the reaction concentration (0.1 M versus 0.9 M) provided the cleanest transformation of **1** to **2** with the highest levels of enantioselectivity. Therefore, the initial optimization of base, solvent, stoichiometry, and reaction concentration led to an exciting entry into enantioselective catalysis of the RC reaction, addressing our first two questions of (1) sufficient reactivity employing a Cys-based catalyst and (2) control of product formation through final elimination and regeneration of the catalyst. Exposure of bis(enone) **1** to catalyst **15** along with *t*-BuOK (1.5 equiv) in acetonitrile (0.1 M) at room temperature afforded the desired product **2** with 36% enantioselectivity (Table 3.3).

Table 3.3: Effects of base stoichiometry and reaction concentration.



<i>t</i> -BuOK (equiv)	reaction outcome ^a	conc (M)	reaction outcome ^b
0.5	2 , 16 , multiple products	0.1	2 : 36% ee , minor by-products
1.0	2 , 16 , by-products	0.3	2 : 35% ee , minor by-products
1.5	2 : 35% ee	0.6	2 : 25% ee , 16 , by-products
2.0	2 : 35% ee , by-products	0.9	2 : 11% ee , 16 , by-products

^a reaction performed at 0.1 M.

^b reaction performed with 1.5 equiv *t*-BuOK.

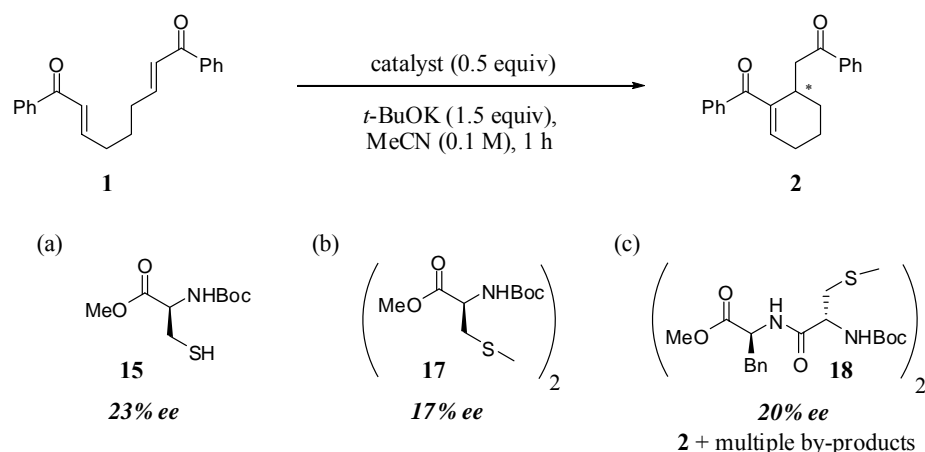
3.3.3 Cystine Catalysis

Our next goal was to address the third question that we initially posed: would we be able to catalyze the desired transformation with discernable levels of stereinduction using a cysteine-based nucleophile embedded in a peptide? In our attempts to answer this question and investigate optimization of the cysteine moiety, we remained enthusiastic that such a simple catalyst (**15**) was able to show measurable levels of stereinduction and we were therefore optimistic that an elaborate secondary structure may not ultimately be required to achieve high levels of enantioselectivity.

Although cysteine is stable, it is known that dipeptides containing a cysteine residue are readily oxidized to the corresponding disulfide dimer. Therefore, before synthesizing various dipeptides to examine the Cys amino acid embedded into more complex secondary structures, we were interested in the possibility of catalyzing the transformation with the corresponding dimer of the protected cysteine catalyst, **17**. To

our surprise, employment of the Boc-protected cysteine catalyst (**17**) promoted cyclization of bis(enone) **1** to **2** with comparable enantioselectivity (17% ee) to that of monomeric Boc-protected cysteine (**15**, 23% ee), using *sub-stoichiometric* catalyst loading (Figure 3.8). One dipeptide (**18**) was synthesized using solution phase peptide synthesis and tested in the analogous reaction. Although stereinduction was similar (20% ee), the reaction suffered from poor chemoselectivity compared to that of catalyst **15** or **17**, and led to the formation of multiple by-products.

Figure 3.8: Catalysis of the RC reaction with cysteine derivatives.

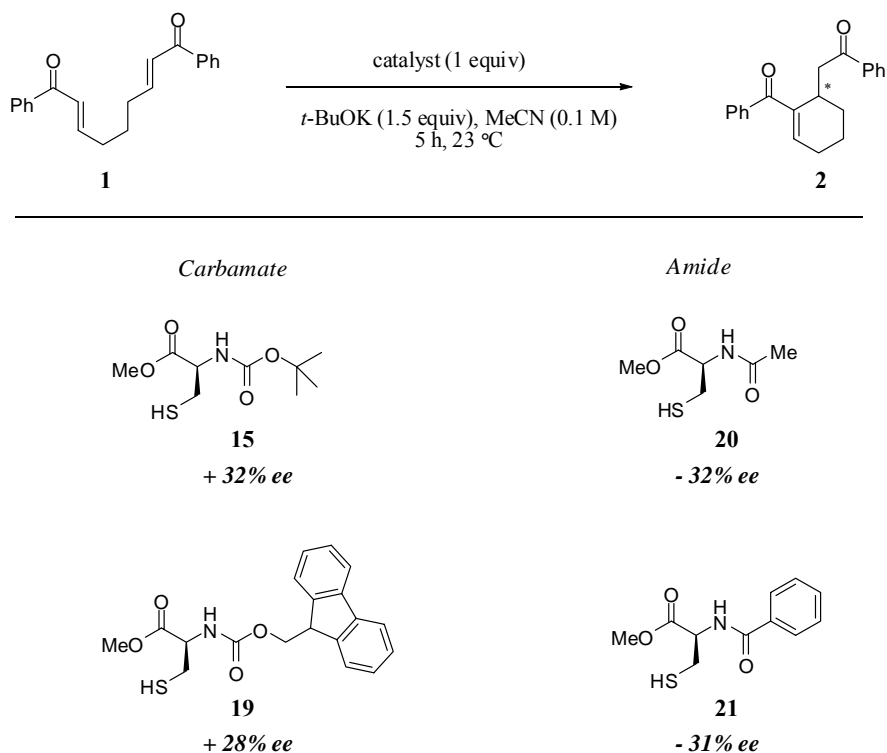


3.3.4 Development of Cysteine Derivatives

While the incorporation of Cys into an oligopeptide was just beginning, we were very interested in maintaining the simplicity of our catalyst. Therefore, we simultaneously began an optimization study of the cysteine component by considering moderate changes. The exploration of simple SAR (structure-activity relationship) around the mono-amino acid led to an intriguing result. Changing the nitrogen protecting group from a carbamate to an amide caused a complete reversal in the sense of

asymmetric induction (Figure 3.9). Under the optimized conditions, Boc-protected (**15**) and Fmoc-protected (**19**) cysteine promoted the cyclization of **1**, providing **2** with 32% and 28% enantiomeric excess, respectively. Amide-protected compounds **20** and **21** led to similar levels of stereoselectivity (-32%, -31% ee), however provided the opposite enantiomer in excess.

Figure 3.9: Simple SAR of the nitrogen protecting group of catalyst **15**.



3.3.5 Protic Additives in the RC Reaction

Research efforts in Morita-Baylis-Hillman-type reactions from other groups have demonstrated the potential of protic additives to accelerate the reaction and affect product

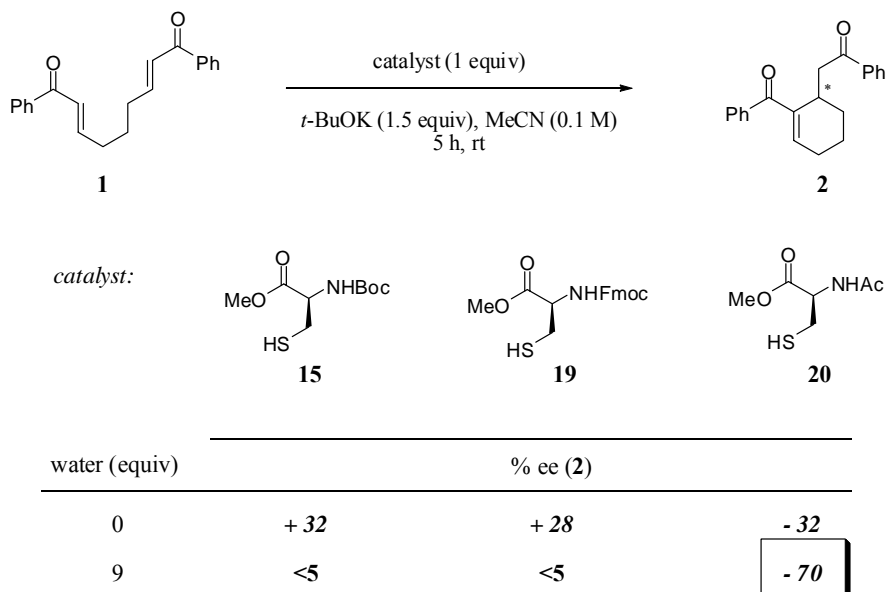
distribution.¹²¹ In our investigation of the Morita-Baylis-Hillman reaction, we learned that protic additives had a dramatic effect not only on the reaction rate and on product distribution, but importantly on the enantioselectivity of the desired transformation as well.¹²² Although, the MBH reaction and Rauhut-Currier reaction have proven to be highly distinct from one another in our laboratory, we were nonetheless interested in exploring the possibility of employing protic additives in this transformation as well.

Interestingly, we discovered that the incorporation of a protic additive did indeed have a dramatic effect on enantioselectivity in the Rauhut-Currier reaction, with the outcome strictly dependent upon the catalyst employed (Figure 3.10). For example, in the catalysis of **1** to **2** employing carbamate-protected catalysts **15** and **19**, the incorporation of water (9 equiv) was completely deleterious to stereoselection and provided only racemic product. *Most excitingly, when water was incorporated in the reaction with amide-protected catalyst 20, we observed a dramatic increase in enantioselectivity to 70% ee.* Hence, we discovered that we could promote the RC reaction with good levels of stereoselection using a single amino acid catalyst, lending credence to our hypothesis that a more complex secondary structure would not be critical to obtaining a highly stereoselective reaction.

¹²¹ (a) Methot, J. L.; Roush, W. R. *Org. Lett.* **2003**, *5*, 4223-4226. (b) Aggarwal, V. K.; Dean, D. K.; Mereu, A.; Williams, R. *J. Org. Chem.* **2002**, *67*, 510-514. (c) Keck, G. E.; Welch, D. S. *Org. Lett.* **2002**, *4*, 3687-3690 and references therein.

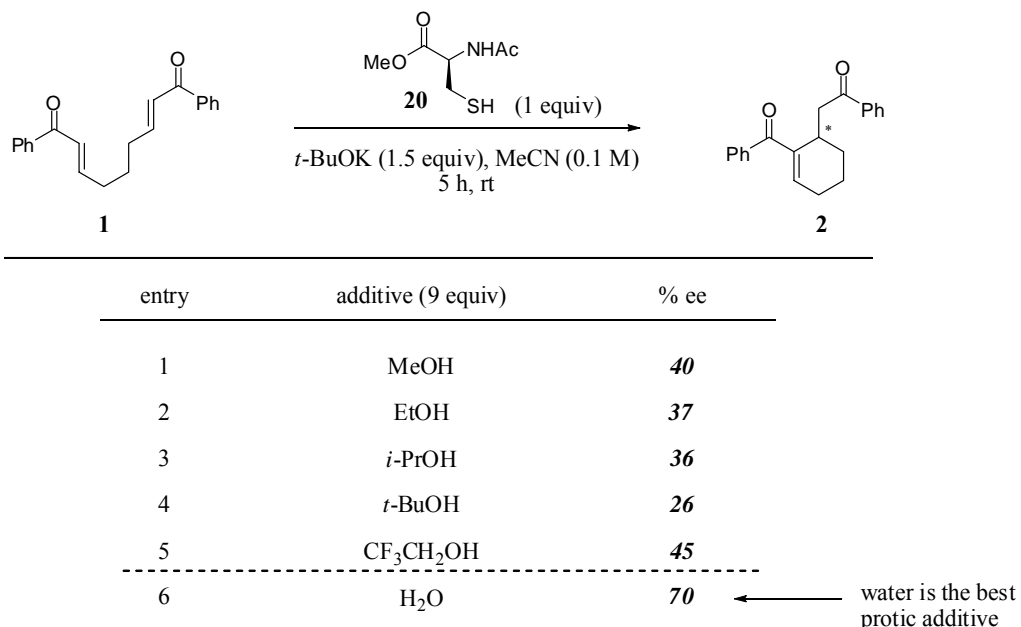
¹²² (a) Methot, J. L.; Roush, W. R. *Org. Lett.* **2003**, *5*, 4223-4226. (b) Aggarwal, V. K.; Dean, D. K.; Mereu, A.; Williams, R. *J. Org. Chem.* **2002**, *67*, 510-514. (c) Keck, G. E.; Welch, D. S. *Org. Lett.* **2002**, *4*, 3687-3690 and references therein.

Figure 3.10: Effects of a protic additive in the cyclization of **1** to **2** promoted by various Cys-protected derivatives.



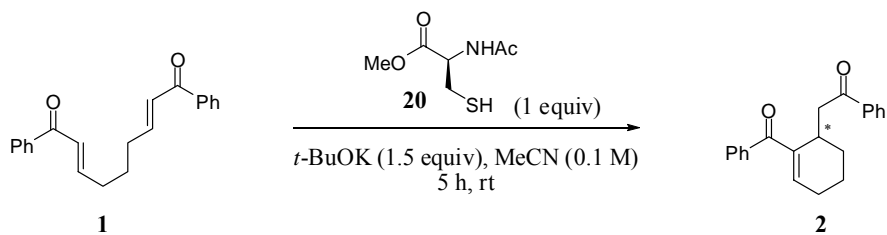
To determine if this effect was unique to water, we were prompted to examine various alternative hydroxylic additives in the transformation of **1** to **2** catalyzed by acetate-protected Cys-derivative **20**. As illustrated in Table 3.4, the addition of methanol, ethanol, and 2-propanol (9 equiv) led to a modest enhancement in selectivity, providing product **2** with approximately a 10% increase in ee over the analogous reaction with no additive (entries 1-3, 40%, 37%, and 36% ee, respectively; cf. 32% ee with no protic additive). The addition of 2,2,2-trifluoroethanol provided a further enhancement in enantioselectivity (45% ee), while incorporation of *t*-butanol led to a slight decrease in enantioselectivity (26% versus 32% ee).

Table 3.4: Effect of various additives in the RC reaction catalyzed by **20**.



With water leading to the most dramatic effect as a protic additive, we next explored the exact requirements of the system. Indeed, we determined that a precise quantity of water was required. Notably, increased selectivity from 42% ee (1 equiv of water, entry 2, Table 3.5) to 81% ee was achieved with the addition of 20 equiv of water to the acetonitrile solvent. A further increase in equivalents of water was deleterious, with a 2:1 mixture of MeCN-H₂O providing the desired product with only 10% enantiomeric excess (entry 11).

Table 3.5: Effects of water additive in the RC reaction catalyzed by **20**.



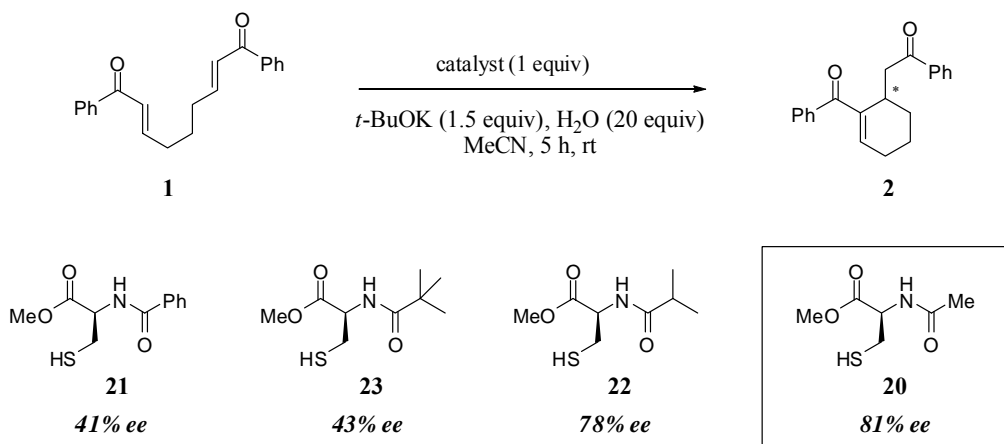
entry	water (equiv)	% ee
1	-	32
2	1	42
3	3	57
4	9	70
5	20	81
6	25	81
7	30	74
8	40	69
9	50	72
10	100	33
11	275	10

3.3.6 Optimization of Cysteine-Based Catalysis

Once we uncovered the dramatic effects of water on enantioselectivity in the RC cyclization, we looked further at the possibility of optimizing the cysteine-based catalyst. With the new reaction conditions in hand (20 equiv of water in bulk acetonitrile), we examined a series of *N*-amide-protected cysteine derivatives. As shown in Figure 3.11, when *N*-benzoyl-protected catalyst **21** was employed in the cyclization of **1** to **2**, a considerable decrease in enantioselectivity was seen (41% ee) as compared with catalyst **20** (81% ee). *N*-isobutyryl catalyst **22** provided comparable results (78% ee), whereas a

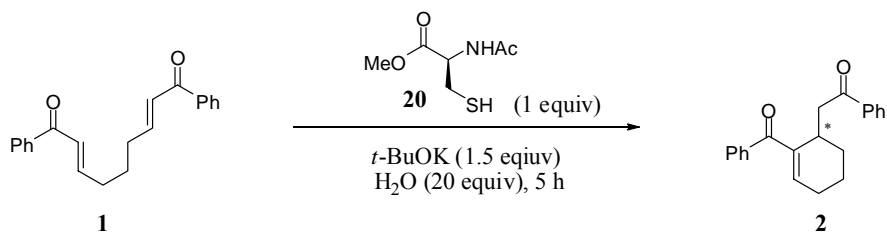
further increase in steric bulk of the protecting group led to a significant decrease in enantioselectivity (*N*-pivaloyl catalyst **23**, 43% ee).

Figure 3.11: Effects of various amide protecting groups on cysteine in the RC cyclization.



A minor study of solvent effects was revisited under the optimized aqueous reaction conditions (20 equiv H₂O in MeCN) in the cyclization reaction promoted by the optimal catalyst, **20**, which mainly led to eroded product enantioselectivity and resulted in the formation of by-products (Figure 3.12). Propionitrile led to a modest decrease in enantioselectivity (77% ee, entry 2), while deleterious results with THF were more pronounced (55% ee, entry 1).

Figure 3.12: Solvent effects with water additive in the RC cyclization of **1** to **2** promoted by **20**.

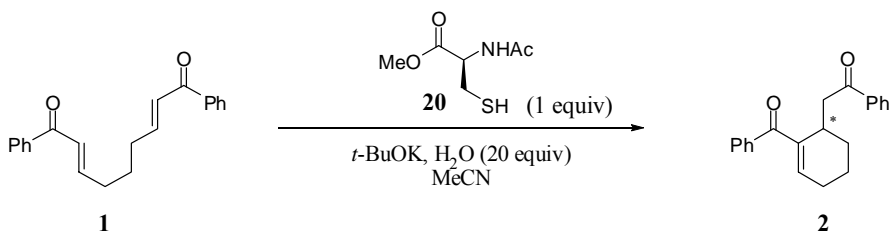


entry	solvent (0.1 M)	% ee
1	THF	55
2	Propionitrile	77
3	MeCN	81

Importantly, because we were able to develop a highly reactive catalytic system, able to promote the conversion of **1** to **2** within 5 hours at 23 °C, we believed there was an opportunity to use temperature control to further enhance the enantioselectivity. In beginning our investigation of temperature effects, we quickly learned there was a delicate balance required between the stoichiometry of the base, the reaction concentration, and the temperature of the reaction. For example, in cooling the reaction to -20 °C, we observed an increase in the level of stereoinduction (92% ee, entry 1, Table 3.6), albeit with a major decrease in the isolated yield (15%). At this reduced temperature, the final elimination step was prohibitive and the major isolated product was intermediate **16**. By fine-tuning the stoichiometry of the base and overall concentration, we were able to obtain excellent results. Consequently, increasing the quantity of t -BuOK led to higher conversions and thus higher isolated yields (4 equiv, 47%, entry 2; 6 equiv, 57%, entry 3). This was demonstrated previously (Table 3.1) in the independent conversion of intermediate **16** to desired product **2** by isolation and subsection to the appropriate base. However, this also led to a simultaneous decrease in the

enantioselectivity of the reaction (84% and 77% ee, respectively). An explanation of the observed decrease in enantioselectivity in the presence of excess base will be proposed in the following discussion of mechanistic details. Nevertheless, by lowering the reaction concentration while maintaining a moderate quantity of base, we were able to preserve the enantioselectivity while obtaining good yield. This trend continued as we decreased the temperature further. For example, in going from -20 °C to -30 °C (entries 5 and 6) and finally to -40 °C (entries 7-10), we observed a continual improvement in enantioselectivity to 95% ee, however with a reduced yield of 39% (6 equiv *t*-BuOK, entry 7). Increasing the amount of base to 9 equiv provided good conversion to product **2** (74% yield, entry 9), again at the cost of selectivity (83% ee). Excitingly, by simply running the reaction for a longer amount of time, 24 h versus 5 h, we were delighted to find that we were able to catalyze the Rauhut-Currier reaction with high levels of enantioselectivity (95% ee) and synthetically useful yields (70%, entry 10).

Table 3.6: Optimization of reaction conditions in the RC cyclization reaction.



entry	temperature (°C)	concentration (M)	$t\text{-BuOK}$ (equiv)	time (h)	% yield	% ee
1	-20	0.1	1.5	5	15	92
2	-20	0.1	4	5	47	84
3	-20	0.1	6	5	57	77
4	-20	0.07	4	5	70	85

5	-30	0.07	4	5	27	94
6	-30	0.07	5	5	67	91

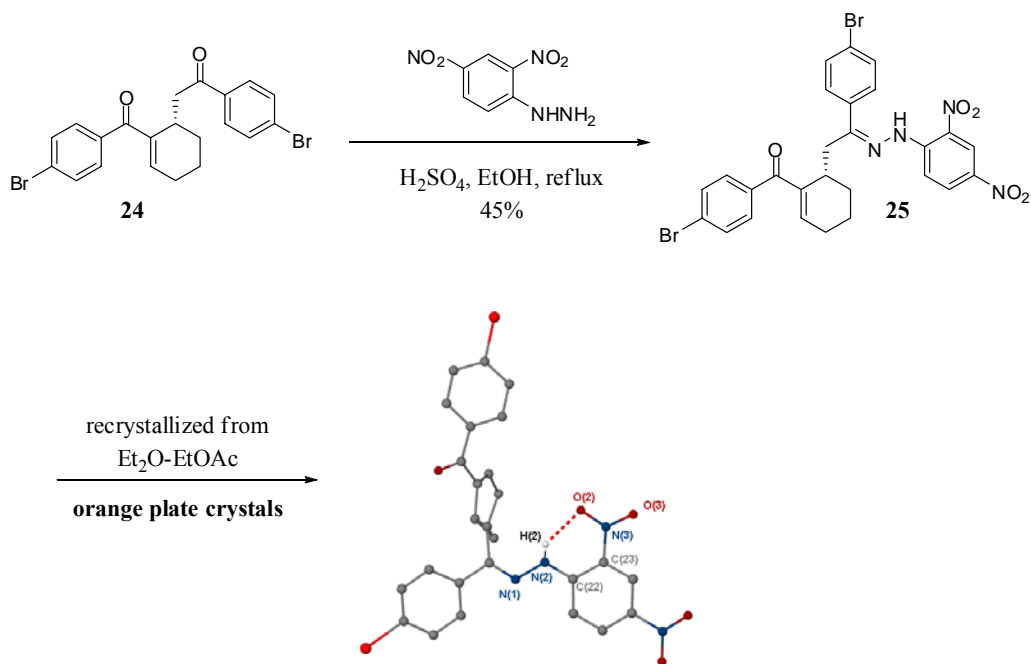
7	-40	0.05	6	5	39	95
8	-40	0.05	8	5	54	92
9	-40	0.05	9	5	74	83
10	-40	0.05	6	24	70	95

3.3.7 Determination of Absolute Stereochemistry

The absolute configuration of cyclization product **24** from the intramolecular RC reaction was determined by X-ray diffraction analysis of crystalline hydrazone derivative **25** following Brady's method.¹²³ As illustrated in Scheme 3.6, optically enriched *para*-bromo-substituted compound **24** (93% ee) was treated with a solution of 2,4-dinitrophenylhydrazine in ethanol and sulfuric acid to provide hydrazone **25** (45% yield), followed by recrystallization of the orange precipitate from diethyl ether and ethyl acetate to provide X-ray quality crystals.

¹²³ (a) Behforouz, M.; Bolan, J. L.; Flynt, M. S. *J. Org. Chem.* **1985**, *50*, 1186-1189. (b) Brady, O. L. *J. Chem. Soc.* **1931**, 756-759.

Scheme 3.6: Formation of hydrazone **25** for crystallization.



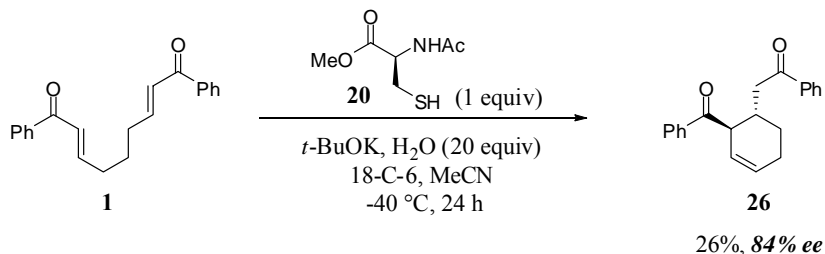
3.4 Mechanistic Studies

Excitingly, we have been able to use a single amino acid derivative to catalyze the first enantioselective Rauhut-Currier reaction. Although the simplicity of our catalytic system was empirically determined, it was initially unexpected, as we believed incorporation of the cysteine moiety into a more elaborate secondary structure would be necessary. Therefore, in order to provide a plausible mechanism of stereinduction, two key experiments were performed.

First, the cycloisomerization of bis(enone) **1** was run under optimized conditions in the presence of 18-crown-6 in order to sequester the potassium ion and determine its role in the reaction (Scheme 3.7). Expected product **2** was not observed; however,

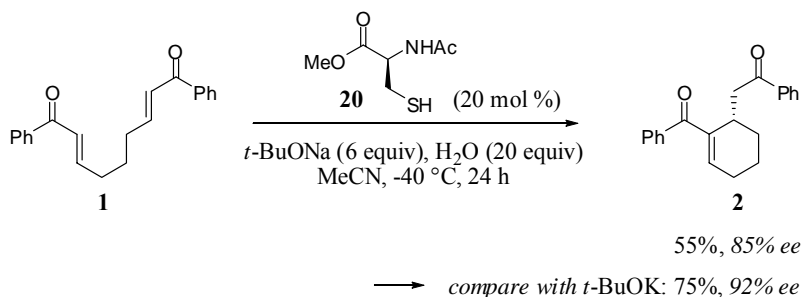
unconjugated cyclized product **26** was found to be the predominant product, albeit in low yield (26%) and with attenuated enantioselectivity (84% ee). Therefore, these results suggest that potassium ion chelation was essential to both product distribution and stereoselectivity.

Scheme 3.7: RC reaction under optimized reaction conditions with 18-crown-6.



In support of this hypothesis, the RC cycloisomerization was performed with catalyst **20** in the presence of sodium *tert*-butoxide versus the optimized conditions including potassium *tert*-butoxide (Scheme 3.8). Under otherwise identical reaction conditions, substitution of potassium with sodium afforded product **2** with attenuated yield (55%) as well as enantioselectivity (85% ee), further demonstrating the importance of the potassium counterion in promoting a highly efficient transformation.

Scheme 3.8: Use of sodium *tert*-butoxide versus potassium *tert*-butoxide in the RC cyclization.

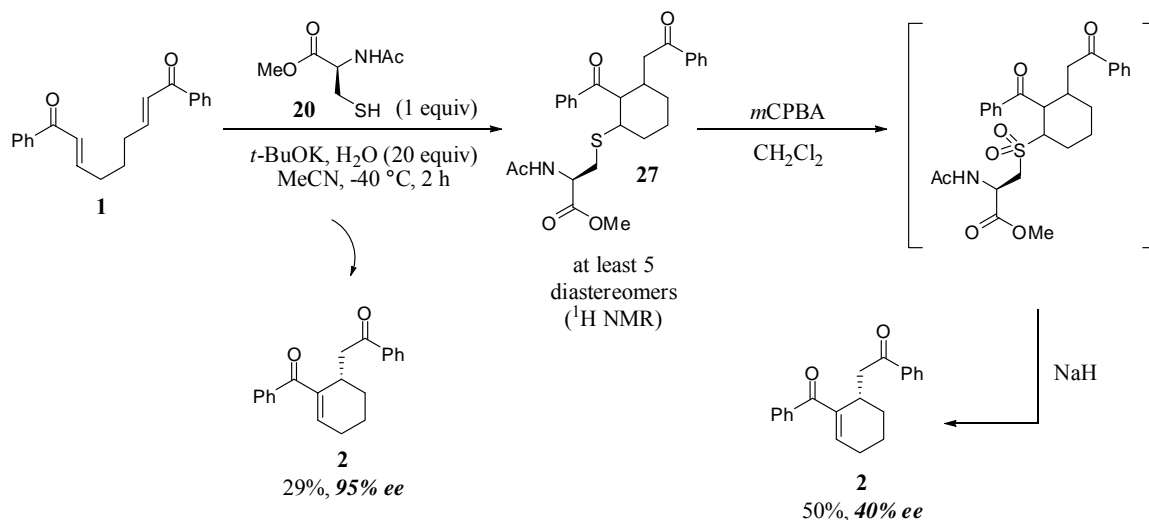


In the second experiment, bis(enone) **1** was subjected to the optimized cycloisomerization reaction conditions, however, the reaction was stopped after only two

hours instead of twenty-four hours (Scheme 3.9). As expected, we obtained the desired product (**2**) with high enantioselectivity (95% ee) and in reduced yield (29%) due to the short reaction time. Additionally, a mixture of five diastereomers of intermediate **27** was isolated, as determined by ¹H NMR. We then subjected intermediate **27** to oxidation and elimination under irreversible conditions (*i.* mCPBA, *ii.* NaH) to determine the enantioselectivity of the desired stereogenic center prior to any potential equilibration. Unlike the outcome under our optimized conditions, product **2** was isolated with reduced enantioselectivity of only 40% ee, which suggested that carbon–carbon bond formation was reversible under the optimized conditions and that abstraction of the α -H atom and extrusion of the catalyst that was the stereochemistry-determining step. These data are in agreement with the most recent mechanistic studies of MBH-type processes by the groups of Aggarwal and McQuade who have also proposed proton transfer/catalyst elimination to be rate-determining.¹²⁴

¹²⁴ For mechanistic studies regarding the MBH reaction, see: (a) Aggarwal, V. K.; Fulford, S.; Lloyd-Jones, G. C. *Angew. Chem., Int. Ed.* **2005**, *44*, 1706-1708. (b) Price, K. E.; Broadwater, S. J.; Walker, B. J.; McQuade, D. T. *J. Org. Chem.* **2005**, *70*, 3980-3987. (c) Price, K. E.; Broadwater, S. J.; Jung, H. M.; McQuade, D. T. *Org. Lett.* **2005**, *7*, 147-150. For mechanistic studies regarding the related aza-MBH reaction, please see: (d) Buskens, P.; Klankermayer, J.; Leitner, W. *J. Am. Chem. Soc.* **2005**, *127*, 16762-16763. (e) Raheem, I. T.; Jacobsen, E. N. *Adv. Synth. Catal.* **2005**, *347*, 1701-1708.

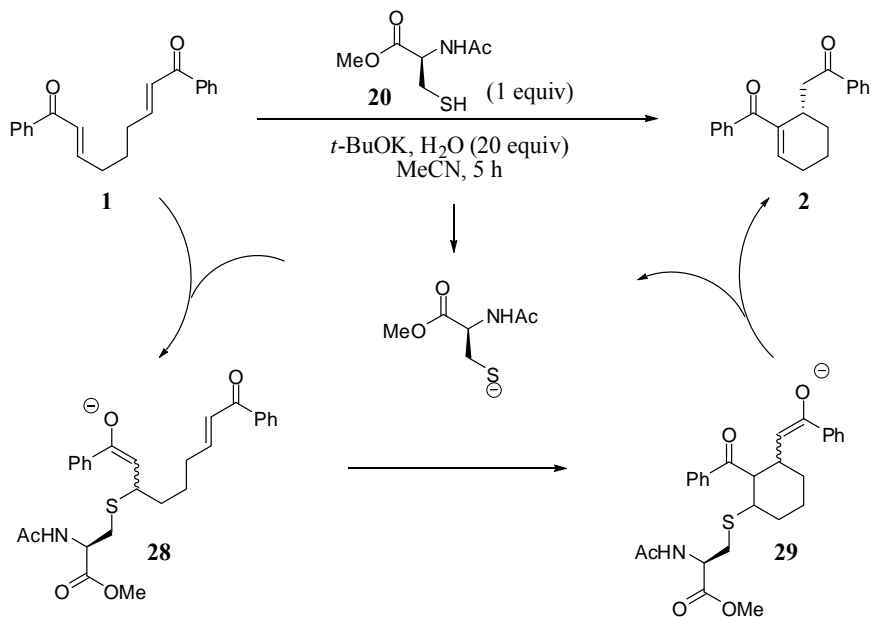
Scheme 3.9: Isolation of intermediate **27** and subjecting to irreversible elimination.



As in our studies of the MBH reaction, the mechanism of the RC reaction is not definitively known. However, based on these experiments and in analogy to the phosphine-catalyzed reactions,¹²⁵ we proposed that the mechanism of the reaction involved conjugate addition of the cysteine-based thiolate to bis(enone) **1** to form enolate **28** (Figure 3.13). Reversible intramolecular Michael addition would then afford cyclized intermediate **29**, followed by irreversible proton transfer and extrusion of the catalyst to generate the RC cyclization product **2** with regeneration of the catalyst. The final step, proceeding from intermediate **29** to desired product **2**, would therefore be the rate-determining and stereo-determining step.

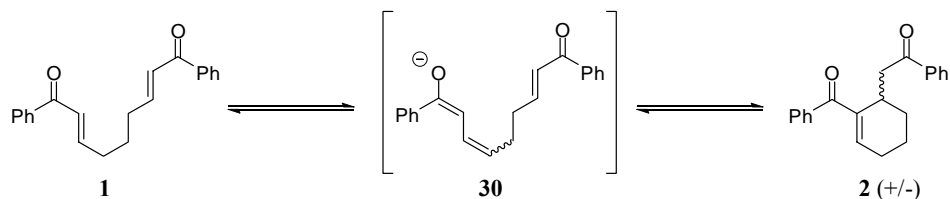
¹²⁵ Methot, J. L.; Roush, W. R. *Adv. Synth. Catal.* **2004**, *346*, 1035-1050.

Figure 3.13: Proposed mechanism of the Cys-catalyzed RC reaction.



As previously disclosed (3.3.6), a significant decrease in enantioselectivity was observed in the cyclization reaction when excess base was employed. We have determined that the integrity of product ee was not diminished by resubjection of the product to reaction conditions. Therefore, the decrease in enantioselectivity was not due to racemization of the product, but possibly due to an alternative mechanism, as shown in Scheme 3.10. In the presence of excess base, γ -deprotonation could lead to intermediate **30** which in turn would undergo cyclization and olefin isomerization to provide **2** (+/-).¹²⁶

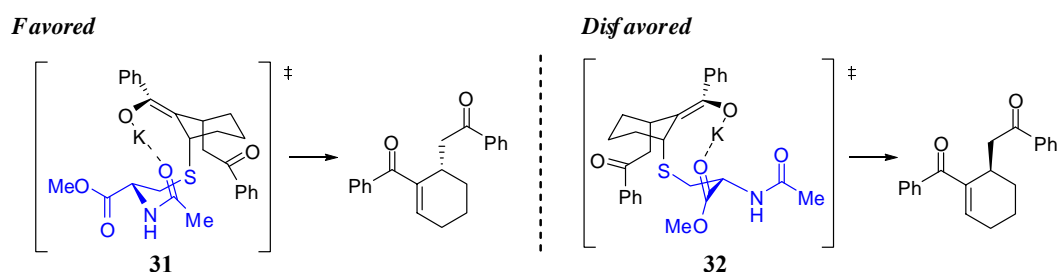
Scheme 3.10: Possible base promoted cyclization to provide racemic product.



¹²⁶ Hwu, J. R.; Hakimelahi, G. H.; Chou, C.-T. *Tetrahedron Lett.* **1992**, 33, 6469-6472.

In order to explain the formation of the observed enantiomer, we have proposed favored (**31**) and disfavored (**32**) transition state models (Figure 3.14). We speculate that the configuration allowing for a more stable potassium chelate between the enolate oxygen and the amide carbonyl on the catalyst would be favored (**31**), versus the analogous ester chelation,¹²⁷ **32**. The greater stability of structure **31** would then lead to a faster rate of elimination with subsequent formation of **2** in high enantiomeric excess.

Figure 3.14: Transition state models to explain formation of the observed enantiomer.



3.5 Reaction Scope

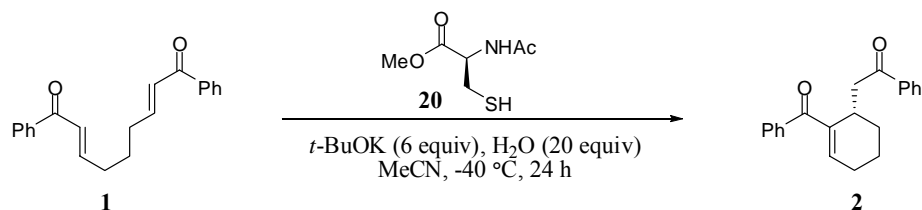
Traditionally, Morita-Baylis-Hillman and Rauhut-Currier-type reactions have been plagued with reactivity and selectivity issues, only to be resolved or partially solved for specific cases and narrow substrate scope. Therefore, it was our desire to not only develop a reactive system that was able to produce a highly enantiomerically enriched product, but also a set of conditions that were amenable to a broad class of substrates providing structurally complex products. Thus, with our set of optimized reaction conditions, we were eager to explore the full scope of this developed methodology.

All the studies presented thus far have included stoichiometric loading of the cysteine-based catalyst. An examination of catalyst loading effects is presented in Table

¹²⁷ Cho, J.-Y.; Iverson, C. N.; Smith, M. R., III *J. Am. Chem. Soc.* **2000**, *122*, 12868-12869.

3.7, and as demonstrated, a substoichiometric amount of catalyst was well tolerated. The cyclization of bis(enone) **1** underwent efficient cyclization with 20 mol % of catalyst **20** to provide **2** with 92% enantiomeric excess in 75% yield after 24 h (entry 2). While lowering the catalyst loading further to 10 mol % maintained high enantioselectivity in the transformation, providing **2** with 91% ee, the efficiency of the reaction was dramatically sacrificed, as the isolated yield was only 41% within the same timeframe. In light of the rate reduction from decreased catalyst loading, and because our Cys-based catalyst was simple and commercially available, we decided to perform the following study of reaction scope employing a full equivalent of **20** to ensure high efficiency and enantioselectivity within a useful timeframe.

Table 3.7: Effect of catalyst loading on the RC reaction of **1** to **2** promoted by **20**.



entry	catalyst (mol %)	yield	ee
1	100	70	95
2	20	75	92
3	10	41	91

Thus, we set out to synthesize various substrates for investigation of the scope of the enantioselective intramolecular Rauht-Currier reaction. Following previous work of

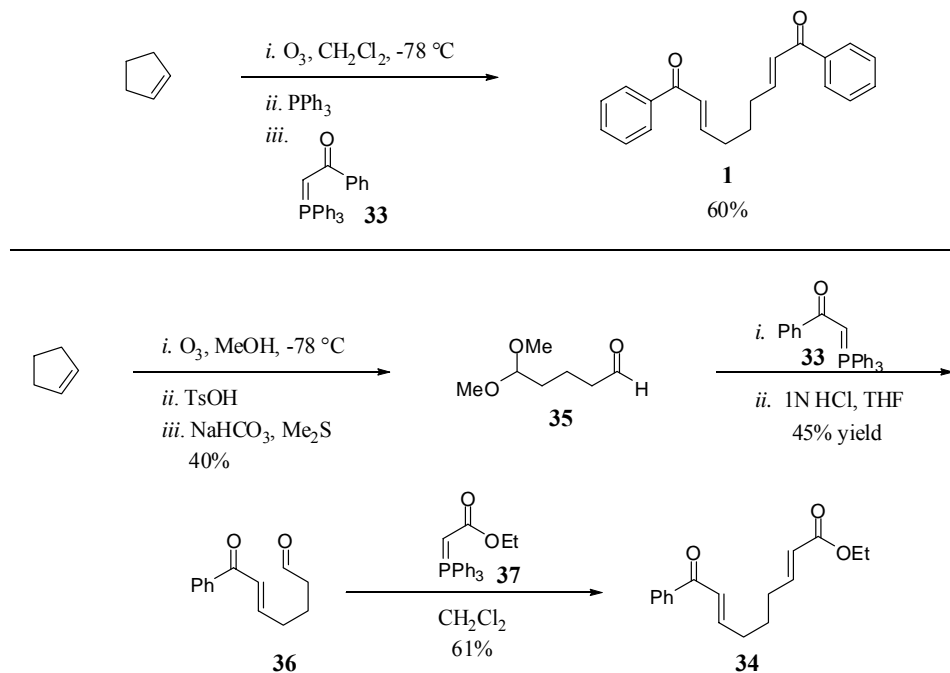
Murphy and co-workers¹²⁸ which documented a synthetic route to accessing the bis(phenyl)-substituted ketone **1**, the substrates were prepared by reaction of a dialdehyde with the requisite phosphorus ylide. As illustrated in Scheme 3.11, ozonolysis of cyclopentene generated the desired dialdehyde which was followed by in situ Wittig olefination with the stabilized phosphorane, **33**. The stabilized Wittig reagents were prepared by subjection of the corresponding α -chloro or bromo halides to triphenylphosphine, followed by elimination under basic conditions.¹²⁹ A variety of symmetrical bis(enones) were therefore prepared via subjection of the desired stabilized Wittig reagents to the ozonolysis reaction. Synthesis of unsymmetrical bis(enone) substrate **34** was achieved by utilizing a procedure disclosed by Schreiber and co-workers for the generation of protected dialdehyde **35**.¹³⁰ Subjection of **35** to stabilized Wittig reagent **33** provided the MBH enone-aldehyde substrate (**36**) after acid deprotection of the methyl acetal. A second Wittig olefination reaction with the desired phosphorane (**37**) afforded unsymmetrical bis(enone) substrate **34**.

¹²⁸ Brown, P. M.; Käppel, N.; Murphy, P. J. *Tetrahedron Lett.* **2002**, *43*, 8707-8710.

¹²⁹ For the preparation of stabilized Wittig salts, please see: (a) Ramirez, F.; Dershowitz, S. *J. Org. Chem.* **1957**, *22*, 41-45. (b) Denney, D. B.; Smith, L. C.; Song, J.; Rossi, C. J.; Hall, C. D. *J. Org. Chem.* **1963**, *28*, 778-780.

¹³⁰ Schreiber, S. L.; Kelly, S. E.; Porco, J. A.; Sammakia, T.; Suh, E. M. *J. Am. Chem. Soc.* **1988**, *110*, 6210-6218.

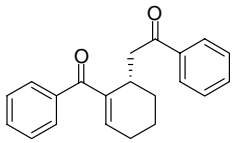
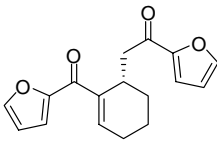
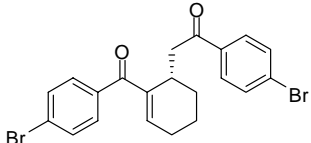
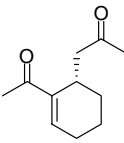
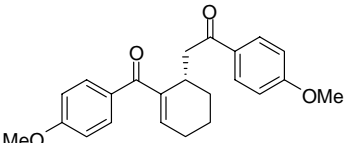
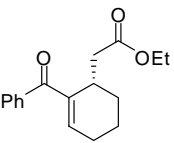
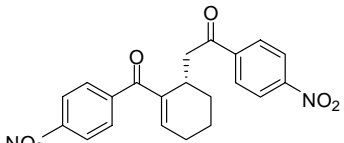
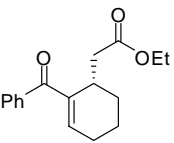
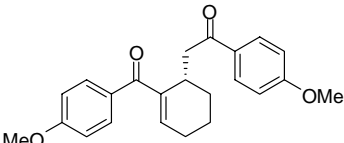
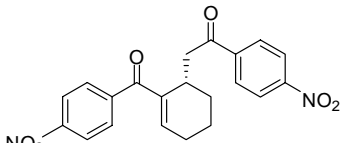
Scheme 3.11: Synthesis of symmetrical and unsymmetrical RC substrates.



Excitingly, we determined that the RC cycloisomerization could be extended to include electron-deficient and electron-rich aryl symmetrical bis(enones) as well as aliphatic and heteroaromatic bis(enones) while maintaining high levels of enantioselectivity.¹¹¹ As previously demonstrated (3.3.6) and reiterated in the following discussion, a delicate balance existed between the amount of base and the concentration of the reaction. Rauhut-Currier cyclization leading to *para*-bromo-substituted compound **24** was performed using 5 equiv of *t*-BuOK at a slightly higher dilution (0.03 M) to provide 70% yield and 93% enantiomeric excess (Table 3.8). Unlike the case with bis(phenyl) compound **1**, a decrease in catalyst loading (20 mol %) was deleterious to enantioselectivity, providing **24** with 74% ee and 81% yield in the same timeframe. Analogous *para*-methoxy substitution of symmetrical bis(phenyl) compound **1** was also well tolerated, producing compound **38** with 90% ee in 73% yield (7 equiv *t*-BuOK, 0.01

M). Performing this cyclization with lowered catalyst loading (20 mol %) provided comparable enantioselectivity (90% ee), yet with reduced efficiency (57% yield). A slight decrease in stereoinduction was observed in the cyclization leading to *para*-NO₂-substituted compound **39** with 84% ee and 71% yield within 4 h (2 equiv *t*-BuOK, 0.01 M). Heteroaromatic furan-substituted **40** was delivered with high enantiomeric excess (92%) and modest yield (54%) in 48 h. Fine-tuning of the reaction conditions provided aliphatic bis(methylketone) **41** with high selectivity and moderate yield (90% ee, 55% yield) or slightly decreased enantioselectivity (81% ee) and higher yield (68%). Finally, unsymmetrical keto ester **42** showed a decrease in enantioselectivity (67% ee). We are optimistic that unsymmetrical substrates will not be a limitation and with further optimization of catalyst and reaction conditions this will be a viable class of substrates.

Table 3.8: Substrate scope in the enantioselective Rauhut-Currier reaction promoted by catalyst **20**.

product ^a	yield, ee (<i>t</i> -BuOK, conc, time)	product ^a	yield, ee (<i>t</i> -BuOK, conc, time)
	70%, 95% ee (6 equiv, 0.05 M, 24 h)		54%, 92% ee (6 equiv, 0.05 M, 48 h)
	70%, 93% ee (5 equiv, 0.03 M, 24 h)		55%, 90% ee (4 equiv, 0.008 M, 40 h)
	81%, 74% ee (20 mol % 20)		68%, 81% ee (4 equiv, 0.01 M, 40 h)
	73%, 90% ee (7 equiv, 0.01 M, 24 h)		66%, 67% ee (6 equiv, 0.05 M, 24 h)
	57%, 90% ee (20 mol % 20)		
	71%, 84% ee (2 equiv, 0.01M, 4 h)		

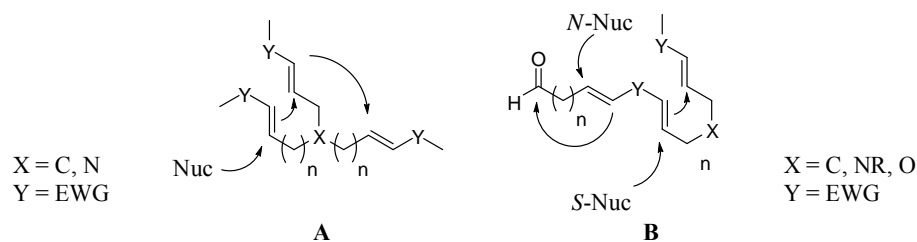
^a Reactions were conducted at -40 °C with 20 equiv H₂O in MeCN (see Experimental section for details).

3.6 Conclusion

The Rauhut-Currier reaction is a powerful transformation with the capability of providing structurally complex enantiopure compounds through the generation of a new carbon-carbon bond. Although progress in the development of this forty five year old reaction has been slow due to difficulties in controlling reactivity, it has recently become a more prominent reaction with the development of the intramolecular version. We have

been able to contribute to the further advancement of this transformation by establishing a method to perform the first enantioselective intramolecular Rauhut-Currier reaction in high yield and enantioselectivity using convenient reagents and conditions. Moreover, our report documents the first use of a simple cysteine derivative as an asymmetric catalyst. An initial substrate scope was examined and we determined that electron-deficient and electron-rich aryl symmetrical bis(enones) as well as aliphatic and heteroaromatic bis(enones) were viable substrates under this catalytic system. Unsymmetrical substrates proved to be more difficult and will be the subject of further explorations.

Many opportunities for growth persist in the development of both the MBH and RC reactions. Further expansion of the substrate scope to include more complex substrates will involve the design of novel molecules, hopefully amenable to catalysis under our Cys-based catalyst. For example, a relay system of RC transformations is possible in a substrate such as compound **A** where the latent enolate from one RC reaction would be trapped by a second such cyclization.



Additionally, opportunities exist in the development of orthogonal conditions in the promotion of the MBH and RC reactions; the MBH reaction is promoted by nitrogen-based catalysis, while the RC reaction is promoted by sulfur-based catalysis and not

nitrogen. If the MBH reaction was inert to specific Cys-based catalytic conditions, we would be able to access interesting scaffolds in a tandem one-pot transformation including sequential MBH/RC reactions (represented by compound **B**). Finally, the facile and widespread application of this methodology to the synthesis of natural products and non-natural target molecules will be the next frontier.

3.7 Experimental

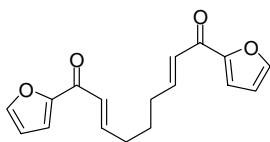
General. Proton NMR spectra were recorded on a 500 or 400 MHz spectrometer. Proton chemical shifts are reported in ppm (δ) relative to internal tetramethylsilane (TMS, δ 0.0 ppm) or with the solvent reference relative to TMS employed as the internal standard (CDCl_3 , δ 7.26 ppm; d_6 -DMSO, δ 2.50 ppm; CD_3OD , δ 3.31 ppm; D_2O , δ 4.79 ppm). Data are reported as follows: chemical shift (multiplicity [singlet (s), doublet (d), triplet (t), quartet (q), and multiplet (m)], coupling constants [Hz], integration). Carbon NMR spectra were recorded at 125 or 100 MHz with complete proton decoupling. Carbon chemical shifts are reported in ppm (δ) relative to TMS with the respective solvent resonance as the internal standard (CDCl_3 , δ 77.0 ppm). Infrared spectra were obtained on a Perkin-Elmer Spectrum 1000 spectrometer. Analytical thin-layer chromatography (TLC) was performed using Silica Gel 60 Å F254 precoated plates (0.25 mm thickness). TLC R_f values are reported. Visualization was accomplished by irradiation with a UV lamp and/or staining with KMnO_4 or cerium ammonium molybdenate (CAM) solutions. Flash column chromatography was performed using Silica Gel 60 Å (32-63 μm).¹³¹ Optical rotations were recorded on a Rudolf Research Analytical Autopol IV Automatic polarimeter at the sodium D line (path length 100 mm). High resolution mass spectra were obtained at the Mass Spectrometry Facility of either Boston College (Chestnut Hill, MA) or the University of Illinois (Urbana-Champaign, IL). The method of ionization is given in parentheses. Analytical normal phase HPLC was performed on a Hewlett-Packard 1100 Series chromatograph equipped with a diode

¹³¹ Still, W.C.; Kahn, M.; Mitra, J. *J. Org. Chem.* **1978**, *43*, 2923.

array detector (214 nm and 254 nm). All reactions were carried out under an argon or nitrogen atmosphere employing oven- and flame-dried glassware. All solvents were purified using a Seca Solvent Purification System by GlassContour. *t*-BuOK was freshly sublimed prior to use.

Experimental Procedures

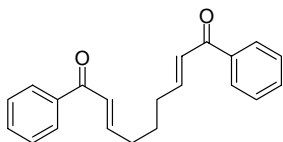
General procedure A: preparation of intramolecular Rauhut-Currier substrates (1, 38b, 24b, 39b, 40b, 41b, and 42b).



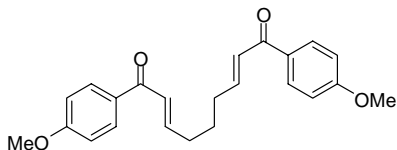
Compound 40b. Cyclopentene (0.52 mL, 5.9 mmol) was dissolved in CH₂Cl₂ (8.7 mL), cooled to -78 °C, and ozone was bubbled through the reaction until the clear solution turned blue. Nitrogen was then bubbled through the solution until the blue color disappeared to remove excess ozone. Triphenylphosphine (2.3 g, 8.9 mmol) was added and the reaction was allowed to stir for 1 h at -78 °C. 1-(2-furanyl)-2-(triphenylphosphoranylidene)-ethanone¹³² (4.6 g, 12.4 mmol) was added at room temperature and the pale yellow solution was allowed to stir for 24 h and then concentrated under reduced pressure. Flash chromatography (hexanes-EtOAc, 5:1)

¹³² (a) Ramirez, F.; Dershowitz, S. *J. Org. Chem.* **1957**, 22, 41-45. (b) Denney, D. B.; Smith, L. C.; Song, J.; Rossi, C. J. *J. Org. Chem.* **1963**, 28, 778-780.

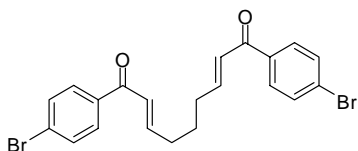
provided **40b** as a pale yellow oil (790 mg, 2.8 mmol, 47%). ^1H NMR (CDCl_3 , 400 MHz) δ 7.63-7.62 (m, 2H), 7.27-7.24 (m, 2H), 7.15 (dt, $J = 15.4, 7.2$ Hz, 2H), 6.84 (d, $J = 15.6$ Hz, 2H), 6.56 (dd, $J = 3.5, 1.8$ Hz, 2H), 2.38 (q, $J = 6.8$ Hz, 4H), 1.78 (quintet, $J = 7.5$ Hz, 2H); ^{13}C NMR (CDCl_3 , 125 MHz) δ 178.3, 153.7, 148.1, 146.9, 125.9, 118.0, 112.7, 32.4, 26.9; IR (film, cm^{-1}) 3124, 2933, 1664, 1620, 1564, 1465, 1392, 1297, 1010; TLC R_f 0.25 (2:1 hexanes-EtOAc); HRMS (ESI) m/z 285.1137 (285.1127 calcd for $\text{C}_{17}\text{H}_{17}\text{O}_4$ $[\text{M}+\text{H}]^+$). Compounds **1**, **38b**, **24b**, **39b**, **41b**, and **42b** were prepared by analogous methodology.



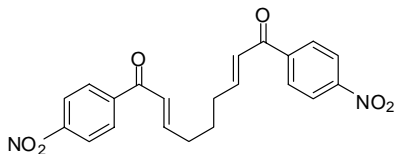
Compound 1. ^1H NMR (CDCl_3 , 500 MHz) δ 7.93 (dd, $J = 8.2, 1.2$ Hz, 4H), 7.55 (t, $J = 7.5$ Hz, 2H), 7.46 (t, $J = 7.6$ Hz, 4H), 7.06 (dt, $J = 15.4, 6.9$ Hz, 2H), 6.92 (d, $J = 15.4$ Hz, 2H), 2.39 (q, $J = 6.8$ Hz, 4H), 1.83-1.75 (m, 2H); ^{13}C NMR (CDCl_3 , 125 MHz) δ 190.6, 148.5, 137.8, 132.7, 128.5, 128.4, 126.4, 32.1, 26.7; IR (film, cm^{-1}) 3056, 2929, 2856, 1671, 1621, 1577, 1446, 1344, 1291, 1221, 1009, 968; TLC R_f 0.46 (3:1 hexanes-EtOAc); HRMS (ESI) m/z 305.1546 (305.1542 calcd for $\text{C}_{21}\text{H}_{21}\text{O}_2$ $[\text{M}+\text{H}]^+$).



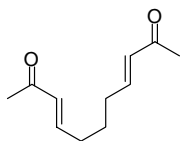
Compound 38b. ^1H NMR (CDCl_3 , 400 MHz) δ 7.95 (d, $J = 8.7$ Hz, 4H), 7.05 (dt, $J = 15.2, 6.9$ Hz, 2H), 6.97-6.90 (m, 6H), 3.88 (s, 6H), 2.39 (q, $J = 7.1$ Hz, 4H), 1.78 (quintet, $J = 7.4$ Hz, 2H); ^{13}C NMR (CDCl_3 , 100 MHz) δ 188.8, 163.4, 147.5, 130.8, 130.7, 126.2, 113.8, 55.5, 32.1, 26.8; IR (film, cm^{-1}) 3010, 2930, 2835, 1662, 1621, 1594, 1570, 1506, 1302, 1259, 1235, 1167; TLC R_f 0.26 (2:1 hexanes-EtOAc); HRMS (ESI) m/z 365.1764 (365.1753 calcd for $\text{C}_{23}\text{H}_{25}\text{O}_4$ $[\text{M}+\text{H}]^+$).



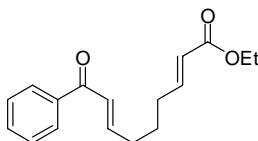
Compound 24b. ^1H NMR (CDCl_3 , 500 MHz) δ 7.79 (d, $J = 8.5$ Hz, 4H), 7.61 (d, $J = 8.5$ Hz, 4H), 7.07 (dt, $J = 15.1, 7.1$ Hz, 2H), 6.82 (d, $J = 15.1$ Hz, 2H), 2.40 (q, $J = 6.8$ Hz, 4H), 1.78 (quintet, $J = 7.5$ Hz, 2H); ^{13}C NMR (CDCl_3 , 125 MHz) δ 189.3, 149.0, 136.5, 131.9, 130.0, 127.9, 126.0, 32.2, 26.6; IR (film, cm^{-1}) 2949, 2886, 2829, 2722, 1721, 1671, 1620, 1583, 1400, 1073, 1010; TLC R_f 0.42 (1:1 hexanes-Et₂O); HRMS (ESI) m/z 460.9771 (460.9752 calcd for $\text{C}_{21}\text{H}_{19}\text{O}_2\text{Br}_2$ $[\text{M}+\text{H}]^+$).



Compound 39b. ^1H NMR (CDCl_3 , 500 MHz) δ 8.32 (d, $J = 8.8$ Hz, 4H), 8.06 (d, $J = 8.8$ Hz, 4H), 7.13 (dt, $J = 15.4, 6.9$ Hz, 2H), 6.91 (d, $J = 15.4$ Hz, 2H), 2.45 (q, $J = 6.9$ Hz, 4H), 1.83 (quintet, $J = 7.5$ Hz, 2H); ^{13}C NMR (CDCl_3 , 125 MHz) δ 189.0, 150.6, 150.1, 142.6, 129.4, 126.1, 123.8, 32.3, 26.6; IR (film, cm^{-1}) 3109, 2934, 2856, 1671, 1617, 1601, 1524, 1344, 1213; TLC R_f 0.32 (2:1 hexanes-EtOAc); HRMS (ESI) m/z 395.1246 (395.1243 calcd for $\text{C}_{21}\text{H}_{19}\text{N}_2\text{O}_6$ $[\text{M}+\text{H}]^+$).

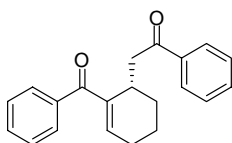


Compound 41b. ^1H NMR (CDCl_3 , 400 MHz) δ 6.78 (dt, $J = 15.9, 6.9$ Hz, 2H), 6.10 (d, $J = 16.0$ Hz, 2H), 2.31-2.24 (m, 10H), 2.39 (q, $J = 7.1$ Hz, 2H), 1.68 (quintet, $J = 7.4$ Hz, 2H); ^{13}C NMR (CDCl_3 , 100 MHz) δ 198.5, 147.0, 131.8, 31.8, 27.0, 26.4; IR (film, cm^{-1}) 3001, 2933, 2856, 1697, 1673, 1620, 1427, 1359, 1254, 1182, 972; TLC R_f 0.29 (2:1 hexanes-EtOAc); HRMS (ESI) m/z 203.1054 (203.1048 calcd for $\text{C}_{11}\text{H}_{16}\text{O}_2\text{Na}$ $[\text{M}+\text{Na}]^+$).



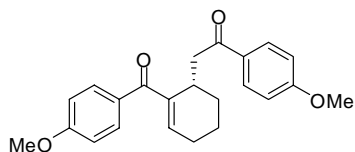
Compound 42b. ^1H NMR (CDCl_3 , 500 MHz) δ 7.93 (d, $J = 7.0$ Hz, 2H), 7.56 (t, $J = 7.3$ Hz, 1H), 7.47 (t, $J = 7.6$ Hz, 2H), 7.07-6.89 (m, 3H), 5.85 (dt, $J = 15.8, 1.5$ Hz, 1H), 4.19 (q, $J = 7.1$ Hz, 2H), 2.36 (q, $J = 6.9$ Hz, 2H), 2.28 (q, $J = 6.9$ Hz, 2H), 1.72 (quintet, $J = 7.3$ Hz, 2H), 1.29 (t, $J = 7.1$ Hz, 3H); ^{13}C NMR (CDCl_3 , 125 MHz) δ 191.0, 166.9, 148.9, 148.4, 138.2, 133.1, 128.9, 128.9, 126.8, 122.4, 60.6, 32.4, 31.9, 26.9, 14.6; IR (film, cm^{-1}) 2980, 2936, 1715, 1672, 1652, 1616, 1442, 1264, 1178; TLC R_f 0.28 (3:1 hexanes-EtOAc); HRMS (ESI) m/z 295.1310 (295.1310 calcd for $\text{C}_{17}\text{H}_{20}\text{O}_3\text{Na}$ $[\text{M}+\text{Na}]^+$).

General procedure B: catalytic intramolecular Rauhut-Currier reactions.



Compound 2. Bisenone **1** (30.0 mg, 0.10 mmol) was dissolved in acetonitrile (2.0 mL) and water (36 μL , 2.0 mmol) and cooled to -40 $^\circ\text{C}$. AcCysOMe (**20**) (17.6 mg, 0.10 mmol) and *t*-BuOK (67.0 mg, 0.59 mmol) were added sequentially and the reaction was allowed to stir for 24 h at -40 $^\circ\text{C}$. The reaction mixture was then filtered through a short plug of silica (hexanes-EtOAc, 1:1), concentrated under reduced pressure, and purified by silica gel chromatography (hexanes-EtOAc, 5:1) to afford **2** as a pale yellow oil (21 mg, 0.069 mmol, 70%). The characterization data for this compound matched that which has

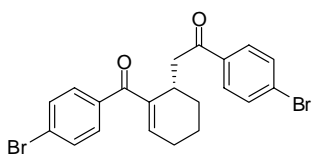
previously been reported.¹³³ $[\alpha]_D -38.6$ (*c* 0.76, CHCl₃, 95% ee); Assay of enantiomeric purity: Enantiomers of product were separated by chiral HPLC employing a Chiralcel AD column (Daicel). Conditions: 96:4 hexanes-isopropanol; Flow rate 0.75 mL/min; 15.1 min (major ent), 20.5 min (minor ent). Compounds **38**, **24**, **39**, **40**, **41**, and **42** were prepared by analogous methodology. **NOTE:** In order to ensure high efficiency and enantioselectivity, the reaction concentration and equivalents of *t*-BuOK must be as described for each respective substrate. For runs employing less than 100 mol% catalyst, reaction parameters other than catalyst loading remain constant.



Compound 38. General procedure B was followed, except that bisenone **38b** (20.0 mg, 0.055 mmol) was employed as starting material with *t*-BuOK (43.2 mg, 0.39 mmol) in acetonitrile (5.5 mL). Yield: 73% (12.8 mg, 0.035 mmol); ¹H NMR (CDCl₃, 500 MHz) δ 8.05 (d, *J* = 8.9 Hz, 2H), 7.74 (d, *J* = 8.8 Hz, 2H), 6.96-9.92 (m, 4H), 6.53 (td, *J* = 3.9, 1.1 Hz, 1H), 3.87 (s, 3H), 3.85 (s, 3H), 3.47-3.45 (m, 1H), 3.34 (dd, *J* = 14.4, 3.2 Hz, 1H), 2.69 (dd, *J* = 14.4, 10.8 Hz, 1H), 2.38-2.29 (m, 1H), 2.23-2.15 (m, 1H), 1.81-1.57 (m, 4H); ¹³C NMR (CDCl₃, 125 MHz) δ 198.7, 197.5, 163.8, 163.2, 142.7, 142.0, 132.1, 131.6, 131.2, 130.3, 114.1, 113.8, 55.9, 55.8, 42.8, 31.6, 27.0, 26.4, 18.8; IR (film, cm⁻¹)

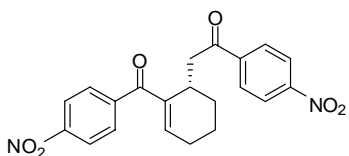
¹³³ (a) Wang, L.-C.; Luis, A. L.; Agapiou, K.; Jang, H.-Y.; Krische, M. J. *J. Am. Chem. Soc.* **2002**, *124*, 2402-2403. (b) Frank, S. A.; Mergott, D. J.; Roush, W. R. *J. Am. Chem. Soc.* **2002**, *124*, 2404-2405.

2925, 2840, 1671, 1630, 1597, 1569, 1507, 1254, 1172, 1029; TLC R_f 0.36 (2:1 hexanes-EtOAc); $[\alpha]_D +7.0$ (c 0.77, CHCl_3 , 90% ee); HRMS (ESI) m/z 365.1766 (365.1753 calcd for $\text{C}_{23}\text{H}_{25}\text{O}_4$ $[\text{M}+\text{H}]^+$); Assay of enantiomeric purity: Enantiomers of product were separated by chiral HPLC employing a Chiralcel AD column (Daicel). Conditions: 80:20 hexanes-isopropanol; Flow rate 0.75 mL/min; 19.3 min (major ent), 28.0 min (minor ent).

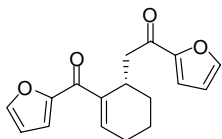


Compound 24. General procedure B was followed, except that bisenone **24b** (30.0 mg, 0.065 mmol) was employed as starting material with *t*-BuOK (36.0 mg, 0.33 mmol) in acetonitrile (2.2 mL). Yield: 70% (21 mg, 0.045 mmol); ^1H NMR (CDCl_3 , 500 MHz) δ 7.93 (d, $J = 8.6$ Hz, 2H), 7.62-7.53 (m, 6H), 6.62 (t, $J = 3.6$ Hz, 1H), 3.43-3.41 (m, 1H), 3.33 (dd, $J = 14.8, 3.5$ Hz, 1H), 2.80 (dd, $J = 14.8, 10.2$ Hz, 1H), 2.38-2.31 (m, 1H), 2.25-2.19 (m, 1H), 1.79-1.61 (m, 4H); ^{13}C NMR (CDCl_3 , 125 MHz) δ 198.9, 197.2, 145.8, 141.6, 137.8, 135.8, 132.3, 131.8, 131.2, 130.4, 128.6, 126.9, 42.8, 30.7, 26.9, 26.5, 18.4; IR (film, cm^{-1}) 2932, 2861, 1679, 1640, 1585, 1393, 1263, 1067, 1008; TLC R_f 0.64 (3:1 hexanes-EtOAc); $[\alpha]_D +9.7$ (c 1.0, CHCl_3 , 93% ee); HRMS (ESI) m/z 460.9751 (460.9752 calcd for $\text{C}_{21}\text{H}_{19}\text{O}_2\text{Br}_2$ $[\text{M}+\text{H}]^+$); Assay of enantiomeric purity: Enantiomers of product were separated by chiral HPLC employing a Chiralcel AD column (Daicel).

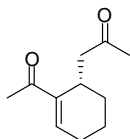
Conditions: 96:4 hexanes-isopropanol; Flow rate 0.75 mL/min; 26.3 min (major ent), 32.8 min (minor ent).



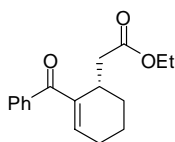
Compound 39. General procedure B was followed, except that bisenone **39b** (20.0 mg, 0.051 mmol) was employed as starting material with *t*-BuOK (11.4 mg, 0.10 mmol) in acetonitrile (5.1 mL) and the reaction was allowed to stir for 4 h. Yield: 71% (14.2 mg, 0.036 mmol); ^1H NMR (CDCl_3 , 400 MHz) δ 8.33 (d, $J = 8.9$ Hz, 2H), 8.30 (d, $J = 8.8$ Hz, 2H), 8.23 (d, $J = 8.9$ Hz, 2H), 7.78 (d, $J = 8.8$ Hz, 2H), 6.69 (t, $J = 3.6$ Hz, 1H), 3.49-3.40 (m, 2H), 2.99 (dd, $J = 15.0, 9.4$ Hz, 1H), 2.45-2.37 (m, 1H), 2.33-2.23 (m, 1H), 1.81-1.69 (m, 4H); ^{13}C NMR (CDCl_3 , 100 MHz) δ 197.9, 195.9, 150.3, 149.4, 148.1, 144.2, 141.1, 141.0, 129.9, 129.4, 123.9, 123.4, 42.8, 29.8, 26.5, 26.4, 17.8; IR (film, cm^{-1}) 2937, 2864, 1689, 1643, 1599, 1522, 1345, 1265; TLC R_f 0.32 (3:1 hexanes-EtOAc); $[\alpha]_D^{25} +15.0$ (c 1.0, CHCl_3 , 84% ee); HRMS (ESI) m/z 395.1259 (395.1243 calcd for $\text{C}_{21}\text{H}_{19}\text{N}_2\text{O}_6$ $[\text{M}+\text{H}]^+$); Assay of enantiomeric purity: Enantiomers of product were separated by chiral HPLC employing a Chiralcel AD column (Daicel). Conditions: 80:20 hexanes-isopropanol; Flow rate 0.75 mL/min; 42.9 min (major ent), 39.0 min (minor ent).



Compound 40. General procedure B was followed, except that bisenone **40b** (30.0 mg, 0.11 mmol) was employed as starting material with *t*-BuOK (74.0 mg, 0.66 mmol) in acetonitrile (2.2 mL) and the reaction was allowed to stir for 40 h. Yield: 54% (13.7 mg, 0.048 mmol); ¹H NMR (CDCl₃, 500 MHz) δ 7.62 (dd, *J* = 1.7, 0.7 Hz, 1H), 7.57 (dd, *J* = 1.7, 0.6 Hz, 1H), 7.41 (d, *J* = 3.7 Hz, 1H), 7.11 (dd, *J* = 3.6, 0.6 Hz, 1H), 7.00 (td, *J* = 3.9, 1.0 Hz, 1H), 6.53-6.51 (m, 2H), 3.48-3.45 (m, 1H), 3.11 (dd, *J* = 14.6, 3.2 Hz, 1H), 2.66 (dd, *J* = 14.6, 10.6 Hz, 1H), 2.39-2.21 (m, 2H), 1.78-1.63 (m, 4H); ¹³C NMR (CDCl₃, 125 MHz) δ 188.2, 183.7, 152.4, 152.3, 146.5, 146.4, 142.1, 140.9, 119.1, 118.2, 112.1, 111.7, 42.3, 30.6, 26.3, 26.1, 18.0; IR (film, cm⁻¹) 3130, 2934, 2860, 1673, 1628, 1564, 1463, 1390, 1285; TLC R_f 0.32 (2:1 hexanes-EtOAc); [α]_D +14 (*c* 0.88, CHCl₃, 92% ee); HRMS (ESI) *m/z* 285.1133 (285.1127 calcd for C₁₇H₁₇O₄ [M+H]⁺); Assay of enantiomeric purity: Enantiomers of product were separated by chiral HPLC employing a Chiralcel AD column (Daicel). Conditions: 80:20 hexanes-isopropanol; Flow rate 0.75 mL/min; 10.2 min (major ent), 14.0 min (minor ent).

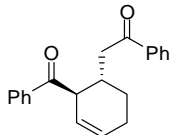


Compound 41. General procedure B was followed, except that bisenone **41b** (20.0 mg, 0.11 mmol) was employed as starting material with *t*-BuOK (37.0 mg, 0.33 mmol) in acetonitrile (5.5 mL) and the reaction was allowed to stir for 40 h. Yield: 55% (7.2 mg, 0.040 mmol); ¹H NMR (CDCl₃, 500 MHz) δ 6.95 (t, *J* = 3.9 Hz, 1H), 3.20-3.15 (m, 1H), 2.60 (dd, *J* = 15.6, 3.2 Hz, 1H), 2.31-2.26 (m, 5H), 2.17 (s, 3H), 1.66-1.52 (m, 5H); ¹³C NMR (CDCl₃, 125 MHz) δ 208.7, 199.2, 142.9, 142.5, 48.0, 30.1, 28.2, 26.6, 26.4, 25.9, 17.4; IR (film, cm⁻¹) 2923, 2854, 1717, 1660, 1635, 1351, 1233, 1160; TLC R_f 0.39 (2:1 hexanes-EtOAc); [α]_D -43 (c 0.42, CHCl₃, 90% ee); HRMS (ESI) *m/z* 203.1056 (203.1048 calcd for C₁₁H₁₆O₂Na [M+Na]⁺); Assay of enantiomeric purity: Enantiomers of product were separated by chiral HPLC employing a Chiralcel AD column (Daicel). Conditions: 97:3 hexanes-isopropanol; Flow rate 0.60 mL/min; 14.9 min (major ent), 16.0 min (minor ent).



Compound 42. General procedure B was followed, except that bisenone **42b** (20.0 mg, 0.073 mmol) was employed as starting material with *t*-BuOK (49.4 mg, 0.44 mmol) in acetonitrile (1.5 mL). Yield: 66% (13.4 mg, 0.049 mmol); ¹H NMR (CDCl₃, 500 MHz)

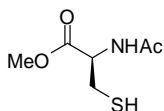
δ 7.67 (d, $J = 6.9$ Hz, 2H), 7.51 (t, $J = 7.4$ Hz, 1H), 7.42 (t, $J = 7.4$ Hz, 2H), 6.54 (t, $J = 3.9$ Hz, 1H), 4.09 (q, $J = 7.1$ Hz, 2H), 3.40-3.33 (m, 1H), 2.59 (dd, $J = 14.9, 4.4$ Hz, 1H), 2.40 (dd, $J = 15.1, 9.1$ Hz, 1H), 2.35-2.26 (m, 1H), 2.23-2.14 (m, 1H), 1.85-1.61 (m, 4H), 1.22 (t, $J = 7.1$ Hz, 3H); ^{13}C NMR (CDCl_3 , 125 MHz) δ 197.6, 172.4, 143.9, 141.2, 138.6, 131.6, 129.3, 128.0, 60.2, 38.1, 30.1, 27.1, 26.0, 18.3, 14.2; IR (film, cm^{-1}) 2927, 2851, 1728, 1641, 1593, 1443, 1368, 1265, 1249, 1173; TLC R_f 0.52 (3:1 hexanes-EtOAc); $[\alpha]_D -62$ (c 0.5, CHCl_3 , 67% ee); HRMS (ESI) m/z 295.1320 (295.1310 calcd for $\text{C}_{17}\text{H}_{20}\text{O}_3\text{Na}$ $[\text{M}+\text{Na}]^+$); Assay of enantiomeric purity: Enantiomers of product were separated by chiral HPLC employing a Chiralcel AD column (Daicel). Conditions: 96:4 hexanes-isopropanol; Flow rate 0.75 mL/min; 11.7 min (major ent), 14.6 min (minor ent).



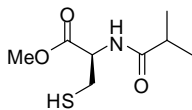
Compound 26. ^1H NMR (CDCl_3 , 500 MHz) δ 7.94 (dd, $J = 8.2, 1.2$ Hz, 2H), 7.78 (dd, $J = 8.2, 1.1$ Hz, 2H), 7.54 (t, $J = 7.25$ Hz, 1H), 7.51-7.42 (m, 3H), 7.35 (t, 7.8 Hz, 2H), 5.96-5.92 (m, 1H), 5.80-5.75 (m, 1H), 4.43 (bs, 1H), 3.06 (dd, $J = 17.0, 7.9$ Hz, 1H), 2.95 (dd, $J = 17.3, 6.0$ Hz, 1H), 2.85-2.78 (m, 1H), 2.20-2.07 (m, 3H), 1.80-1.72 (m, 1H); ^{13}C NMR (CDCl_3 , 125 MHz) δ 201.3, 199.7, 137.2, 137.1, 133.1, 132.9, 129.9, 128.7, 128.5, 128.3, 127.9, 124.1, 45.8, 39.6, 31.9, 25.2, 23.6; IR (film, cm^{-1}) 3060, 3025, 2922, 1682, 1595, 1578, 1446, 1372, 1323, 1283, 1211, 999; TLC R_f 0.52 (3:1 hexanes-EtOAc); $[\alpha]_D +54.3$ (c 0.23, CHCl_3 , 84% ee); HRMS (ESI) m/z 305.1552 (305.1542 calcd for $\text{C}_{21}\text{H}_{21}\text{O}_2$

[M+H]⁺); Assay of enantiomeric purity: Enantiomers of product were separated by chiral HPLC employing a Chiralcel AD column (Daicel). Conditions: 96:4 hexanes-isopropanol; Flow rate 0.75 mL/min; 26.1 min (major ent), 27.9 min (minor ent).

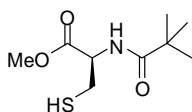
General procedure C: preparation of Rauhut-Currier catalysts.



Compound 20. A white heterogeneous mixture of CysOMe·HCl (1.00 g, 5.82 mmol) in acetonitrile (58 mL) was cooled to 0 °C. *N,N*-Diisopropylethylamine (935 μL, 5.24 mmol) and acetyl chloride (374 μL, 5.24 mmol) were added and the reaction was allowed to stir for 20 min. Saturated aqueous NH₄Cl (50 mL) was added at 0 °C and the reaction mixture was extracted with EtOAc (2 x 100 mL). The combined organic layers were washed with saturated aqueous NaHCO₃ (100 mL), saturated aqueous NaCl (100 mL), dried over Na₂SO₄, and concentrated under reduced pressure. Flash chromatography on silica gel (hexanes-EtOAc, 1:2) yielded **20** as a white fluffy solid (422 mg, 2.38 mmol, 41%). ¹H NMR (CDCl₃, 500 MHz) δ 6.41-6.33 (bs, 1H), 4.90 (dt, *J* = 7.9, 3.8 Hz, 1H), 3.80 (s, 3H), 3.07-2.98 (m, 2H), 2.08 (s, 3H), 1.34 (t, *J* = 8.9 Hz, 1H); ¹³C NMR (CDCl₃, 125 MHz) δ 171.0, 170.1, 53.9, 53.2, 27.2, 23.5; IR (film, cm⁻¹) 3276, 2952, 1748, 1652, 1532, 1437, 1369, 1213; TLC R_f 0.21 (1:2 hexanes-EtOAc); [α]_D +71 (*c* 1.0, CHCl₃); HRMS (ESI) *m/z* 200.0363 (200.0357 calcd for C₆H₁₁NO₃SNa [M+Na]⁺).



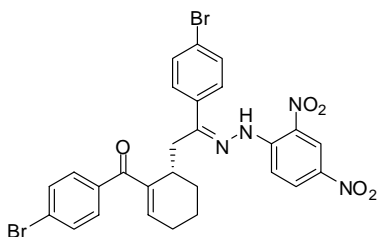
Compound 22. General procedure C was followed, except that CysOMe·HCl (100 mg, 0.58 mmol) was used with isobutyryl chloride (55 μ L, 0.52 mmol) and *N,N*-diisopropylethylamine (94 μ L, 0.52 mmol) in acetonitrile (5.8 mL). Yield: 39% (47 mg, 0.23 mmol). ^1H NMR (CDCl_3 , 500 MHz) δ 6.40-6.33 (bs, 1H), 4.89 (dt, $J = 7.7, 3.7$ Hz, 1H), 3.80 (s, 3H), 3.03 (dd, $J = 8.8, 4.1$ Hz, 2H), 2.47 (quintet, $J = 6.9$ Hz, 1H), 1.31 (t, $J = 8.9$ Hz, 1H), 1.20 (d, $J = 4.1$ Hz, 3H), 1.19 (d, $J = 4.1$ Hz, 3H); ^{13}C NMR (CDCl_3 , 125 MHz) δ 177.1, 171.2, 53.6, 53.2, 35.9, 27.3, 20.0, 19.7; IR (film, cm^{-1}) 3322, 2962, 2921, 1749, 1744, 1650, 1528, 1430, 1340, 1319, 1213; TLC R_f 0.64 (1:2 hexanes-EtOAc); $[\alpha]_D^{25} +59$ (c 1.0, CHCl_3); HRMS (ESI) m/z 206.0858 (206.0851 calcd for $\text{C}_8\text{H}_{16}\text{NO}_3\text{S}$ $[\text{M}+\text{H}]^+$).



Compound 23. General procedure C was followed, except that CysOMe·HCl (200 mg, 1.2 mmol) was used with pivaloyl chloride (123 μ L, 1.0 mmol) and *N,N*-diisopropylethylamine (174 μ L, 1.0 mmol) in acetonitrile (11.6 mL). Yield: 42% (107 mg, 0.49 mmol); ^1H NMR (CDCl_3 , 500 MHz) δ 6.58-6.48 (bs, 1H), 4.85 (dt, $J = 7.9, 3.9$ Hz, 1H), 3.80 (s, 3H), 3.03 (dd, $J = 8.8, 4.1$ Hz, 2H), 1.29 (t, $J = 9.0$ Hz, 1H), 1.25 (s, 9H); ^{13}C NMR (CDCl_3 , 125 MHz) δ 178.7, 171.3, 53.7, 53.2, 39.2, 27.8, 27.2; IR (film,

cm⁻¹) 3349, 2953, 1747, 1653, 1648, 1513, 1438, 1207; TLC R_f 0.73 (1:2 hexanes-EtOAc); [α]_D +55 (c 1.0, CHCl₃); HRMS (ESI) *m/z* 220.1004 (220.1007 calcd for C₉H₁₈NO₃S [M+H]⁺).

Determination of absolute configuration.

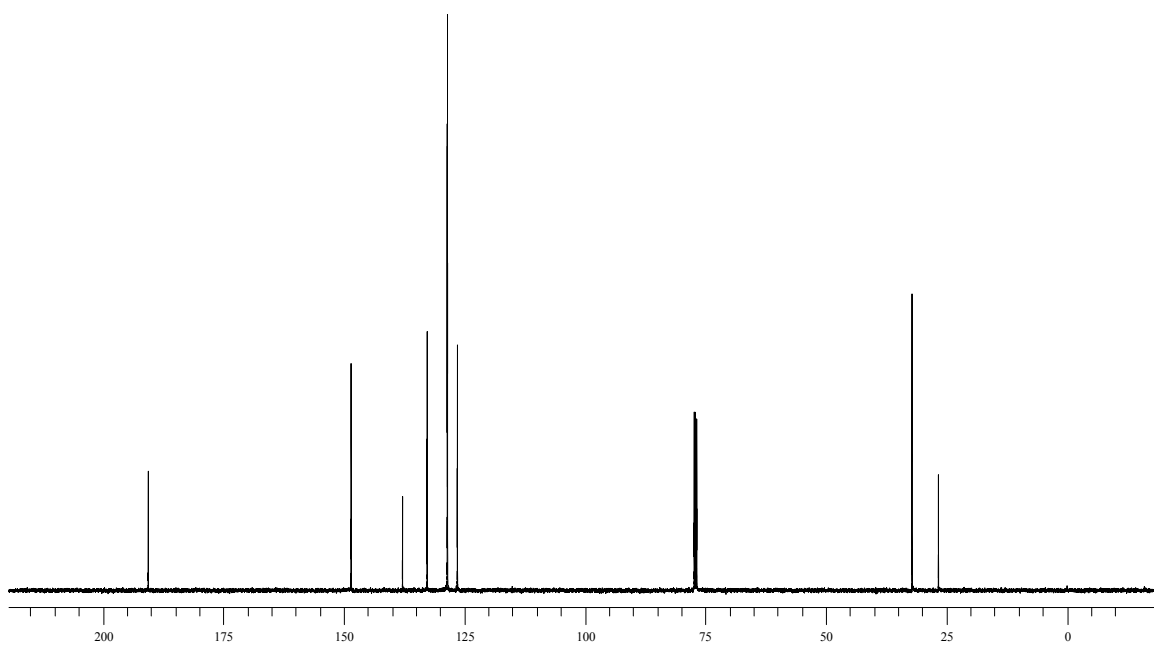
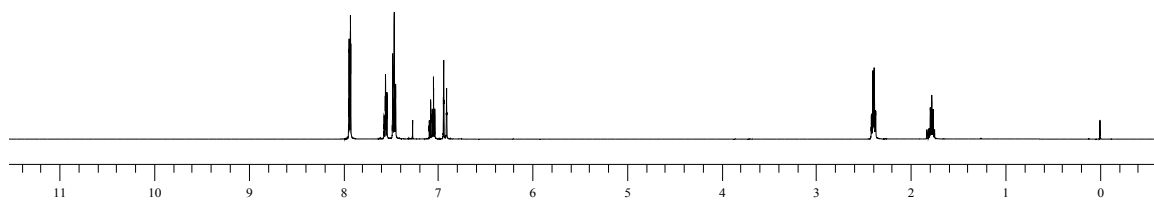
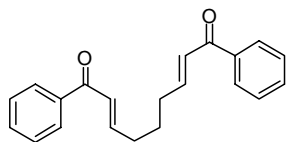


Compound 25. 2,4-dinitrophenylhydrazine (5.4 mg, 0.022 mmol) and 0.5 N H₂SO₄ (22 μL, 0.011 mmol) were added to a solution of **24** (10 mg, 0.022 mmol) in ethanol (100 μL). The red heterogeneous mixture was heated to reflux for 12 h, at which point excess 2,4-dinitrophenylhydrazine (10.8 mg, 0.044 mmol) was added and refluxed for an additional 12 h until the starting material was consumed as indicated by TLC. The solid material was collected and purified by silica gel chromatography (hexanes-EtOAc, 10:1) to afford **25** as an orange solid (6.3 mg, 0.010 mmol, 45%). X-ray quality crystals were prepared by recrystallizing **25** from an Et₂O-ethyl acetate solution affording bright orange plate crystals. ¹H NMR (CDCl₃, 500 MHz) δ 11.6 (s, 1H), 9.17 (d, *J* = 2.5 Hz, 1H), 8.36 (dd, *J* = 9.6, 2.5 Hz, 1H), 8.08 (d, *J* = 9.6 Hz, 1H), 7.87 (d, *J* = 8.6 Hz, 2H), 7.59 (d, *J* = 8.6 Hz, 2H), 7.53 (d, *J* = 8.6 Hz, 2H), 7.42 (d, *J* = 8.6 Hz, 2H), 6.69 (t, *J* = 3.8 Hz, 1H), 3.39-3.30 (m, 1H), 3.24 (dd, *J* = 14.4, 5.6 Hz, 1H), 2.79 (dd, *J* = 14.4, 9.6 Hz, 1H), 2.49-

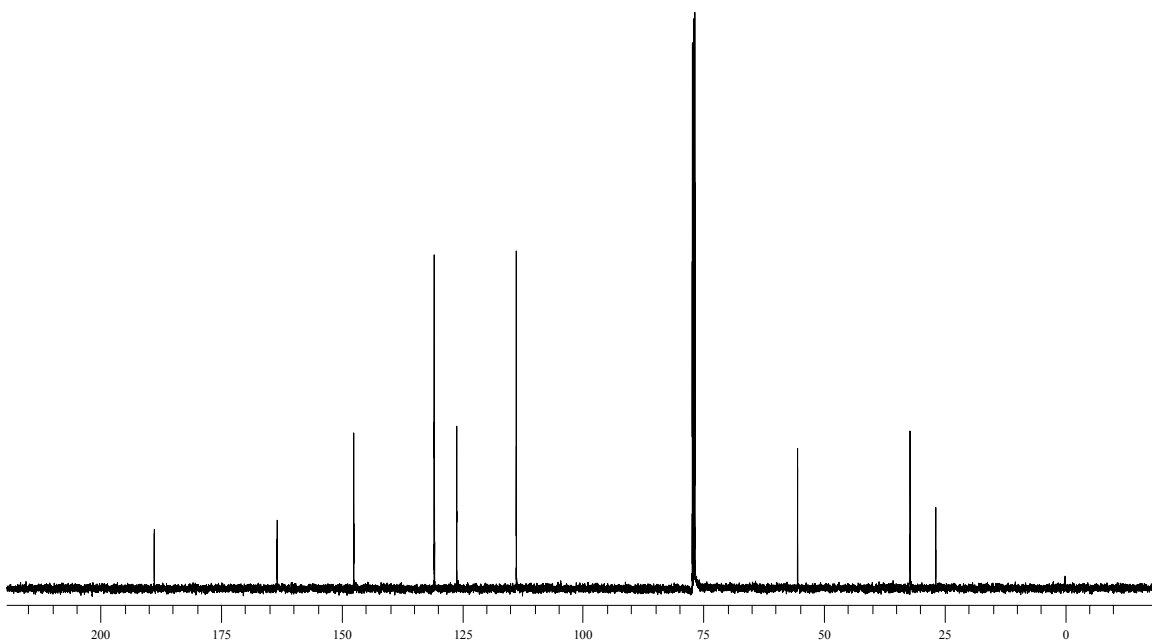
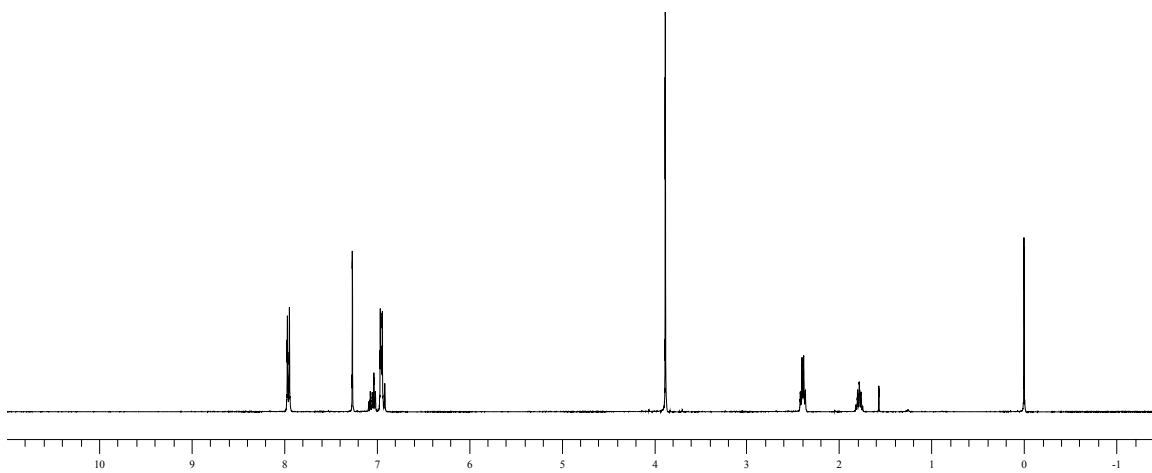
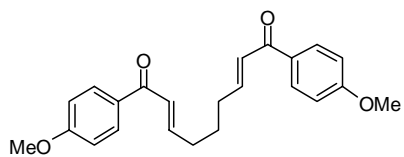
2.39 (m, 1H), 2.29-2.17 (m, 1H), 1.90-1.59 (m, 4H); ^{13}C NMR (CDCl_3 , 125 MHz) δ 196.6, 154.5, 146.9, 145.4, 140.6, 138.8, 137.1, 135.6, 132.3, 131.9, 131.0, 130.6, 130.2, 129.1, 127.2, 125.1, 123.8, 117.3, 31.5, 31.2, 27.3, 26.6, 18.5; IR (film, cm^{-1}) 3317, 2927, 2856, 1645, 1617, 1586, 1514, 1502, 1486, 1331, 1307, 1263; TLC R_f 0.53 (3:1 hexanes-EtOAc); $[\alpha]_D + 50$ (c 0.45, CHCl_3); HRMS (ESI) m/z 641.0034 (641.0035 calcd for $\text{C}_{27}\text{H}_{23}\text{Br}_2\text{N}_4\text{O}_5$ $[\text{M}+\text{H}]^+$).

3.7.1 NMR Spectra

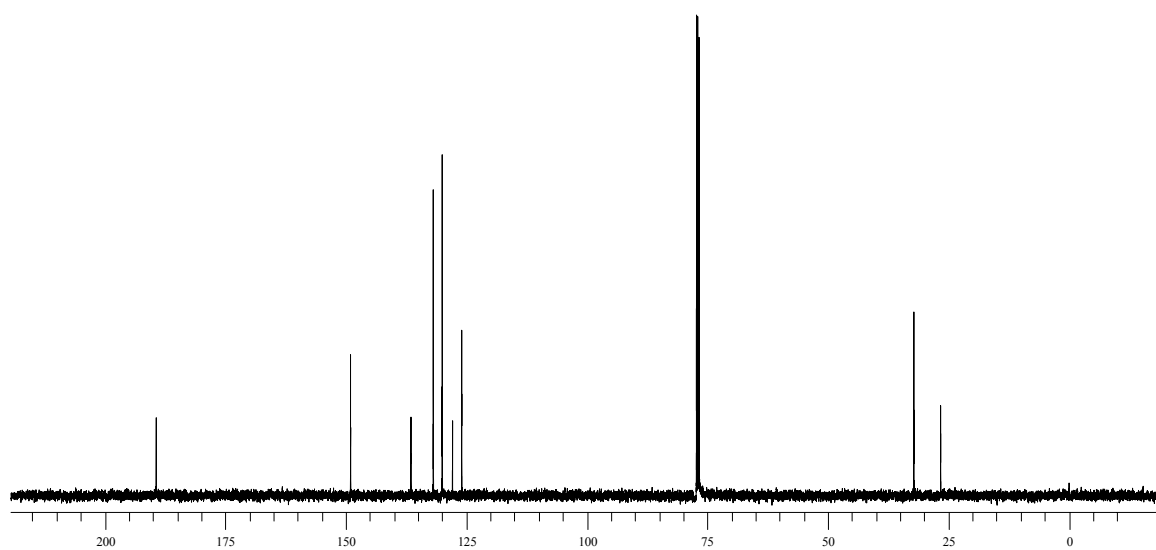
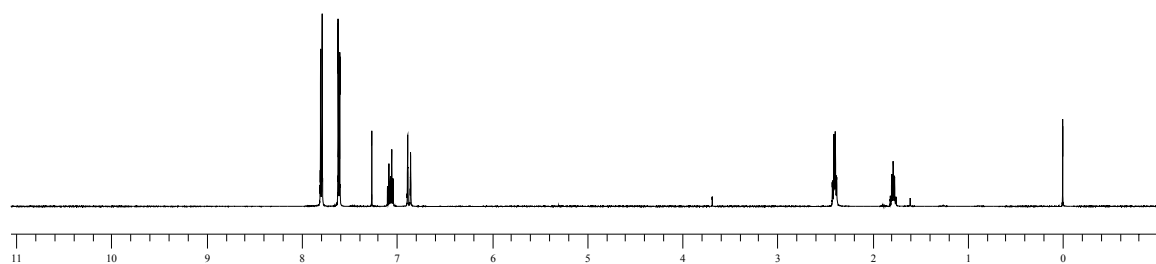
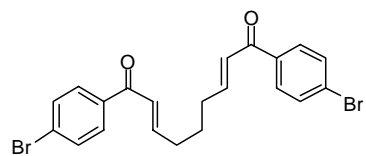
Compound 1.



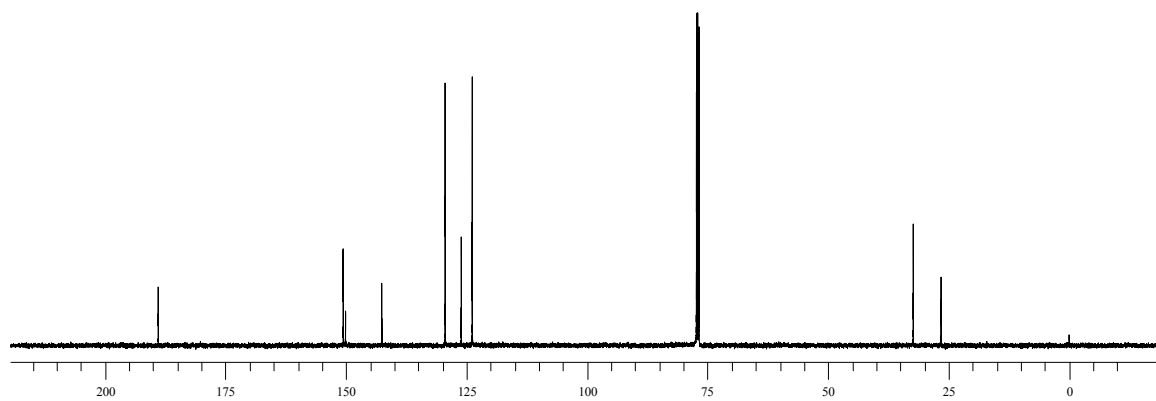
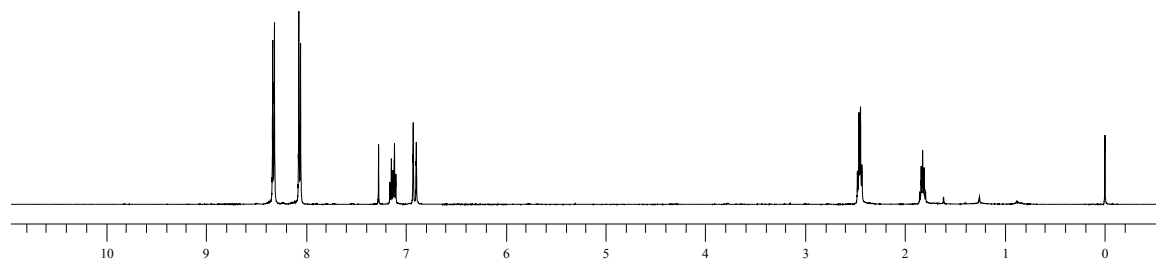
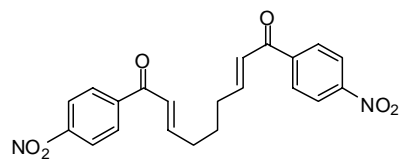
Compound 38b.



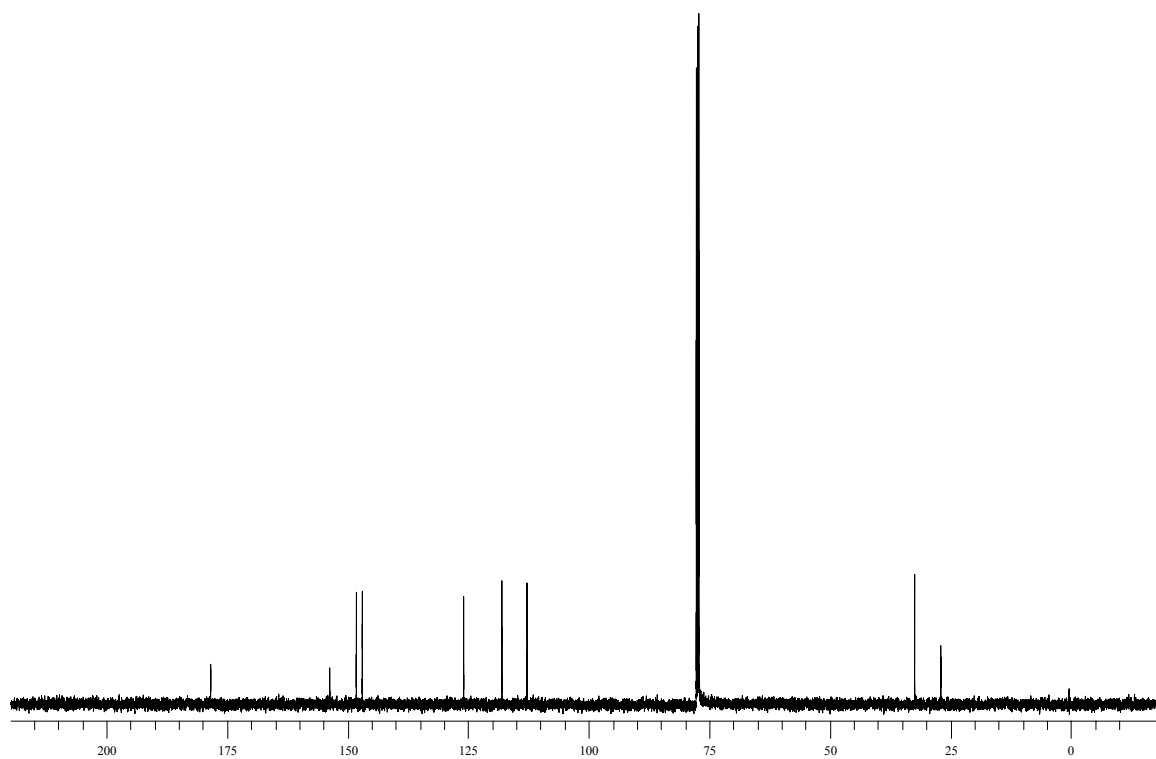
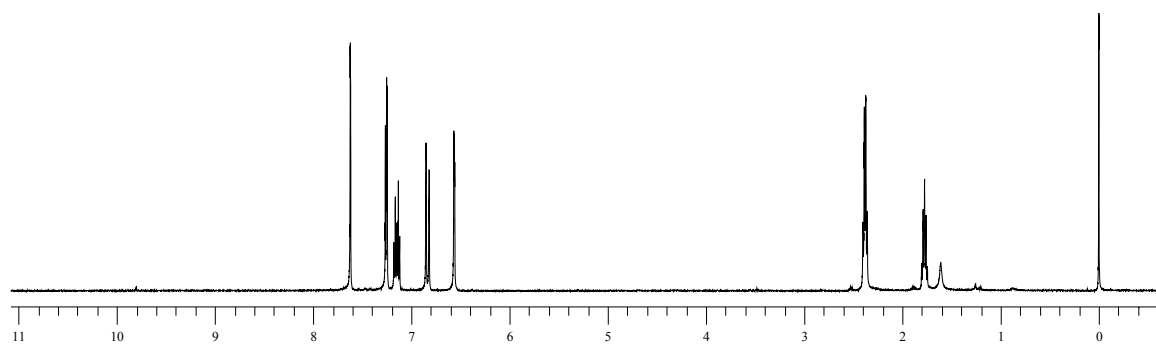
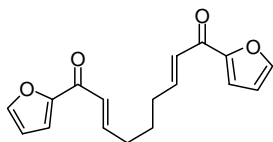
Compound 24b.



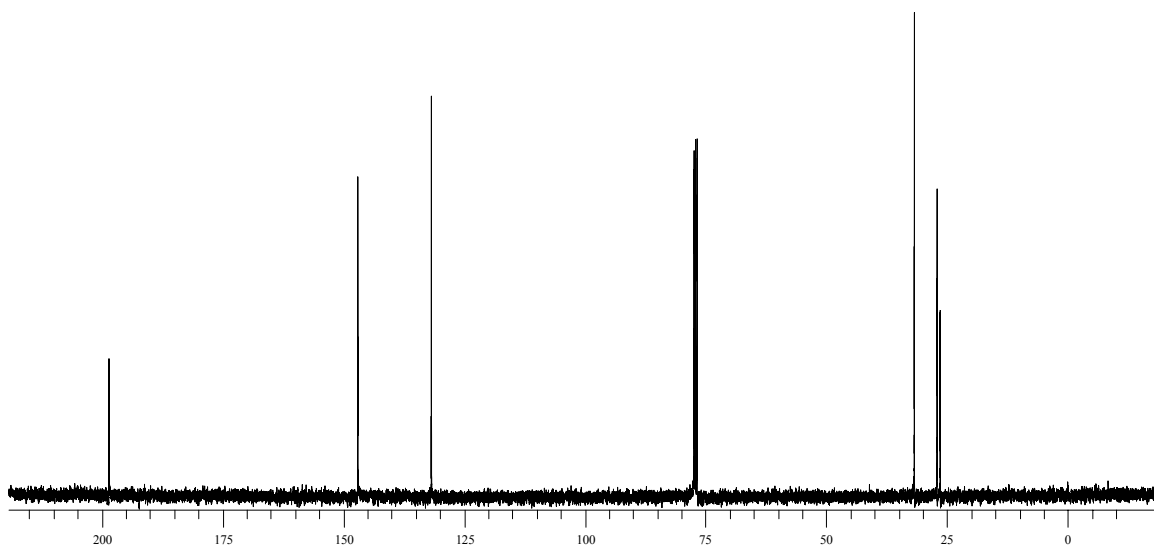
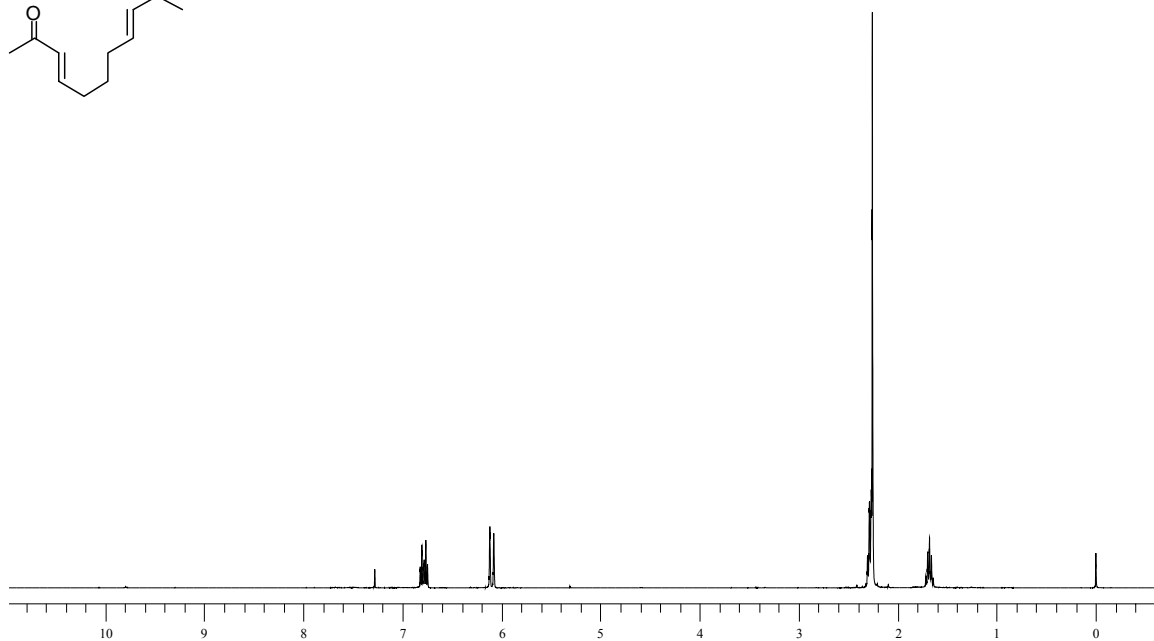
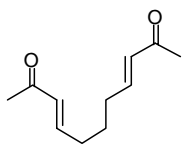
Compound 39b.



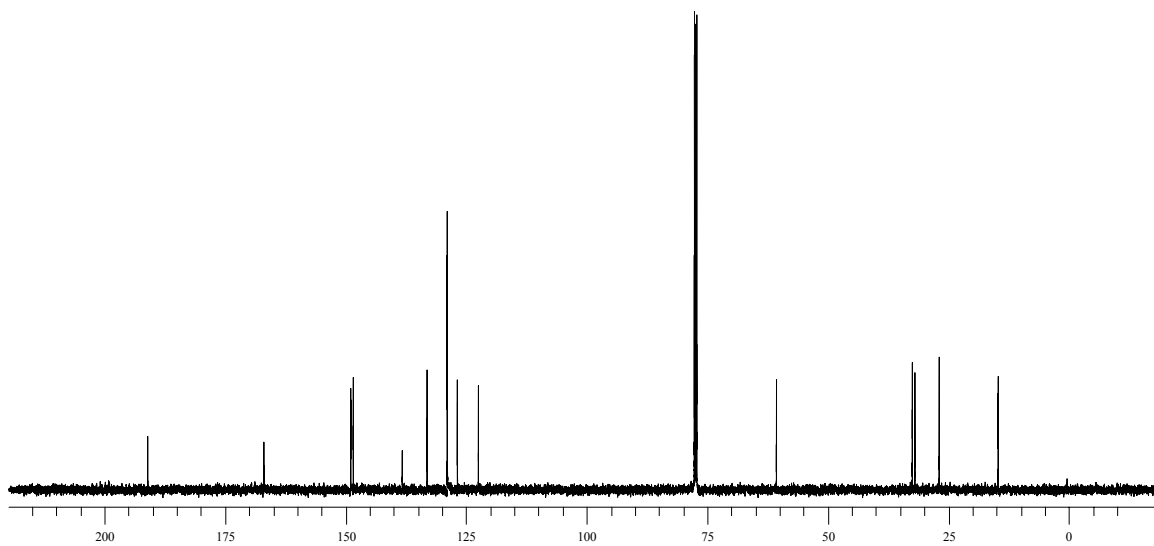
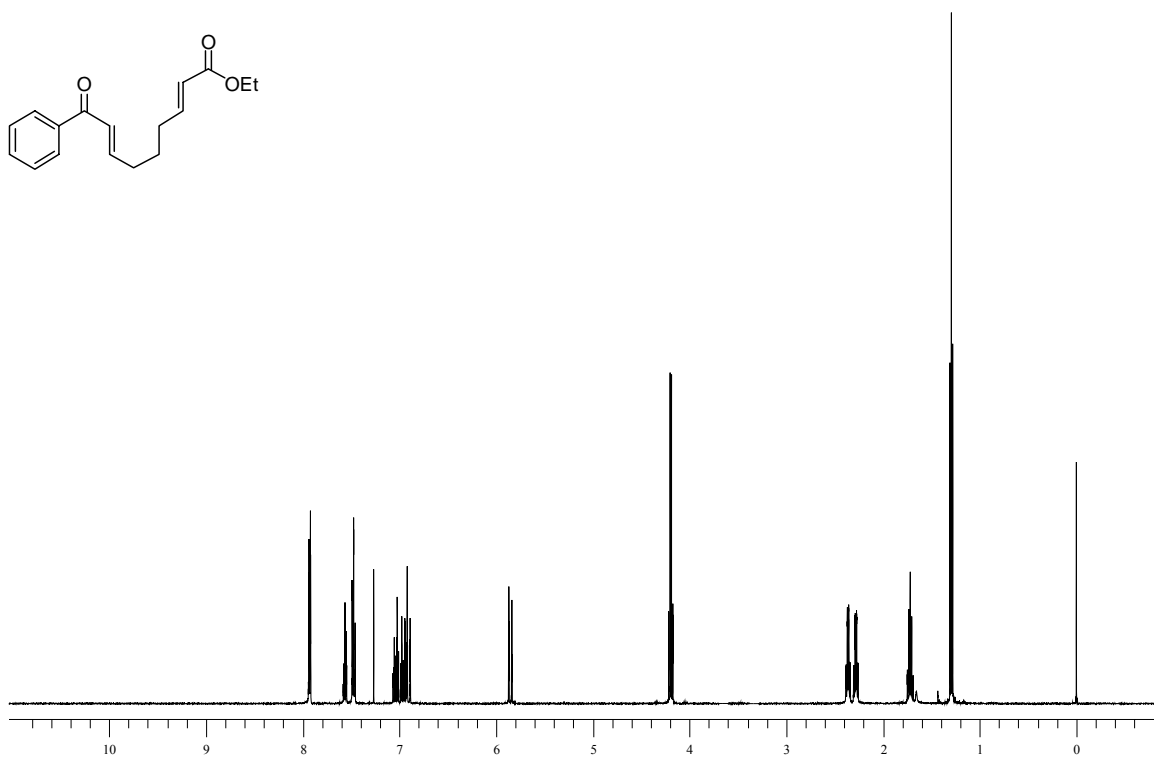
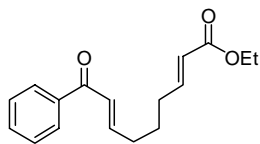
Compound 40b.



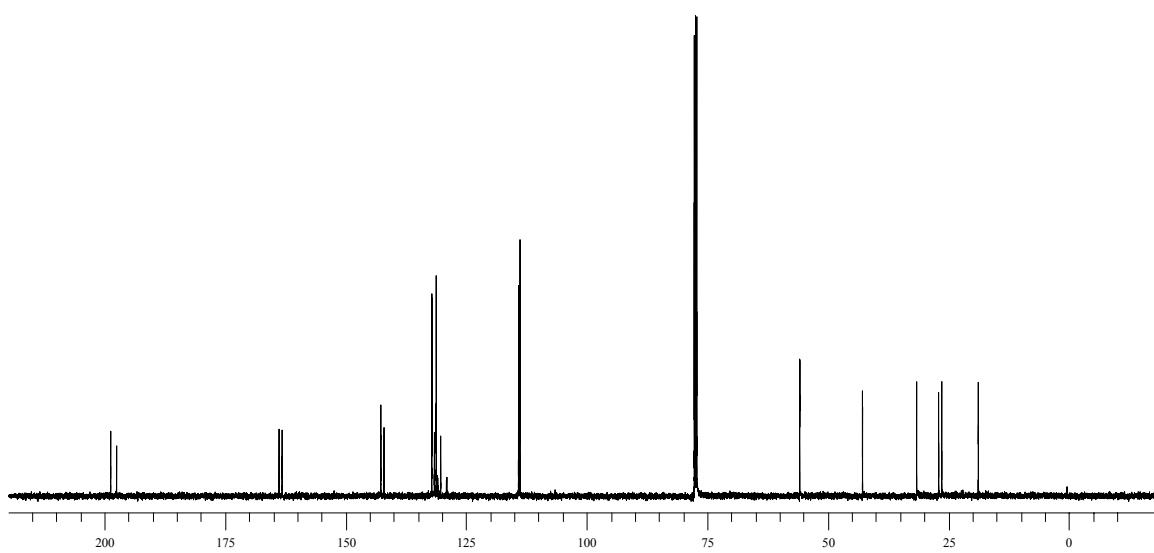
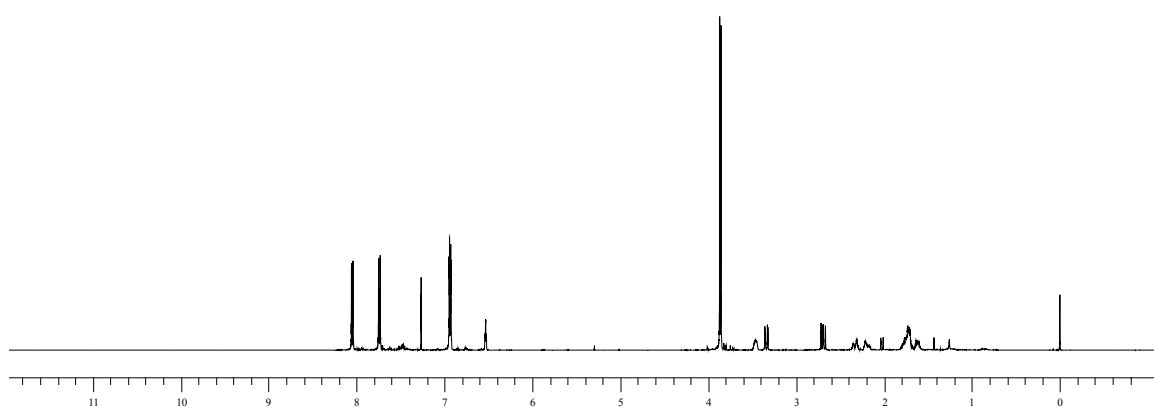
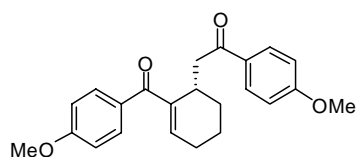
Compound 41b.



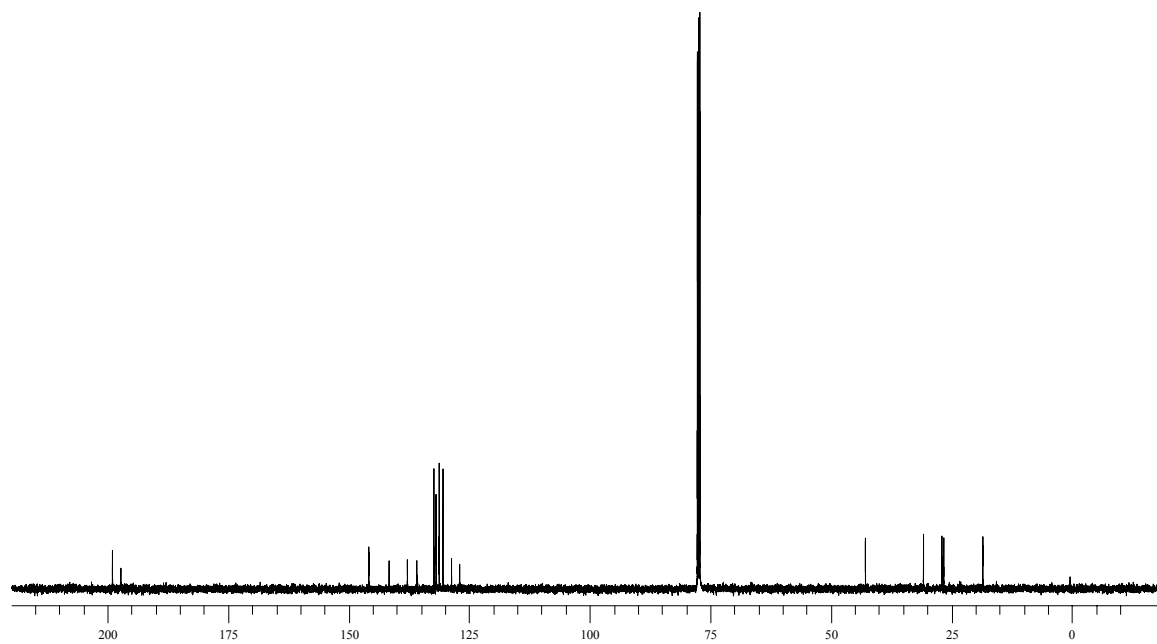
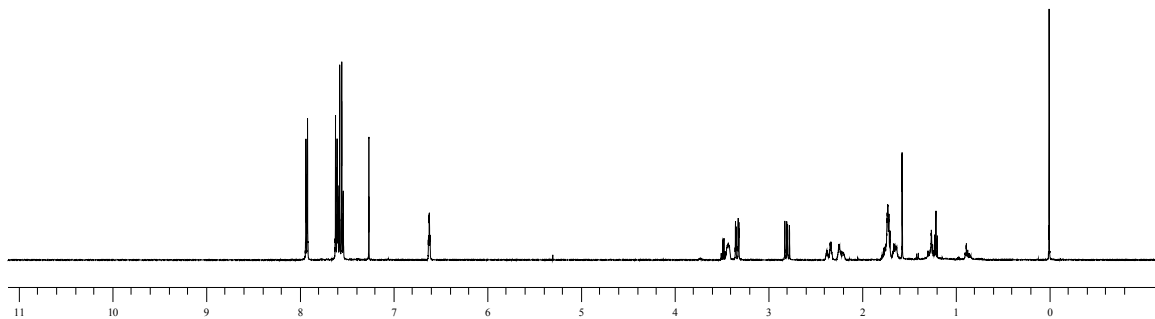
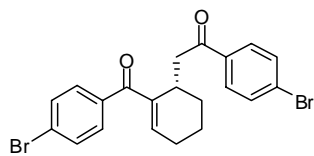
Compound 42b.



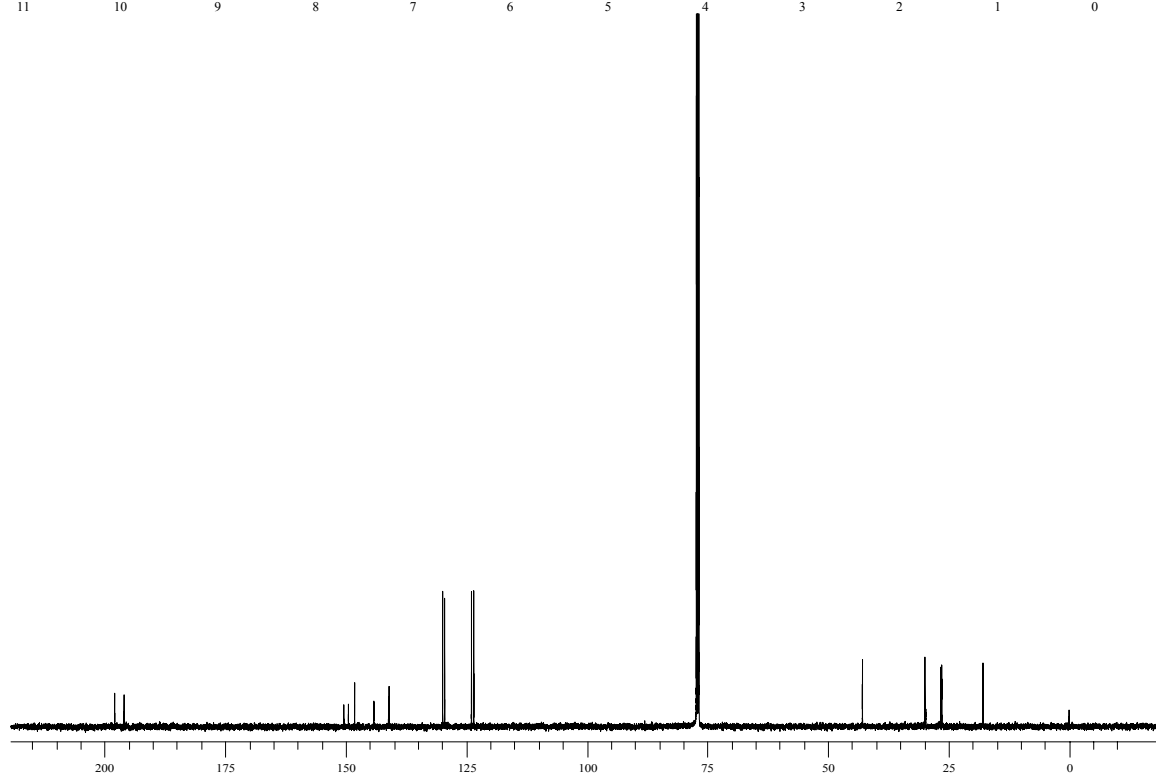
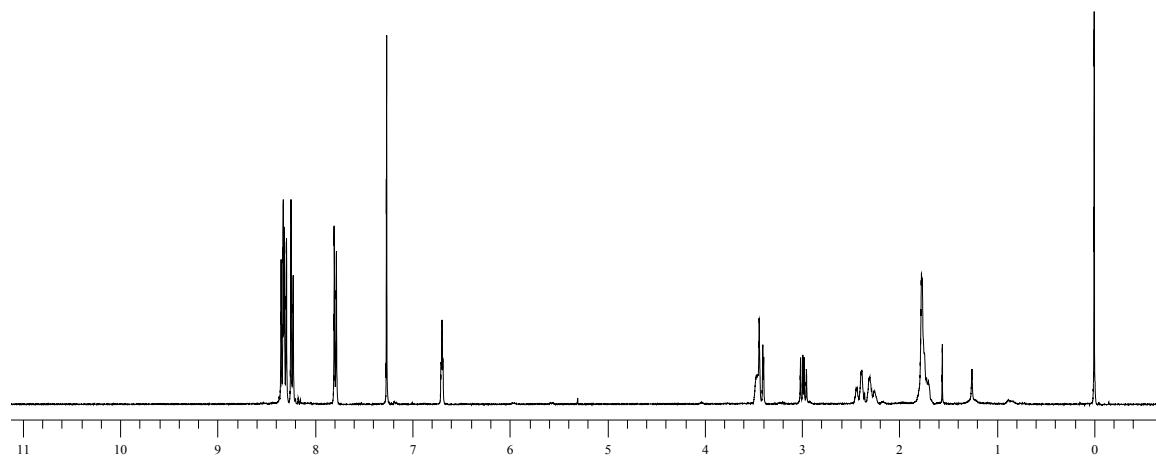
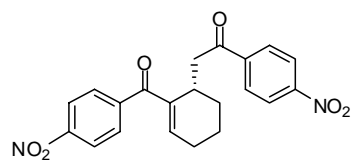
Compound 38.



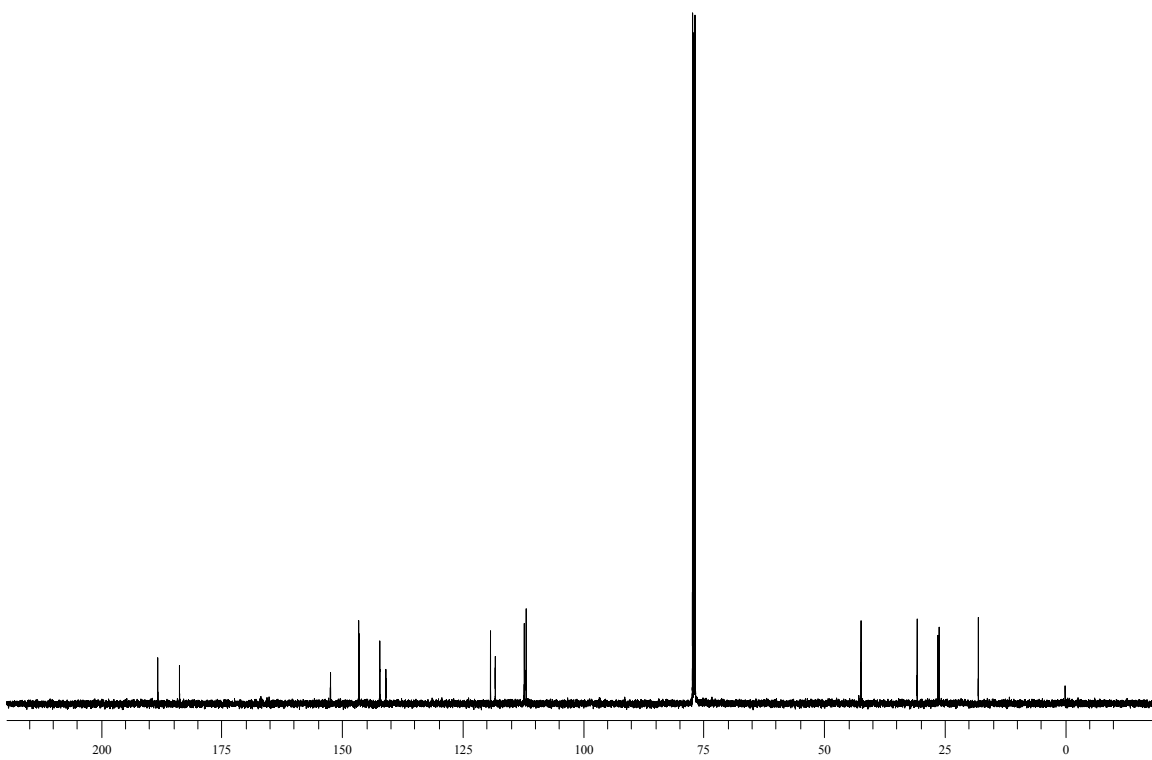
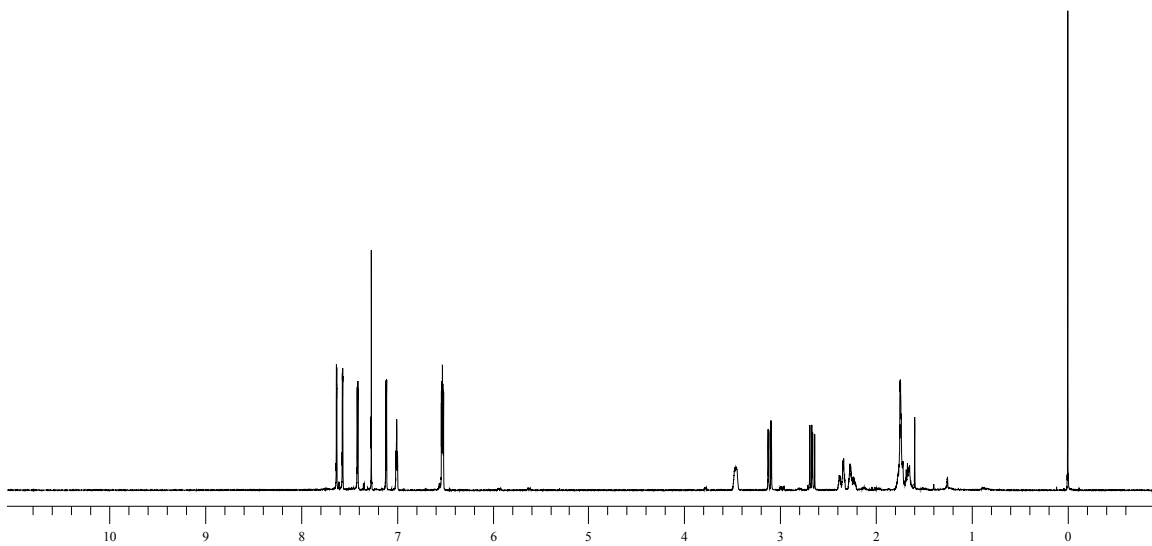
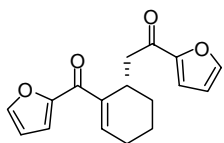
Compound 24.



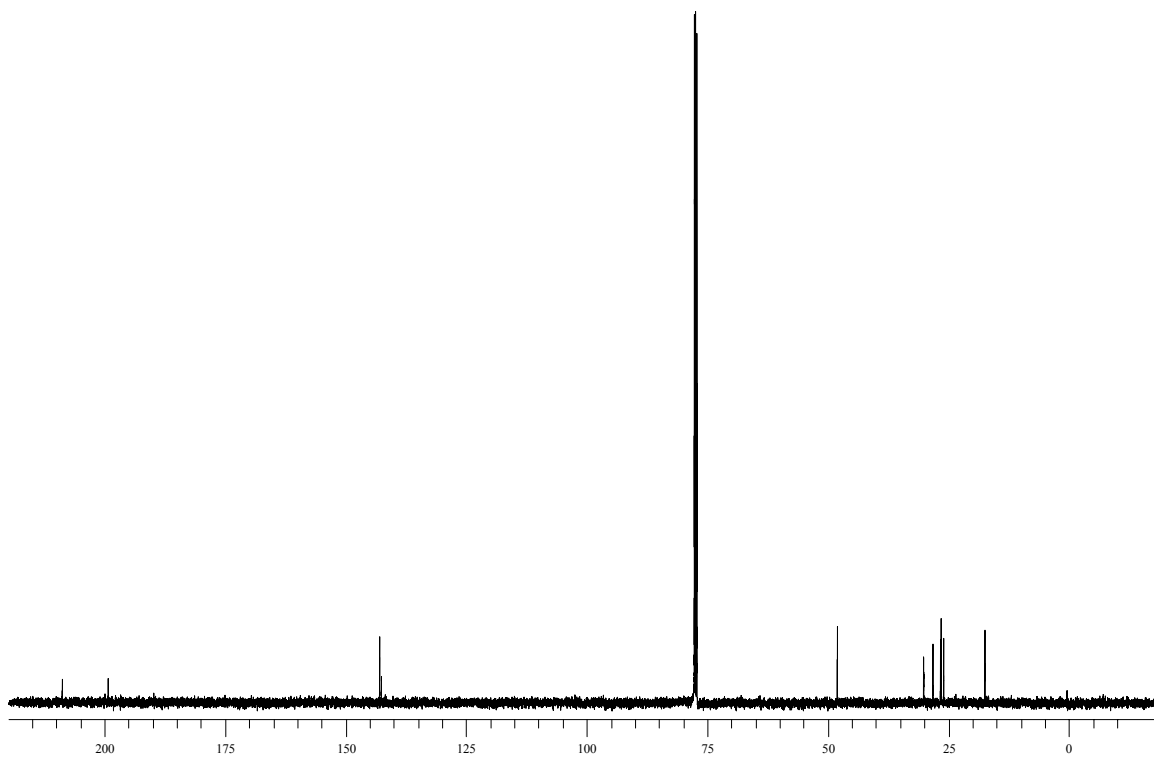
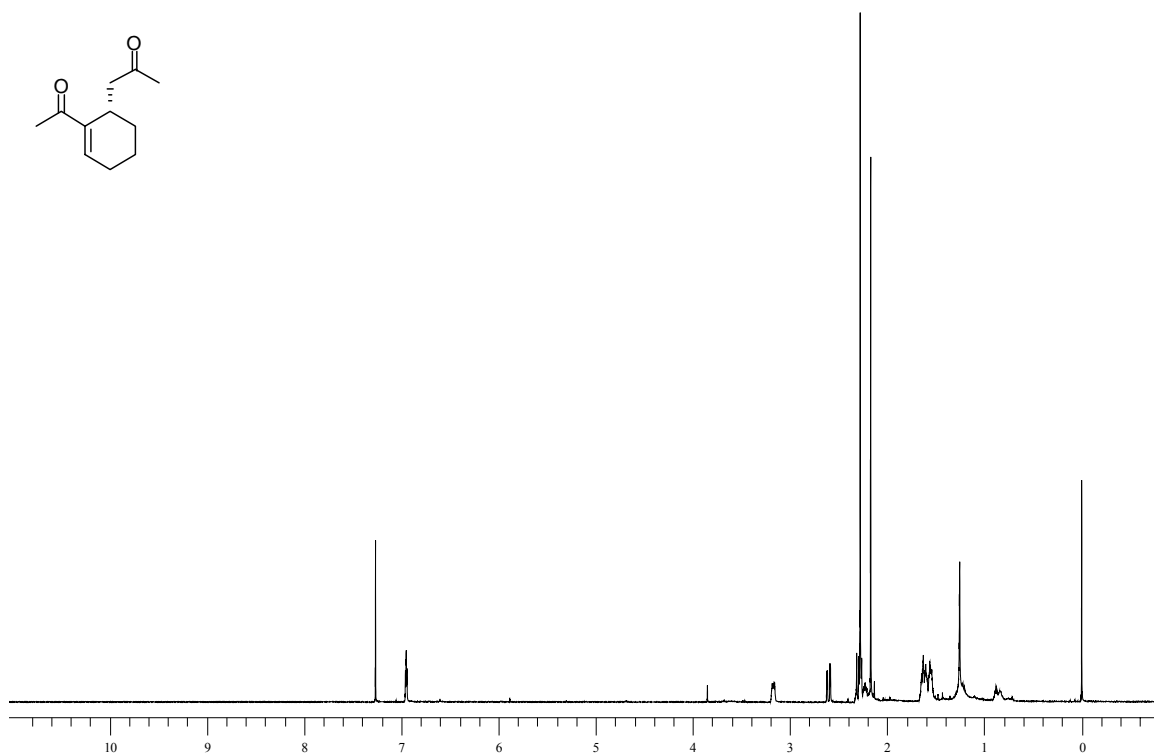
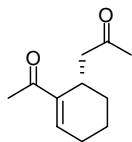
Compound 39.



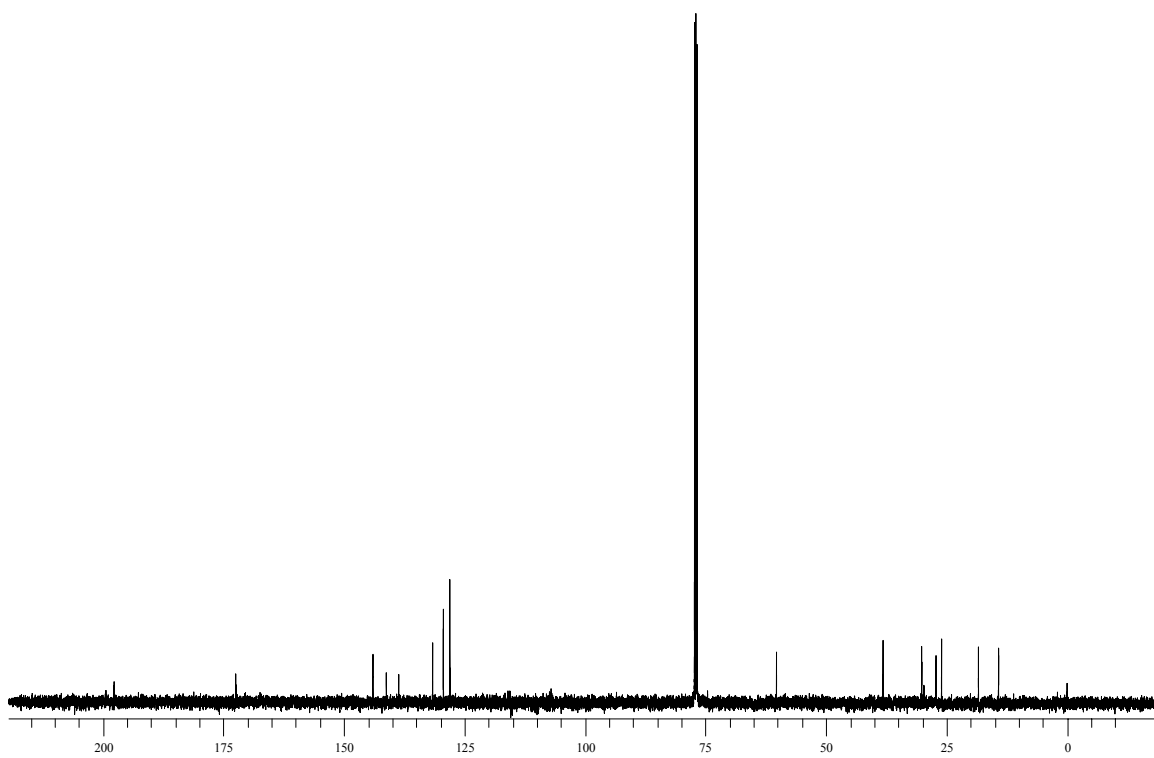
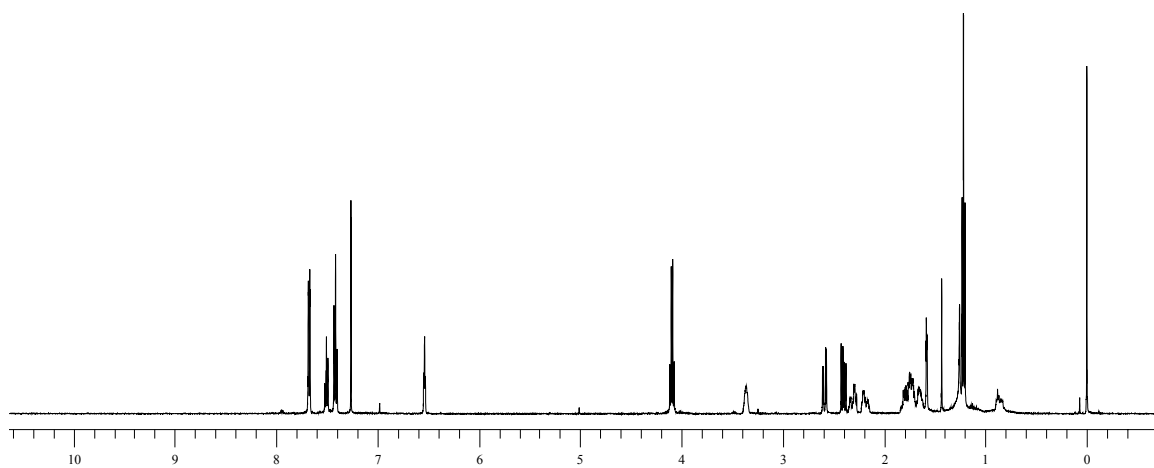
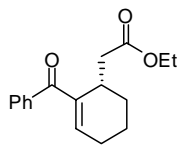
Compound 40.



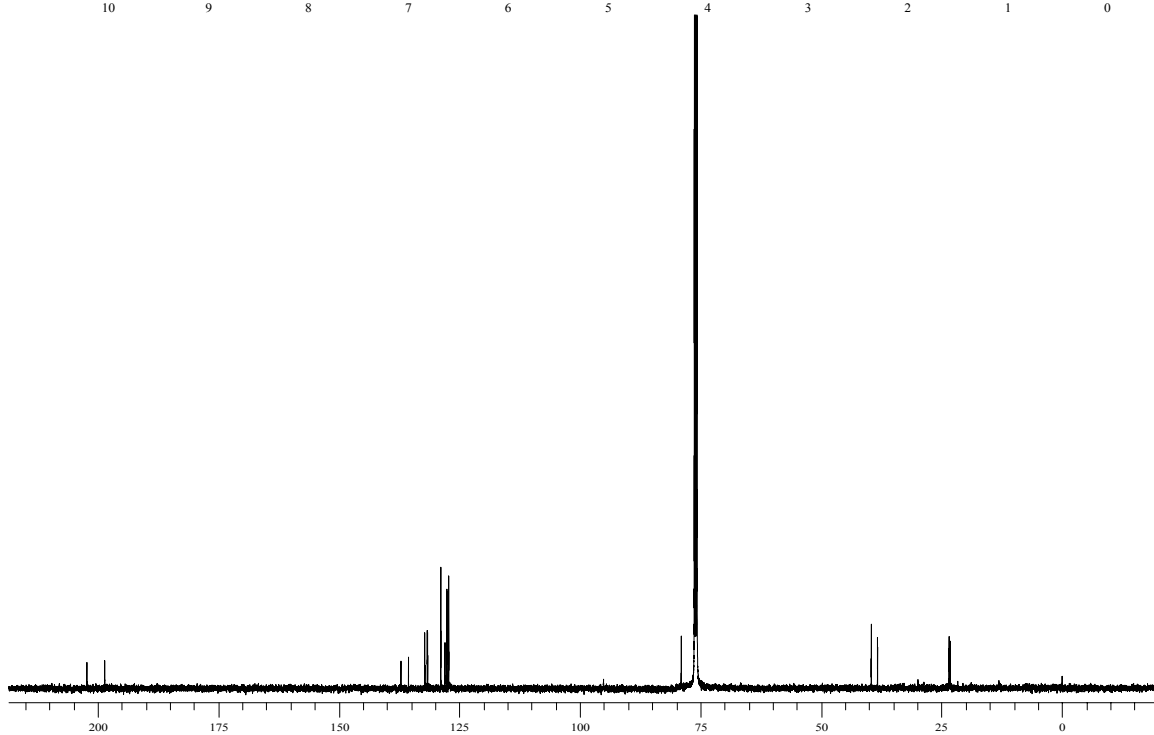
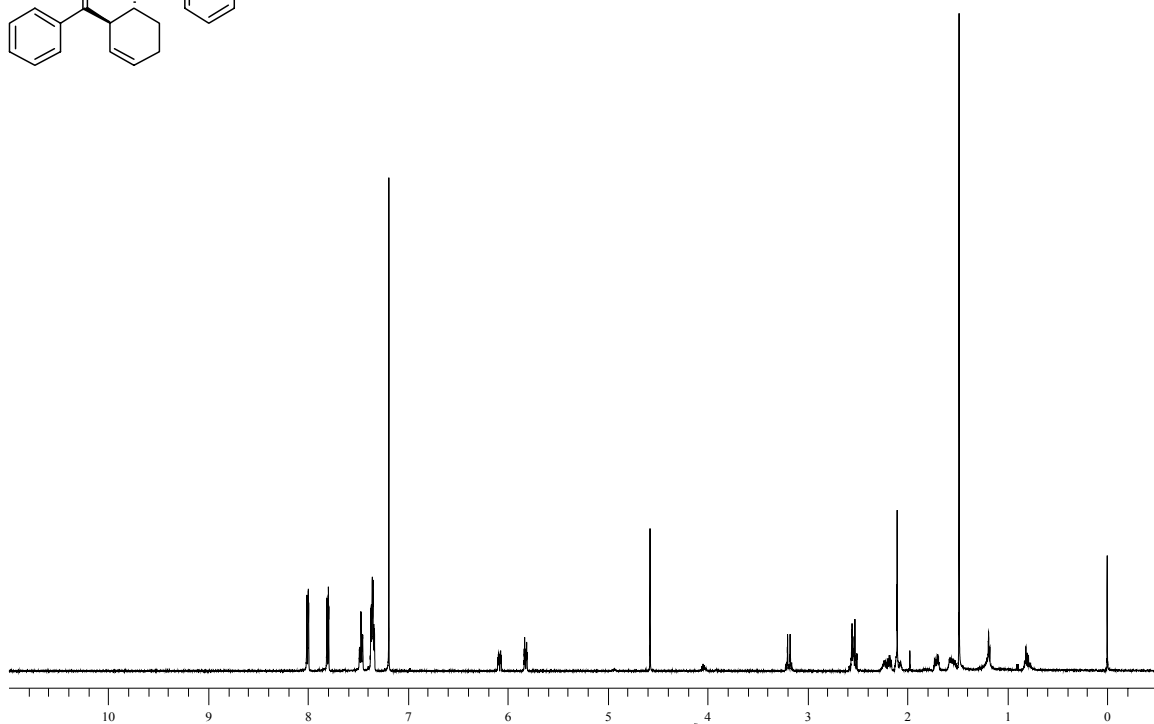
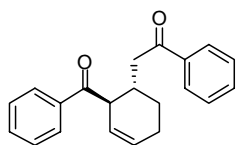
Compound 41.



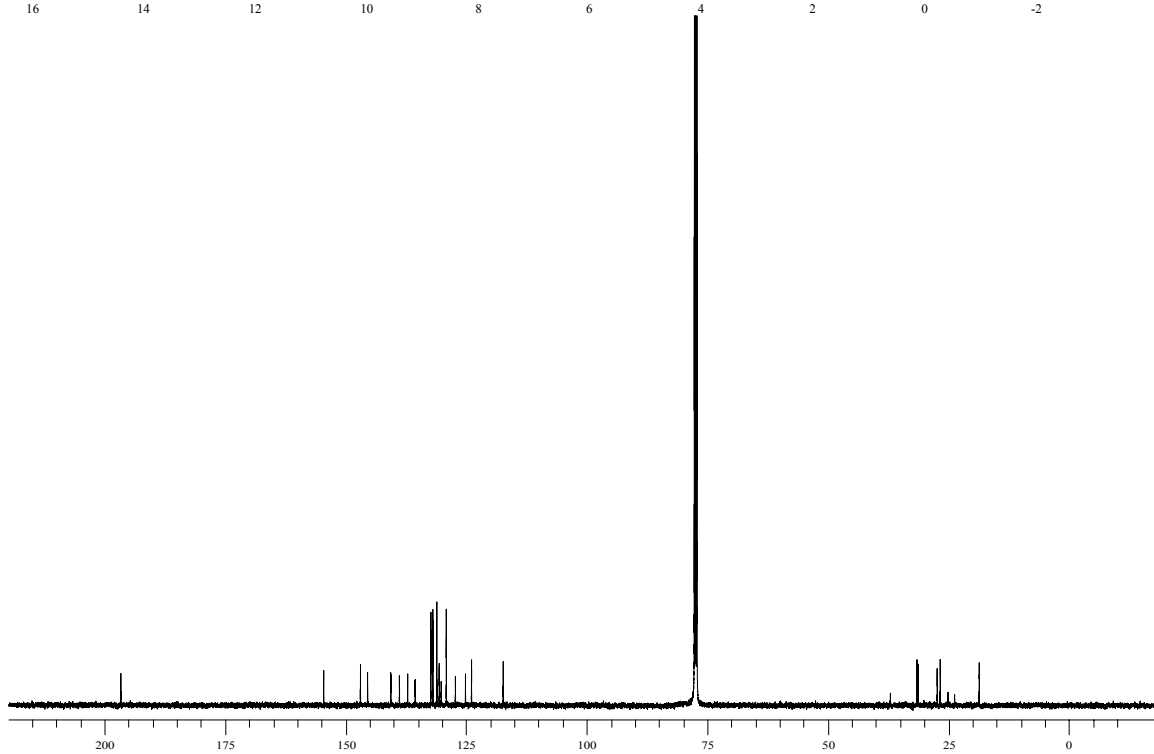
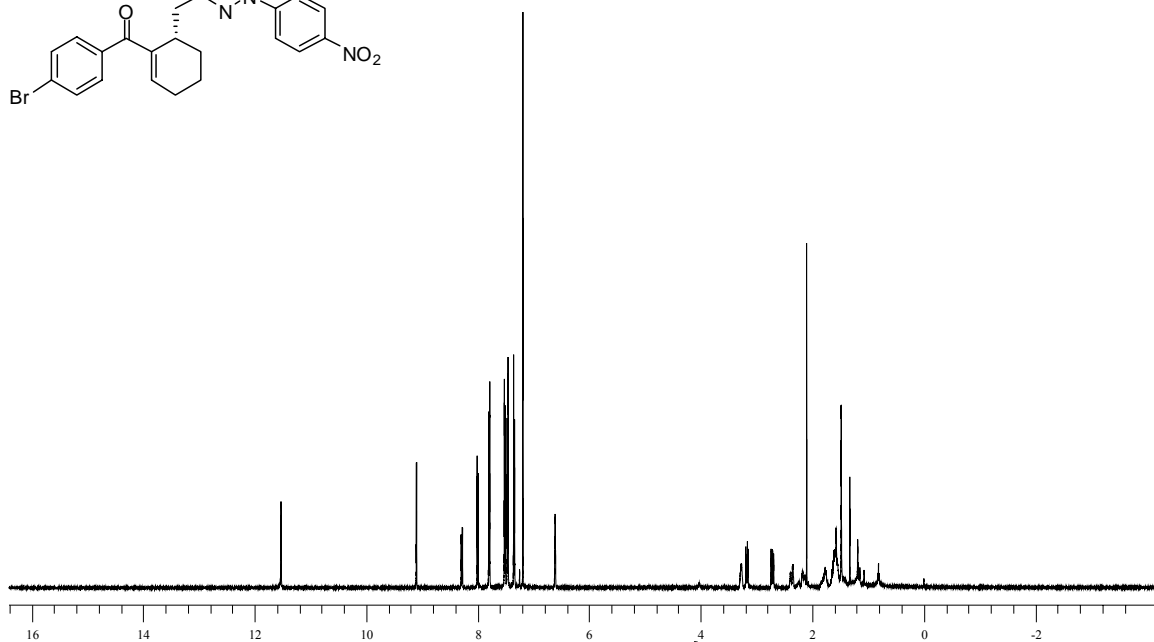
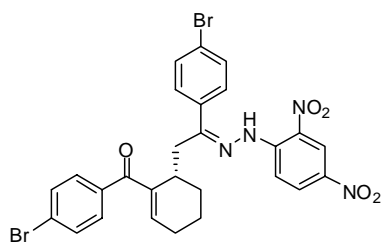
Compound 42.



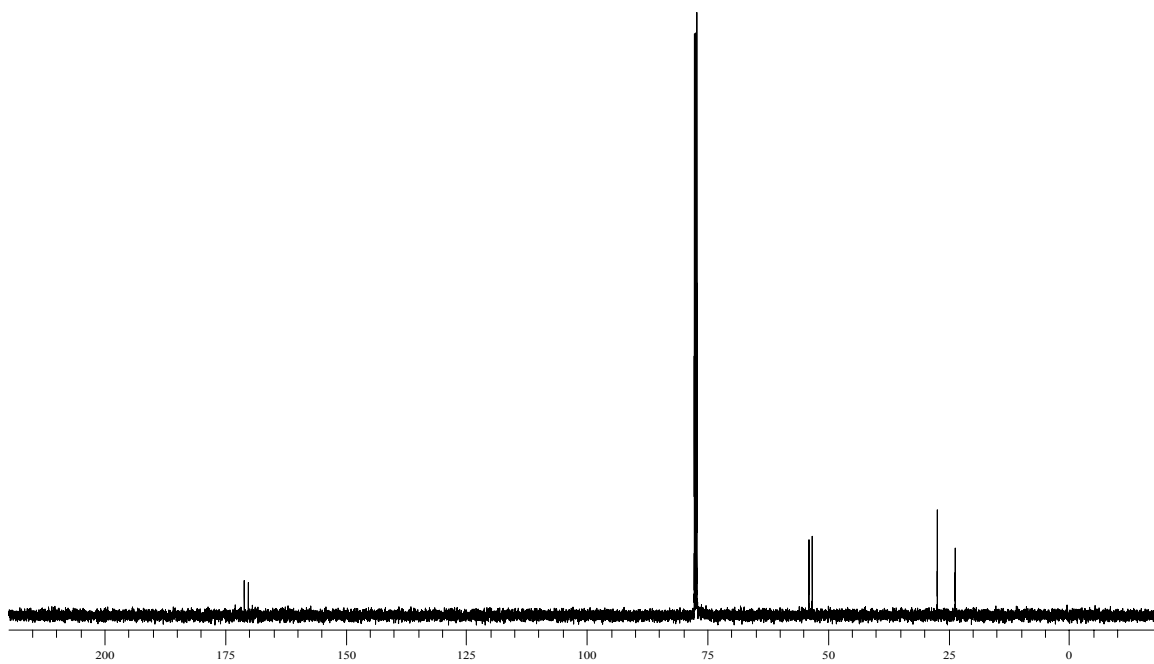
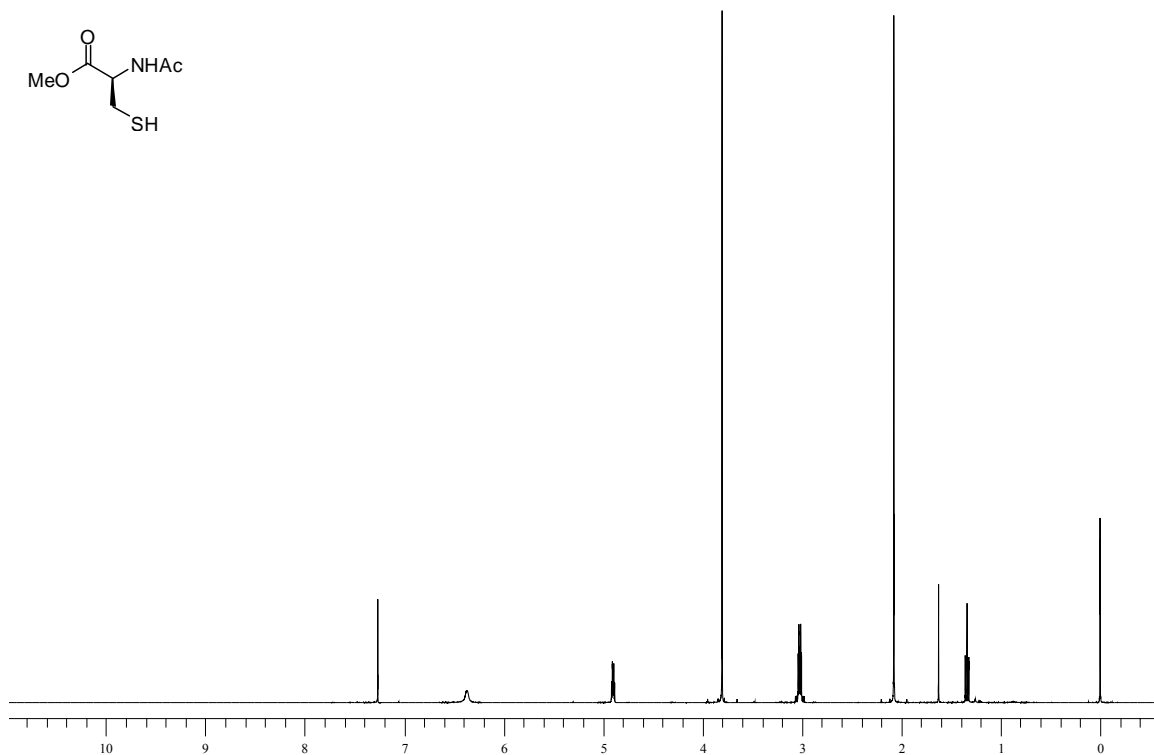
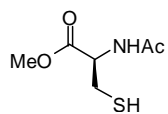
Compound 26.



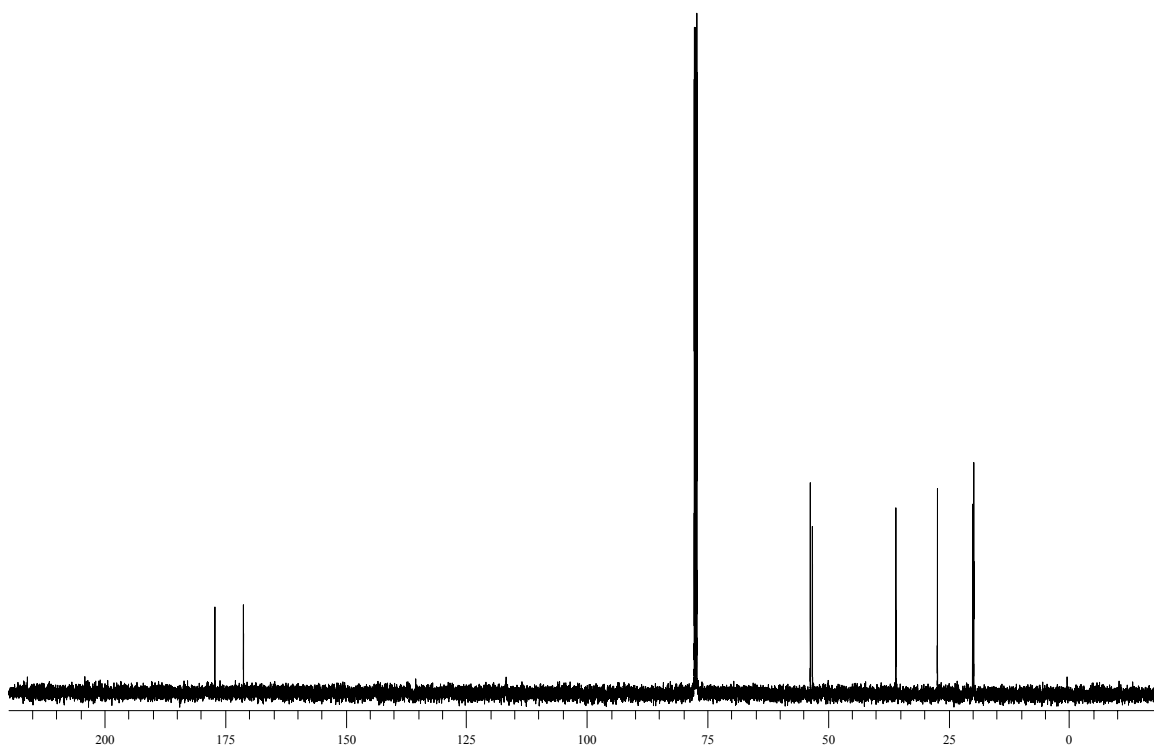
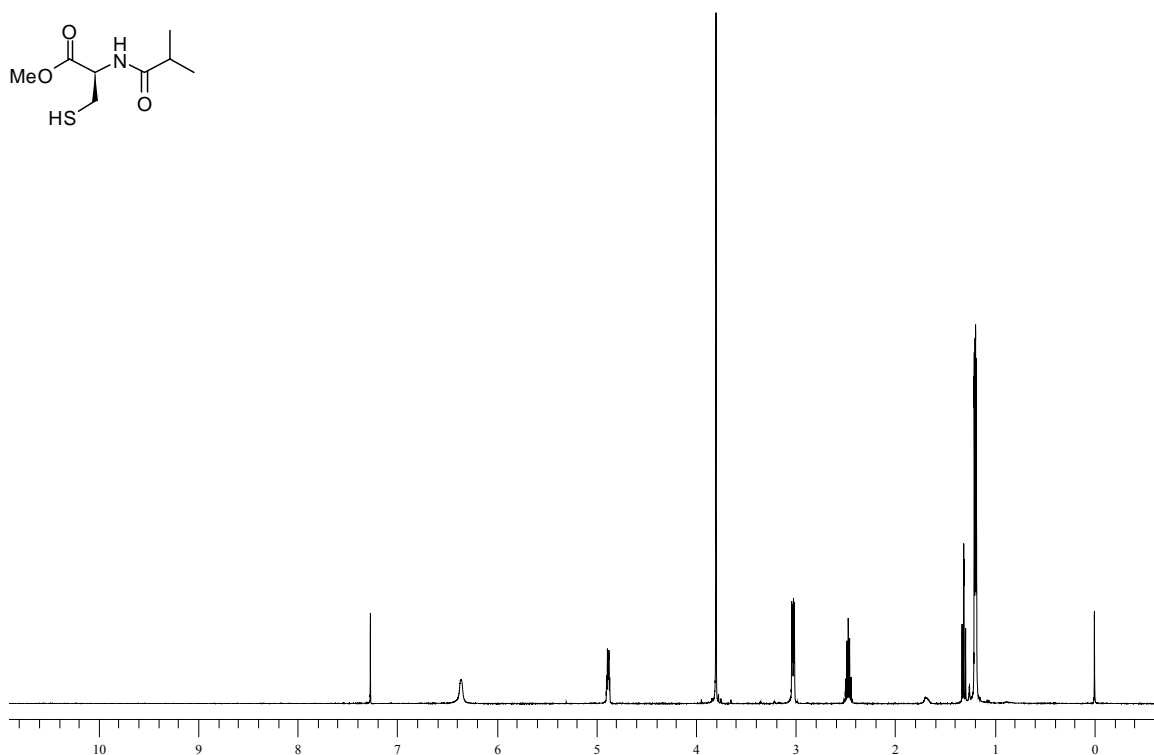
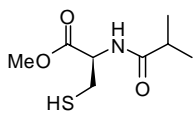
Compound 25.



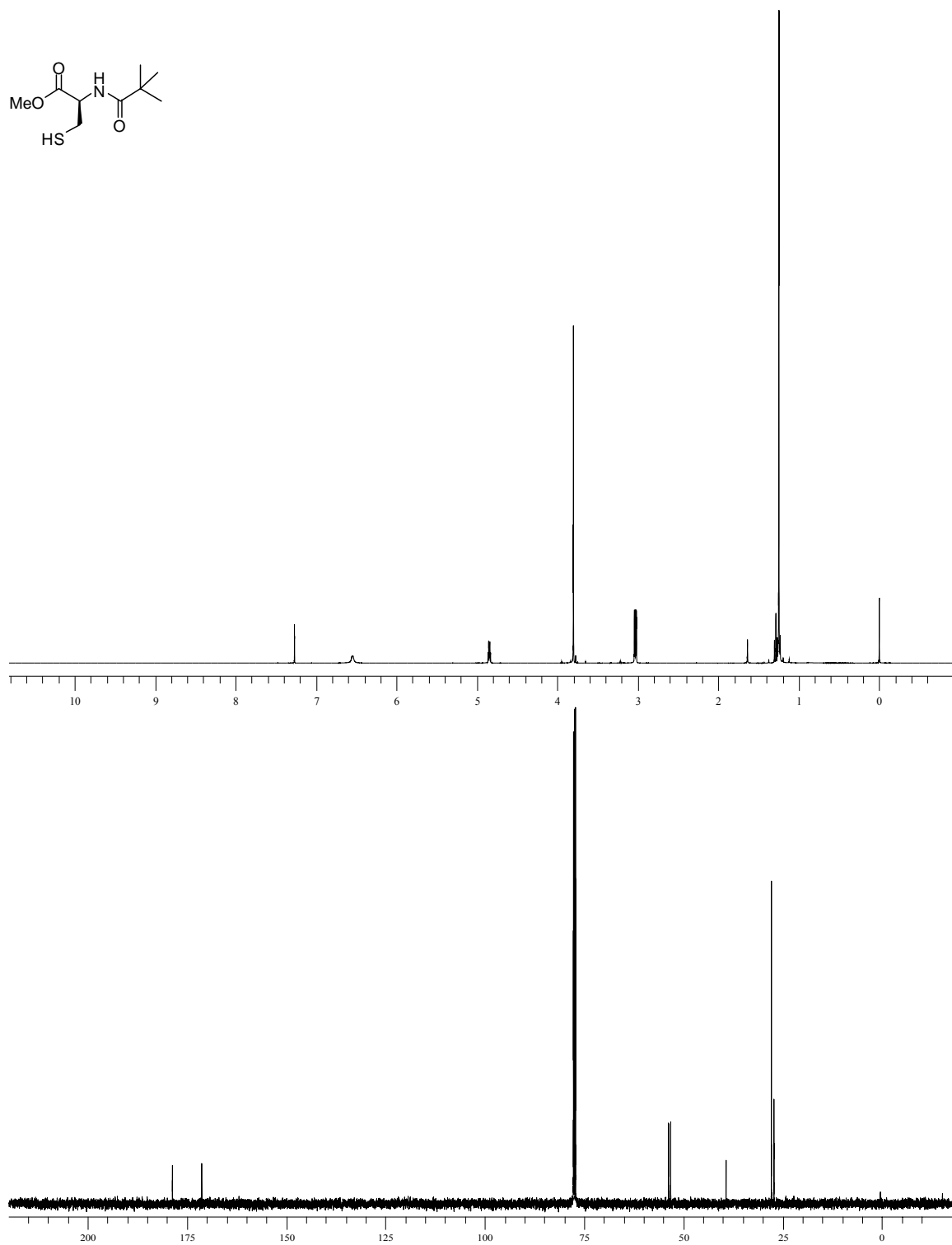
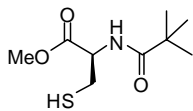
Compound 20.



Compound 22.



Compound 23.

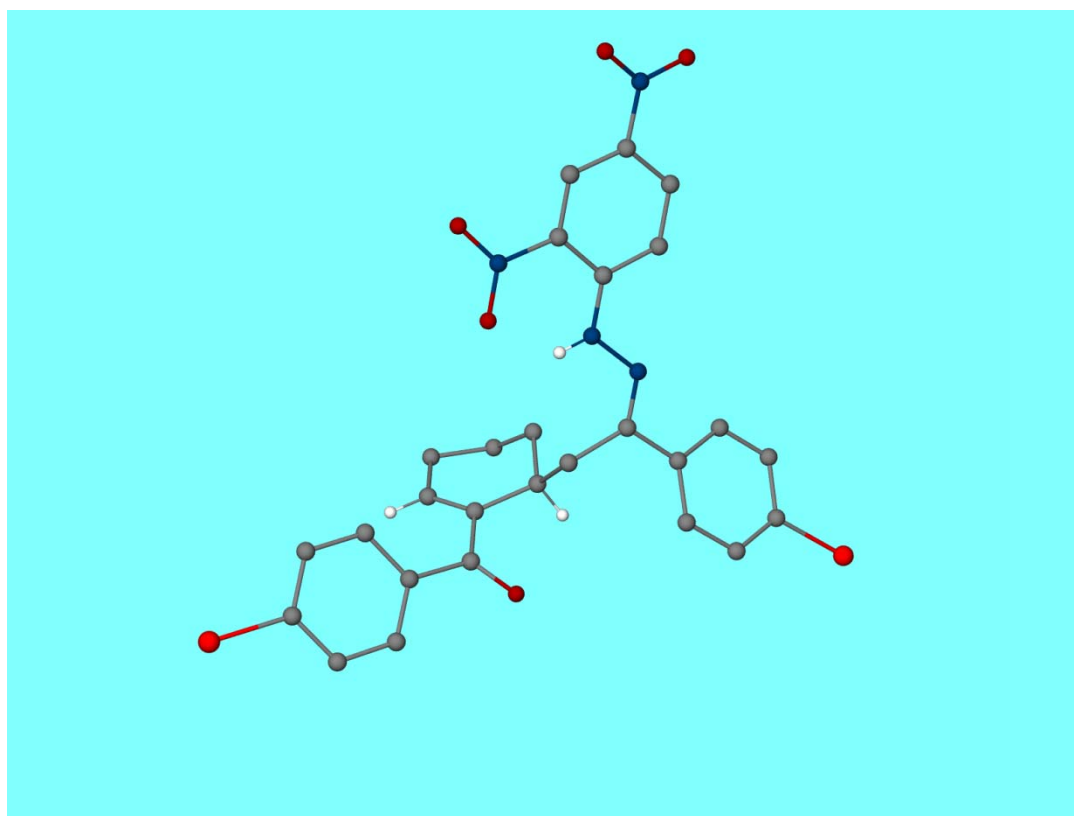


3.7.2 Appendix: Crystallographic Data for Compound 25

YALE CHEMICAL INSTRUMENTATION CENTER

X-Ray Structure Report
Reference Number: MILLER_CA01

September 29, 2006



YALE CHEMICAL INSTRUMENTATION CENTER

X-Ray Structure Report
Reference Number: MILLER_CA01

September 29, 2006

Data Collection

An orange plate crystal of $C_{27}H_{22}Br_2N_4O_5$ having approximate dimensions of 0.20 x 0.20 x 0.10 mm³ was mounted with epoxy cement on the tip of a fine glass fiber. All measurements were made on a Nonius KappaCCD diffractometer with graphite monochromated Mo-K α radiation.

Cell constants and an orientation matrix for data collection corresponded to a primitive orthorhombic cell with dimensions:

$$\begin{aligned} a &= 7.3503(15) \text{ \AA} & \alpha &= 90^\circ \\ b &= 11.878(2) \text{ \AA} & \beta &= 90^\circ \\ c &= 33.132(7) \text{ \AA} & \gamma &= 90^\circ \\ V &= 2892.6(10) \text{ \AA}^3 \end{aligned}$$

For $Z = 4$ and F.W. = 642.31, the calculated density is 1.475 g/cm³. Based on a statistical analysis of intensity distribution, and the successful solution and refinement of the structure, the space group was determined to be $P2_12_12_1$ (#19).

The data were collected at a temperature of 173(2) K to a maximum 2θ value of 58.22°. Three omega scans consisting of 108, 108, and 87 data frames, respectively, were collected with a frame width of 0.7° and a detector-to-crystal distance, D_x , of 43.0 mm. Each frame was exposed twice (for the purpose of de-zinger) for a total of 21 s. The data frames were processed and scaled using the DENZO software package.¹³⁴

Data Reduction

A total of 7386 reflections were collected of which 7386 were unique and observed ($R_{\text{int}} = 0.000$, Friedel pairs not merged). The linear absorption coefficient, μ , for Mo-K α radiation is 28.44 cm⁻¹, and no absorption correction was applied. The data were corrected for Lorentz and polarization effects.

¹³⁴ Z. Otwinowski and W. Minor, "Processing of X-Ray Diffraction Data Collected in Oscillation Mode," Methods in Enzymology, vol. 276: Macromolecular Crystallography, part A, 307-326, 1997, C.W. Carter, Jr. & R.M. Sweet, Eds., Academic Press.

Structure Solution and Refinement

The structure was solved by direct methods and expanded using Fourier techniques.¹³⁵ The non-hydrogen atoms were refined anisotropically, and hydrogen atoms, with exceptions noted, were treated as idealized contributions. The final cycle of full-matrix least-squares refinement¹³⁶ on F was based on 7386 observed reflections ($I > 2.00\sigma(I)$) and 347 variable parameters and converged with unweighted and weighted agreement factors of:

$$R = \Sigma ||F_o| - |F_c|| / \Sigma |F_o| = 0.0521$$
$$R_w = \{ \Sigma [w (F_o^2 - F_c^2)^2] / \Sigma [w(F_o^2)^2] \}^{1/2} = 0.1252$$

The maximum and minimum peaks on the final difference Fourier map corresponded to 0.990 and $-0.442 \text{ e}^-/\text{\AA}^3$ respectively.

Structural Description

The compound crystallized in the chiral orthorhombic space group $P2_12_12_1$ with one molecule in the asymmetric unit and four molecules in the unit cell.

H(2) was located from the residual electron difference map and freely refined with isotropic displacement parameters. No geometric restraints were applied to the N(2)-H(2) bond, which refined to a distance of 0.76(5) Å. As illustrated in Figure 3, H(2) is hydrogen bonded to O(2) of the adjacent nitro-group. Interatomic distances are 2.03 Å for H(2)⋯O(2) and 2.60 Å for N(2)⋯O(2). The N(2)-H(2)⋯O angle is 131.3 °.

Extensive π -stacking is present in the crystal lattice. As illustrated in Figures 4 and 5, the π -stacking is present between the dinitro-substituted phenyl ring, C(22-27) and

¹³⁵ *SHELXTL*, v.6.12, Bruker-AXS, Madison, WI, 2001.

¹³⁶ Least Squares function minimized: $\Sigma w(F_o^2 - F_c^2)^2$

one of the bromo-substituted phenyl rings, C(16-21). Interplane separations are approximately 3.6 Å and the stacking propagates along the crystallographic a-axis.

The absolute molecular configuration was unambiguously determined [Flack = - 0.013(10)]. ORTEPs, packing diagrams and full crystallographic tables follow.

Figure 1

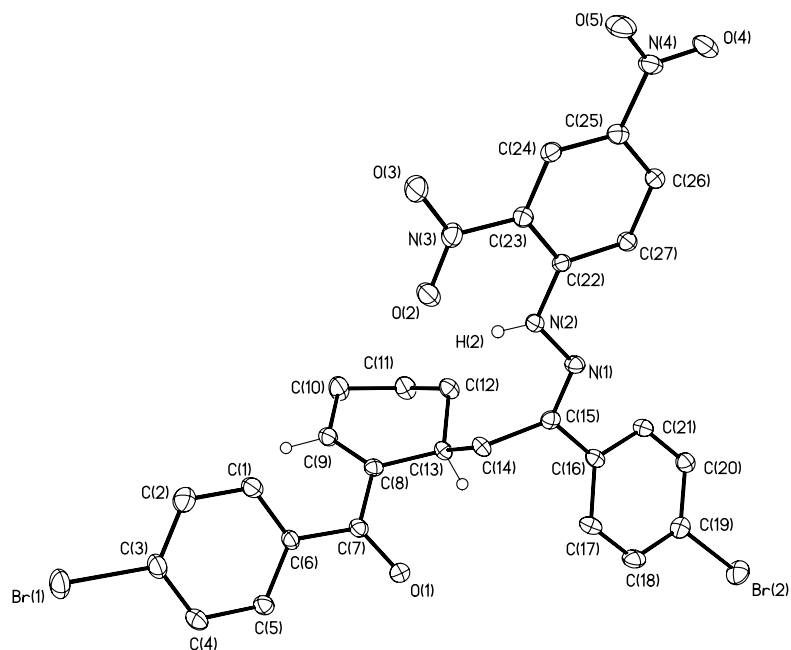


Figure 3

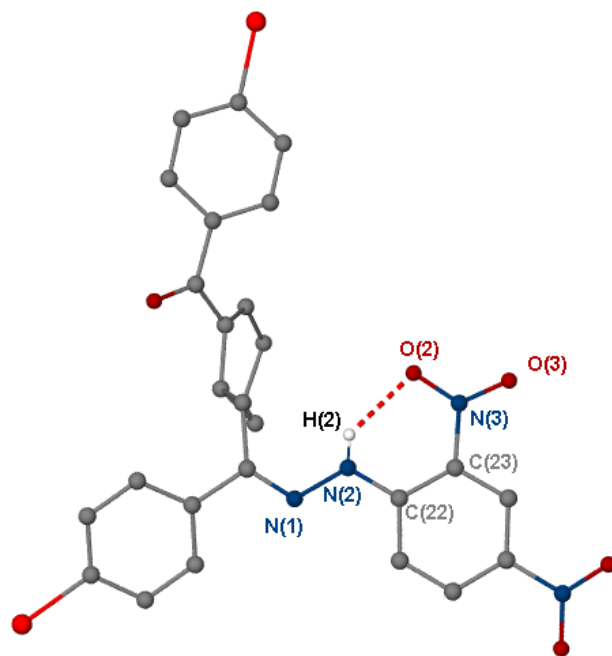


Figure 4

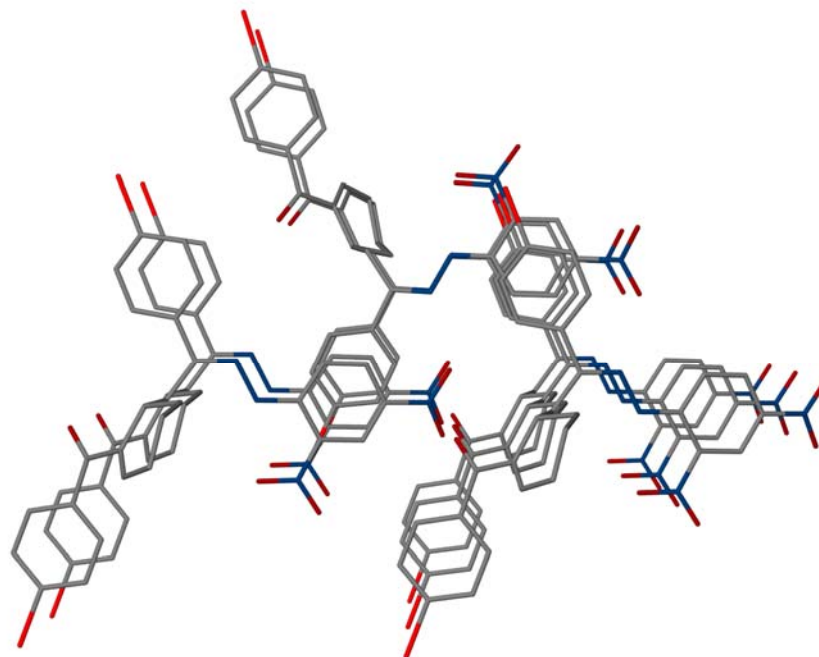
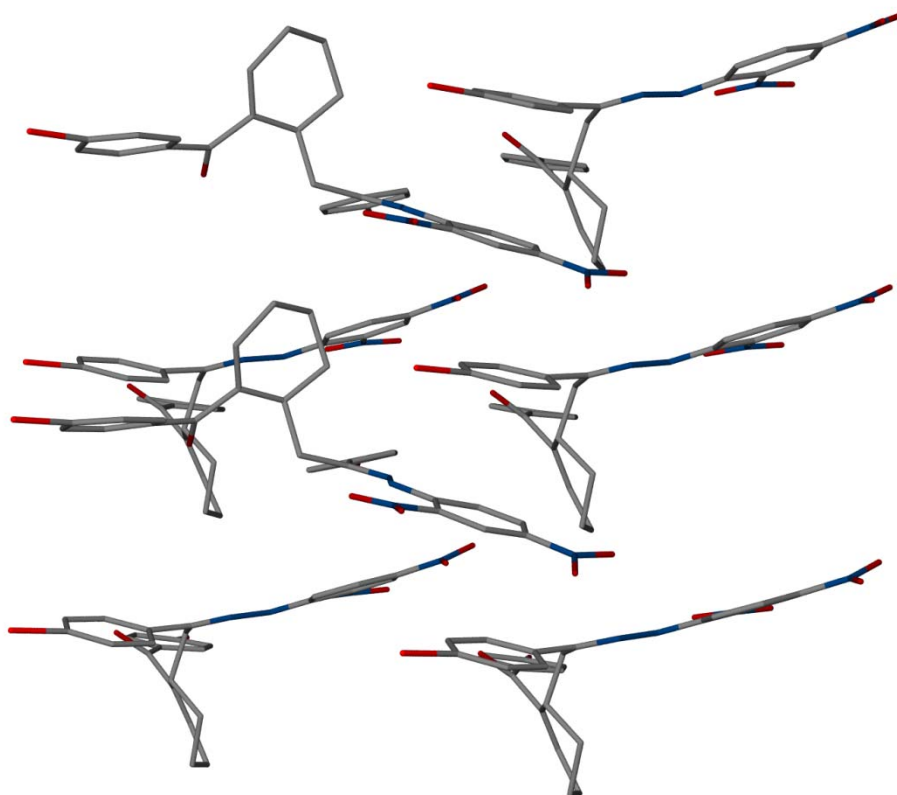
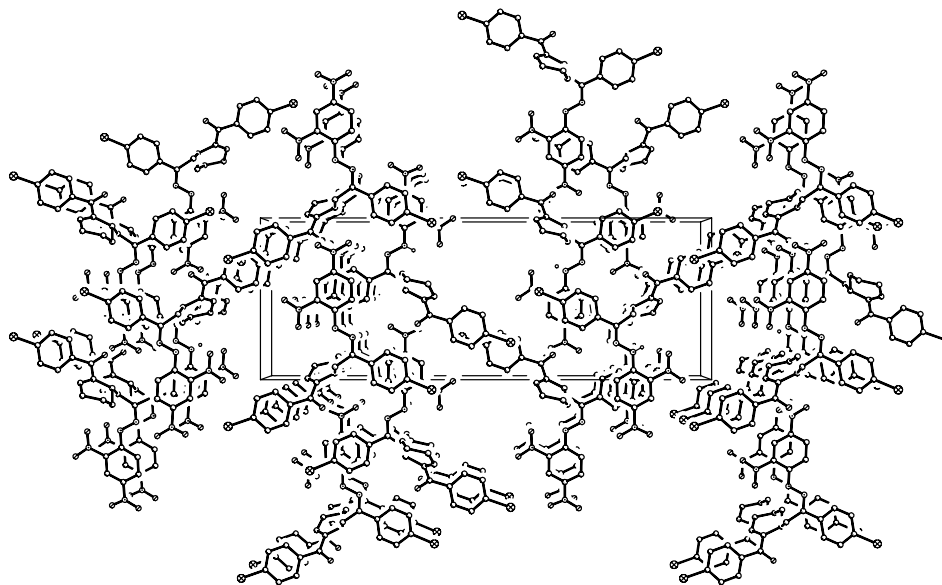


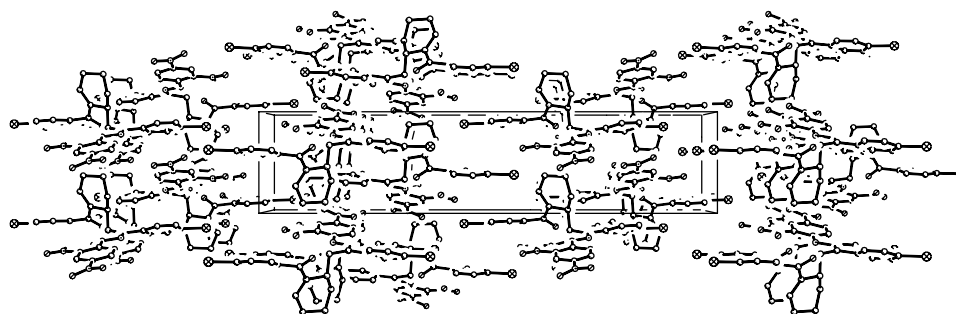
Figure 5



Packing diagram – View down the a-axis



Packing diagram – View down the b-axis



Packing diagram – View down the c-axis

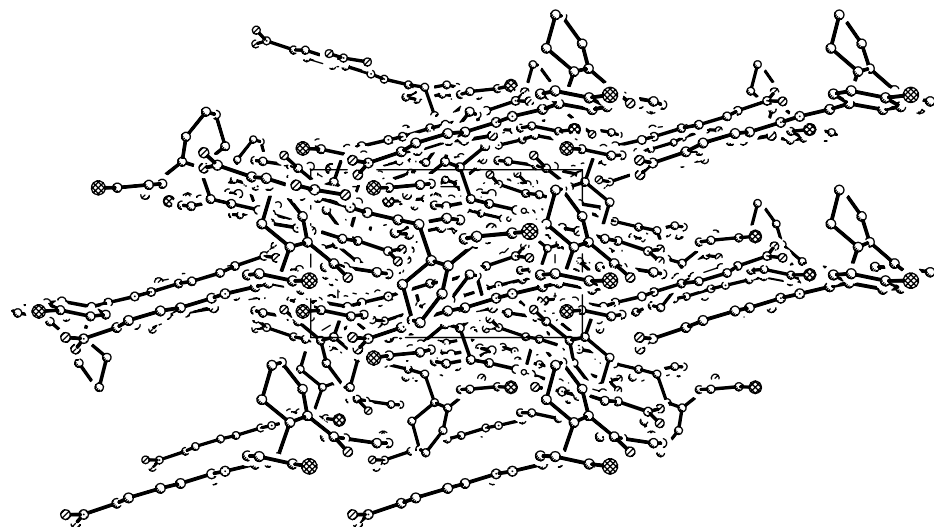


Table 1. Crystal data and structure refinement for miller_ca01.

Identification code	miller_ca01	
Empirical formula	C ₂₇ H ₂₂ Br ₂ N ₄ O ₅	
Formula weight	642.31	
Temperature	173(2) K	
Wavelength	0.71073 Å	
Crystal system	Orthorhombic	
Space group	P2(1)2(1)2(1)	
Unit cell dimensions	a = 7.3503(15) Å	α = 90°.
	b = 11.878(2) Å	β = 90°.
	c = 33.132(7) Å	γ = 90°.
Volume	2892.6(10) Å ³	
Z	4	
Density (calculated)	1.475 g/cm ³	
Absorption coefficient	28.44 cm ⁻¹	
F(000)	1288	
Crystal size	0.20 x 0.20 x 0.10 mm ³	
Theta range for data collection	2.84 to 29.11°.	
Index ranges	-10 ≤ h ≤ 10, -16 ≤ k ≤ 16, -44 ≤ l ≤ 45	
Reflections collected	7386	
Independent reflections	7386 [R(int) = 0.0000]	
Completeness to theta = 29.11°	98.9 %	
Absorption correction	None	
Max. and min. transmission	0.7641 and 0.6001	
Refinement method	Full-matrix least-squares on F ²	
Data / restraints / parameters	7386 / 0 / 347	
Goodness-of-fit on F ²	1.008	
Final R indices [I > 2σ(I)]	R1 = 0.0521, wR2 = 0.1252	
R indices (all data)	R1 = 0.0891, wR2 = 0.1417	
Absolute structure parameter	-0.013(10)	
Largest diff. peak and hole	0.990 and -0.442 e.Å ⁻³	

Table 2. Atomic coordinates ($\times 10^4$) and equivalent isotropic displacement parameters ($\text{\AA}^2 \times 10^3$) for miller_ca01. $U(\text{eq})$ is defined as one third of the trace of the orthogonalized U^{ij} tensor.

	x	y	z	$U(\text{eq})$
Br(1)	8864(1)	7359(1)	4467(1)	48(1)
Br(2)	8544(1)	9560(1)	8834(1)	45(1)
O(1)	8632(5)	8496(2)	6489(1)	35(1)
O(2)	6852(5)	13348(3)	6016(1)	43(1)
O(3)	6366(6)	14939(3)	5730(1)	51(1)
O(4)	5269(5)	18273(3)	7107(1)	41(1)
O(5)	4519(5)	18139(3)	6476(1)	43(1)
N(1)	7735(5)	12705(3)	7152(1)	25(1)
N(2)	7469(5)	13253(3)	6786(1)	27(1)
N(3)	6577(5)	14366(3)	6033(1)	34(1)
N(4)	5157(5)	17751(3)	6790(1)	31(1)
C(1)	9217(6)	9414(4)	5471(1)	33(1)
C(2)	9104(7)	9028(4)	5076(1)	41(1)
C(3)	8932(7)	7886(4)	5006(1)	36(1)
C(4)	8799(7)	7122(4)	5316(1)	36(1)
C(5)	8912(6)	7516(4)	5710(1)	29(1)
C(6)	9196(6)	8653(3)	5790(1)	25(1)
C(7)	9431(5)	9019(3)	6222(1)	26(1)
C(8)	10658(6)	9946(3)	6327(1)	25(1)
C(9)	12158(6)	10147(4)	6107(1)	30(1)
C(10)	13724(7)	10880(4)	6227(2)	42(1)
C(11)	13630(6)	11154(4)	6676(2)	36(1)
C(12)	11688(5)	11489(4)	6788(1)	29(1)
C(13)	10377(5)	10513(4)	6731(1)	24(1)
C(14)	8394(6)	10936(3)	6768(1)	25(1)
C(15)	8133(5)	11655(3)	7142(1)	24(1)
C(16)	8366(5)	11131(3)	7545(1)	24(1)
C(17)	8016(6)	9992(3)	7603(1)	30(1)
C(18)	8097(6)	9535(4)	7982(2)	35(1)

C(19)	8511(6)	10187(4)	8307(1)	30(1)
C(20)	8901(6)	11328(4)	8260(1)	31(1)
C(21)	8825(6)	11791(3)	7877(1)	28(1)
C(22)	6924(5)	14348(3)	6788(1)	22(1)
C(23)	6490(6)	14924(3)	6423(1)	27(1)
C(24)	5916(6)	16034(3)	6422(1)	27(1)
C(25)	5797(5)	16587(3)	6785(1)	26(1)
C(26)	6232(7)	16069(3)	7147(1)	28(1)
C(27)	6772(6)	14956(3)	7149(1)	26(1)

Table 3. Bond lengths [Å] and angles [°] for miller_ca01.

Br(1)-C(3)	1.895(4)	C(17)-C(18)	1.367(6)
Br(2)-C(19)	1.900(4)	C(18)-C(19)	1.360(7)
O(1)-C(7)	1.230(5)	C(19)-C(20)	1.394(6)
O(2)-N(3)	1.228(5)	C(20)-C(21)	1.383(6)
O(3)-N(3)	1.223(5)	C(22)-C(27)	1.402(6)
O(4)-N(4)	1.225(5)	C(22)-C(23)	1.426(6)
O(5)-N(4)	1.230(5)	C(23)-C(24)	1.385(6)
N(1)-C(15)	1.282(5)	C(24)-C(25)	1.372(6)
N(1)-N(2)	1.388(5)	C(25)-C(26)	1.386(6)
N(2)-H(2)	0.76(5)	C(26)-C(27)	1.381(6)
N(2)-C(22)	1.361(5)		
N(3)-C(23)	1.452(5)	C(15)-N(1)-N(2)	117.8(4)
N(4)-C(25)	1.460(5)	H(2)-N(2)-C(22)	119(4)
C(1)-C(2)	1.389(6)	H(2)-N(2)-N(1)	121(4)
C(1)-C(6)	1.391(6)	C(22)-N(2)-N(1)	119.0(4)
C(2)-C(3)	1.382(7)	O(3)-N(3)-O(2)	122.0(4)
C(3)-C(4)	1.372(7)	O(3)-N(3)-C(23)	118.1(4)
C(4)-C(5)	1.390(6)	O(2)-N(3)-C(23)	119.8(4)
C(5)-C(6)	1.392(6)	O(4)-N(4)-O(5)	124.2(4)
C(6)-C(7)	1.507(6)	O(4)-N(4)-C(25)	117.9(4)
C(7)-C(8)	1.465(6)	O(5)-N(4)-C(25)	117.9(4)
C(8)-C(9)	1.344(6)	C(2)-C(1)-C(6)	120.1(4)
C(8)-C(13)	1.513(6)	C(3)-C(2)-C(1)	119.1(5)
C(9)-C(10)	1.497(6)	C(4)-C(3)-C(2)	122.0(4)
C(10)-C(11)	1.524(7)	C(4)-C(3)-Br(1)	119.0(3)
C(11)-C(12)	1.528(6)	C(2)-C(3)-Br(1)	118.9(4)
C(12)-C(13)	1.520(6)	C(3)-C(4)-C(5)	118.4(4)
C(13)-C(14)	1.546(6)	C(4)-C(5)-C(6)	120.9(4)
C(14)-C(15)	1.516(6)	C(5)-C(6)-C(1)	119.2(4)
C(15)-C(16)	1.482(6)	C(5)-C(6)-C(7)	118.5(4)
C(16)-C(17)	1.391(6)	C(1)-C(6)-C(7)	122.2(4)
C(16)-C(21)	1.393(6)	O(1)-C(7)-C(8)	120.2(4)

O(1)-C(7)-C(6)	118.8(4)	C(24)-C(25)-N(4)	118.9(4)
C(8)-C(7)-C(6)	120.9(4)	C(26)-C(25)-N(4)	119.0(4)
C(9)-C(8)-C(7)	120.7(4)	C(27)-C(26)-C(25)	119.8(4)
C(9)-C(8)-C(13)	120.9(4)	C(26)-C(27)-C(22)	120.8(4)
C(7)-C(8)-C(13)	117.4(4)		
C(8)-C(9)-C(10)	126.2(4)		
C(9)-C(10)-C(11)	110.4(4)		
C(10)-C(11)-C(12)	109.7(4)		
C(13)-C(12)-C(11)	111.3(3)		
C(8)-C(13)-C(12)	111.3(3)		
C(8)-C(13)-C(14)	110.1(3)		
C(12)-C(13)-C(14)	109.9(3)		
C(15)-C(14)-C(13)	111.5(3)		
N(1)-C(15)-C(16)	114.3(4)		
N(1)-C(15)-C(14)	126.7(4)		
C(16)-C(15)-C(14)	118.9(3)		
C(17)-C(16)-C(21)	118.8(4)		
C(17)-C(16)-C(15)	120.9(4)		
C(21)-C(16)-C(15)	120.2(4)		
C(18)-C(17)-C(16)	120.4(4)		
C(19)-C(18)-C(17)	120.7(4)		
C(18)-C(19)-C(20)	120.7(4)		
C(18)-C(19)-Br(2)	120.5(3)		
C(20)-C(19)-Br(2)	118.8(3)		
C(21)-C(20)-C(19)	118.7(4)		
C(20)-C(21)-C(16)	120.7(4)		
N(2)-C(22)-C(27)	121.3(4)		
N(2)-C(22)-C(23)	121.4(4)		
C(27)-C(22)-C(23)	117.3(4)		
C(24)-C(23)-C(22)	121.8(4)		
C(24)-C(23)-N(3)	116.4(4)		
C(22)-C(23)-N(3)	121.7(4)		
C(25)-C(24)-C(23)	118.2(4)		
C(24)-C(25)-C(26)	122.1(4)		

Symmetry transformations used to generate equivalent atoms:

Table 4. Anisotropic displacement parameters ($\text{\AA}^2 \times 10^3$) for miller_ca01. The anisotropic displacement factor exponent takes the form: $-2\pi^2 [h^2 a^{*2} U^{11} + \dots + 2 h k a^* b^* U^{12}]$

	U ¹¹	U ²²	U ³³	U ²³	U ¹³	U ¹²
Br(1)	48(1)	67(1)	31(1)	-16(1)	5(1)	-21(1)
Br(2)	52(1)	47(1)	35(1)	13(1)	0(1)	7(1)
O(1)	49(2)	28(2)	29(2)	0(1)	7(2)	-6(2)
O(2)	68(3)	29(2)	33(2)	-4(1)	-2(2)	6(2)
O(3)	86(3)	41(2)	25(2)	3(1)	-1(2)	14(2)
O(4)	55(2)	24(2)	45(2)	-9(2)	1(2)	3(2)
O(5)	55(2)	28(2)	45(2)	5(2)	-10(2)	12(2)
N(1)	29(2)	20(2)	27(2)	2(2)	-2(1)	2(2)
N(2)	38(2)	21(2)	22(2)	-1(2)	2(2)	2(2)
N(3)	38(2)	37(2)	26(2)	2(2)	1(2)	5(2)
N(4)	32(2)	20(2)	42(2)	-1(2)	3(2)	-1(2)
C(1)	43(2)	25(2)	30(2)	-3(2)	-3(2)	-2(2)
C(2)	49(3)	45(3)	30(2)	2(2)	0(2)	-6(2)
C(3)	38(3)	41(3)	29(2)	-12(2)	2(2)	-7(2)
C(4)	41(3)	32(2)	36(2)	-10(2)	-1(2)	-10(2)
C(5)	25(2)	27(2)	34(2)	-5(2)	3(2)	-4(2)
C(6)	27(2)	25(2)	23(2)	-6(2)	-1(2)	-2(2)
C(7)	26(2)	22(2)	31(2)	-2(2)	3(2)	2(2)
C(8)	27(2)	20(2)	27(2)	2(2)	-1(2)	4(2)
C(9)	30(2)	25(2)	34(3)	-4(2)	6(2)	-4(2)
C(10)	32(2)	48(3)	45(3)	-14(2)	10(2)	-9(2)
C(11)	24(2)	43(3)	43(3)	-9(2)	0(2)	-3(2)
C(12)	22(2)	29(2)	37(2)	-6(2)	0(2)	3(2)
C(13)	24(2)	23(2)	26(2)	-3(2)	-1(2)	4(2)
C(14)	26(2)	22(2)	26(2)	-6(2)	-3(2)	2(2)

C(15)	19(2)	26(2)	29(2)	1(2)	0(2)	-4(2)
C(16)	19(2)	22(2)	31(2)	-3(2)	-2(2)	3(2)
C(17)	32(2)	20(2)	39(3)	-2(2)	-4(2)	1(2)
C(18)	38(2)	22(2)	45(3)	4(2)	0(2)	5(2)
C(19)	27(2)	34(2)	29(2)	7(2)	-2(2)	8(2)
C(20)	34(2)	30(2)	30(2)	-3(2)	0(2)	0(2)
C(21)	30(2)	22(2)	31(2)	-1(2)	-3(2)	-1(2)
C(22)	22(2)	21(2)	24(2)	2(2)	1(2)	-1(2)
C(23)	29(2)	26(2)	27(2)	-2(2)	3(2)	-3(2)
C(24)	30(2)	25(2)	25(2)	4(2)	2(2)	1(2)
C(25)	21(2)	24(2)	32(2)	1(2)	0(2)	2(2)
C(26)	34(2)	24(2)	26(2)	-3(2)	2(2)	-3(2)
C(27)	34(2)	23(2)	21(2)	1(2)	-3(2)	3(2)

Table 5. Hydrogen coordinates ($\times 10^4$) and isotropic displacement parameters ($\text{\AA}^2 \times 10^{-3}$) for miller_ca01.

	x	y	z	U(eq)
H(2)	7640(70)	12960(40)	6587(15)	30(14)
H(1A)	9309	10198	5523	39
H(2A)	9146	9542	4857	50
H(4A)	8633	6344	5262	44
H(5A)	8794	7001	5928	35
H(9A)	12230	9791	5851	36
H(10A)	13693	11587	6068	50
H(10B)	14882	10489	6167	50
H(11A)	14474	11779	6739	44
H(11B)	14004	10488	6835	44
H(12A)	11658	11737	7074	35
H(12B)	11298	12130	6618	35
H(13A)	10603	9948	6949	29
H(14A)	8077	11382	6526	30
H(14B)	7562	10281	6781	30
H(17A)	7720	9528	7379	36
H(18A)	7861	8756	8018	42
H(20A)	9213	11779	8486	37
H(21A)	9088	12567	7840	33
H(24A)	5613	16403	6177	32
H(26A)	6159	16479	7392	34
H(27A)	7043	14598	7398	32

4 Synthetic Studies Toward the Synthesis of (+)-Sch 642305 via Selective Transannular Rauhut-Currier Reaction

4.1 Introduction

An ongoing question in our research group has been concerned with the issue of utilizing *catalyst* control to override *substrate* control. It is well established that the conformational rigidity of macrocycles can be employed as a controlling element for various stereospecific transformations.¹³⁷ Transannular reactions have the ability to incorporate high degrees of both stereo and architectural complexity in a single step, traditionally directed by the conformational properties of the reacting macrocycle.¹³⁸ The ability to control the outcome of these reactions through the use of a chiral catalyst would enable the efficient synthesis of not only desired complex molecules, but analogs of these products as well.

In 2004, Roush and coworkers reported the synthesis of Spinosyn A in which they effectively used trimethylphosphine to catalyze a diastereoselective transannular Rauhut-Currier (RC) reaction (Figure 4.1).¹³⁹ They utilized the predefined conformational preference of the macrocycle in order to achieve high diastereoselectivity and set the C3 stereocenter. The stereochemical issues were dependent upon the intrinsic properties of the macrocycle, and not of the achiral catalyst. However, an alternative approach would be necessary if the inherent reactivity provided the opposite diastereomer

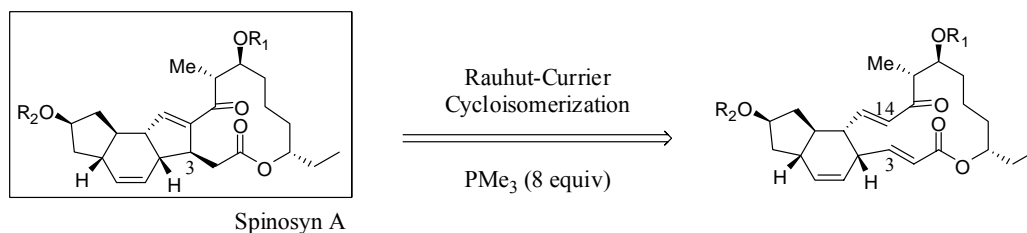
¹³⁷ Still, W. C.; Galynker, I. *Tetrahedron* **1981**, *37*, 3981-3996.

¹³⁸ For a recent example, please see: Scheerer, J. R.; Lawrence, J. F.; Wang, G. C.; Evans, D. A. *J. Am. Chem. Soc.* **2007**, *129*, 8968-8969 and references therein.

¹³⁹ (a) Mergott, D. J.; Frank, S. A.; Roush, W. R. *Proc. Natl. Acad. Sci. U.S.A.* **2004**, *101*, 11955-11959. (b) Winbush, S. M.; Mergott, D. J.; Roush, W. R. *J. Org. Chem.* **2008**, *73*, 1818-1829.

from that desired, or to obtain an unnatural epimer of the natural product. We are intrigued with the prospect of using chiral catalysts to override the inherent selectivity dictated by macromolecular conformation, thereby granting access to otherwise difficult to obtain stereoisomers.

Figure 4.1: Use of macrocyclic control of the Rauhut-Currier Reaction in the synthesis of Spinosyn A by Roush and co-workers.



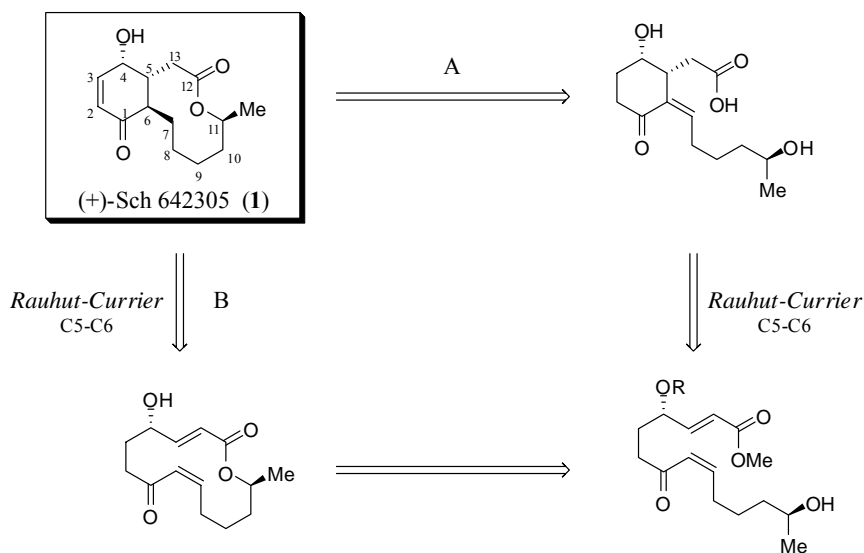
Inspired by the synthesis of Spinosyn A, we sought a molecule that would provide a forum in which we could explore this challenge. As illustrated in Scheme 4.1, the application of our enantioselective Rauhut-Currier methodology¹⁴⁰ to the stereoselective synthesis of (+)-Sch 642305 (**1**) will allow the us to address three major challenges: 1) the ability of our catalyst to dictate the stereoselectivity of the key step (*catalyst control*) and allow the synthesis of the natural product and unnatural stereoisomeric analogs, 2) the application of our newly developed RC methodology in a complex reaction setting, further demonstrating the utility of the transformation, and 3) the demonstration that this new methodology for generating a carbon–carbon bond with exquisite control of stereochemistry will provide an expedient synthesis of natural product **1**.

Herein we present the initial investigations into addressing each of these challenges in the synthesis of (+)-Sch 642305. Crucially, we have synthesized the key

¹⁴⁰ Please refer to Chapter 3 for an in-depth discussion of our methodology study.

Rauhut-Currier substrate in both pathways and have begun preliminary studies in that context. The findings that will be discussed lay the groundwork for an ongoing in-depth study.

Scheme 4.1: Application of our developed enantioselective Rauhut-Currier reaction to the synthesis of (+)-Sch 642305 (**1**).



4.2 Biological Significance: Anti-bacterial and Anti-HIV

In 2003, scientists at Schering-Plough reported the isolation of 10-membered macrolide (+)-Sch642305 (**1**) from *Penicillium verrucosum*.¹⁴¹ The compound was shown to inhibit bacterial DNA primase (Dna G), a novel target for the discovery of new antibiotics, with an EC₅₀ value of 70 μM.¹⁴² Dna G is a DNA-dependent RNA polymerase which is required for chromosomal DNA replication in Gram-positive and Gram-negative bacteria. With the emergence of multiple drug resistant organisms, the

¹⁴¹ Chu, M.; Mierzwa, R.; Xu, L.; He, L.; Terracciano, J.; Patel, M.; Gullo, V.; Black, T.; Zhao, W. J.; Chan, T. M.; McPhail, A.T. *J. Nat. Prod.* **2003**, *66*, 1527-1530.

¹⁴² Agarwal, A.; Louise-May, S.; Thanassi, J. A.; Podos, S. D.; Cheng, J.; Thoma, C.; Liu, C.; Wiles, J. A.; Nelson, D. M.; Phadke, A. S.; Bradbury, B. J.; Deshpande, M. S.; Pucci, M. J. *Bioorg. Med. Chem. Lett.* **2007**, *17*, 2807-2810.

identification and development of new targets to address the challenge of antibacterial resistance is of great interest worldwide.

The 10-membered macrolide was also isolated from the fungus *Septofusidium* sp. in 2005 by a group at Merck.¹⁴³ It was shown to inhibit HIV-1 Tat-dependent transactivation with an IC₅₀ value of 1.0 μM. Human immunodeficiency virus-1 tat (HIV-tat) is a proinflammatory cytokine and one of six regulatory proteins encoded by HIV that are essential for viral replication. The Tat protein is known to affect various cellular responses, playing a critical role in the pathogenesis of AIDS, and therefore represents an attractive target for the development of a new class of therapeutics in the treatment of HIV infections.

4.3 Previous Synthesis of (+)-Sch 642305

In addition to its interesting biological activities, (+)-Sch 642305 (**1**) is structurally novel with a decalactone ring *trans*-fused to a 4-hydroxycyclohexenone ring and includes four stereogenic centers, three of which are contiguous. Accordingly, the synthesis of **1** presents interesting challenges and has been the subject of attention of various research groups, leading to six total syntheses reported in the five years since its discovery in 2003.¹⁴⁴⁻¹⁴⁹

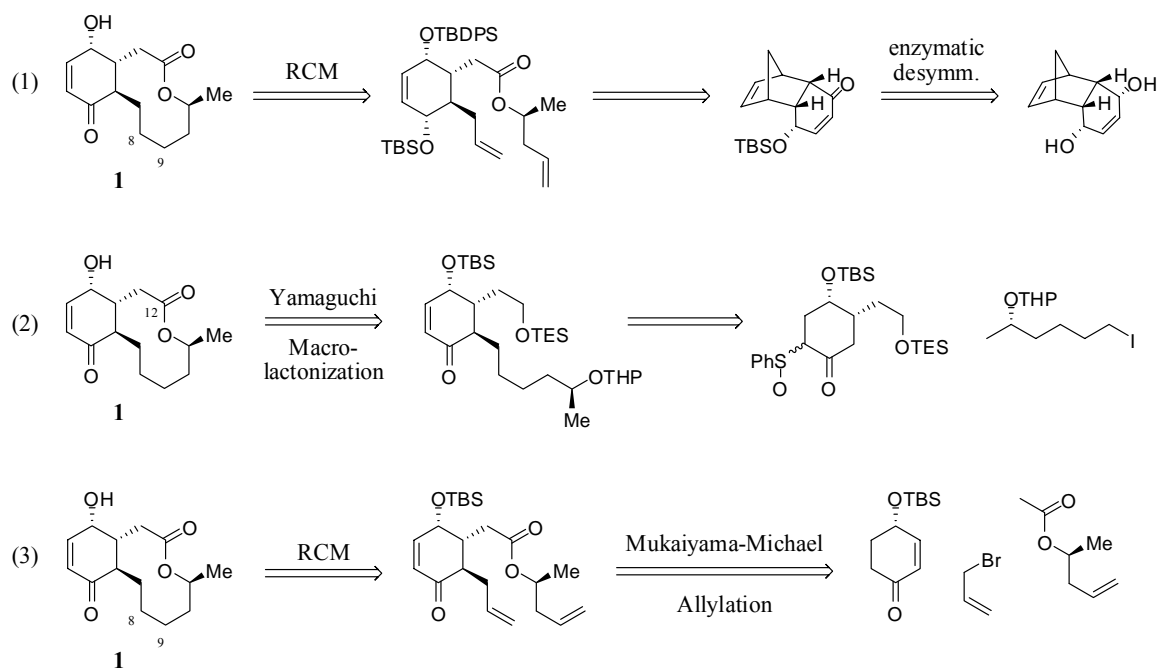
As illustrated in Figure 4.2 (eq 1), Mehta and Shinde¹⁴⁴ reported the first enantioselective total synthesis of compound **1** in 2005. The key steps of their synthesis

¹⁴³ Jayasuriya, H.; Zink, D. L.; Polishook, J. D.; Bills, G. F.; Dombrowski, A. W.; Genilloud, O.; Pelaez, F. F.; Herranz, L.; Quamina, D.; Lingham, R. B.; Danzeizen, R.; Graham, P. L.; Tomassini, J. E.; Singh, S. B. *Chem. Biodiversity* **2005**, 2, 112-122.

¹⁴⁴ Mehta, G.; Shinde, H. M. *J. Chem. Soc., Chem. Commun.* **2005**, 3703-3705.

included ring-closing metathesis (RCM) to construct the decalactone ring along the C8-C9 bond as well as a lipase-mediated enzymatic desymmetrization to generate the enantiopure substituted cyclohexenone. Watanabe and co-workers¹⁴⁵ reported a synthesis in 2006 that featured a highly functionalized enantiopure cyclohexanone derivative obtained through two stereoselective enzymatic reductions (baker's yeast), stereoselective dianion alkylation of a β -keto-sulfoxide, and finally Yamaguchi macrolactonization (Figure 4.2, eq 2). An enantioselective synthesis by Trauner and co-workers employed a Mukaiyama-Michael addition/allylation sequence to establish the syn-anti relationship of the three contiguous stereocenters followed by RCM to form the 10-membered lactone.¹⁴⁶

Figure 4.2: Synthesis of compound **1** by the groups of (1) Mehta, (2) Watanabe, and (3) Trauner.



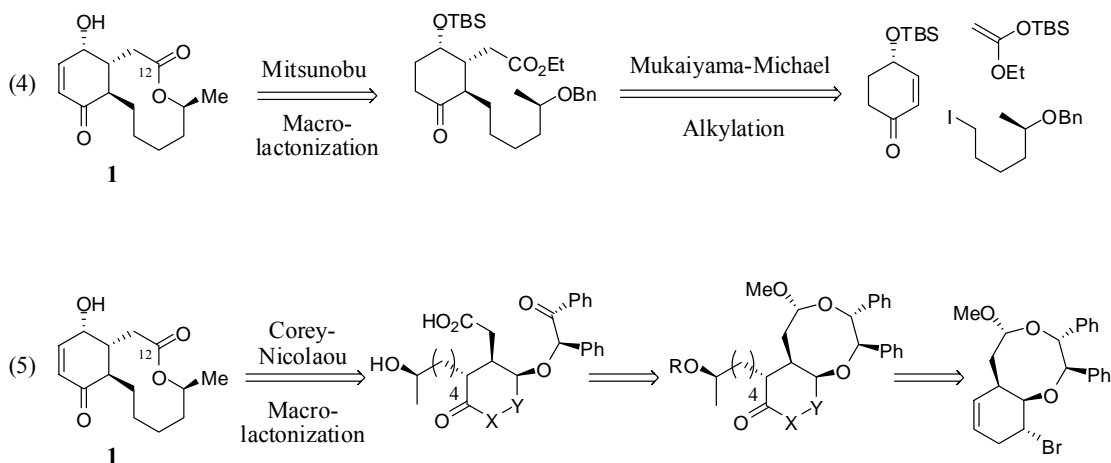
¹⁴⁵ Ishigami, K.; Katsuta, R.; Watanabe, H. *Tetrahedron* **2006**, 62, 2224-2230.

¹⁴⁶ Wilson, E. M.; Trauner, D. *Org Lett.* **2007**, 9, 1327-1329.

More recently, Carda and co-workers¹⁴⁷ have presented a stereoselective synthesis relying on a similar Mukaiyama-Michael addition/allylation sequence, as employed by the Trauner laboratory, as well as a macrolactonization via the Mitsunobu procedure (Figure 4.3, eq 4). The strategy of employing a single chiral auxiliary to set multiple stereocenters was employed by Fujioka and co-workers to promote both regio- and stereoselective transformations while serving as a protecting group (Figure 4.3, eq 5).

148

Figure 4.3: Synthesis of compound **1** by the groups of (4) Carda and (5) Fujioka.



Finally, Snider and coworkers presented a biomimetic synthesis of **1** where they utilized macrocyclic conformational control in a transannular Michael reaction (Scheme 4.2).¹⁴⁹ It was proposed that the cyclization reaction may be diastereoselective, providing only one of four possible stereoisomers, due to the rigid conformation of the macrocycle

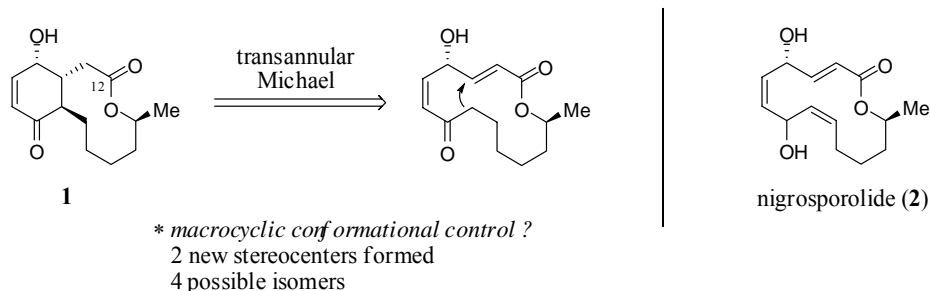
¹⁴⁷ Garcia-Fortanet, J.; Carda, M.; Marco, J. A. *Tetrahedron* **2007**, *63*, 12131-12137.

¹⁴⁸ Fujioka, H.; Ohba, Y.; Nakahara, K.; Takatsuji, M.; Murai, K.; Ito, M.; Kita, Y. *Org. Lett.* **2007**, *9*, 5605-5608.

¹⁴⁹ Snider, B. B.; Zhou, J. *Org. Lett.* **2006**, *8*, 1283-1286.

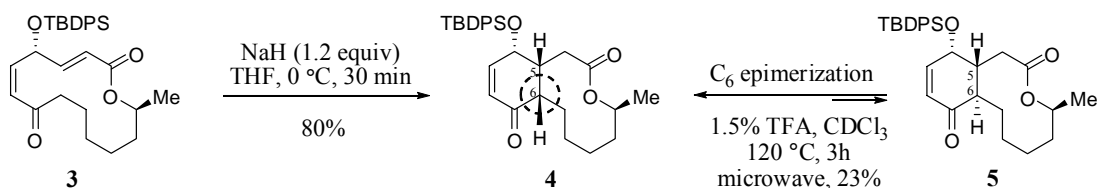
as well as its close relationship to the macrolactone nigrosporolide (**2**, an isomer of which could be involved in the biosynthesis of **1**).

Scheme 4.2: Proposed biomimetic synthesis of **1** by Snider and co-workers.



Accordingly, treatment of advanced intermediate **3** with NaH affected the transannular Michael reaction to provide **4**, however, the transformation led predominately to the undesired epimer at C6 (Scheme 4.3). Equilibration to provide the desired stereoisomer (**5**) required forcing conditions, even though MM2 calculations suggested compound **5** should be 1 kcal/mol lower in energy than **4**. In this case, an alternative approach, such as the application of a chiral catalyst, would be imperative to controlling the diastereoselectivity of the transformation. Snider's synthesis therefore provided an excellent forum in which to test our previously stated questions while underscoring the importance of being able to use a chiral catalyst to override the inherent selectivity of a molecule and the ability to actively select for the desired stereochemistry.

Scheme 4.3: Transannular Michael reaction leading to the opposite epimer at C6.

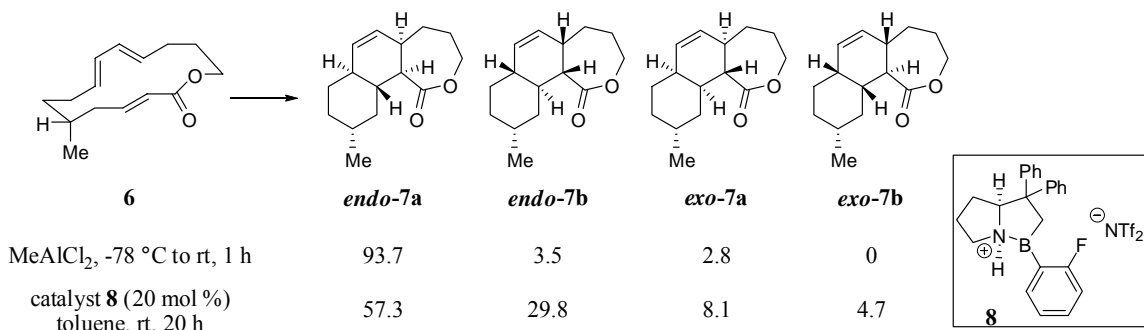


During our work on the synthesis of (+)-Sch 642305, Jacobsen and co-workers elegantly demonstrated the successful application of this strategy by employing a chiral catalyst to alter the inherent diastereoselectivity of a transannular Diels-Alder (TADA) reaction, controlling the stereochemical outcome of the transformation.¹⁵⁰ Importantly, in the case of conformationally biased substrates, the formation of disfavored diastereomeric products would require a chiral catalyst capable of overcoming a substantially higher activation barrier. For example, in order to maintain the methyl group in a pseudoequatorial position, biased macrocycle **6** was expected to adopt a conformation leading predominantly to one of four possible diastereomeric products (Scheme 4.4). As anticipated, when promoting the TADA reaction of **6** with an achiral Lewis acid (MeAlCl₂, 0.8 equiv) or under thermal conditions, high diastereoselectivity was achieved, providing *endo-7a* as the major product. On the other hand, when macrocycle **6** was subjected to catalyst **8** (20 mol %), an oxazaborolidine derivative based on catalysts developed by Corey and co-workers for inter- and intramolecular Diels-Alder reactions,¹⁵¹ they were able to alter the product distribution. While *endo-7a* remained the major product, the authors were nonetheless able to produce diastereomer *endo-7b* in 30% yield. Although the inherent selectivity could not be completely overridden, they were able to affect the outcome, leading to a diastereomeric ratio (dr) of 2:1 from 27:1, and synthesize and otherwise inaccessible compound.

¹⁵⁰ Balskus, E. P.; Jacobsen, E. N. *Science*, **2007**, *317*, 1736-1740.

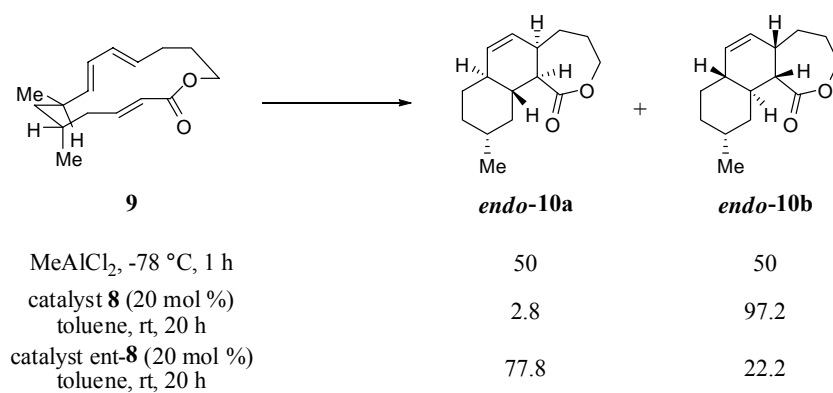
¹⁵¹ (a) Corey, E. J.; Shibata, T.; Lee, T. W. *J. Am. Chem. Soc.* **2002**, *124*, 3808-3809. (b) Ryu, D. H.; Corey, E. J. *J. Am. Chem. Soc.* **2003**, *125*, 6388-6389. (c) Zhou, G.; Hu, Q.-Y.; Corey, E. J. *Org. Lett.* **2003**, *5*, 3979-3982.

Scheme 4.4: Catalyst-controlled diastereoselective TADA of a biased macrocycle.



Jacobsen and co-workers were able to demonstrate catalyst control in a similar TADA reaction of an unbiased macrocycle (**9**). Using an achiral catalyst, or under thermal conditions, poor selectivity was achieved due to the presence of 1,3-*anti* methyl substitution (Figure 4.4). On the other hand, exquisite control was obtained when macrocycle **9** was exposed to catalyst **8** and *endo-10b* was obtained in 34:1 dr. The selective formation of *endo-10a* was achieved by use of the opposite enantiomer of catalyst **8**, ent-**8**.

Figure 4.4: Catalyst-controlled diastereoselective TADA of unbiased macrocycle **8**.

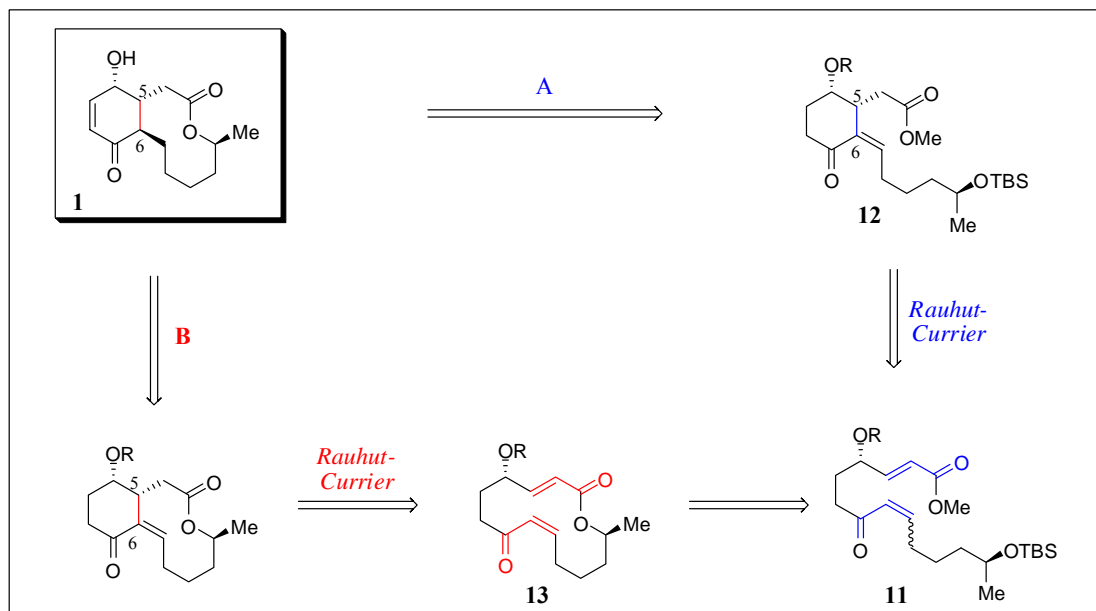


4.4 Retrosynthetic Analysis

Our synthesis of (+)-Sch 642305 (**1**) will allow for the examination of the Rauhut-Currier methodology in more than one setting: first, in an acyclic reaction reminiscent of our previous work, and secondly, in a yet untested setting of a transannular reaction (Scheme 4.5). The importance of controlling chemoselectivity and diastereoselectivity will be critical to both reactions. Once the inherent selectivity of our system is established through the use of an achiral catalyst in both pathways, we will attempt to override it using either our previously discovered chiral RC catalyst, or a peptide derivative thereof, in concert with our continuing interest regarding peptidic structures as elements of stereocontrol.

We envisage **1** arising from two alternative approaches that diverge from a common intermediate, **11** (Scheme 4.5). In pathway **A**, the decalactone ring would be generated through macrolactonization of compound **12** which would be prepared from common intermediate **11** using our RC methodology to form the C5-C6 bond. Alternatively in plan **B**, disconnection of the decalactone yields transannular RC substrate **13** which would be derived from **11** via macrolactonization. In both cases, we rely on our newly developed RC catalyst to dictate stereochemistry in the key reaction regardless of the starting olefin geometry or inherent conformational bias.

Scheme 4.5: Retrosynthetic analysis displaying two alternative routes, **A** and **B**.



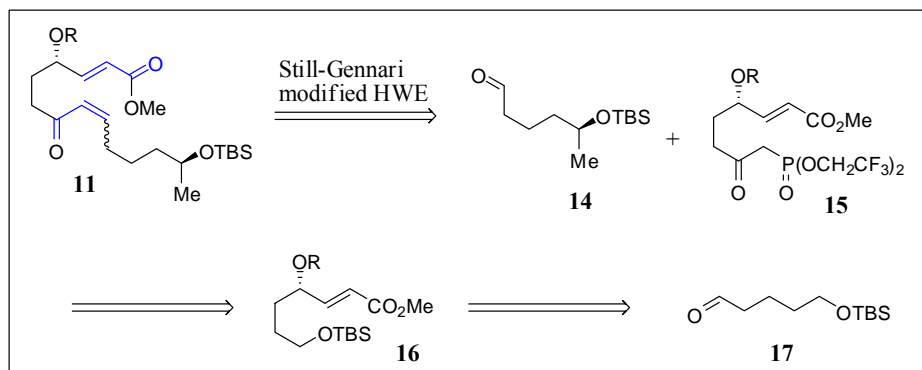
Common intermediate **11** can be disassembled to afford intermediates **14** and **15** through a modified Still-Gennari HWE reaction (Scheme 4.6).¹⁵² We envision phosphonate **15** ultimately arising from an α -aminooxylation reaction followed by an *in situ* HWE reaction of known aldehyde **17**.¹⁵³ Protected aldehyde **14** can ultimately be derived from epoxide opening of commercially available (*S*)-propylene oxide with 3-butenylmagnesium bromide¹⁵⁴ followed by ozonolysis.

¹⁵² Still, W. C.; Gennari, C. *Tetrahedron Lett.* **1983**, 24, 4405-4408.

¹⁵³ Mangion, I. K.; MacMillan, D. W. C. *J. Am. Chem. Soc.* **2005**, 127, 3696-3697.

¹⁵⁴ Dixon, D. J.; Ley, S. V.; Tate, E. W. *J. Chem. Soc., Perkin Trans. 1* **2000**, 2385-2394.

Scheme 4.6: Retrosynthetic analysis of common intermediate **11**.



4.5 Synthesis of (+)-Sch 642305: Route A

4.5.1 Synthesis of Divergent Intermediate 11

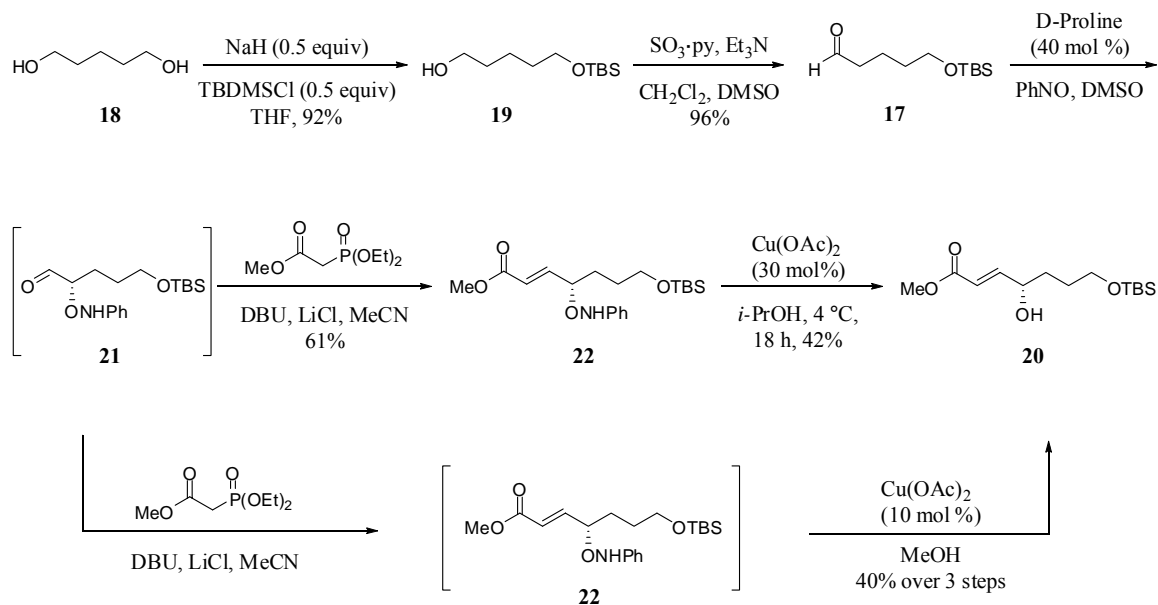
Our synthesis commenced with the execution of pathway **A** in which the RC reaction was used to promote the first cyclization, followed by macrolactonization. To begin, aldehyde **17** was synthesized by mono-TBS protection (92%)¹⁵⁵ of commercially available pentane-1,5-diol (**18**) followed by Parikh-Doering¹⁵⁶ oxidation of **19** (96%) (Scheme 4.7). Using the one pot aminooxylation/ Horner-Wadsworth-Emmons (HWE)/ N-O cleavage reaction described by MacMillan and coworkers,¹⁵⁷ we then obtained alcohol **20** in 40% yield over three steps. Since aldehyde **21** was oligomeric in solution, the HWE reaction was performed in situ.

¹⁵⁵ McDougal, P. G.; Rico, J. G.; Oh, Y.-I.; Codon, B. D. *J. Org. Chem.* **1986**, *51*, 3388-3390.

¹⁵⁶ Parikh, J. R.; Doering, W. von E. *J. Am. Chem. Soc.* **1967**, *89*, 5505-5507.

¹⁵⁷ (a) Mangion, I. K.; MacMillan, D. W. C. *J. Am. Chem. Soc.* **2005**, *127*, 3696-3697. (b) Zhong, G.; Yu, Y. *Org. Lett.* **2004**, *6*, 1637-1639. (c) Varseev, G. N.; Maier, M. E. *Org. Lett.* **2007**, *9*, 1461-1464.

Scheme 4.7: In-situ aminooxylation/ HWE/ N-O Cleavage:



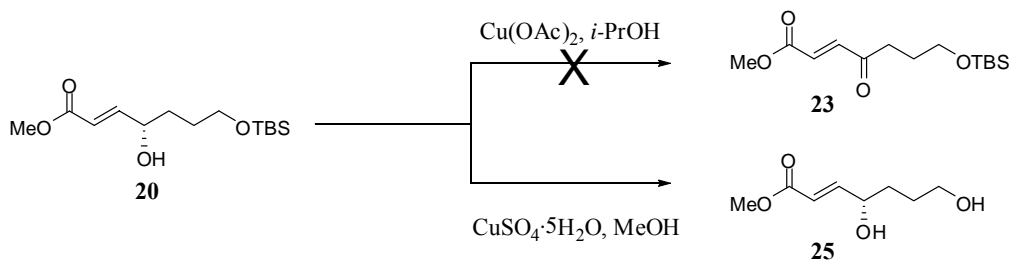
A stepwise procedure, where intermediate **22** was isolated and subjected to a separate N-O cleavage step, was examined as well and found to be less efficient. Accordingly, a screen of various reagents demonstrated that cleavage with copper(II) acetate was optimal, providing desired product **20** (42%) in addition to by-product **23** (26%, Table 4.1). Copper(II) sulfate afforded **20** in slightly diminished yield (36%) in addition to another by-product (**24**). N-O cleavage promoted by alternative reagents led to unsatisfactory results: Zn/THF/AcOH provided alcohol **20** in low yield (29%) due to TBS deprotection, Mo(CO)₆ provided 37% yield of **20**, possibly due to molybdenum coordination to the olefin, and MeOH/NH₄Cl led to recovered starting material.

Table 4.1: N-O cleavage experiments.

<i>conditions:</i>	20	23	24
Cu(OAc) ₂ , <i>i</i> -PrOH	42%	26%	0%
CuSO ₄ ·5H ₂ O, MeOH	36%	0%	15%
Zn/THF/AcOH	29%	-	-
Mo(CO) ₆	37%	-	-
MeOH/NH ₄ Cl	0%	-	-

Furthermore, resubjection of product **20** to the reaction conditions employing copper(II) acetate afforded to recovered starting material, without formation of by-product **23** (Scheme 4.8). Analogous resubjection of **20** to copper(II) sulfate resulted in TBS deprotection, providing bis(alcohol) by-product **25** without the formation of **24**. Thus, it appeared that by-product formation in the copper-catalyzed cleavage reactions was not due to oxidation or further reaction of product **20**. Ultimately, a one-pot reaction sequence was more favorable compared to the less efficient stepwise procedures involving isolation of intermediate **22**.¹⁵⁸

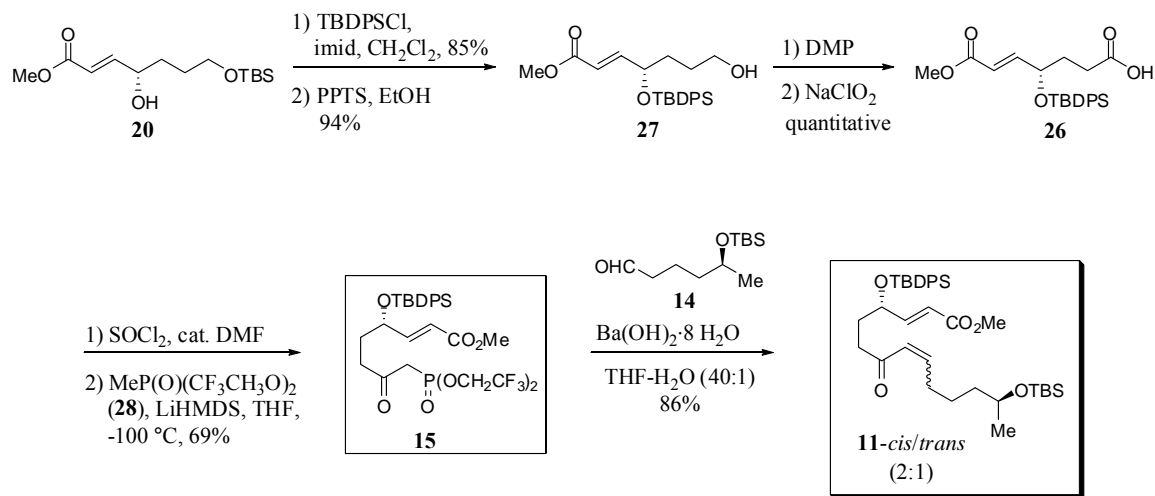
Scheme 4.8: Resubjection of alcohol **20** to reaction conditions with copper(II) species.



¹⁵⁸ Additionally, intermediate **22** was not stable to silica gel chromatography and decomposed in part to desired alcohol **20**, in addition to multiple unidentifiable by-products.

As illustrated in Scheme 4.9, alcohol **20** was then subjected to silylation using *tert*-butyldiphenylchlorosilane (85%) followed by selective deprotection of the primary TBS group with PPTS (94%). Dess-Martin¹⁵⁹ oxidation to the corresponding aldehyde and further oxidation under Kraus-Pinnick¹⁶⁰ conditions with NaClO₂ provided acid **26** quantitatively. A one step oxidation procedure of alcohol **27** using PDC and DMF¹⁶¹ was less efficient and led to a diminished yield of 24%. Acid **26** was then converted to the corresponding acid chloride using thionyl chloride, which was reacted immediately with the lithium anion of methyl phosphonate **28**. This two-step procedure provided β -ketophosphonate **15** in 69% yield.

Scheme 4.9: Synthesis of common intermediate **11**.



The aldehyde coupling partner, **14**, was prepared in a three-step sequence involving copper catalyzed epoxide ring opening of (-)-(*S*)-propylene oxide with 3-butenylmagnesium bromide,¹⁵⁴ and subsequent conversion to the silyl ether followed

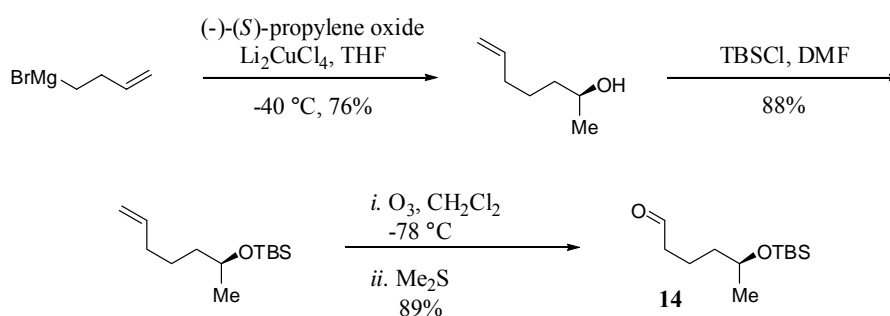
¹⁵⁹ Dess, D. B.; Martin, J. C. *J. Org. Chem.* **1983**, *48*, 4155.

¹⁶⁰ (a) Lindgren, B. O.; Nilsson, T. *Acta. Chem. Scand.* **1973**, *27*, 888-890. (b) Bal, B. S.; Childers, W. E. J.; Pinnick, H. W. *Tetrahedron* **1981**, *37*, 2091-2096.

¹⁶¹ Corey, E. J.; Schmidt, G. *Tetrahedron Lett.* **1979**, *5*, 399-402.

by ozonolysis of the terminal olefin (Scheme 4.10).¹⁶² Next, Still-Gennari modified HWE coupling of advanced phosphonate **15** with aldehyde **14** produced enone-enoate **11** as a 2:1 mixture of *Z* and *E* olefins. These isomers were easily separable, allowing us to test our hypothesis that equilibration under our reaction conditions would enable the catalyst to override the diastereoselectivity of the RC reaction using either isomer, obviating the need to control the geometry of this olefin in our final synthetic route.

Scheme 4.10: Synthesis of aldehyde fragment **14**.

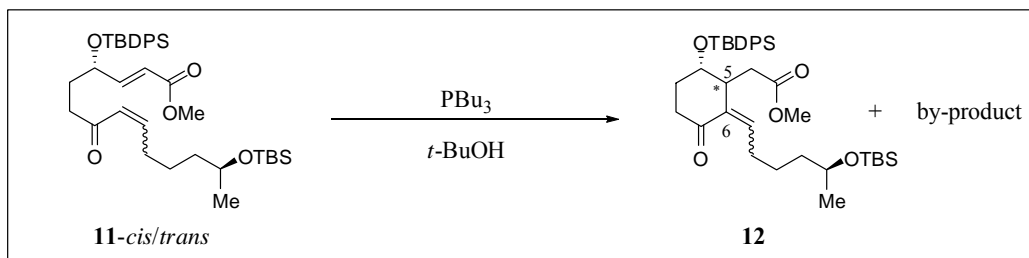


4.5.2 Preliminary Studies of the RC Reaction in *Route A*

With both isomers of common enone-enoate **11** in hand, we were able to test our key Rauhut-Currier step under pathway **A**. Crucially, we have been able to demonstrate catalysis using an achiral catalyst, PBU_3 , in the cycloisomerization of enone-enoate **11** to generate intermediate **12** (Scheme 4.11). Initial experiments showed that both *cis* and *trans* isomers underwent catalysis at room temperature and led to the desired product (as determined by ^1H NMR and HRMS) in addition to an unidentifiable by-product.

¹⁶² The characterization data for compound **14**, including optical rotation, matched that which has previously been reported, please see the Experimental and: Ernst, B.; Wagner, B. *Helv. Chim. Acta* **1989**, *72*, 165-171.

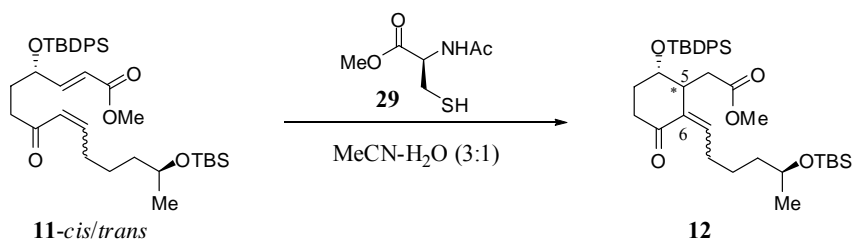
Scheme 4.11: Initial study of the key RC reaction in route A with an achiral catalyst.



On the other hand, preliminary exploration into catalysis with our protected cysteine derivative (**29**) proved to be more difficult. Reaction under previously optimized conditions¹⁶³ (-40 °C, $t\text{-BuOK}$ (4 equiv); entries 1 and 2, Table 4.2) as well as at elevated temperatures (23 °C, 70 °C; entries 3 and 4, Table 4.2) led only to recovered starting material. In the case of enone-enoate **11-cis**, isomerization to **11-trans** was rapid (less than 1 h) and in each case only *trans* starting material was recovered. Interestingly, in the absence of base (entry 5, Table 4.2) no isomerization was seen and **11-cis** was recovered.

¹⁶³ Please refer to Chapter 3 for a full discussion.

Table 4.2: Preliminary experiments in the Rauhut-Currier reaction in route A catalyzed by protected cysteine catalyst **29**.



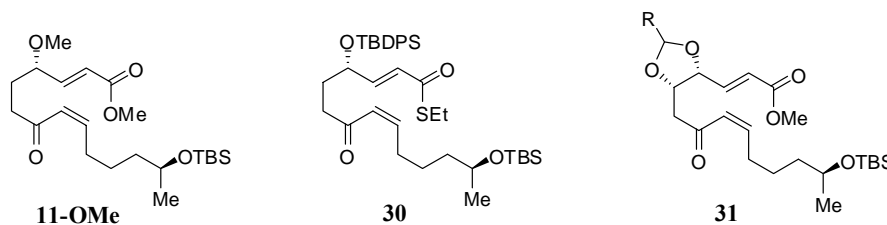
entry	11	base (equiv)	conc (M)	temp (°C)	rxn outcome
1	<i>cis</i>	<i>t</i> -BuOK (4)	0.02	-40	conv to 11-trans
2	<i>trans</i>	<i>t</i> -BuOK (4)	0.02	-40	rec 11-trans
3	<i>cis</i>	<i>t</i> -BuOK (1.5)	0.05	23	conv to 11-trans
4	<i>cis</i>	<i>t</i> -BuOK (1.5)	0.05	70	2 d, conv to 11-trans
5	<i>cis</i>	-	0.05	23	rec 11-cis

While the further exploration of this reaction is currently on-going in our laboratory, we simultaneously investigated the possibility of employing alternative derivatives of **11** in the key RC transformation. We speculated that the steric environment imposed by the large silyl ether may impede the cycloisomerization, and therefore investigated the RC reaction of analogous methyl ether **11-OMe** (Figure 4.5). Additionally, methyl esters are known to be poor coupling partners in the RC reaction, demonstrating low reactivity.¹⁶⁴ Consequently, the possibility of employing analogous thioester **30** was considered (Figure 4.5). Furthermore, due to the high reactivity displayed by achiral phosphine catalyst PBu₃ in this reaction, the use of a chiral phosphine catalyst will be discussed subsequently. Finally, it is possible that the rotational freedom of substrate **11** is too great, precluding cyclization. Substrate **31** could

¹⁶⁴ (a) Agapiou, K.; Krische, M. J. *Org. Lett.* **2003**, *5*, 1737-1740. (b) Aroyan, C. E.; Miller, S. J. *J. Am. Chem. Soc.* **2007**, *129*, 256-257 and references therein.

test this hypothesis, bringing the reacting olefins into close proximity, as well as leading to a more expeditious endgame with a simultaneous dehydration/deprotection step (Figure 4.5).

Figure 4.5: Possible substrates for the Rauhut-Currier reaction in Route A.



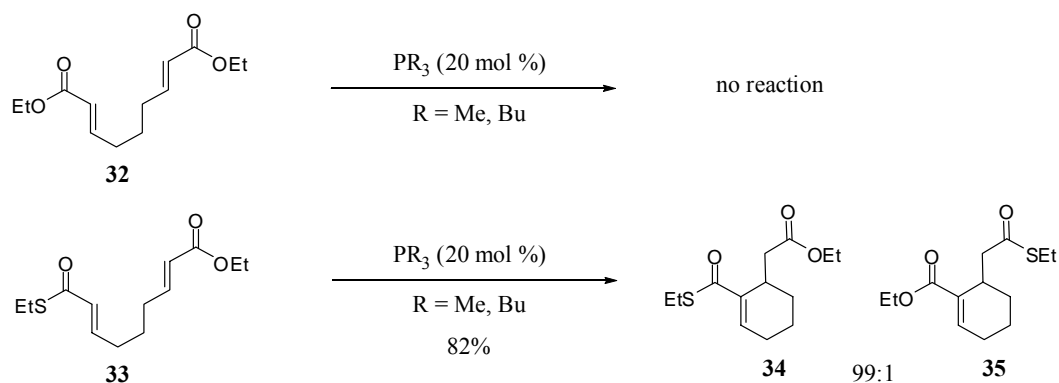
4.5.3 Thioenoates as Reactive Rauhut-Currier Substrates

Although enoates have been shown to be viable electrophilic partners in Rauhut-Currier reactions by our group as well as the groups of Krische¹⁶⁴ and Roush,¹⁶⁵ they are nonetheless, much less reactive towards conjugate addition than their enone counterparts. Thioenoates, on the other hand, have demonstrated superior reactivity to enoates with their reactivity lying closer to that of enones.¹⁶⁶ In addition, the cycloisomerization of bis(enoates) has been shown to be problematic (as in the case of substrate **32**, Figure 4.6), while the use of mixed thioenoate-enoate **33** was demonstrated to be highly efficient, providing cyclohexene **34** in 82% yield (Figure 4.6). It is important to note that the reaction displayed high chemoselectivity as well, with **34** as the exclusive cycloisomerization product (99:1).

¹⁶⁵ Frank, S. A.; Mergott, D. J.; Roush, W. R. *J. Am. Chem. Soc.* **2002**, *124*, 2404-2405.

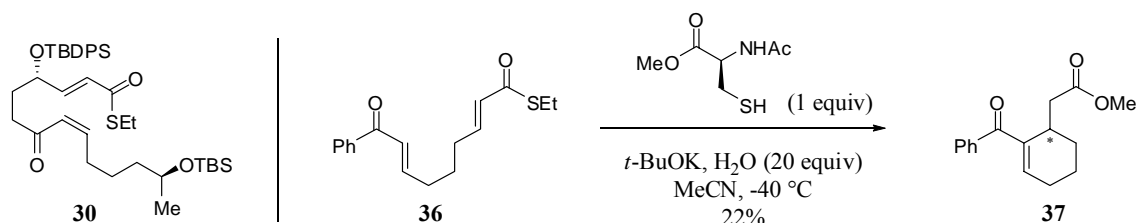
¹⁶⁶ Keck, G. E.; Welch, D. S. *Org. Lett.* **2002**, *4*, 3687-3690.

Figure 4.6: Heightened thioenoate reactivity in the RC reaction.



In view of this heightened reactivity and high chemoselectivity, the possibility of employing thiol ester **30** in our synthesis provided an intriguing opportunity to enhance the reactivity of our system under sulfur-based catalysis (Figure 4.7). Hence, substrate **36** was synthesized as a model compound to further test the scope of our reaction conditions and investigate the effects of a thioenoate in lieu of an enoate. Unfortunately, enone-*thioenoate* **36** was not a viable substrate under our catalytic system, providing enone-*enoate* product **37** in low yield (22%, Figure 4.7). The abnormal reactivity displayed by this system is not fully understood at this time and is currently being explored further.¹⁶⁷

Figure 4.7: Model system employing a thiol ester electrophilic partner.



¹⁶⁷ This abnormal reactivity was determined during the further exploration of reaction scope of our previously reported Rauhut-Currier reaction. Thioenoates are of general interest in the RC reaction and the related Morita-Baylis-Hillman reaction and will therefore be investigated further. It is worth noting that while we are interested in this substrate class, we would nonetheless like to find a more general catalytic system which would not require substrate manipulation.

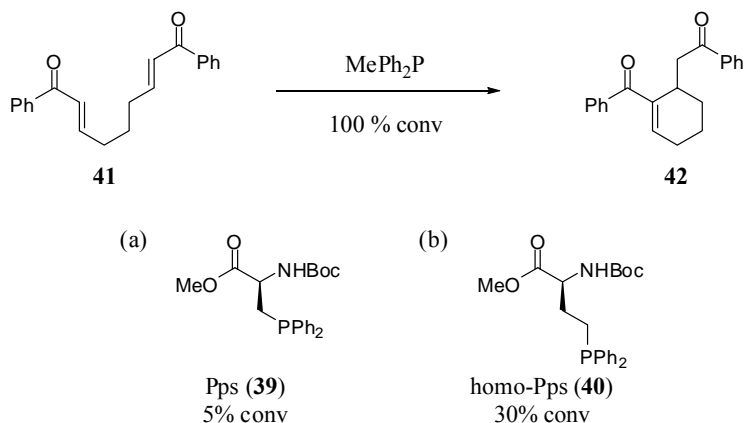
4.5.4 Phosphine Catalysis

As illustrated in section 4.5.2, PBu_3 was found to be an excellent catalyst for the acyclic Rauhut-Currier reaction. Although our work in the RC reaction revealed sulfur-based catalyst **29** as the optimal catalyst, we had prior experience using a chiral phosphine catalyst as well in the context of amino acid diphenylphosphinoserine (Pps, **39**).¹⁶⁸ In analogy to other reports using phosphine-based catalysts, our work on the RC reaction empirically determined the order of reactivity to increase with the number of aliphatic substituents: $\text{Bu}_3\text{P} > \text{MePh}_2\text{P} \gg \gg \text{homo-Pps (40)} \gg \text{Pps (39)} > \text{Ph}_3\text{P}$. As illustrated in Figure 4.8, our model catalyst (MePh_2P) was sufficiently reactive to catalyze the cycloisomerization of bis(enone) **41** to generate cyclized product **42** in 100% conversion. However, when this moiety was incorporated into an amino acid (Pps, **39**),¹⁶⁹ the reaction no longer proceeded with a useful level of conversion (5%). Homo-Pps (**40**) was tested as well in an attempt to minimize the electron withdrawing effects of the amino acid and decrease steric bulk near the phosphorous center, however, was found to provide only a modest increase in reactivity.

¹⁶⁸ Please refer to Chapter 3 for a discussion of our work using phosphine-based catalysts in the Rauhut-Currier reaction.

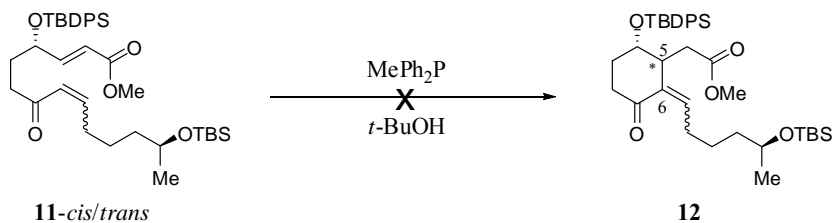
¹⁶⁹ Gilbertson, S. R.; Chen, G.; McLoughlin, M. *J. Am. Chem. Soc.* **1994**, *116*, 4481.

Figure 4.8: Phosphine catalysis in the Rauhut-Currier reaction.



With this knowledge of phosphine reactivity in a model system, we examined the possibility of employing a phosphine-based catalytic system with the more complex substrate **11**. Excited that Bu_3P was able to catalyze the cyclization of enone-enoate **11** to **12** (section 4.5.2), we next turned to catalysis with MePh_2P . Unfortunately, this catalyst was ineffective in our new system and provided recovered starting material at room temperature as well as at elevated temperatures (Scheme 4.12). While this catalyst was not reactive with the acyclic substrate in route **A**, we were optimistic that we would be able to fine-tune the reactivity of our system under sulfur-based catalysis. Additionally, we have not dismissed the possibility of returning to a phosphine-based catalyst in the further study of route **B**.

Scheme 4.12: Phosphine catalysis in Route A.



4.5.5 Examination of Sterics: Synthesis of **11-OMe**

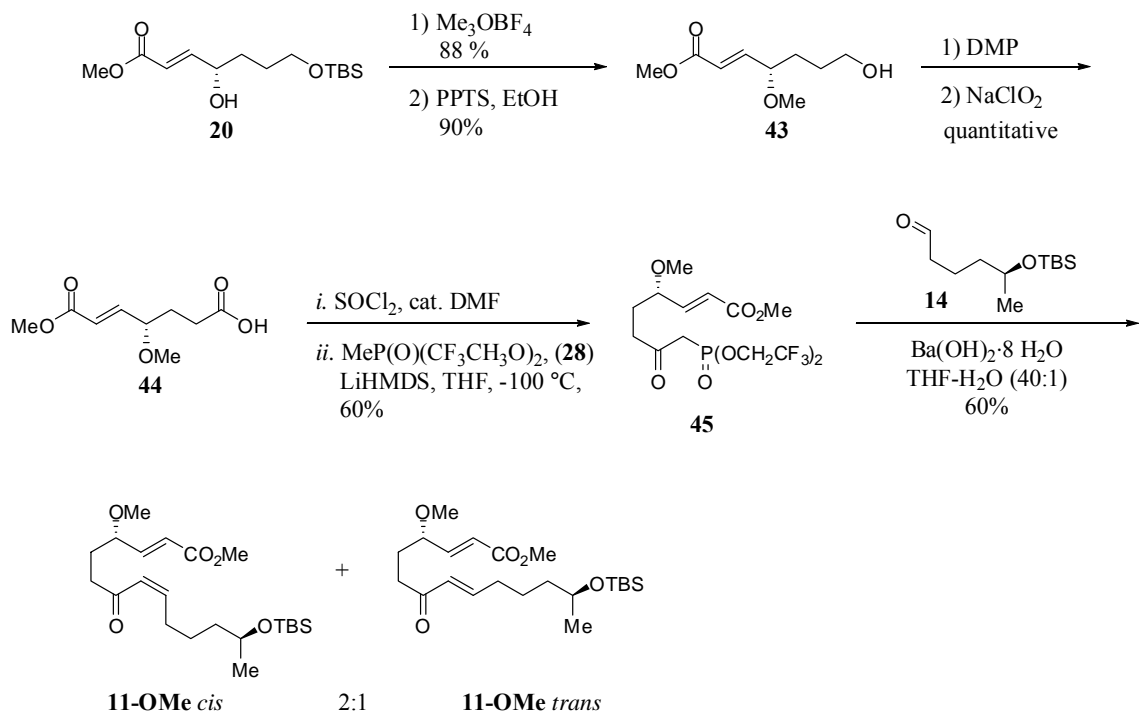
To address the possibility that Rauhut-Currier cyclization of substrate **11** was impeded due to steric hindrance from the bulky silyl ether, we elected to synthesize an analogous substrate that would unambiguously answer the question of steric interference. After considering various alternative protecting groups, we decided the use of a methyl ether protecting group would best address the initial question we set out to answer; the ability of a chiral catalyst to override the inherent diastereoselectivity of a reaction involving a chiral molecule. This objective presents a complex challenge, as it potentially requires the chiral catalyst to overcome a substantially higher activation barrier of the pathway leading to the disfavored diastereomer. Therefore, we set out to test the RC reaction with the analogous methyl ether compound, **11-OMe**, which would examine the cycloisomerization in the absence of a potentially dominating bulky protecting group.

As illustrated in Scheme 4.13, the successful synthesis of **11-OMe** was analogous to the synthesis we reported for **11-OTBDPS** (see section 4.5.1). Beginning with alcohol **20**, methylation with Meerwein's salt (88%) followed by deprotection of the primary TBS group with PPTS (90%) cleanly provided methyl ether **43**. Dess-Martin¹⁵⁹ oxidation followed by Kraus-Pinnick¹⁷⁰ oxidation provided quantitative conversion to the corresponding acid (**44**). Acid **44** was then converted to β -ketophosphonate **45** in 60% yield. Finally, Still-Gennari modified HWE coupling of advanced phosphonate **45** with aldehyde **14** produced enone-enoate **11-OMe**. We obtained a similar ratio of

¹⁷⁰ (a) Lindgren, B. O.; Nilsson, T. *Acta. Chem. Scand.* **1973**, 27, 888-890. (b) Bal, B. S.; Childers, W. E. J.; Pinnick, H. W. *Tetrahedron* **1981**, 37, 2091-2096.

approximately a 2:1 mixture of *Z* and *E* olefins which were easily separable in this case as well, allowing both isomers to be carried forward independently.

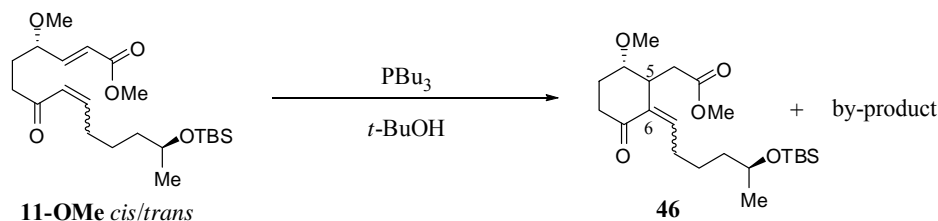
Scheme 4.13: Synthesis of analogous **11-Ome** *cis/trans*.



4.5.6 Preliminary Rauhut-Currier Studies in *Route A*: **11-Ome**

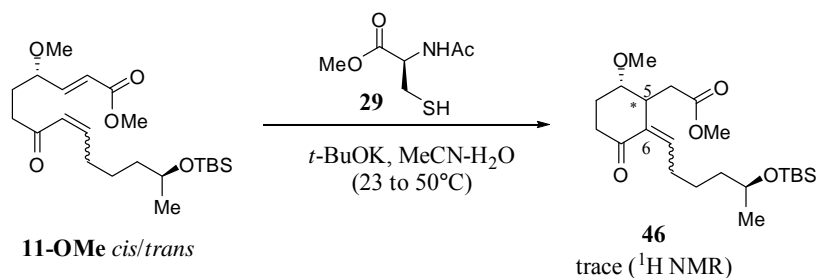
With both isomers of enone-enoate **11-Ome** in hand, we were able to reinvestigate our key Rauhut-Currier step under pathway **A** and test our hypothesis that the steric environment with the TBDPS protected substrate was preventing cyclization. Initial experiments demonstrated that we were able once again to promote the cycloisomerization of both *cis* and *trans* isomers of **11-Ome** using an achiral catalyst, PBU₃, affording desired product **46** (as determined by ¹H NMR and HRMS) in addition to an unidentified by-product (Scheme 4.14).

Scheme 4.14: Initial study of the RC reaction of **11-OMe** in route **A** with an achiral phosphine-based catalyst.



Excitingly, while **11-OTBDPS** did not lead to the desired product using our Cys-derived catalyst **29**, catalysis of the RC reaction of **11-OMe** generated trace amounts of the desired product after 24 h at 50 °C,¹⁷¹ suggesting that our hypothesis about the effect of the bulky protecting group on the C4 hydroxyl group could be correct (Scheme 4.15). We are encouraged by these initial results and are optimistic that with a multidimensional study of the reaction parameters (solvent, temperature, concentration, and catalyst loading) we will be able to efficiently catalyze this transformation. The RC reaction has been utilized successfully in the synthesis of several natural products, with each case proving to be highly substrate dependent and requiring an independent optimization study.¹⁷²

Scheme 4.15: Preliminary experiments in the Rauhut-Currier reaction of **11-OMe** catalyzed by protected cysteine catalyst **29**.



¹⁷¹ As determined by ^1H nuclear magnetic resonance analysis.

¹⁷² Please refer to chapter 2 for a full discussion of the application of the Rauhut-Currier reaction to the synthesis of natural products.

4.5.7 Synthesis in *Route A*

After the key Rauhut-Currier reaction, our synthesis would proceed in six steps to provide the natural product, **1**, as well as the C5 epimer of the natural product (Scheme 4.16). Reduction of enone **46** with triethylsilane in the presence of Wilkinson's catalyst would provide ketone **47** after treatment of the resultant silyl enol ether with K_2CO_3 in MeOH, establishing the syn-anti relationship of the three contiguous stereocenters.¹⁷³ Conjugate reduction could also be effected using sodium borohydride ($NaBH_4$) in pyridine, as demonstrated by Krische and co-workers in the synthesis of (\pm) ricciocarpin A.¹⁷⁴ Deprotection of the secondary alcohol followed by hydrolysis of the methyl ester would provide advanced cyclohexanone derivative **49**, which would serve as the substrate for a Yamaguchi macrocyclization to generate the decalactone, **50**. Saegusa-Ito¹⁷⁵ oxidation, as reported by the groups of Trauner¹⁴⁶ and Carda,¹⁴⁷ would deliver the penultimate unsaturated protected intermediate, **51**. Alternatively, dehydration via a phenylselenation-selenoxide elimination sequence could be employed, as by Mehta and co-workers,¹⁴⁴ whereas IBX-mediated dehydrogenation¹⁷⁶ was reported to be unsuccessful. Final deprotection of **51**, (**51**-OTBDPS; TBAF/HOAc, 1:1)¹⁴⁴ or (**51**-OMe; Me_3SiI or BBr_3 , CH_2Cl_2),¹⁷⁷ would provide natural product **1** as well as the C5 epimer of (+)-Sch 642305.

¹⁷³ (a) Sakai, M.; Sasaki, M.; Tanino, K.; Miyashita, M. *Tetrahedron Lett.* **2002**, *43*, 1705-1708. (b) Ojima, I.; Kogure, T.; Nagai, Y. *Tetrahedron Lett.* **1972**, *13*, 5035-5038.

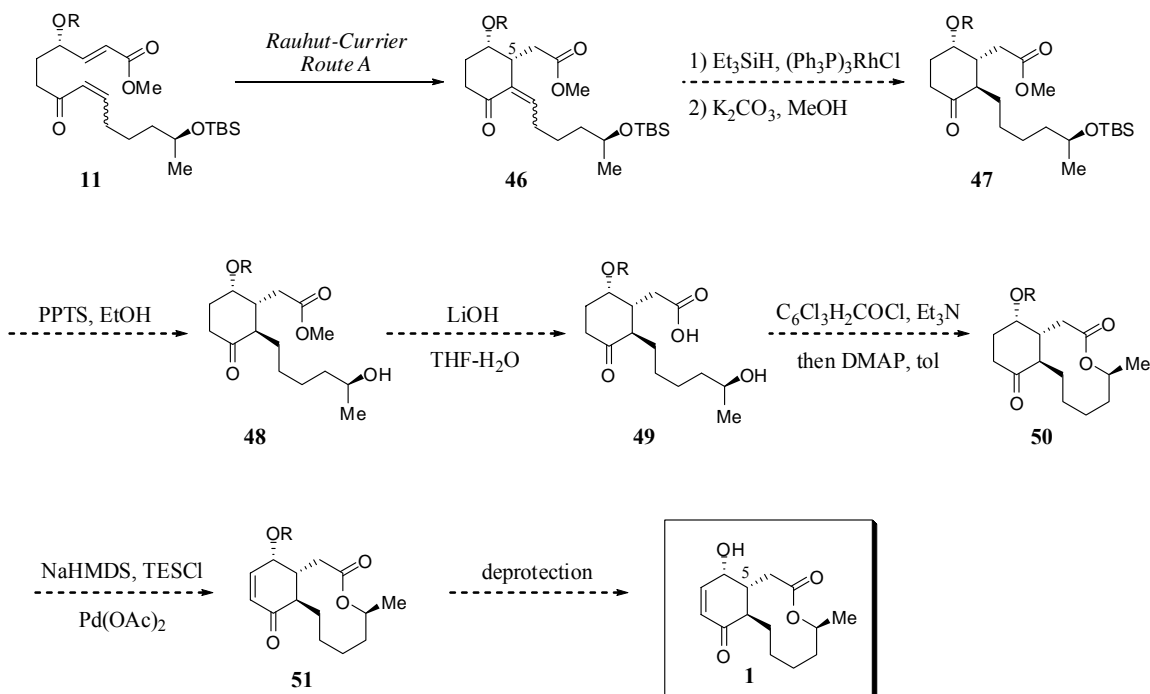
¹⁷⁴ (a) Agapiou, K.; Krische, M. *J. Org. Lett.* **2003**, *5*, 1737-1740. (b) Jackson, W. R.; Zurqiyah, A. *J. Chem. Soc.* **1965**, 5280-5287.

¹⁷⁵ Ito, Y.; Hirao, T.; Saegusa, T. *J. Org. Chem.* **1978**, *43*, 1011-1013.

¹⁷⁶ Nicolaou, K. C.; Zhong, Y. L.; Baran, P. S. *J. Am. Chem. Soc.* **2000**, *122*, 7596-7597.

¹⁷⁷ Greene, T. W.; Wuts, P. G. M. *Protective Groups in Organic Synthesis*, 4th ed.; John Wiley & Sons: New York, 2006; pp 25-29.

Scheme 4.16: Synthesis of (+)-Sch 642305 in *route A*.

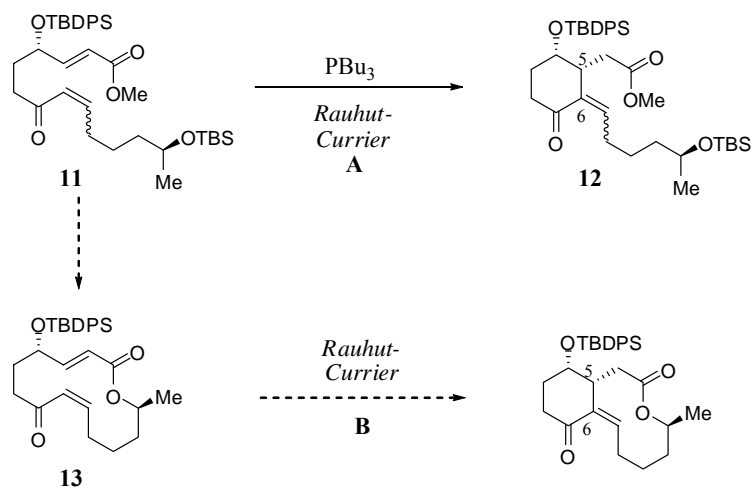


4.6 Synthesis of (+)-Sch 642305: *Route B*

4.6.1 Synthetic Plan for *Route B*

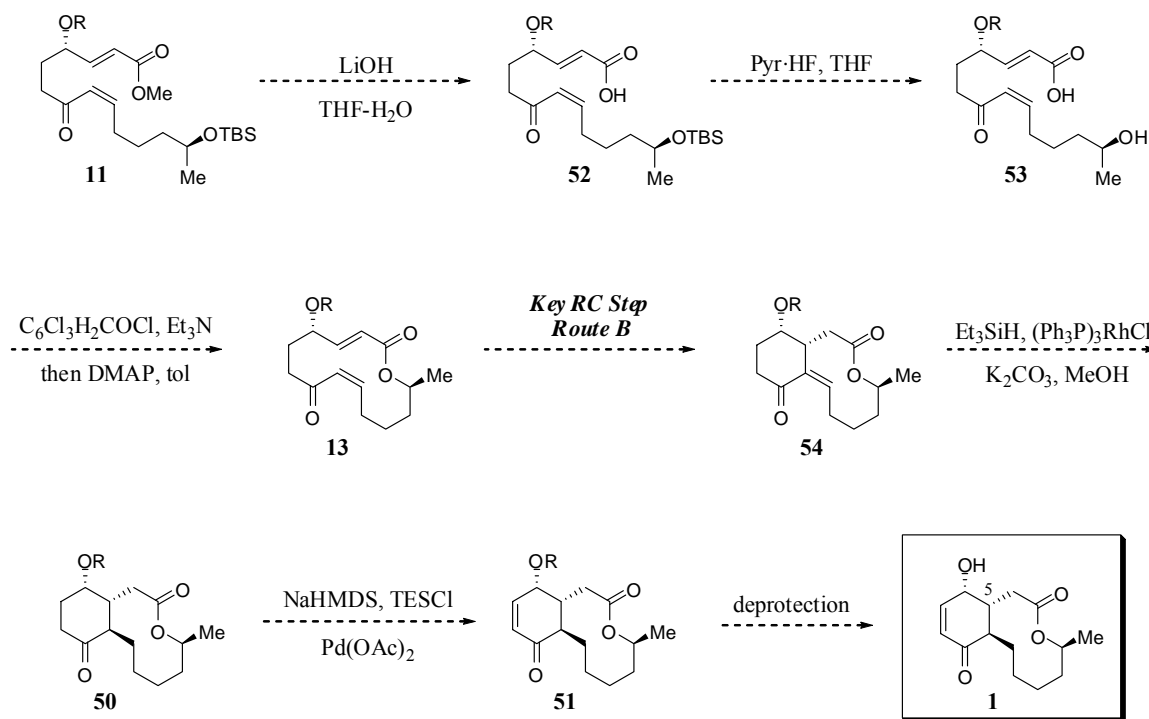
As mentioned earlier, our synthetic plan for (+)-Sch 642305 allows for the examination of the Rauhut-Currier methodology in two alternative settings. While optimization of the Rauhut-Currier reaction was proceeding on the acyclic substrate in *route A*, we were eager to test the reaction simultaneously in a previously unexplored transannular mode (Figure 4.9). This would allow us first to establish the inherent diastereoselectivity of the cyclization reaction on this chiral macrocycle, and second, to attempt to override this preference using our chiral catalyst, overcoming a potentially substantially higher activation barrier leading to the alternative diastereomer.

Figure 4.9: Application of the Rauhut-Currier reaction in *route B*.



The exploration of route **B** required that common intermediate **11** be carried forward to the transannular substrate **13** (Scheme 4.17). We envisioned that this could be achieved by hydrolysis of the methyl ester followed by deprotection of the secondary alcohol and Yamaguchi macrocyclization to provide **13**. Once the key Rauhut-Currier step is optimized, the remaining steps would parallel those presented in route **A**. The synthesis would proceed in three steps to produce the desired natural product, **1**, as well as the C5 epimer of the natural product.

Scheme 4.17: Synthesis of (+)-Sch 642305 in *route B*.



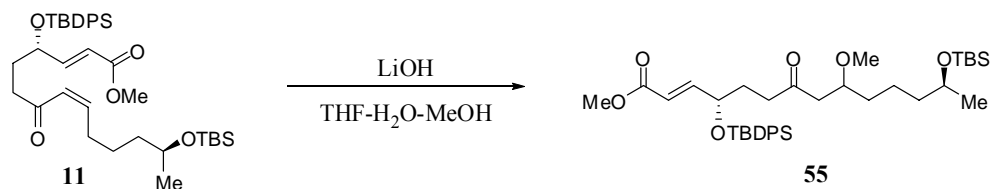
4.6.2 Synthesis with TBDPS Protecting Group

By investigating *route A* we learned that the bulky TBDPS protecting group of common intermediate **11** interfered with the acyclic Rauhut-Currier reaction. Because *route B* involved catalysis of the cycloisomerization in a completely new forum as a transannular reaction, the steric and electronic requirements of this system were unknown. Therefore, we proceeded with both the TBDPS and methyl ether protected compounds, beginning first with the bulkier silyl protected compound.

Exploration of *route B* began from common intermediate **11** with cleavage of the methyl ester using LiOH in THF-H₂O-MeOH (Scheme 4.18). However, instead of hydrolysis of the methyl ester, these conditions led exclusively to the conjugate addition of methoxide into the α,β -unsaturated carbonyl affording **55**. The high electrophilicity of

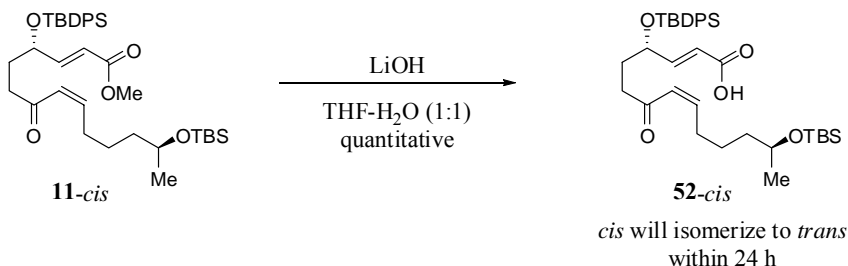
this enone towards conjugate addition was determined to be problematic at later points in the synthesis as well, and will be revisited throughout the discussion of route **B**.

Scheme 4.18: Hydrolysis of divergent intermediate **4**.



Fortunately, we were able to overcome this undesired reactivity in the hydrolysis step and found that quantitative cleavage could be obtained at room temperature in the absence of methanol (THF-H₂O, 1:1) providing advanced carboxylic acid **52-cis** (Scheme 4.19). Although the *cis*-acid was configurationally unstable, isomerizing to **52-trans** within 24 h when stored either under vacuum at ambient temperature or under nitrogen at -20 °C, isolation and immediate use was sufficient to overcome this problem.

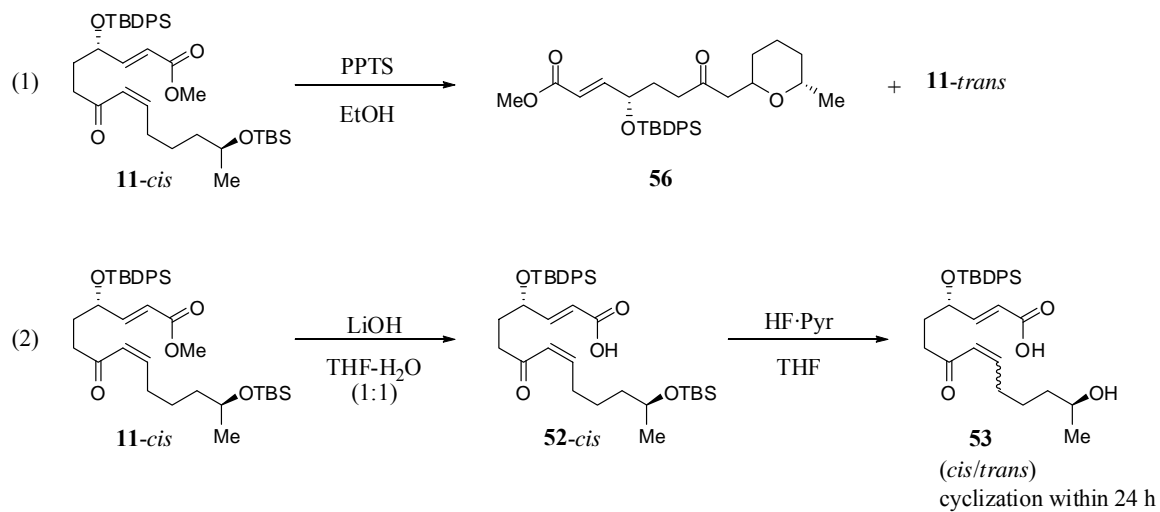
Scheme 4.19: Successful hydrolysis of methyl ester **11**.



Simultaneous investigation into silyl deprotection of common intermediate **11** was met with greater difficulty. We were able to selectively deprotect the secondary TBS ether over the TBDPS ether using PPTS in ethanol or HF·pyridine. However, the desired product was not stable under these deprotection conditions (eq 1, Scheme 4.20). Instead, we isolated tetrahydropyran **56**, the product of silyl deprotection followed by

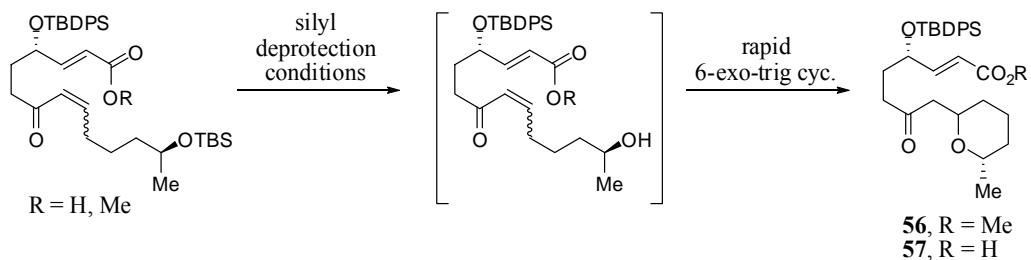
intramolecular conjugate addition, as the major product in addition to recovered starting material. It is important to note that the recovered starting material was no longer in the *cis* configuration, but that it had isomerized under these conditions to the *trans* configuration.

Scheme 4.20: Selective silyl deprotection.



A similar outcome ensued when HF·pyridine was used in the deprotection step (eq 2, Scheme 4.20). Initial hydrolysis of the methyl ester of **11-cis** (LiOH, THF-H₂O) provided carboxylic acid **52-cis**. Subsequent deprotection with HF·pyridine provided the desired product, **53**, and unlike under deprotection conditions using PPTS we were now able to isolate the desired product. Yet, **53** was highly configurationally unstable; the *cis* olefin rapidly isomerized to the *trans* geometry and furthermore the generated free hydroxyl group rapidly underwent conjugate addition into the α,β -unsaturated ketone to provide **57** (Figure 4.10).

Figure 4.10: Rapid 6-exo-trig cyclization leading to undesired cyclic by-product.

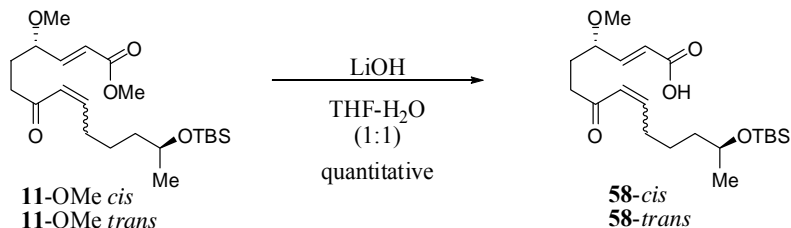


Although we were able to isolate a small amount of **53** for a fleeting moment, we were apprehensive of continuing forward with this route. The next step in the synthesis is a Yamaguchi macrocyclization. Once **53** is subjected to the reaction conditions for the macrocyclization, the alcohol or alkoxide will be poised for rapid intramolecular 6-exo-trig cyclization to produce undesired by-product **57** (Figure 4.10). This pathway should be more facile, forming a 6-membered ring, than the desired 14-membered ring formation required in the macrolactonization.

4.6.3 Synthesis with Me Ether Protecting Group

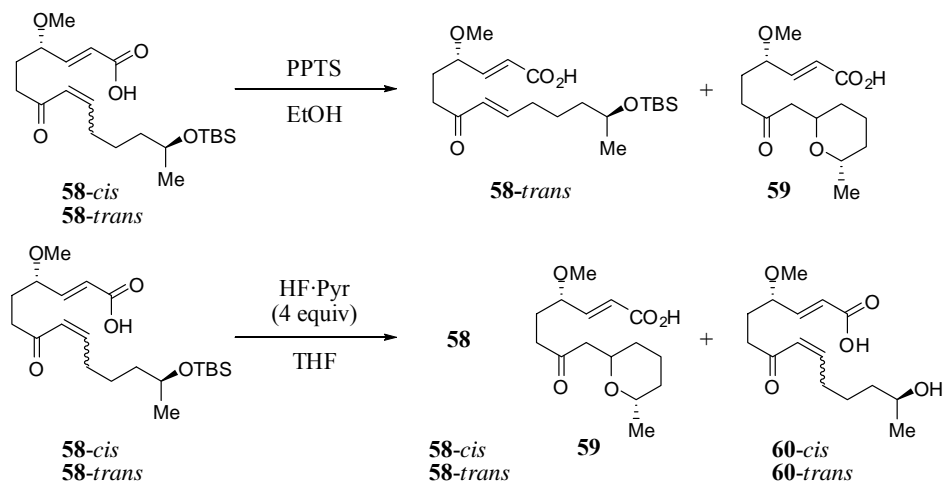
In analogy to our work with the TBDPS-protected compound, we explored route **B** with the sterically smaller methyl ether-protected compound, **11-OMe**. We began by studying **11-OMe cis** and **11-OMe trans**, which were independently subjected to the optimized hydrolysis conditions (LiOH, THF-H₂O) to provide quantitative conversion to acid **58-cis** and **58-trans**, respectively (Scheme 4.21).

Scheme 4.21: Hydrolysis of **11-OMe cis** and **11-OMe trans**.



As illustrated in Scheme 4.22, the advanced *cis* and *trans* acids were then subjected to silyl deprotection with both PPTS and HF·pyridine. Similarly, under PPTS deprotection conditions, we were not able to isolate the desired free secondary alcohol and isolated tetrahydropyran **59** as the major product in addition to recovered starting material (**58-*trans*** in both cases). Deprotection using HF·pyridine led to a mixture of recovered starting material (**58-*cis*** did not undergo isomerization), tetrahydropyran by-product **59**, and trace amounts of the desired product (**60-*cis*** and **60-*trans***, respectively). As with compound **53**, we were able to isolate **60** in only trace quantities and were cognizant that the next step would require the formation of a 14-membered ring versus the extremely facile 6-membered ring. Consequently, we decided it would be judicious to modify this route and investigate protection of the α,β -unsaturated ketone.

Scheme 4.22: Silyl deprotection of **58-*cis*** and **58-*trans***.

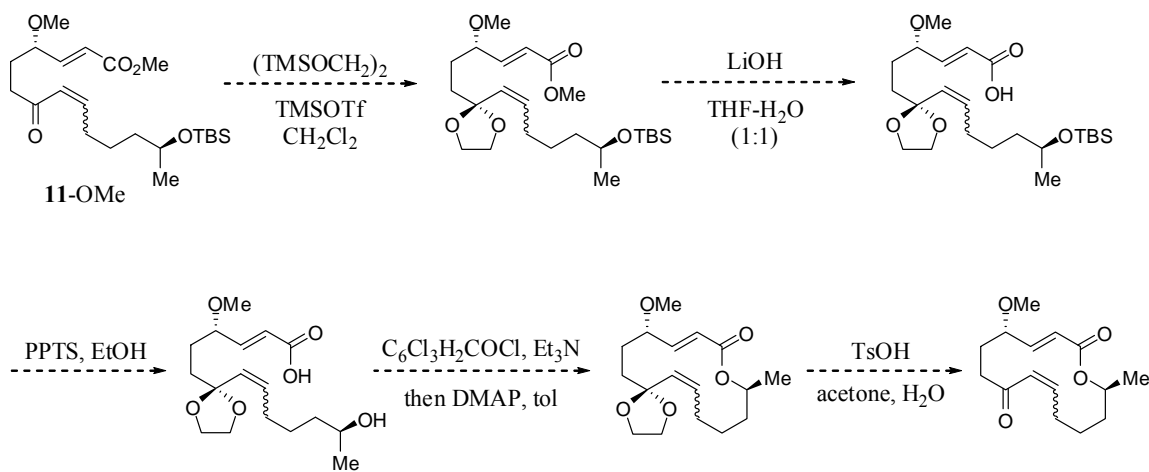


4.6.4 1,3-Dioxolane

Our apprehension about the instability of compounds **53** and **60** compelled us to modify route **B** by investigating protection of the α,β -unsaturated ketone as a 1,3-

dioxolane. The new synthetic plan for (+)-Sch 642305 would parallel that already disclosed for this route with the addition of a protection and deprotection step. Hence, ketalization would be followed by hydrolysis of the methyl ester, deprotection of the secondary alcohol, Yamaguchi macrolactonization, and finally deprotection of the 1,3-dioxolane as reported by Snider and co-workers,¹⁴⁹ providing the original substrate for the Rauhut-Currier reaction (Scheme 4.23). Completion of the synthesis would be identical to that described in section 4.6.1.

Scheme 4.23: Synthetic plan for (+)-Sch 642305 in *route B* with a ketal protected α,β -unsaturated ketone.

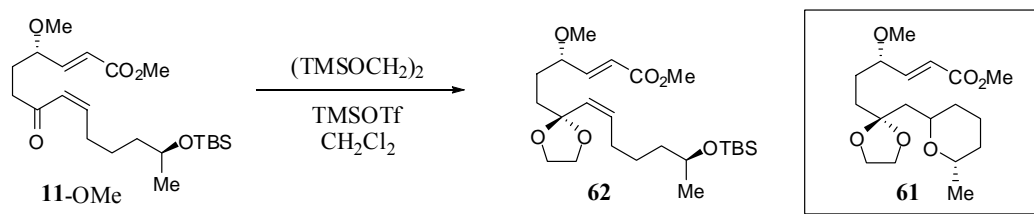


Ketal protection of α,β -unsaturated ketone **11-OMe** was attempted under mild conditions reported by Noyori and coworkers¹⁷⁸ (Scheme 4.24). However, upon subjection to bis-*O*-(trimethylsilyl)ethylene glycol and catalytic trimethylsilyl trifluoromethanesulfonate (TMSOTf) we obtained undesired product **61** as the sole product, and not the desired 1,3-dioxolane, **62**. We found that ketalization did occur; however, it occurred after 6-exo-trig cyclization/silyl deprotection. Once again, the

¹⁷⁸ Tsunoda, T.; Suzuki, M.; Noyori, R. *Tetrahedron Lett.* **1980**, *21*, 1357-1358.

electrophilicity of the α,β -unsaturated ketone drove the reaction outcome and required us to modify our system.

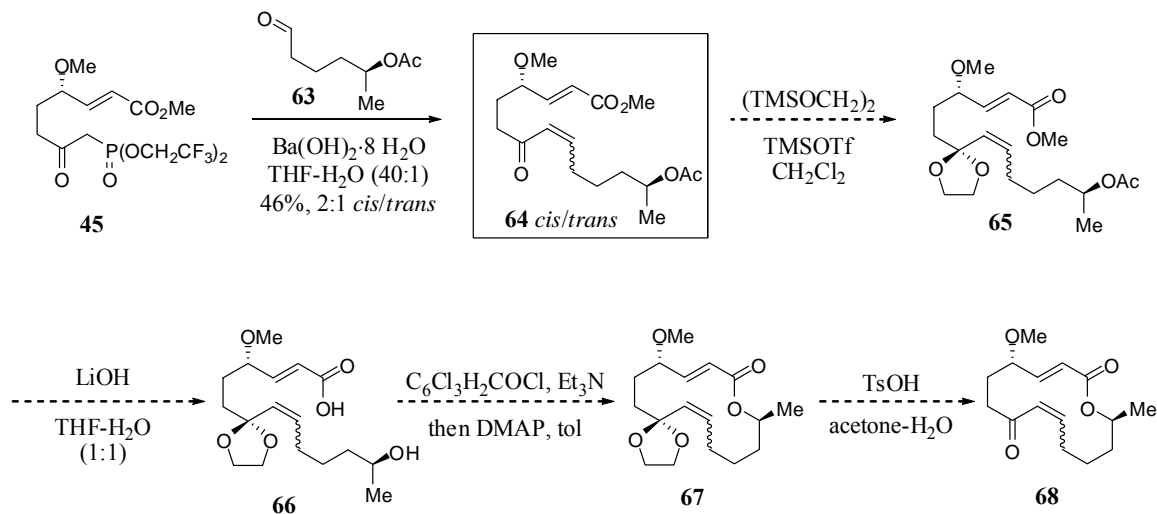
Scheme 4.24: Attempted ketalization of **11-OMe**.



4.6.5 1,3-Dioxolane with OAc Protecting Group

As illustrated in Scheme 4.25, our revised plan incorporated an orthogonal protecting group on the secondary alcohol, to replace the TBS protecting group with an acetate group, which will remain intact under the ketalization conditions. The amended synthesis began with a Still-Gennari modified HWE coupling of advanced phosphonate **45** and known aldehyde **63** to provide acetate-protected intermediate **64** in 46% yield and 2:1 *cis:trans* ratio. To complete the synthesis, intermediate **66** would be synthesized via ketalization of the α,β -unsaturated ketone followed by simultaneous deprotection of the methyl ester and secondary alcohol. Macrolactonization and deprotection of the ketal would then provide transannular RC substrate **68**.

Scheme 4.25: Synthetic plan incorporating a modified protecting group scheme.



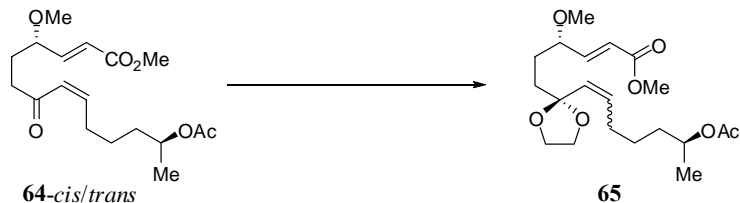
With acetate-protected intermediate **64** in hand, we were able to attempt the ketalization once again. Initial experiments with the mild Noyori protocol¹⁷⁸ (subjection to bis-*O*-(trimethylsilyl)ethylene glycol and catalytic TMSOTf at -78 °C) led to recovered starting material and olefin isomerization in the case of **64-cis** to **64-trans** (entries 1 and 2, Table 4.3). Under identical conditions with modest warming of the reaction mixture (-78 °C to -50 °C) we obtained isomerized starting material in addition to multiple unidentifiable by-products (entry 3).¹⁷⁹ Alternative conditions employing ethylene glycol and triethyl orthoformate with catalytic *p*-toluenesulfonic acid also led to multiple unidentifiable by-products (entry 4).¹⁸⁰ Finally, a report from Wicha and co-workers described irreproducible yields when employing the Noyori conditions and found that a

¹⁷⁹ NMR experiments suggest that one of the many by-products is the product of olefin migration from the α,β position to the β,γ position. This is a known issue in the ketalization of α,β -unsaturated ketones and was expected as we increased to warmer reaction conditions. Noyori's anhydrous conditions were developed in part to overcome this side reactivity. Please see reference 178.

¹⁸⁰ a) Becher, E.; Albrecht, R.; Bernhard, K.; Leuenberger, H. G. W.; Mayer, H.; Müller, R. K.; Schüep, W.; Wagner, H. P. *Helv. Chim. Acta.* **1981**, *64*, 2419-2435. b) Rao, K. S.; Reddy, D. S.; Mukkanti, K.; Pal, M.; Iqbal, J. *Tetrahedron Lett.* **2006**, *47*, 6623-6626.

5:1 ratio of bis-*O*-(trimethylsilyl)ethylene glycol to ethylene glycol with TMSOTf was critical to obtain consistent high yields.¹⁸¹ However, our system was unreactive under these conditions and we recovered starting material for both the *cis* and *trans* isomers (entries 5 and 6).

Table 4.3: Ketalization conditions tested in the protection of α,β -unsaturated ketone **64**.



entry	64	conditions (equiv)	catalyst (0.1 equiv)	temp (°C)	rxn outcome
1	<i>cis</i>	(TMSOCH ₂) ₂ (1.5)	TMSOTf	-78	64-<i>trans</i>
2	<i>trans</i>	(TMSOCH ₂) ₂ (1.5)	TMSOTf	-78	64-<i>trans</i>
3	<i>cis</i>	(TMSOCH ₂) ₂ (1.5)	TMSOTf	-78 to -50	64-<i>trans</i> + by-products
4	<i>cis</i>	HO(CH ₂) ₂ OH (1.5) CH(OC ₂ H ₅) ₃	TsOH	23	multiple by-products
5	<i>cis</i>	(TMSOCH ₂) ₂ (2.5) HO(CH ₂) ₂ OH (0.5)	TMSOTf	-78	64-<i>cis</i>
6	<i>trans</i>	(TMSOCH ₂) ₂ (2.5) HO(CH ₂) ₂ OH (0.5)	TMSOTf	-78	64-<i>trans</i>

4.6.6 Masked α,β -Unsaturated Carbonyl

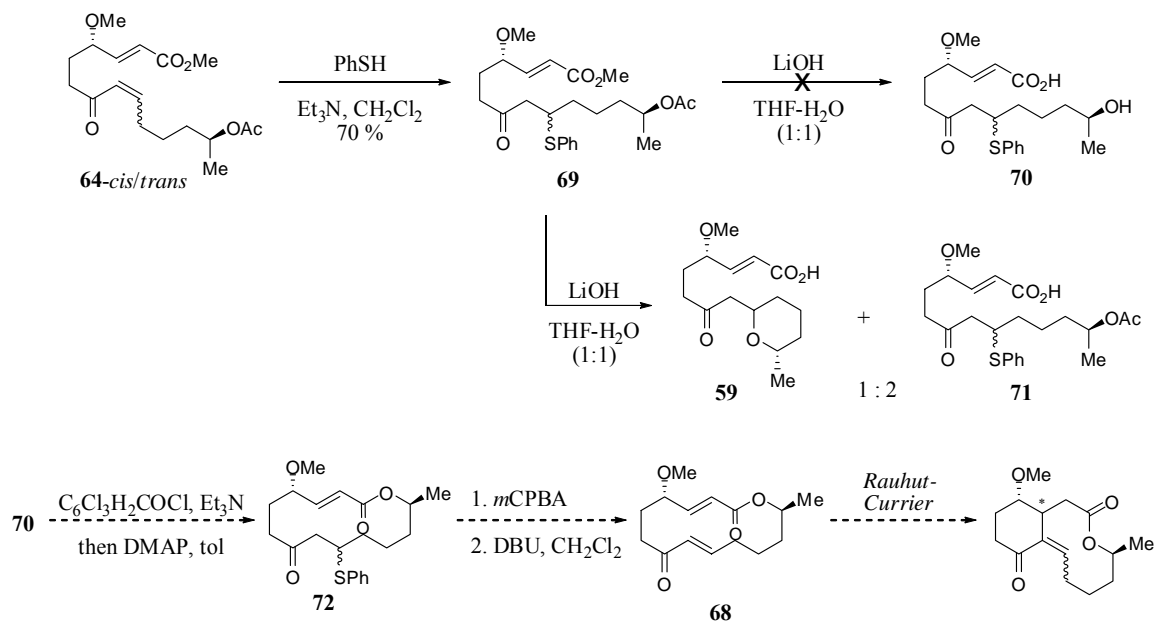
Protection of the α,β -unsaturated ketone as a 1,3-dioxolane in both the TBS protected compound (**11-OMe**) as well as the acetate protected compound (**64-OMe**) proved to be problematic for several reasons as described above. This prompted us to explore an alternative approach to protect the enone. In our new plan, the α,β -unsaturated ketone would be converted to a β -thioether (**69**) to mask the highly reactive enone moiety

¹⁸¹ Chochrek, P.; Kurek-Tyrlik, A.; Michalak, K.; Wicha, J. *Tetrahedron Lett.* **2006**, *47*, 6017-6020.

until regeneration prior to the Rauhut-Currier cyclization. The synthesis, as outlined in Scheme 4.26, involved the conversion of α,β -unsaturated ketone **64** to intermediate **69** as a mixture of diastereomers using benzenethiol with catalytic triethylamine (70% yield). Simultaneous hydrolysis of the methyl ester and acetate protecting group using LiOH in THF-H₂O did not lead to the desired product, **70**, and instead produced undesired by-products, tetrahydropyran **59** and partially deprotected intermediate **71**, in a 1:2 ratio. Moreover, upon re-subjection to the reaction conditions, **71** was readily converted to tetrahydropyran **59**. Monitoring the reaction revealed that ester hydrolysis and elimination of benzenethiol were rapid whereas cleavage of the acetate protecting group was more sluggish.¹⁸² Therefore, the α,β -unsaturated ketone was regenerated and unmasked prior to deprotection of the acetate group, leading to rapid cyclization upon liberation of the free alkoxide. Because the thioester was not stable to hydrolysis/deprotection conditions, an alternative approach was required.

¹⁸² By ¹H NMR and TLC.

Scheme 4.26: Synthesis of masked α,β -unsaturated ketone **69**.

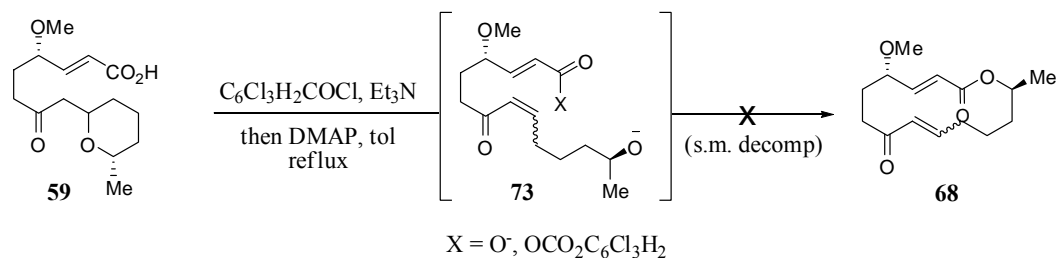


4.6.7 Initial Yamaguchi Cyclization

A brief attempt at the Yamaguchi macrolactonization was explored with by-product tetrahydropyran **59** (obtained during silyl deprotection of **58** as well as hydrolysis of β -thioether **69**). This reaction would require retro-conjugate addition of the secondary alcohol to generate α,β -unsaturated ketone intermediate **73** and subsequent macrocyclization. As illustrated in Scheme 4.27, subjection of **59** to cyclization conditions led to decomposition of the starting material with no detectable product (**68**).¹⁸³

¹⁸³ Mulzer, J.; Kirstein, H. M.; Buschmann, J.; Lehmann, C.; Luger, P. *J. Am. Chem. Soc.* **1991**, *113*, 910-923.

Scheme 4.27: Initial attempt at the Yamaguchi macrolactonization with substrate **59**.

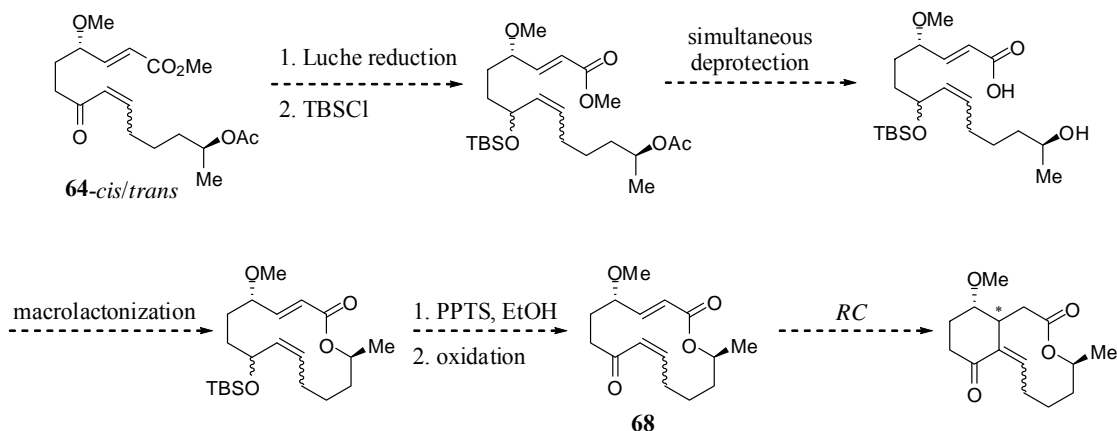


4.6.8 Carbonyl Reduction/Protection

Thus far, we have been exploring the synthesis of (+)-Sch 642305 in *route B* with several modifications of our original plan (1,3-dioxolane protection and β -thioether formation) in order to control the high electrophilicity of the α,β -unsaturated ketone. Ultimately, we found that a carbonyl reduction/protection sequence was successful.

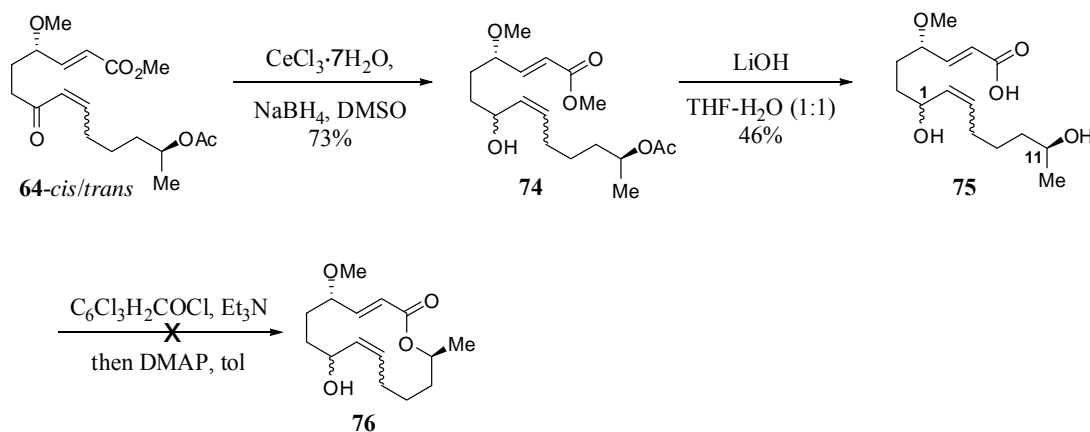
Proceeding with acetate protected compound **64**, the synthesis would continue with a Luche reduction of the α,β -unsaturated ketone followed by TBS protection of the allylic alcohol (Scheme 4.28). Hydrolysis of the methyl ester and acetate protecting group would be effected in one step followed by macrolactonization. A final deprotection of the allylic alcohol and subsequent oxidation would generate **68** for the key transannular Rauhut-Currier reaction.

Scheme 4.28: Synthetic plan employing a reduction/protection sequence.



Alternatively, selective macrolactonization could be achieved on fully deprotected substrate **75** (Scheme 4.29). This would require exclusive ring closure resulting from the C11 hydroxyl group with no by-product formed from ring closure of the hydroxyl at C1. This is effectively a competition between 14-membered macrolide formation and 8-membered macrolide formation, with the former being preferred.¹⁸⁴

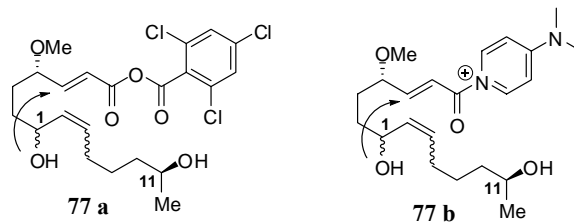
Scheme 4.29: Synthesis employing carbonyl reduction and macrolactonization on fully deprotected intermediate **75**.



¹⁸⁴ (a) Schreiber, S. L.; Kelly, S. E.; Porco, J. A.; Sammakia, T.; Suh, E. M. *J. Am. Chem. Soc.* **1988**, *110*, 6210-6218. (b) White, J. D.; Blakemore, P. R.; Browder, C. C.; Hong, J.; Lincoln, C. M.; Nagorny, P. A.; Robarge, L. A.; Wardrop, D. J. *J. Am. Chem. Soc.* **2001**, *123*, 8593-8595.

As illustrated in Scheme 4.29, Luche reduction¹⁸⁵ of intermediate **64** provided allylic alcohol **74** (73%) which then underwent deprotection of both the methyl ester and the acetate protecting group to provide substrate **75** for the selective macrolactonization. However, upon subjection of fully deprotected intermediate **75** to Yamaguchi cyclization conditions,¹⁸⁴ the starting material was fully consumed and an unidentifiable mixture of by-products was formed. One point of concern was the potential for 6-exo-trig intramolecular conjugate addition of the C1 hydroxyl once the carboxylic acid was activated as either the corresponding mixed anhydride (**77a**) or as the acetylpyridinium ion (**77b**) (Figure 4.11).

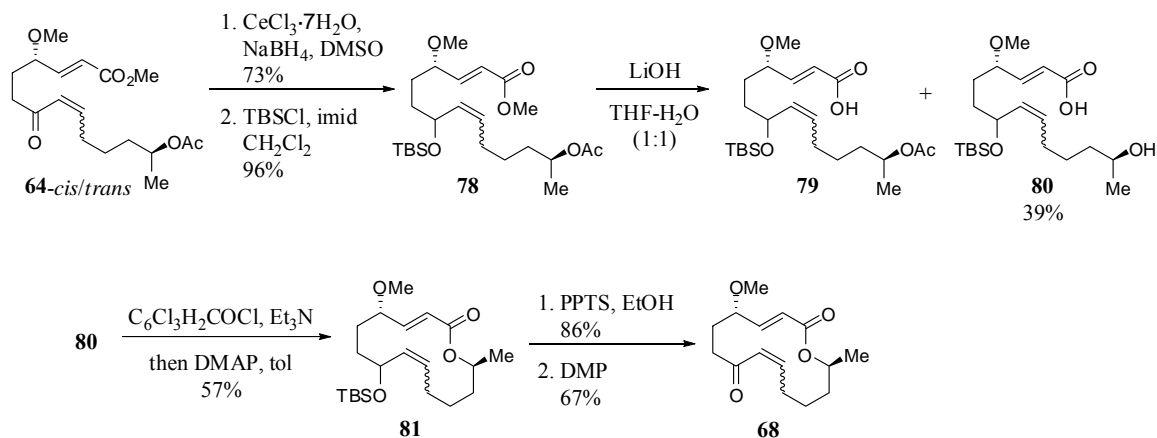
Figure 4.11: Potential side reactivity in macrolactonization of the fully deprotected intermediate.



To avoid these aforementioned complications, we proceeded with the protected compound (Scheme 4.30). Once again, Luche reduction was followed by silylation using *tert*-butylchlorodimethylsilane (**78**, 96%) and hydrolysis of both the methyl ester and acetate protecting groups with LiOH. Acetate cleavage was significantly slower than ester hydrolysis, leading to a mixture of partially deprotected **79** and fully deprotected **80** (39%). In the initial attempt, intermediate **79** was re-subjected to the reaction conditions for full conversion to **80**, however, future syntheses of this route will simply be run under longer times.

¹⁸⁵ Adams, C. *Synth. Commun.* **1984**, *14*, 1349-1353.

Scheme 4.30: Synthesis employing carbonyl reduction/protection.



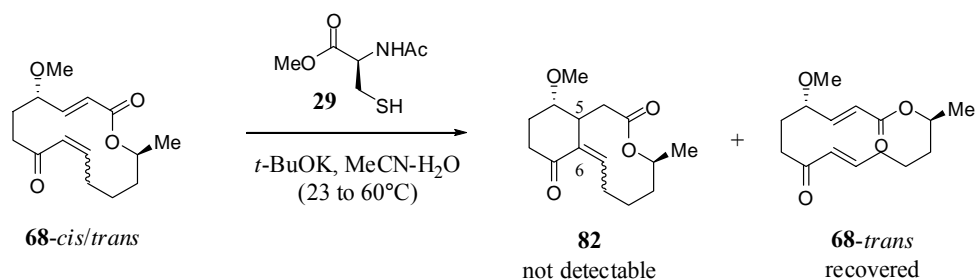
With substrate **80** in hand, we were able to perform an initial test of the final reaction sequence on small scale. Yamaguchi macrocyclization of the C1 hydroxyl-protected compound was successful, providing compound **81** in 57% un-optimized yield. Deprotection of the allylic alcohol with PPTS (86%) followed by Dess-Martin¹⁵⁹ oxidation finally provided the key transannular Rauhut-Currier substrate (**68**, 2 mg) in a 1:1 *cis* to *trans* ratio for preliminary examination.

4.6.9 Preliminary Studies of the Rauhut-Currier Reaction in *Route B*

Exploration of the Rauhut-Currier reaction in *route A* involved the use of an acyclic substrate, while synthesis of (+)-Sch 642305 in *route B* demanded that our Rauhut-Currier methodology could be expanded to include a transannular cyclization. With intermediate **68** in hand, we were able to test our key step under this alternative pathway. Preliminary examination of this cycloisomerization on very small scale (2 mg) has demonstrated that an optimization study will be critical in *route B*. Subjection of macrolide **68** to protected cysteine derivative **29** under previously optimized conditions (23 °C, *t*-BuOK, 1.5 equiv) as well as at elevated temperatures (up to 60 °C) led to the

recovery of starting material in the *trans* configuration (Scheme 4.31). As mentioned previously, we are optimistic that a systematic variation of reaction parameters, including solvent, concentration, temperature, and possibly catalyst structure, will ultimately lead to the successful catalysis of the key RC reaction in both the acyclic reaction as well as the transannular reaction. Once sufficient catalysis is demonstrated, we will be able to determine the inherent diastereoselectivity of the reaction using an achiral catalyst and then attempt to override it using our chiral catalyst.

Scheme 4.31: Rauhut-Currier reaction in route **B**.



4.7 Conclusion

Our study of the synthesis of (+)-Sch 642305 (**1**) has provided an exciting forum in which to address several on-going questions in our laboratory. We are interested in the ability to utilize catalyst control to drive reaction selectivity as well as demonstrate the application of our previously developed Rauhut-Currier methodology in a complex setting. Excitingly, we have presented our initial investigations into these questions, demonstrating a viable route to both key Rauhut-Currier substrates in pathways **A** and **B** (**11** and **68**) and have begun preliminary optimization studies thereof. We are inspired by our initial success in the acyclic RC transformation and are eager to continue studying the application of this methodology in full detail. Once we are able to establish the inherent

diastereoselectivity of the cyclization reaction on the acyclic substrate and the macrolide, we will study the use of a chiral catalyst to override this preference. This is a great challenge, as it may necessitate overcoming a substantially higher activation barrier if the substrate conformation strongly favors formation of one diastereomer over another. Then, using the newly developed methodology for setting the stereocenter at C5, we hope to actively select for the exclusive formation of the natural product (**1**) in addition to difficult-to-obtain unnatural analogs. This synthesis would then satisfy our original goals, to address our continuing interest regarding elements of stereocontrol, demonstrate the application of our RC methodology in a complex setting, and finally provide an expedient synthesis of (+)-Sch 642305.

4.8 Experimental

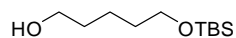
General. Proton NMR spectra were recorded on a 500 or 400 MHz spectrometer. Proton chemical shifts are reported in ppm (δ) relative to internal tetramethylsilane (TMS, δ 0.0 ppm) or with the solvent reference relative to TMS employed as the internal standard (CDCl_3 , δ 7.26 ppm; d_6 -DMSO, δ 2.50 ppm; CD_3OD , δ 3.31 ppm; D_2O , δ 4.79 ppm). Data are reported as follows: chemical shift (multiplicity [singlet (s), doublet (d), triplet (t), quartet (q), and multiplet (m)], coupling constants [Hz], integration). Carbon NMR spectra were recorded at 125 or 100 MHz with complete proton decoupling. Carbon chemical shifts are reported in ppm (δ) relative to TMS with the respective solvent resonance as the internal standard (CDCl_3 , δ 77.0 ppm). Infrared spectra were obtained on a Perkin-Elmer Spectrum 1000 spectrometer. Analytical thin-layer chromatography (TLC) was performed using Silica Gel 60 Å F254 precoated plates (0.25 mm thickness). TLC R_f values are reported. Visualization was accomplished by irradiation with a UV lamp and/or staining with KMnO_4 or cerium ammonium molybdenate (CAM) solutions. Flash column chromatography was performed using Silica Gel 60 Å (32-63 μm).¹⁸⁶ Optical rotations were recorded on a Rudolf Research Analytical Autopol IV Automatic polarimeter at the sodium D line (path length 100 mm). High resolution mass spectra were obtained at the Mass Spectrometry Facility of either Boston College (Chestnut Hill, MA) or the University of Illinois (Urbana-Champaign, IL). The method of ionization is given in parentheses. Analytical normal phase HPLC was performed on a Hewlett-Packard 1100 Series chromatograph equipped with a diode

¹⁸⁶ Still, W.C.; Kahn, M.; Mitra, J. *J. Org. Chem.* **1978**, *43*, 2923.

array detector (214 nm and 254 nm). All reactions were carried out under an argon or nitrogen atmosphere employing oven- and flame-dried glassware. All solvents were purified using a Seca Solvent Purification System by GlassContour. *t*-BuOK was freshly sublimed prior to use.

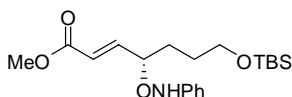
Experimental Procedures – *Route A*

Synthesis of Intermediate 11.



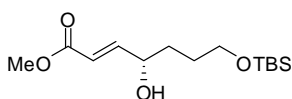
5-(*tert*-butyldimethylsilyloxy)pentan-1-ol (19). A mixture of NaH (95%, 2.18 g, 86.4 mmol) and THF (173 mL) was cooled to 0 °C and 1,5-pentanediol (18.1 mL, 173 mmol) was added dropwise over 5 minutes. The ice bath was removed after 5 minutes and the reaction mixture was allowed to stir at room temperature for 30 minutes. The mixture was then cooled to 0 °C and *tert*-butyldimethylchlorosilane (13.0 g, 86.4 mmol) was added portionwise over 10 minutes. After 15 minutes, the mixture was allowed to warm to room temperature and stir for an additional 2 h. The reaction mixture was cooled to 0 °C and quenched by the slow addition of water (100 mL). The mixture was diluted with Et₂O (200 mL) and washed with 10% aqueous K₂CO₃ (200 mL). The aqueous layer was extracted with Et₂O (2 x 100 mL) and the combined organic layers were washed with 10% aqueous K₂CO₃ (100 mL), saturated aqueous NaCl (100 mL), dried over MgSO₄, and concentrated under reduced pressure in a 0 °C bath. The crude oil was purified by

silica gel chromatography (hexanes-EtOAc, 9:1 to 5:1) to afford **19** as a clear oil (17.4 g, 79.6 mmol, 92%). ^1H NMR (CDCl_3 , 500 MHz) δ 3.61-3.57 (m, 4H), 1.95 (bs, 1H), 1.58-1.49 (m, 4H), 1.40-1.34 (m, 2H), 0.86 (s, 9H), 0.02 (s, 6H); ^{13}C NMR (CDCl_3 , 125 MHz) δ 63.1, 62.7, 32.5, 32.4, 25.9, 22.0, 18.3, -5.4; IR (film, cm^{-1}) 3346, 2934, 2856, 1475, 1474, 1389, 1360, 1254, 1099, 1038, 833, 772; TLC R_f 0.29 (4:1 hexanes-EtOAc); HRMS (ESI) m/z 219.1787 (219.1780 calcd for $\text{C}_{11}\text{H}_{27}\text{O}_2\text{Si}$ $[\text{M}+\text{H}]^+$).



Compound 22. Nitrosobenzene (2.16 g, 20.2 mmol) was added to a solution of aldehyde **17** (5.24 g, 24.2 mmol) in anhydrous DMSO (97 mL) followed by D-proline (1.16 g, 10.1 mmol). After stirring at ambient temperature for 15 min, the teal solution turned bright orange and was cooled to $-15\text{ }^\circ\text{C}$. A premixed solution of methyl diethylphosphonoacetate (11.1 mL, 60.5 mmol), DBU (9.12 mL, 60.5 mmol), and LiCl (2.56 g, 60.5 mmol) in CH_3CN (97 mL) was cooled to $-15\text{ }^\circ\text{C}$ and added quickly via cannula. The resulting solution was maintained at $-15\text{ }^\circ\text{C}$ until the reaction was determined to be complete by TLC (35 min), at which point cooled ($0\text{ }^\circ\text{C}$) saturated aqueous NH_4Cl (200 mL) was added. The mixture was extracted with ethyl acetate (3 x 200 mL) and the combined organic layers were washed with water (3 x 100 mL), saturated aqueous NaCl (150 mL), and dried over MgSO_4 to provide **22** as an orange oil (4.70 g, 12.4 mmol, 61%) after silica gel chromatography (hexanes- Et_2O , 18:1 to 9:1). ^1H NMR (CDCl_3 , 400 MHz) δ 7.23-7.18 (m, 2H), 6.93-6.85 (m, 5H), 6.00 (d, $J = 17.1$

Hz, 1H), 4.40-4.35 (m, 1H), 3.71 (s, 3H), 3.62-3.59 (m, 2H), 1.83-1.55 (m, 4H), 0.85 (s, 9H), 0.02 (s, 6H); ^{13}C NMR (CDCl_3 , 100 MHz) δ 166.5, 148.2, 147.3, 128.9, 122.4, 122.0, 114.3, 82.7, 62.6, 51.6, 29.6, 28.2, 25.9, 18.2, -5.3; IR (film, cm^{-1}) 3289, 2950, 2925, 2856, 1728, 1659, 1601, 1495, 1254; TLC R_f 0.44 (2:1 hexanes- Et_2O); HRMS (ESI) m/z 380.2251 (380.2257 calcd for $\text{C}_{20}\text{H}_{34}\text{NO}_4\text{Si}$ $[\text{M}+\text{H}]^+$).

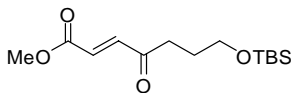


Compound 20. Nitrosobenzene (2.66 g, 24.9 mmol) was added to a solution of aldehyde **17** (5.38 g, 24.9 mmol) in anhydrous DMSO (96 mL) followed by D-proline (1.14 g, 9.9 mmol). After stirring at ambient temperature for 30 min, the teal solution turned bright orange and was cooled to 0 °C. A premixed solution of methyl diethylphosphonoacetate (11.4 mL, 62.2 mmol), DBU (9.40 mL, 62.2 mmol), and LiCl (2.60 g, 62.2 mmol) in CH_3CN (96 mL) was cooled to -15 °C and added quickly via cannula. The resulting solution was maintained at 0 °C for 30 min and then diluted with cooled (0 °C) methanol (500 mL) and NH_4Cl (3.33g, 62.2 mmol) and $\text{Cu}(\text{OAc})_2$ (0.45 g, 2.5 mmol) were added. The mixture was allowed to warm to ambient temperature and was maintained for 2 d. Methanol was then removed under reduced pressure and the mixture was diluted with water (500 mL) and extracted with Et_2O (3 x 150 mL). The combined organic layers were washed with water (2 x 150 mL), saturated aqueous NaCl (150 mL), and dried over sodium sulfate. Flash chromatography (hexanes- EtOAc , 8:1 to 2:1) provided alcohol **20** as a pale orange oil (3.01 g, 10.4 mmol, 42%) with >98% ee. ^1H NMR (CDCl_3 , 500

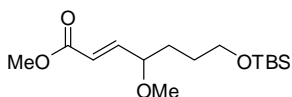
MHz) δ 6.95 (dd, $J = 15.4, 4.4$ Hz, 1H), 6.09 (d, $J = 15.5$ Hz, 1H), 4.36-4.31 (m, 1H), 3.74 (s, 3H), 3.68-3.66 (m, 2H), 3.48 (d, $J = 4.4$ Hz, 1H), 1.84-1.78 (m, 1H), 1.74-1.61 (m, 3H), 0.91 (s, 9H), 0.08 (s, 6H); ^{13}C NMR (CDCl_3 , 125 MHz) δ 167.1, 150.6, 119.6, 70.5, 63.3, 51.5, 34.3, 28.6, 25.8, 18.3, -5.4; IR (film, cm^{-1}) 3438, 2952, 2928, 2853, 1726, 1651, 1473, 1433, 1311; TLC R_f 0.14 (2:1 hexanes- Et_2O); HRMS (ESI) m/z 289.1835 (289.1835 calcd for $\text{C}_{14}\text{H}_{29}\text{O}_4\text{Si}$ $[\text{M}+\text{H}]^+$); Assay of enantiomeric purity: Enantiomers of product were separated by chiral HPLC employing a Chiralcel OD column (Daicel). Conditions: 94:6 hexanes-isopropanol; Flow rate 0.70 mL/min; 10.1 min (major ent), 11.4 min (minor ent).

Representative procedure for separate N-O cleavage.

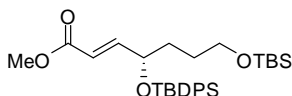
$\text{Cu}(\text{OAc})_2$ (1.10 g, 6.10 mmol) was added to a solution of **22** (4.40 g, 20.3 mmol) in *i*-PrOH (203 mL) at 0 °C. The mixture was allowed to stir for 15 h at 4.1 °C and then quenched with cooled (0 °C) saturated aqueous NH_4Cl (100 mL). The yellow mixture was extracted with ethyl acetate (3 x 1500 mL) and the combined organic layers were washed with water (2 x 100 mL), saturated aqueous NaCl (150 mL), and dried over Na_2SO_4 . The crude material was purified by silica gel chromatography (hexanes- Et_2O , 9:1 to 4:1) to provide **20** as a pale orange oil (2.46 g, 8.53 mmol, 42%) as well as by-product **23** (1.51 g, 5.28 mmol, 26%).



Compound 23. ^1H NMR (CDCl_3 , 400 MHz) δ 7.08 (d, $J = 15.9$ Hz, 1H), 6.68 (d, $J = 15.9$ Hz, 1H), 3.81 (s, 3H), 3.64 (t, $J = 5.9$ Hz, 2H), 2.72 (t, $J = 7.1$ Hz, 2H), 1.88-1.82 (m, 2H), 0.88 (s, 9H), 0.03 (s, 6H); ^{13}C NMR (CDCl_3 , 125 MHz) δ 199.5, 166.0, 139.6, 130.0, 61.8, 52.2, 37.9, 26.7, 25.8, 18.2, -5.4; TLC R_f 0.63 (1:1 hexanes- Et_2O); HRMS (ESI) m/z 309.1501 (309.1498 calcd for $\text{C}_{14}\text{H}_{26}\text{O}_4\text{NaSi}$ [$\text{M}+\text{Na}$] $^+$).

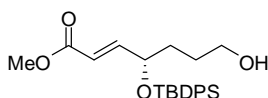


Compound 24. ^1H NMR (CDCl_3 , 500 MHz) δ 6.80 (dd, $J = 15.8, 6.3$ Hz, 1H), 6.98 (d, $J = 15.8$ Hz, 1H), 3.77-3.75 (m, 4H), 3.63-3.58 (m, 2H), 2.30 (s, 3H), 1.65-1.52 (m, 4H), 0.88 (s, 9H), 0.04 (s, 6H); ^{13}C NMR (CDCl_3 , 125 MHz) δ 166.6, 148.4, 121.5, 80.3, 62.7, 56.9, 51.5, 31.1, 28.2, 25.9, 18.2, -5.3; TLC R_f 0.43 (6:1 hexanes- EtOAc); HRMS (ESI) m/z 303.1992 (303.1992 calcd for $\text{C}_{15}\text{H}_{31}\text{O}_4\text{Si}$ [$\text{M}+\text{H}$] $^+$).



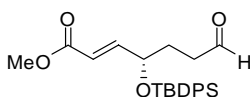
Compound 20b. Alcohol **20** (1.40 g, 4.85 mmol) was dissolved in CH_2Cl_2 (24 mL) and cooled to 0 $^\circ\text{C}$. Imidazole (0.76 g, 11.2 mmol) and *tert*-butyldiphenylchlorosilane (1.90 mL, 7.28 mmol) were successively added and the orange mixture was allowed to stir for

30 min, then at room temperature for 12 h. Water (30 mL) was added and the solution was extracted with CH₂Cl₂ (3 x 50 mL) and washed with saturated aqueous NH₄Cl (50 mL), NaCl (50 mL), dried over MgSO₄, and concentrated under reduced pressure. The crude oil was purified by silica gel chromatography (hexanes-Et₂O, 10:1 to 8:1) to afford the bis-silyl ether **20b** as a clear oil (2.17 g, 4.12 mmol, 85%). ¹H NMR (CDCl₃, 500 MHz) δ 7.68 (d, *J* = 6.6 Hz, 2H), 7.62 (d, *J* = 6.6 Hz, 2H), 7.46-7.35 (m, 6H), 6.89 (dd, *J* = 15.5, 5.0 Hz, 1H), 5.95 (d, *J* = 15.8 Hz, 1H), 4.43-4.41 (m, 1H), 3.73 (s, 3H), 3.51-3.41 (m, 2H), 1.56-1.39 (m, 4H), 1.10 (s, 9H), 0.87 (s, 9H), 0.03 (d, *J* = 3.15 Hz, 6H); ¹³C NMR (CDCl₃, 125 MHz) δ 166.9, 150.3, 135.7, 133.8, 133.4, 129.7, 129.7, 127.6, 127.5, 119.9, 72.1, 62.9, 51.4, 33.1, 27.2, 27.0, 25.9, 19.3, 18.2, -5.3; IR (film, cm⁻¹) 3074, 2953, 2929, 2887, 2852, 1725, 1661, 1109; TLC R_f 0.45 (4:1 hexanes-Et₂O); HRMS (ESI) *m/z* 527.3008 (527.3013 calcd for C₃₀H₄₇O₄Si₂ [M+H]⁺).

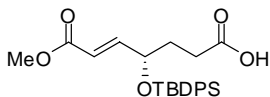


Compound 27. Bis-silyl ether **20b** (1.36 g, 2.58 mmol) was dissolved in absolute EtOH (14 mL) and pyridinium *p*-toluenesulfonate (259 mg, 1.03 mmol) was added in one portion. The pale yellow solution was allowed to stir at room temperature for 18 h and then concentrated under reduced pressure. The crude oil was purified by silica gel chromatography (hexanes-Et₂O, 9:1 to 1:2) to afford **27** as a clear oil (1.01 g, 2.45 mmol, 94%). ¹H NMR (CDCl₃, 500 MHz) δ 7.66 (dd, *J* = 8.0, 1.4 Hz, 2H), 7.59 (dd, *J* = 7.9, 1.3 Hz, 2H), 7.43-7.32 (m, 6H), 6.85 (dd, *J* = 15.8, 5.2 Hz, 1H), 5.93 (dd, *J* = 15.8, 1.4 Hz,

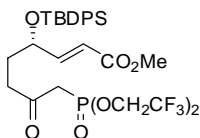
1H), 4.44-4.40 (m, 1H), 3.69 (s, 3H), 3.45-3.42 (m, 2H), 1.57-1.38 (m, 5H), 1.08 (s, 9H); ¹³C NMR (CDCl₃, 125 MHz) δ 166.8, 149.9, 135.7, 133.7, 133.1, 129.8, 129.7, 127.6, 127.5, 120.0, 71.9, 62.5, 51.4, 32.8, 27.0, 26.9, 19.2; IR (film, cm⁻¹) 3431, 2950, 2858, 1724, 1660, 1427, 1303, 1275, 1111, 702; TLC R_f 0.28 (2:1 hexanes-EtOAc); HRMS (ESI) *m/z* 435.1969 (435.1968 calcd for C₂₄H₃₂O₄SiNa [M+Na]⁺).



Compound 27b. Alcohol **27** (1.32 g, 3.15 mmol) was dissolved in CH₂Cl₂ (10 mL) and added dropwise to a stirred suspension of Dess-Martin periodinane (1.47 g, 3.47 mmol) in CH₂Cl₂ (12 mL) at 0 °C. The resulting mixture was allowed to warm to room temperature and maintained for 1.5 h, then filtered over celite and concentrated under reduced pressure. The crude residue was purified by silica gel chromatography (hexanes-EtOAc, 10:1 to 4:1) to aldehyde **27b** as a clear oil (1.30 g, 3.16 mmol, quantitative). ¹H NMR (CDCl₃, 500 MHz) δ 9.61 (s, 1H), 7.65 (d, *J* = 7.9 Hz, 2H), 7.59 (d, *J* = 8.1 Hz, 2H), 7.46-7.34 (m, 6H), 6.79 (dd, *J* = 15.5, 5.0 Hz, 1H), 5.94 (d, *J* = 17.0 Hz, 1H), 4.52-4.49 (m, 1H), 3.72 (s, 3H), 2.50-2.31 (m, 2H), 1.83-1.72 (m, 2H), 1.09 (s, 9H); ¹³C NMR (CDCl₃, 125 MHz) δ 201.3, 166.5, 149.0, 135.7, 135.7, 133.4, 133.0, 130.0, 129.9, 127.7, 127.6, 120.8, 71.0, 51.5, 38.2, 28.5, 27.0, 19.3; IR (film, cm⁻¹) 2949, 2929, 2853, 1994, 1723, 1429, 1110; TLC R_f 0.39 (3:1 hexanes-EtOAc); HRMS (ESI) *m/z* 411.2002 (411.1992 calcd for C₂₄H₃₁O₄Si [M+H]⁺).

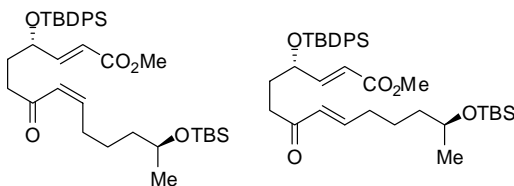


Compound 26. Silyl-protected aldehyde **27b** (1.35 g, 3.29 mmol) was dissolved in *tert*-butanol (33 mL) and 2-methyl-2-butene (6.30 mL, 59.2 mmol). A clear solution of sodium chlorite (0.60 g, 6.58 mmol) and sodium dihydrogen phosphate (2.72 g, 19.7 mmol) in water (33 mL) was added via cannula over 10 min. After 3 h, the reaction mixture was diluted with saturated aqueous NaCl (50 mL) and extracted with CH₂Cl₂ (3 x 50 mL). The combined organic layers were washed with saturated aqueous NaCl (50 mL) and dried over Na₂SO₄ to provide **26** as a clear oil (1.41 g, 3.30 mmol, quantitative) after silica gel chromatography (hexanes-EtOAc, 2:1 to 1:2). ¹H NMR (CDCl₃, 400 MHz) δ 10.79 (bs, 1H), 7.66 (d, *J* = 6.6 Hz, 2H), 7.62 (d, *J* = 6.6 Hz, 2H), 7.46-7.33 (m, 6H), 6.83 (dd, *J* = 15.7, 5.3 Hz, 1H), 5.93 (d, *J* = 15.7 Hz, 1H), 4.50-4.46 (m, 1H), 3.71 (s, 3H), 2.43-2.23 (m, 2H), 1.82-1.76 (m, 2H), 1.09 (s, 9H); ¹³C NMR (CDCl₃, 125 MHz) δ 178.5, 166.6, 148.9, 135.7, 135.7, 133.3, 133.0, 129.9, 129.8, 127.7, 127.6, 120.8, 71.0, 51.5, 30.9, 28.2, 27.0, 19.3; IR (film, cm⁻¹) 3068, 2954, 2934, 2856, 1728, 1708, 1426, 1307, 1275, 1111; TLC R_f 0.46 (1:2 hexanes-EtOAc); HRMS (ESI) *m/z* 427.1985 (427.1941 calcd for C₂₄H₃₁O₅Si [M+H]⁺).



Compound 15. Acid **26** (0.20 g, 0.47 mmol) was dissolved in thionyl chloride (2 mL) with catalytic DMF (0.1 mL) and was allowed to stir for 1.5 h at ambient temperature. The crude acid chloride was then concentrated under reduced pressure and dried under vacuum for 30 min. Lithium hexamethyldisilazide (1M in THF, 0.99 mL, 0.99 mmol) was added dropwise over 5 min to bis(2,2,2-trifluoroethyl) methylphosphonate (0.24 g, 0.94 mmol) in THF (3.1 mL) at -100 °C. After 15 min, the acid chloride was dissolved in THF (3.1 mL) and added dropwise over 10 min. The reaction mixture was maintained at -100 °C for 1 h and then quenched with saturated aqueous NH₄Cl (5 mL) and allowed to warm to room temperature. After dilution with saturated aqueous NH₄Cl (20 mL), the mixture was extracted with CH₂Cl₂ (3 x 20 mL) and the combined organic extracts were washed with saturated aqueous NaCl (50 mL), dried (Na₂SO₄), and purified via silica gel chromatography (toluene-EtOAc, 9:1 to 4:1) to provide **15** as a clear oil (0.22 g, 0.32 mmol, 69%). ¹H NMR (CDCl₃, 500 MHz) δ 7.65 (d, *J* = 6.6 Hz, 2H), 7.58 (d, *J* = 6.6 Hz, 2H), 7.46-7.34 (m, 6H), 6.78 (dd, *J* = 15.4, 4.7 Hz, 1H), 5.97 (d, *J* = 15.4 Hz, 1H), 4.51-4.36 (m, 5H), 3.72 (s, 3H), 3.16-3.03 (m, 2H), 2.57-2.42 (m, 2H), 1.75-1.71 (m, 2H), 1.08 (s, 9H); ¹³C NMR (CDCl₃, 125 MHz) δ 125.7, 125.7, 123.5, 123.4, 121.3, 121.2, 119.1, 119.0, 120.7, 127.8, 127.7, 130.0, 129.9, 133.4, 132.8, 135.7, 135.6, 149.0, 166.5, 200.2, 200.2, 70.7, 62.7, 62.7, 62.4, 62.4, 62.1, 62.1, 61.8, 61.8, 51.5, 41.6, 40.5, 38.6, 38.5, 29.5, 19.2, 26.9; IR (film, cm⁻¹) 2962, 2929, 2857, 1717, 1297, 1265, 1164,

1103, 1067; TLC R_f 0.68 (2:1 toluene-EtOAc); HRMS (ESI) m/z 691.1691 (691.1692 calcd for $C_{29}H_{35}F_6O_7NaSiP [M+Na]^+$).

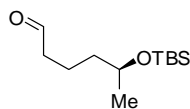


Compounds 11-cis and 11-trans. Barium hydroxide (0.16 g, 0.52 mmol) was added to a solution of phosphonate **15** (0.43 g, 0.65 mmol) in THF (18 mL) and allowed to stir for 30 min. Aldehyde **14** (0.15 g, 0.65 mmol) was dissolved in THF-H₂O (40:1, 4 mL) and added to the mixture. After 4 h, the reaction mixture was diluted with CH₂Cl₂ (100 mL), washed with saturated aqueous NaHCO₃, and extracted with CH₂Cl₂ (2 x 100 mL). The combined organic layers were washed with saturated aqueous NaCl (50 mL), dried (Na₂SO₄), and the crude oil was purified via silica gel chromatography (petroleum ether-Et₂O, 15:1 to 7:1) to provide **11-cis** (0.25 g, 0.39 mmol, 61%) and **11-trans** (0.11 g, 0.16 mmol, 25%) in 86% overall yield as a clear oil.

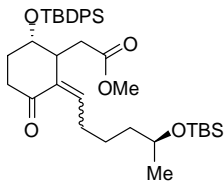
11-cis. ¹H NMR (CDCl₃, 400 MHz) δ 7.62-7.54 (m, 4H), 7.41-7.29 (m, 6H), 6.76 (dd, $J = 15.5, 5.1$ Hz, 1H), 6.00-5.92 (m, 2H), 5.88 (dd, $J = 15.5, 1.5$ Hz, 1H), 4.45-4.41 (m, 1H), 3.77-3.71 (m, 1H), 3.70 (s, 3H), 2.55-2.26 (m, 4H), 1.76-1.70 (m, 2H), 1.47-1.31 (m, 4H), 1.08 (d, $J = 6.1$ Hz, 3H), 1.06 (s, 9H), 0.85 (s, 9H), 0.02 (d, $J = 3.5$ Hz, 6H); ¹³C NMR (CDCl₃, 125 MHz) δ 200.3, 166.6, 149.6, 148.6, 135.8, 135.7, 133.5, 133.1, 129.9, 129.8, 127.7, 127.6, 126.4, 120.4, 71.3, 68.2, 51.4, 39.1, 38.3, 30.2, 29.6, 29.3, 27.0, 25.8,

25.3, 23.7, 19.3, 18.1, -4.3, -4.7; TLC R_f 0.50 (3:1 petroleum ether-Et₂O); HRMS (ESI) m/z 637.3730 (637.3745 calcd for C₃₇H₅₇O₅Si₂ [M+H]⁺).

11-trans. ¹H NMR (CDCl₃, 500 MHz) δ 7.65 (d, J = 6.6 Hz, 2H), 7.59 (d, J = 6.6 Hz, 2H), 7.45-7.33 (m, 6H), 6.83 (dd, J = 15.8, 5.0 Hz, 1H), 6.70 (dt, J = 15.8, 6.9 Hz, 1H), 5.98 (dt, J = 15.8, 1.6 Hz, 1H), 5.93 (dd, J = 15.7, 1.26 Hz, 1H), 4.50-4.47 (m, 1H), 3.81-3.77 (m, 1H), 3.72 (s, 3H), 2.58-2.38 (m, 2H), 2.19-2.15 (m, 2H), 1.81-1.75 (m, 2H), 1.57-1.36 (m, 4H), 1.12 (d, J = 6.3 Hz, 3H), 1.09 (s, 9H), 0.89 (s, 9H), 0.04 (s, 6H); ¹³C NMR (CDCl₃, 125 MHz) δ 199.5, 166.7, 149.6, 147.1, 135.8, 135.7, 133.5, 133.1, 130.1, 130.0, 129.8, 127.7, 127.6, 120.4, 71.4, 68.1, 51.5, 39.0, 34.2, 32.4, 30.4, 30.2, 27.0, 25.8, 24.1, 23.8, 19.3, 18.0, -4.3, -4.7; TLC R_f 0.31 (3:1 petroleum ether-Et₂O); HRMS (ESI) m/z 637.3750 (637.3745 calcd for C₃₇H₅₇O₅Si₂ [M+H]⁺).

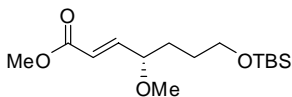


Compound 14. The characterization data for this compound matched that which has previously been reported.¹⁶² $[\alpha]_D^{25} +15$ (c 1.0, CHCl₃).



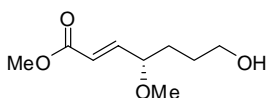
Compound 12. Tributylphosphine (46 μL , 0.19 mmol) was added to a solution of **11-cis** (12 mg, 0.019 mmol) in *tert*-butanol (1 mL). The clear solution was allowed to stir for 24 h at 23 $^{\circ}\text{C}$ at which point the reaction was diluted with EtOAc (20 mL) and washed with water (2 x 20 mL), saturated aqueous NaCl (20 mL), and dried over Na_2SO_4 . Flash chromatography (hexanes-EtOAc, 10:1) afforded compound **12** as a clear oil for characterization. ^1H NMR (CDCl_3 , 500 MHz) δ 7.65-7.62 (m, 4H), 7.47-7.33 (m, 6H), 6.67 (t, $J = 5.0$ Hz, 1H), 4.10 (bs, 1H), 3.79-3.73 (m, 1H), 3.47 (s, 3H), 3.38-3.34 (m, 1H), 2.83-2.76 (m, 1H), 2.39-2.34 (m, 2H), 2.18-2.14 (m, 4H), 1.93-1.85 (m, 2H), 1.46-1.38 (m, 3H), 1.12-1.09 (m, 3H), 1.04 (s, 9H), 0.89 (s, 9H), 0.05 (s, 6H); HRMS (ESI) m/z 659.3565 (659.3564 calcd for $\text{C}_{37}\text{H}_{56}\text{O}_5\text{NaSi}_2$ [$\text{M}+\text{Na}$] $^+$).

Synthesis of Intermediate 11-OMe.



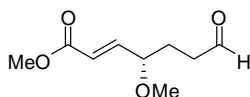
Compound 20c. Alcohol **20** (1.82 g, 6.31 mmol) was dissolved in CH_2Cl_2 (79 mL) and cooled to 0 $^{\circ}\text{C}$. Proton SpongeTM (8.10 g, 37.9 mmol) and trimethyloxonium tetrafluoroborate (4.70 g, 1.03 mmol) were added sequentially and the pale brown

mixture was allowed to stir at room temperature for 2 h. The reaction mixture was then quenched with saturated aqueous NaHCO₃ (100 mL) and extracted with CH₂Cl₂ (3 x 100 mL). The organic layers were combined and washed with 0.5 N HCl (2 x 100 mL), saturated aqueous NaCl (100 mL), dried (MgSO₄), and filtered over a 2.5 cm plug of silica gel, flushing with hexanes-Et₂O, 1:1 (300 mL) to afford **20c** as a pale yellow oil (1.65 g, 5.46 mmol, 87%). ¹H NMR (CDCl₃, 500 MHz) δ 6.77 (dd, *J* = 15.8, 6.6 Hz, 1H), 5.95 (d, *J* = 15.8 Hz, 1H), 3.76-3.69 (m, 4H), 3.61-3.54 (m, 2H), 3.27 (s, 3H), 1.63-1.48 (m, 4H), 0.85 (s, 9H), 0.01 (s, 6H); ¹³C NMR (CDCl₃, 125 MHz) δ 166.5, 148.3, 121.5, 80.2, 62.7, 56.9, 51.4, 31.0, 28.1, 25.8, 18.2, -5.4; IR (film, cm⁻¹) 2954, 2925, 2856, 1728, 1659, 1475, 1438, 1254, 1168, 1099, 833, 772; TLC R_f 0.43 (6:1 hexanes-EtOAc); HRMS (ESI) *m/z* 303.2001 (303.1992 calcd for C₁₅H₃₁O₄Si [M+H]⁺).

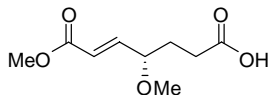


Compound 43. Methyl ether **20c** (415 mg, 1.37 mmol) was dissolved in absolute EtOH (7.6 mL) and pyridinium *p*-toluenesulfonate (138 mg, 0.55 mmol) was added in one portion. The pale yellow solution was allowed to stir at room temperature for 19 h and then concentrated under reduced pressure. The crude oil was purified by silica gel chromatography (hexanes-Et₂O, 10:1 to 1:4) to afford **43** as a clear oil (232 mg, 1.23 mmol, 90%). ¹H NMR (CDCl₃, 400 MHz) δ 6.80 (dd, *J* = 15.7, 6.3 Hz, 1H), 5.99 (d, *J* = 15.7 Hz, 1H), 3.82-3.77 (m, 1H), 3.75 (s, 3H), 3.66-3.62 (m, 2H), 3.32 (s, 3H), 1.89-1.83 (m, 1H), 1.63-1.48 (m, 4H); ¹³C NMR (CDCl₃, 125 MHz) δ 166.5, 147.9, 121.7, 80.3,

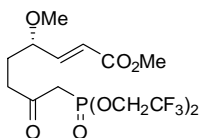
62.4, 57.0, 51.6, 31.3, 28.3; IR (film, cm^{-1}) 3423, 2947, 2870, 1724, 1659, 1438, 1304, 1272, 1163; TLC R_f 0.29 (1:4 hexanes-Et₂O); $[\alpha]_D$ -27.0 (*c* 1.0, CHCl₃); HRMS (ESI) m/z 211.0940 (211.0946 calcd for C₉H₁₆O₄Na [M+Na]⁺).



Compound 43b. Alcohol **43** (1.30 g, 6.90 mmol) was dissolved in CH₂Cl₂ (20 mL) and added dropwise to a stirred suspension of Dess-Martin periodinane (3.22 g, 7.60 mmol) in CH₂Cl₂ (33 mL) at 0 °C. The resulting mixture was allowed to warm to room temperature and maintained for 1.5 h, then filtered over celite and concentrated under reduced pressure. The crude residue was purified by silica gel chromatography (hexanes-Et₂O, 9:1 to 5:1) to afford **43b** as a clear oil (1.22 g, 6.56 mmol, 95%). ¹H NMR (CDCl₃, 400 MHz) δ 9.69 (t, *J* = 1.2 Hz, 1H), 6.72 (dd, *J* = 15.8, 6.2 Hz, 1H), 5.95 (dd, *J* = 15.8, 1.1 Hz, 1H), 3.78-3.72 (m, 1H), 3.70 (s, 3H), 3.23 (s, 3H), 2.55-2.41 (m, 2H), 1.93-1.75 (m, 2H); ¹³C NMR (CDCl₃, 100 MHz) δ 201.5, 166.3, 147.1, 122.0, 79.0, 56.9, 51.5, 39.2, 26.9; IR (film, cm^{-1}) 2950, 2934, 2826, 1720, 1431, 1303, 1271, 1163, 1115; TLC R_f 0.42 (1:1 hexanes-EtOAc); $[\alpha]_D$ -29.0 (*c* 1.0, CHCl₃); HRMS (ESI) m/z 209.0790 (209.0790 calcd for C₉H₁₄O₄Na [M+Na]⁺).

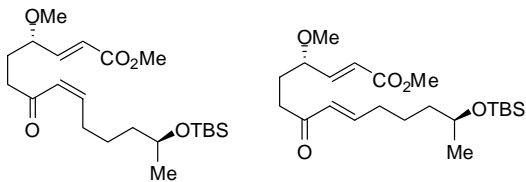


Compound 44. 43b (0.230 g, 1.24 mmol) was dissolved in *tert*-butanol (12 mL) and 2-methyl-2-butene (2.36 mL, 22.2 mmol). A clear solution of sodium chlorite (224 mg, 2.48 mmol) and sodium dihydrogen phosphate (1.03 g, 7.44 mmol) in water (12 mL) was added via cannula over 10 min. After 3 h, the reaction mixture was diluted with saturated aqueous NaCl (50 mL) and extracted with CH₂Cl₂ (3 x 50 mL). The combined organic layers were washed with saturated aqueous NaCl (50 mL) and dried over Na₂SO₄ to provide **44** as a clear oil (0.252 g, 1.24 mmol, quantitative) after silica gel chromatography (hexanes-EtOAc, 2:1 to 1:2). ¹H NMR (CDCl₃, 500 MHz) δ 10.41 (bs, 1H), 6.79 (dd, *J* = 15.8, 6.0 Hz, 1H), 6.02 (d, *J* = 15.8 Hz, 1H), 3.85-3.81 (m, 1H), 3.76 (s, 3H), 3.31 (s, 3H), 2.50-2.42 (m, 2H), 1.97-1.82 (m, 2H); ¹³C NMR (CDCl₃, 125 MHz) δ 178.9, 166.4, 147.2, 122.1, 79.0, 57.1, 51.6, 29.4, 29.3; IR (film, cm⁻¹) 2950, 2827, 1728, 1658, 1438, 1307, 1275, 1168, 1111; TLC R_f 0.30 (1:2 hexanes-EtOAc); [α]_D -17.0 (*c* 0.89, CHCl₃); HRMS (ESI) *m/z* 225.0750 (225.0739 calcd for C₉H₁₄O₅Na [M+Na]⁺).



Compound 45. Acid **44** (0.733 g, 3.63 mmol) was dissolved in thionyl chloride (7 mL) with catalytic DMF (0.1 mL) and was allowed to stir for 1.5 h at ambient temperature. The crude acid chloride was then concentrated under reduced pressure and dried under

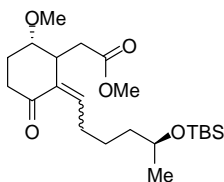
vacuum for 30 min. Lithium hexamethyldisilazide (1M in THF, 7.99 mL, 7.99 mmol) was added dropwise over 10 min to bis(2,2,2-trifluoroethyl) methylphosphonate (1.89 g, 7.26 mmol) in THF (24 mL) at -100 °C. After 15 min, the acid chloride was dissolved in THF (24 mL) and added dropwise over 10 min. The reaction mixture was maintained at -100 °C for 1 h and then quenched with saturated aqueous NH₄Cl (30 mL) and allowed to warm to room temperature. After dilution with saturated aqueous NH₄Cl (75 mL), the mixture was extracted with CH₂Cl₂ (3 x 50 mL) and the combined organic extracts were washed with saturated aqueous NaCl (100 mL), dried (Na₂SO₄), and purified via silica gel chromatography (hexanes-EtOAc, 5:1) to provide **45** as a clear oil (0.966 g, 2.18 mmol, 60%). ¹H NMR (CDCl₃, 500 MHz) δ 6.76 (dd, *J* = 15.8, 6.0 Hz, 1H), 6.01 (d, *J* = 15.8 Hz, 1H), 4.48-4.41 (m, 4H), 3.81-3.77 (m, 1H), 3.76 (s, 3H), 3.32-3.26 (m, 5H), 2.72-2.59 (m, 2H), 1.98-1.91 (m, 1H), 1.84-1.77 (m, 1H); ¹³C NMR (CDCl₃, 125 MHz) δ 200.7, 200.6, 166.7, 147.4, 126.2, 124.0, 122.6, 121.7, 119.2, 79.2, 62.9, 62.6, 57.4, 52.0, 42.2, 41.1, 40.1, 40.0, 28.6; IR (film, cm⁻¹) 2950, 2831, 1720, 1442, 1418, 1303, 1258, 1176, 1103, 1074; TLC R_f 0.35 (1:1 toluene-EtOAc); [α]_D -13.0 (*c* 1.0, CHCl₃); HRMS (ESI) *m/z* 445.0855 (445.0851 calcd for C₁₄H₂₀F₆O₇P [M+H]⁺).



Compounds 11-OMe *cis* and **11-OMe *trans***. Barium hydroxide (491 mg, 1.56 mmol) was added to a solution of phosphonate **45** (864 mg, 0.65 mmol) in THF (53 mL) and allowed to stir for 30 min. Aldehyde **14** (448 mg, 1.95 mmol) was dissolved in THF-H₂O (40:1, 12 mL) and added to the mixture via cannula. After 4 h, the reaction mixture was diluted with CH₂Cl₂ (250 mL), washed with saturated aqueous NaHCO₃, and extracted with CH₂Cl₂ (2 x 200 mL). The combined organic layers were washed with saturated aqueous NaCl (150 mL), dried (Na₂SO₄), and the crude oil was purified via silica gel chromatography (petroleum ether-Et₂O, 15:1 to 7:1) to provide **11-OMe *cis*** (338 mg, 0.82 mmol, 42%) and **11-OMe *trans*** (144 mg, 0.35 mmol, 18%) in 60% overall yield as a clear oil.

11-OMe *cis*. ¹H NMR (CDCl₃, 500 MHz) δ 6.77 (dd, *J* = 15.8, 6.3 Hz, 1H), 6.12-5.97 (m, 3H), 3.82-3.75 (m, 2H), 3.74 (s, 3H), 3.27 (s, 3H), 2.61-2.50 (m, 4H), 1.94-1.77 (m, 2H), 1.52-1.35 (m, 4H), 1.09 (d, *J* = 6.3 Hz, 3H), 0.86 (s, 9H), 0.01 (d, *J* = 3.5, Hz, 6H); ¹³C NMR (CDCl₃, 125 MHz) δ 200.4, 166.5, 148.7, 147.7, 126.5, 121.8, 79.2, 68.2, 57.0, 51.6, 39.1, 39.0, 29.3, 28.4, 25.8, 25.3, 23.7, 18.0, -4.4, -4.7; IR (film, cm⁻¹) 2954, 2929, 2851, 1724, 1691, 1617, 1437, 1274, 1254, 1164, 1094; TLC R_f 0.42 (2:1 petroleum ether-Et₂O); HRMS (ESI) *m/z* 435.2534 (435.2543 calcd for C₂₂H₄₀O₅NaSi [M+Na]⁺).

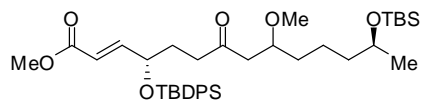
11-OMe trans. ^1H NMR (CDCl_3 , 500 MHz) δ 6.85-6.77 (m, 2H), 6.08 (d, $J = 16.1$ Hz, 1H), 6.00 (d, $J = 15.8$ Hz, 1H), 3.83-3.77 (m, 2H), 3.75 (s, 3H), 3.29 (s, 3H), 2.69-2.56 (m, 2H), 2.22-2.18 (m, 2H), 1.97-1.78 (m, 2H), 1.60-1.38 (m, 4H), 1.10 (d, $J = 6.3$ Hz, 3H), 0.88 (s, 9H), 0.04 (d, $J = 3.2$ Hz, 6H); ^{13}C NMR (CDCl_3 , 125 MHz) δ 199.6, 166.5, 147.7, 147.4, 130.2, 121.8, 79.2, 68.1, 57.0, 51.6, 39.0, 34.8, 32.4, 28.6, 25.8, 24.1, 23.7, 18.0, -4.3, -4.7; IR (film, cm^{-1}) 2951, 2926, 2853, 1726, 1693, 1669, 1629, 1433, 1270, 1254; TLC R_f 0.32 (2:1 petroleum ether- Et_2O); HRMS (ESI) m/z 435.2545 (435.2543 calcd for $\text{C}_{22}\text{H}_{40}\text{O}_5\text{NaSi}$ $[\text{M}+\text{Na}]^+$).



Compound 46. Tributylphosphine (92 μL , 0.37 mmol) was added to a solution of **11-OMe cis** (15.4 mg, 0.037 mmol) in *tert*-butanol (1.85 mL). The clear solution was allowed to stir for 24 h at 23 $^\circ\text{C}$ at which point the reaction was diluted with EtOAc (20 mL) and washed with water (2 x 20 mL), saturated aqueous NaCl (20 mL), and dried over Na_2SO_4 . Flash chromatography (petroleum ether- Et_2O , 10:1 to 2:1) afforded compound **46** as a clear oil for characterization. ^1H NMR (CDCl_3 , 500 MHz) δ 6.61 (t, $J = 7.6$ Hz, 1H), 3.81-3.75 (m, 2H), 3.69 (s, 3H), 3.37 (s, 3H), 2.61-2.53 (m, 2H), 2.39-2.33 (m, 2H), 2.23-1.96 (m, 6H), 1.52-1.35 (m, 3H), 1.11 (d, $J = 6.0$ Hz, 3H), 0.91-0.84 (m,

9H), 0.05-0.03 (m, 6H); TLC R_f 0.21 (1:1 petroleum ether-Et₂O); HRMS (ESI) m/z 435.2527 (435.2543 calcd for C₂₂H₄₀O₅NaSi [M+Na]⁺).

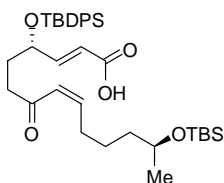
Experimental Procedures – Route B



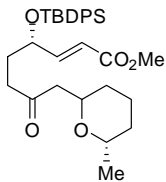
Compound 55. 11-*trans* (12 mg, 0.02 mmol) was dissolved in THF-H₂O-MeOH (2:2:1, 2.0 mL) and aqueous LiOH (2N, 0.1 mL) was added. After 12 h at ambient temperature, the reaction mixture was acidified to pH 3 with 1N HCl and extracted with EtOAc (3 x 15 mL). The combined organic layers were washed with saturated aqueous NaCl (15 mL) and dried (Na₂SO₄) to afford **55** (12 mg, 0.018 mmol, 90%) as a mixture of diastereomers after purification via silica gel chromatography (hexanes-EtOAc, 10:1). ¹H NMR (CDCl₃, 500 MHz) δ 7.65 (d, J = 6.6 Hz, 4H), 7.58 (d, J = 6.6 Hz, 4H), 7.46-7.29 (m, 12H), 6.82-6.77 (m, 2H), 5.93 (d, J = 15.8, 6.9 Hz, 2H), 4.47-4.44 (m, 2H), 3.80-3.75 (m, 2H), 3.72 (s, 6H), 3.60-3.56 (m, 2H), 3.26 (s, 3H), 3.24 (s, 3H), 2.55-2.25 (m, 8H), 1.76-1.69 (m, 4H), 1.41-1.21 (m, 12H), 1.12-1.10 (m, 6H), 1.08 (s, 18H), 0.88 (s, 18H), 0.04 (s, 12H); TLC R_f 0.49 (3:1 hexanes-EtOAc); HRMS (ESI) m/z 669.4021 (669.4007 calcd for C₃₈H₆₁O₆Si₂ [M+H]⁺).

Representative procedure for methyl ester hydrolysis.

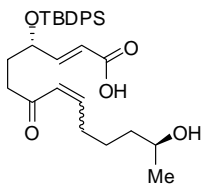
11-cis (125 mg, 0.20 mmol) was dissolved in THF-H₂O (1:1, 10 mL) and aqueous LiOH (2N, 1.0 mL) was added. After 12 h at ambient temperature, the reaction mixture was acidified to pH 3 with 1N HCl (3 mL), extracted with EtOAc (3 x 75 mL). The combined organic layers were washed with saturated aqueous NaCl (75 mL) and dried (Na₂SO₄) to afford **52-cis** (124 mg, 0.20 mmol, quantitative) and used without further purification.



Compound 52-cis. ¹H NMR (CDCl₃, 400 MHz) δ 7.66-7.59 (m, 4H), 7.46-7.34 (m, 6H), 6.95-6.87 (m, 1H), 6.00-5.90 (m, 3H), 4.52-4.47 (m, 1H), 3.81-3.74 (m, 1H), 2.58-2.32 (m, 4H), 1.83-1.72 (m, 2H), 1.52-1.35 (m, 4H), 1.11 (d, *J* = 6.1 Hz, 3H), 1.09 (s, 9H), 0.87 (s, 9H), 0.05-0.03 (m, 6H); ¹³C NMR (CDCl₃, 100 MHz) δ 200.5, 171.3, 152.2, 148.9, 135.8, 133.5, 133.1, 130.0, 129.9, 127.7, 127.6, 126.5, 120.0, 71.3, 68.4, 39.2, 38.3, 30.2, 29.4, 27.1, 25.9, 25.3, 23.8, 19.4, 18.2, -4.3, -4.7; IR (film, cm⁻¹) 3070, 2957, 2925, 2893, 2852, 1697, 1648, 1423, 1113; TLC R_f 0.57 (1:1 hexanes-EtOAc).

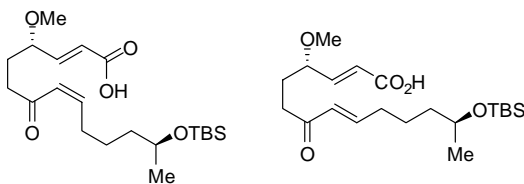


Compound 56. **11-cis** (10 mg, 0.016 mmol) was dissolved in absolute EtOH (0.53 mL) and pyridinium *p*-toluenesulfonate (1.6 mg, 0.006 mmol) was added in one portion. The clear solution was allowed to stir at room temperature for 12 h and then diluted with EtOAc (10 mL), washed with saturated aqueous NaCl (15 mL) and dried (Na₂SO₄). Crude ¹H NMR analysis indicated a 1:3 mixture of **11-trans** and by-product **56**. Flash chromatography (hexanes-Et₂O, 10:1) afforded compound **56** as a clear oil for characterization. ¹H NMR (CDCl₃, 500 MHz) δ 7.64 (d, *J* = 6.6 Hz, 2H), 7.59 (d, *J* = 6.6 Hz, 2H), 7.44-7.33 (m, 6H), 6.78 (dd, *J* = 15.5, 5.0 Hz, 1H), 5.91 (d, *J* = 15.5 Hz, 1H), 4.47-4.43 (m, 1H), 3.72-3.67 (m, 4H), 3.44-3.37 (m, 1H), 2.57-2.27 (m, 4H), 1.79-1.71 (m, 2H), 1.56-1.47 (m, 6H), 1.10 (d, *J* = 6.0 Hz, 3H), 1.08 (s, 9H); TLC R_f 0.42 (4:1 hexanes-EtOAc); HRMS (ESI) *m/z* 523.2881 (523.2880 calcd for C₃₁H₄₃O₅Si [M+H]⁺).



Compound 53-cis/trans. HF·pyridine (21 μL, 0.064 mmol) was added to a solution of **52-cis** (10 mg, 0.016 mmol) in THF (0.32 mL) at 0 °C. The reaction was allowed to warm to room temperature and stir for 5 h, at which point it was quenched with saturated

aqueous NaHCO₃ (5 mL) until the evolution of CO₂ ceased. The mixture was extracted with EtOAc (2 x 10 mL) and the combined organic extracts were washed with saturated aqueous NaCl (10 mL) and dried over Na₂SO₄ to afford a mixture of desired product **53-cis/trans** and **52-cis/trans**. Purification via silica gel chromatography afforded **53-cis/trans** as a mixture of diastereomers for characterization. ¹H NMR (CDCl₃, 400 MHz) δ 7.66-7.59 (m, 4H), 7.45-7.34 (m, 6H), 6.90-6.69 (m, 2H), 6.00-5.92 (m, 2H), 4.52-4.45 (m, 1H), 3.85-3.80 (m, 1H), 2.62-2.211 (m, 4H), 1.88-1.73 (m, 3H), 1.59-1.41 (m, 4H), 1.18 (d, *J* = 6.3 Hz, 3H), 1.09 (s, 9H); TLC R_f 0.15 (1:1 hexanes-EtOAc).

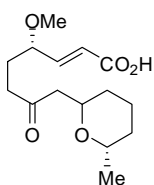


Compounds **58-cis** and **58-trans**.

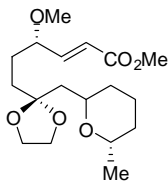
58-cis. Prepared according to the general procedure for methyl ester hydrolysis from **11-OMe cis** (50 mg, 0.12 mmol) to afford **58-cis** (48 mg, 0.12 mmol, quantitative) and used without further purification. ¹H NMR (CDCl₃, 400 MHz) δ 10.98 (bs, 1H), 6.89 (dd, *J* = 15.6, 5.8 Hz, 1H), 6.14-5.99 (m, 3H), 3.89-3.76 (m, 2H), 3.31 (s, 3H), 2.63-2.53 (m, 4H), 1.90-1.80 (m, 2H), 1.53-1.34 (m, 4H), 1.11 (d, *J* = 5.8 Hz, 3H), 0.88 (s, 9H), 0.04 (d, *J* = 3.5, Hz, 6H); TLC R_f 0.64 (6:1 CH₂Cl₂-MeOH).

58-trans. Prepared according to the general procedure for methyl ester hydrolysis from **11-OMe trans** (113 mg, 0.27 mmol) to afford **58-trans** (107 mg, 0.27 mmol, quantitative)

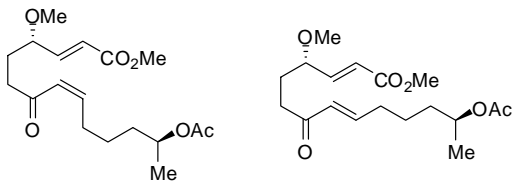
and used without further purification. ^1H NMR (CDCl_3 , 500 MHz) δ 10.25 (bs, 1H), 6.93-6.81 (m, 2H), 6.09 (d, $J = 15.8$ Hz, 1H), 6.02 (d, $J = 15.8$ Hz, 1H), 3.88-3.77 (m, 2H), 3.31 (s, 3H), 2.68-2.47 (m, 3H), 2.23-2.19 (m, 1H), 1.99-1.79 (m, 2H), 1.56-1.39 (m, 4H), 1.12 (d, $J = 6.0$ Hz, 3H), 0.89 (s, 9H), 0.04 (d, $J = 2.8$ Hz, 6H); TLC R_f 0.64 (6:1 CH_2Cl_2 -MeOH).



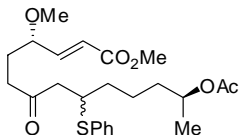
Compound 59. **58-*cis*** (17 mg, 0.06 mmol) was dissolved in absolute EtOH (3 mL) and pyridinium *p*-toluenesulfonate (6.6 mg, 0.02 mmol) was added in one portion. The clear solution was allowed to stir at room temperature for 12 h and then diluted with EtOAc (10 mL), washed with saturated aqueous NaCl (15 mL) and dried (Na_2SO_4). Purification via silica gel chromatography (6:1 CH_2Cl_2 -MeOH) afforded **59** for characterization. ^1H NMR (CDCl_3 , 400 MHz) δ 10.88 (bs, 1H), 6.88 (dd, $J = 15.8, 6.1$ Hz, 1H), 6.00 (d, $J = 15.7$ Hz, 1H), 3.85-3.73 (m, 2H), 3.47-3.39 (m, 1H), 3.30 (s, 3H), 2.70-2.37 (m, 4H), 1.96-1.74 (m, 3H), 1.61-1.46 (m, 3H), 1.21-1.14 (m, 2H), 1.12 (d, $J = 6.1$, 3H); TLC R_f 0.73 (6:1 CH_2Cl_2 -MeOH).



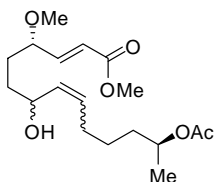
Compound 61. Trimethylsilyl trifluoromethanesulfonate (TMSOTf, 0.9 μ L, 0.005 mmol) was added to **11-OMe cis** (20 mg, 0.048 mmol) and ethylene glycol bis(trimethylsilyl ether) (99 mg, 0.48 mmol) at -78 $^{\circ}$ C. Methylene chloride (50 μ L) and TMSOTf (0.9 μ L, 0.005 mmol) were added after 1.5 h, as no reaction had occurred by TLC analysis. No reaction was determined after 6 h at -78 $^{\circ}$ C, and the reaction was allowed to warm to -25 $^{\circ}$ C over 12 h and stir for an additional 12 h. Saturated aqueous NaHCO_3 (5 mL) was added and the mixture was extracted with CH_2Cl_2 (2 x 5 mL), washed with saturated aqueous NaCl (5 mL) and dried (Na_2SO_4). Purification via silica gel chromatography (9:1 hexanes-EtOAc) provided **61** for characterization. ^1H NMR (CDCl_3 , 500 MHz) δ 6.81-6.75 (m, 1H), 6.00-5.95 (m, 1H), 3.92-3.88 (m, 3H), 3.76-3.72 (m, 4H), 3.48-3.62 (m, 2H), 3.29 (s, 3H), 1.89-1.46 (m, 10H), 1.25-1.15 (m, 3H), 1.12 (d, $J = 6.3$ Hz, 3H); ^{13}C NMR (CDCl_3 , 125 MHz) δ 166.6, 148.4, 121.5, 110.6, 80.4, 74.2, 73.7, 64.8, 64.7, 56.9, 51.5, 43.7, 33.0, 32.9, 32.2, 28.6, 23.8, 22.1; TLC R_f 0.34 (3:1 hexanes-EtOAc).



Compounds 64-*cis* and **64-*trans***. Barium hydroxide (235 mg, 0.74 mmol) was added to a solution of phosphonate **45** (415 mg, 0.93 mmol) in THF (25 mL) and allowed to stir for 30 min. Aldehyde **63** (150 mg, 0.93 mmol) was dissolved in THF-H₂O (40:1, 6 mL) and added dropwise over 5 min. After 4 h, the reaction mixture was concentrated under reduced pressure and the crude mixture was purified via silica gel chromatography (hexanes-EtOAc, 8:1 to 1:1) to provide **64-*cis*** (97 mg, 0.28 mmol) and **64-*trans*** (50 mg, 0.15 mmol) in 46% overall yield as a clear oil. **64-*cis***. ¹H NMR (CDCl₃, 400 MHz) δ 6.79 (dd, *J* = 15.9, 6.3 Hz, 1H), 6.15-5.98 (m, 3H), 4.93-4.85 (m, 1H), 3.84-3.79 (m, 1H), 3.75 (s, 3H), 3.29 (s, 3H), 2.64-2.52 (m, 4H), 2.02 (s, 3H), 1.96-1.77 (m, 2H), 1.64-1.39 (m, 4H), 1.20 (d, *J* = 6.3 Hz, 3H); ¹³C NMR (CDCl₃, 100 MHz) δ 200.4, 170.7, 166.4, 147.9, 147.7, 126.8, 121.8, 79.2, 70.7, 57.0, 51.6, 39.0, 35.4, 29.1, 28.3, 24.9, 21.3, 19.9; TLC R_f 0.61 (2:1 hexanes-EtOAc). **64-*trans***. ¹H NMR (CDCl₃, 400 MHz) δ 6.84-6.77 (m, 2H), 6.08 (d, *J* = 15.9 Hz, 1H), 6.01 (d, *J* = 15.9 Hz, 1H), 4.93-4.87 (m, 1H), 3.84-3.79 (m, 1H), 3.75 (s, 3H), 3.29 (s, 3H), 2.65-2.60 (m, 2H), 2.25-2.19 (m, 2H), 2.03 (s, 1H), 1.99-1.78 (m, 2H), 1.62-1.44 (m, 4H), 1.21 (d, *J* = 6.3 Hz, 3H); TLC R_f 0.57 (2:1 hexanes-EtOAc).

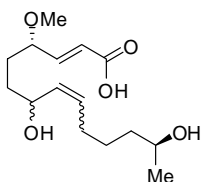


Compound 69. Benzenethiol (5.6 μL , 0.055 mmol) and Et_3N (0.014 M in CH_2Cl_2 , 175 μL , 0.0025 mmol) were added to a solution of **64-cis** (17 mg, 0.050 mmol) in CH_2Cl_2 (0.5 mL) and the mixture was allowed to stir at ambient temperature for 24 h. Direct purification via silica gel chromatography (CH_2Cl_2 -EtOAc, 10:1 to 5:1) provide **69** (15.4 mg, 0.34 mmol) as a mixture of diastereomers in 70% yield. ^1H NMR (CDCl_3 , 500 MHz) δ 7.33-7.31 (m, 2H), 7.24-7.16 (m, 4H), 6.68 (dd, $J = 15.8, 5.9$ Hz, 1H), 5.91 (d, $J = 15.8$ Hz, 1H), 4.82-4.75 (m, 1H), 3.72-3.68 (m, 4H), 3.53-3.48 (m, 1H), 3.19 (s, 3H), 2.67-2.49 (m, 2H), 2.46-2.32 (m, 2H), 1.95 (s, 3H), 1.85-1.75 (m, 1H), 1.72-1.64 (m, 1H), 1.53-1.35 (m, 5H), 1.14-1.11 (m, 3H); ^{13}C NMR (CDCl_3 , 125 MHz) δ 207.9, 170.6, 166.4, 147.6, 147.5, 134.4, 134.3, 132.4, 132.3, 128.9, 127.1, 122.0, 121.9, 79.1, 79.0, 70.6, 70.5, 57.0, 51.6, 48.3, 48.2, 43.7, 43.6, 38.5, 38.4, 35.4, 34.7, 34.5, 28.1, 22.7, 22.6, 21.3, 19.9, 19.8; TLC R_f 0.56 (6:1 CH_2Cl_2 -EtOAc).



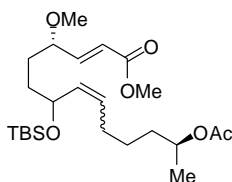
Compound 74. Cerium trichloride heptahydrate (19.7 mg, 0.053 mmol) was added to a solution of **64-cis/trans** (18 mg, 0.053 mmol) in DMSO (0.53 mL) until the cerium salt was fully dissolved (approx. 20 min). NaBH_4 (2 mg, 0.053 mmol) was added and the

mixture was allowed to stir at 23 °C for 1 h, at which point the reaction was quenched by the addition of saturated aqueous NH₄Cl (2 mL) and extracted with Et₂O (3 x 5 mL). The combined organic extracts were washed with water (5 mL), saturated aqueous NaCl (5 mL), and dried over Na₂SO₄ to afford **74** as a mixture of diastereomers (13.2 mg, 0.039 mmol, 73%) after purification via silica gel chromatography. ¹H NMR (CDCl₃, 400 MHz) δ 6.79 (dd, *J* = 15.9, 6.6 Hz, 2H), 5.98 (d, *J* = 15.9 Hz, 2H), 5.65-5.57 (m, 1H), 5.48-5.37 (m, 3H), 4.92-4.85 (m, 2H), 4.43-4.38 (m, 1H), 4.06-4.02 (m, 1H), 3.80-3.75 (m, 2H), 3.74 (s, 6H), 3.30 (s, 6H), 2.18-1.97 (m, 10H), 1.70-1.54 (m, 10H), 1.51-1.34 (m, 8H), 1.18 (d, *J* = 6.1 Hz, 6H); ¹³C NMR (CDCl₃, 125 MHz) δ 171.1, 166.9, 148.4, 148.3, 133.5, 131.9, 131.8, 122.2, 122.1, 80.8, 80.8, 73.0, 72.9, 71.2, 71.1, 57.4, 51.9, 35.8, 35.7, 33.2, 33.1, 32.3, 32.2, 31.1, 25.2, 25.2, 21.7, 20.3; TLC R_f 0.44 (1:1 hexanes-EtOAc).



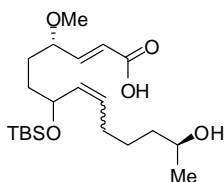
Compound 75. Prepared according to the general procedure for methyl ester hydrolysis from **74** (13 mg, 0.038 mmol) to afford **75** (5 mg, 0.017 mmol, 46%) after silica gel chromatography (CH₂Cl₂-MeOH, 7:1). ¹H NMR (CDCl₃, 400 MHz) δ 6.89 (dd, *J* = 15.5, 6.1 Hz, 1H), 6.00 (d, *J* = 15.4 Hz, 1H), 5.68-5.62 (m, 1H), 5.49-5.43 (m, 1H), 4.09-4.04 (m, 1H), 3.85-3.78 (m, 2H), 3.33 (s, 3H), 2.08-2.03 (m, 2H), 1.69-1.57 (m, 4H), 1.50-

1.39 (m, 6H), 1.26-1.24 (m, 1H), 1.18 (d, $J = 6.1$ Hz, 3H); TLC R_f 0.21 (7:1 CH_2Cl_2 -MeOH).

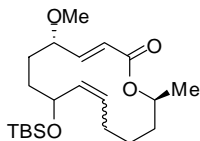


Compound 78. Allylic alcohol **74** (35 mg, 0.102 mmol) was dissolved in CH_2Cl_2 (1 mL) and DMF (0.25 mL) and cooled to 0°C . Imidazole (16 mg, 0.235 mmol) and *tert*-butyldimethylchlorosilane (23 mg, 0.153 mmol) were successively added and the white mixture was allowed to stir for 30 min, then at room temperature for 3.5 h. Water (10 mL) was added and the solution was extracted with CH_2Cl_2 (3 x 10 mL) and washed with saturated aqueous NH_4Cl (10 mL), NaCl (10 mL), dried over Na_2SO_4 , and concentrated under reduced pressure. The crude oil was purified by silica gel chromatography (hexanes-EtOAc, 10:1) to afford **78** as a mixture of diastereomers (45 mg, 0.099 mmol, 96%). ^1H NMR (CDCl_3 , 500 MHz) δ 6.80-6.75 (m, 2H), 5.97 (d, $J = 15.8$ Hz, 2H), 5.51-5.46 (m, 1H), 5.38-5.27 (m, 3H), 4.90-4.86 (m, 2H), 4.41-4.35 (m, 1H), 4.05-4.00 (m, 1H), 3.75-3.69 (m, 8H), 3.28 (s, 6H), 2.05-1.98 (m, 10H), 1.64-1.25 (m, 16H), 1.18 (d, $J = 6.1$ Hz, 6H), 0.87 (s, 18H), 0.01 (d, $J = 3.5$, Hz, 12H); ^{13}C NMR (CDCl_3 , 125 MHz) δ 170.7, 170.6, 166.5, 148.4, 148.3, 134.2, 134.1, 133.8, 133.7, 130.0, 128.7, 128.6, 121.6, 121.5, 80.6, 80.5, 80.4, 73.4, 73.2, 70.9, 70.7, 70.6, 68.5, 68.3, 56.9, 51.5, 35.8, 35.6, 35.4, 33.8, 33.7, 33.6, 31.7, 30.5, 30.2, 29.6, 27.6, 25.9, 25.8, 25.4, 25.3,

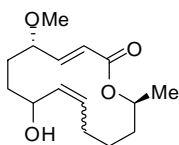
25.0, 21.2, 19.9, 18.2, 18.1, 18.0, -4.1, -4.2, -4.4, -4.7, -4.8; TLC R_f 0.59 (10:1 hexanes-EtOAc).



Compound 80. Prepared according to the general procedure for methyl ester hydrolysis from **78** (44 mg, 0.098 mmol) to afford **80** (15.1 mg, 0.038 mmol, 39%) after silica gel chromatography (CH₂Cl₂-MeOH, 7:1). ¹H NMR (CDCl₃, 500 MHz) δ 6.88 (dd, J = 15.7, 6.1 Hz, 2H), 6.52 (bs, 2H), 5.98 (d, J = 15.7 Hz, 2H), 5.54-5.48 (m, 1H), 5.39-5.28 (m, 3H), 4.42-4.37 (m, 1H), 4.09-4.01 (m, 1H), 3.84-3.74 (m, 4H), 3.30 (s, 6H), 2.08-1.98 (m, 4H), 1.68-1.36 (m, 18H), 1.18 (d, J = 6.0 Hz, 6H), 0.87-0.86 (m, 18H), 0.02-0.01 (m, 12H); ¹³C NMR (CDCl₃, 125 MHz) δ 171.0, 151.0, 150.9, 134.5, 134.4, 134.0, 133.9, 130.7, 130.7, 129.3, 129.3, 121.6, 121.6, 80.8, 80.7, 73.7, 73.6, 68.9, 68.8, 68.6, 68.4, 68.3, 57.5, 57.4, 39.3, 39.2, 39.1, 39.0, 34.1, 34.0, 33.9, 32.3, 30.7, 30.5, 30.4, 28.2, 28.1, 26.3, 26.2, 26.1, 26.0, 25.7, 23.8, 23.7, 18.6, 18.5, -3.7, -3.8, -4.3, -4.4.

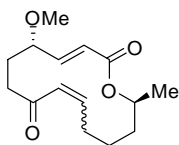


Compound 81. Acid **80** (15 mg, 0.037 mmol) in THF (2 mL) was treated with Et₃N (25.8 μ L, 0.185 mmol) for 10 min at 23 °C. 2,4,6-trichlorobenzoyl chloride (17.6 μ L) was added and the mixture was allowed to stir for 2 h. The reaction mixture was then diluted with toluene (11 mL) and added to a refluxing solution of DMAP (54.2 mg, 0.44 mmol) in toluene (24 mL) via syringe pump through a Vigreux column over 9 h. Once the reaction was cooled to ambient temperature, saturated aqueous NaHCO₃ (75 mL) was added and the mixture was extracted with EtOAc (3 x 100 mL). The combined organic extracts were washed with 0.1N HCl (75 mL), saturated aqueous NaCl (100 mL) and dried over Na₂SO₄. Flash chromatography (hexanes-EtOAc, 10:1) provided **81** (8.1 mg, 0.021 mmol, 57%) as a clear oil. ¹H NMR (CDCl₃, 500 MHz) δ 6.92-6.70 (m, 2H), 6.09-5.89 (m, 2H), 5.62-5.55 (m, 1H), 5.43-5.21 (m, 3H), 5.09-4.98 (m, 2H), 4.37-3.81 (m, 4H), 3.34-3.31 (m, 6H), 2.04-1.40 (m, 20H), 1.32-1.26 (m, 6H), 0.89-0.86 (m, 18H), 0.08-0.01 (m, 12H); TLC R_f 0.4, 0.37 (8:1 hexanes-EtOAc).



Compound 81b. **81** (5 mg, 0.013 mmol) was dissolved in absolute EtOH (1 mL) and pyridinium *p*-toluenesulfonate (4.2 mg, 0.017 mmol) was added in one portion. The clear

solution was allowed to stir at room temperature for 12 h at which point excess pyridinium *p*-toluenesulfonate (4.2 mg, 0.017 mmol) was added. After 24 h, the reaction was diluted with EtOAc (10 mL) and washed with saturated aqueous NaHCO₃ (10 mL). The aqueous phase was extracted with EtOAc (2 x 10 mL) and the combined organic layers were washed with saturated aqueous NaCl (10 mL) and dried (Na₂SO₄). Flash chromatography (CH₂Cl₂-EtOAc, 10:1 to 1:10) afforded compound **81b** (3 mg, 0.011 mmol, 86%) as a clear oil. ¹H NMR (CDCl₃, 500 MHz) δ 6.88-6.72 (m, 2H), 6.12-5.92 (m, 2H), 5.79-5.42 (m, 2H), 5.39-5.30 (m, 2H), 5.12-4.94 (m, 2H), 4.41-3.78 (m, 4H), 3.37-3.30 (m, 6H), 2.15-1.45 (m, 22H), 1.30-1.25 (m, 6H); ¹³C NMR (CDCl₃, 125 MHz) δ 166.3, 166.2, 149.4, 149.0, 147.3, 133.5, 133.4, 133.2, 132.9, 132.8, 132.7, 131.7, 131.4, 124.3, 123.7, 123.1, 122.2, 121.2, 81.2, 80.1, 79.7, 79.6, 73.0, 72.9, 72.8, 71.4, 71.0, 70.6, 67.5, 67.1, 57.3, 57.2, 35.5, 36.5, 35.1, 34.7, 34.3, 32.9, 32.1, 32.0, 31.0, 30.8, 30.7, 30.2, 30.0, 29.8, 29.3, 29.1, 28.6, 28.3, 27.7, 26.7, 26.2, 26.1, 26.0, 24.8, 24.7, 23.6, 21.3, 21.1, 20.7, 19.5; TLC R_f 0.39, 0.30 (1:1 CH₂Cl₂ -EtOAc).

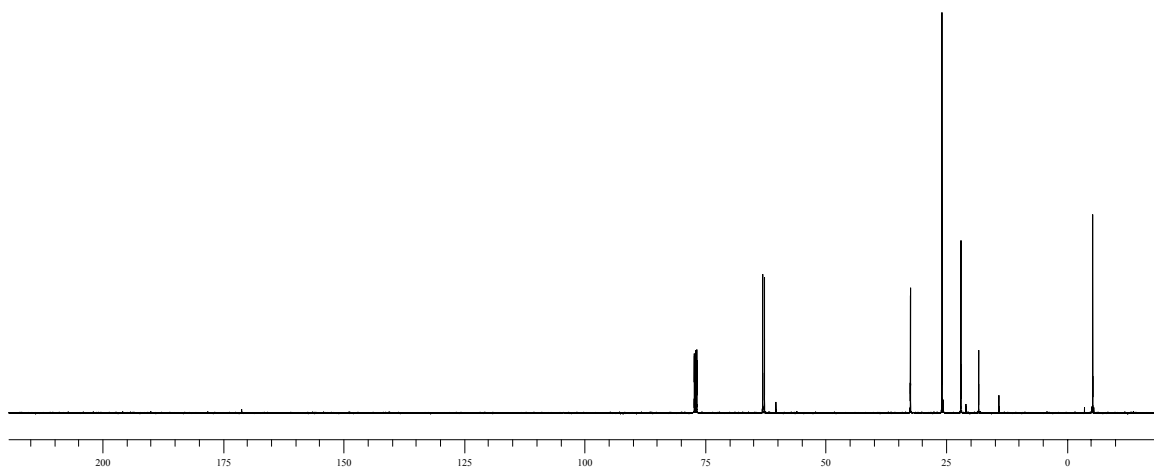
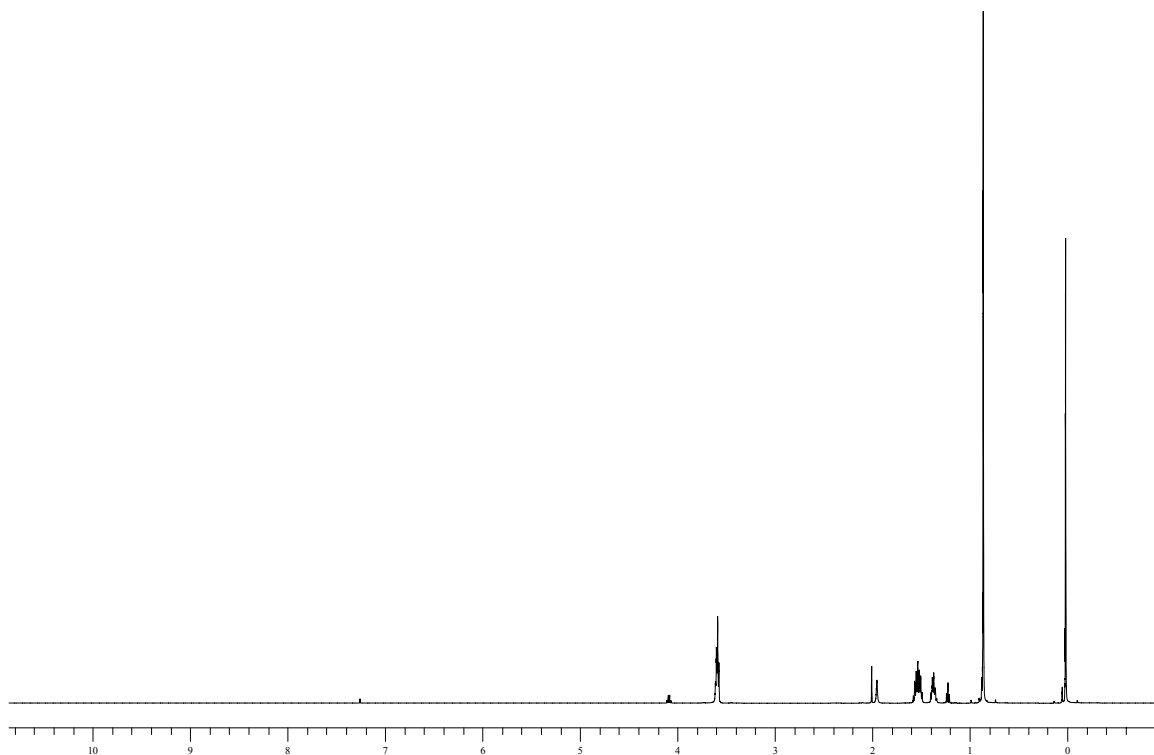
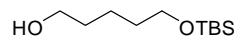


Compound 68-cis/trans. Alcohol **81b** (3 mg, 0.011 mmol) was dissolved in CH₂Cl₂ (1 mL) and Dess-Martin periodinane (5.2 mg, 0.012 mmol) was added at 0 °C. The resulting mixture was allowed to warm to room temperature and maintained for 1 h, then filtered over celite and concentrated under reduced pressure. The crude residue was

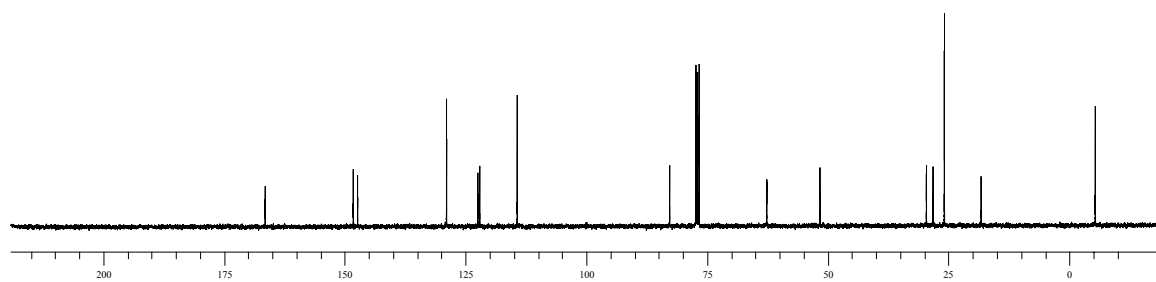
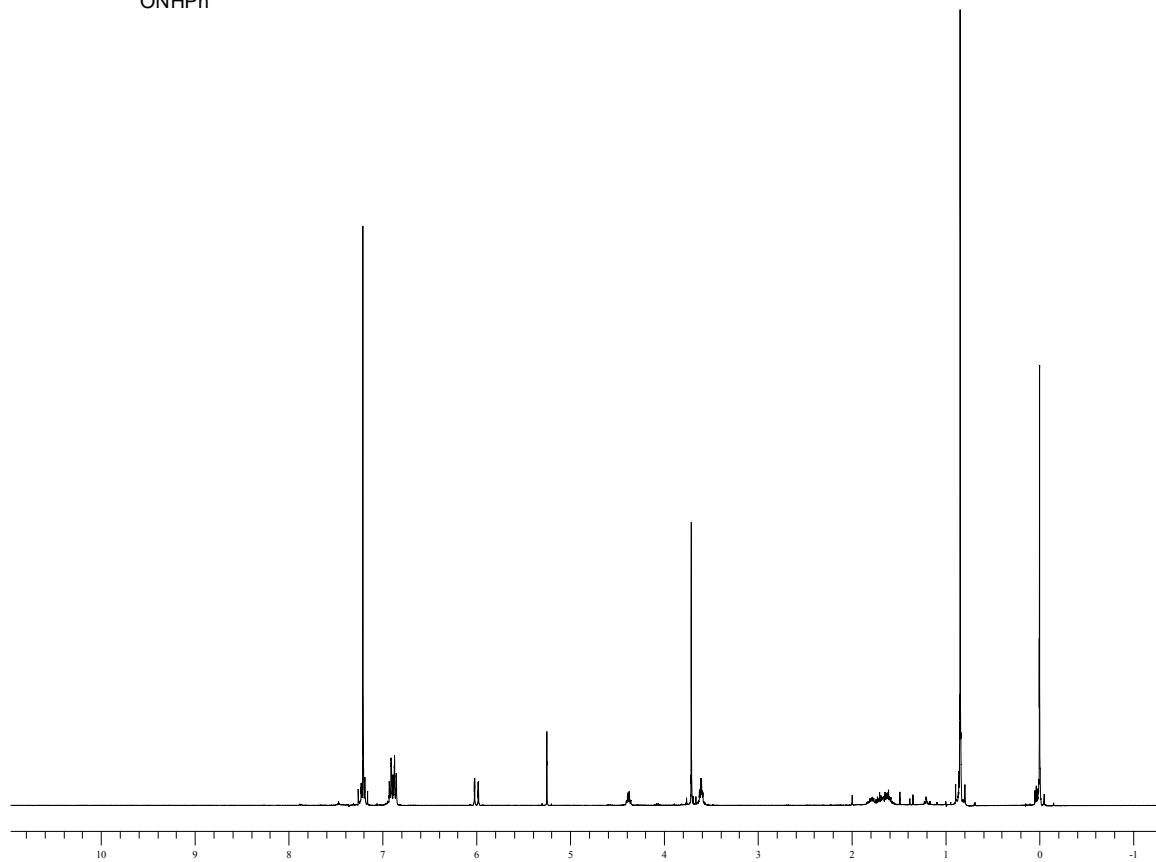
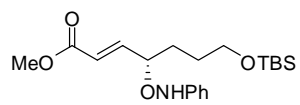
purified by silica gel chromatography (CH₂Cl₂-EtOAc, 10:1 to 1:1) to afford **68-cis/trans** as a clear oil (2 mg, 0.0075 mmol, 67%) in approximately a 1:1 *cis* to *trans* ratio. ¹H NMR (CDCl₃, 400 MHz) δ 6.77-6.44 (m, 3H), 6.16-5.87 (m, 5H), 5.11-5.01 (m, 2H), 3.91-3.72 (m, 2H), 3.35-3.29 (m, 7H), 2.96-2.88 (m, 1H), 2.64-2.03 (m, 12H), 1.82-1.46 (m, 6H), 1.27-1.19 (m, 6H); TLC R_f 0.82, 0.75 (1:1 CH₂Cl₂ -EtOAc); LRMS (ESI) *m/z* 289.11 (289.14 calcd for C₁₅H₂₂O₄NaSi [M+Na]⁺). Recovered **68-trans**. ¹H NMR (CDCl₃, 400 MHz) δ 6.70-6.63 (m, 1H), 6.47-6.41 (m, 1H), 6.02 (d, *J* = 15.7 Hz, 1H), 5.84 (d, *J* = 15.8 Hz, 1H), 5.02-4.92 (m, 1H), 3.79-3.68 (m, 1H), 3.27-3.20 (m, 4H), 2.44-2.07 (m, 6H), 1.68-1.50 (m, 3H), 1.17-1.14 (m, 3H); TLC R_f 0.75 (1:1 CH₂Cl₂ -EtOAc).

4.8.1 NMR Spectra

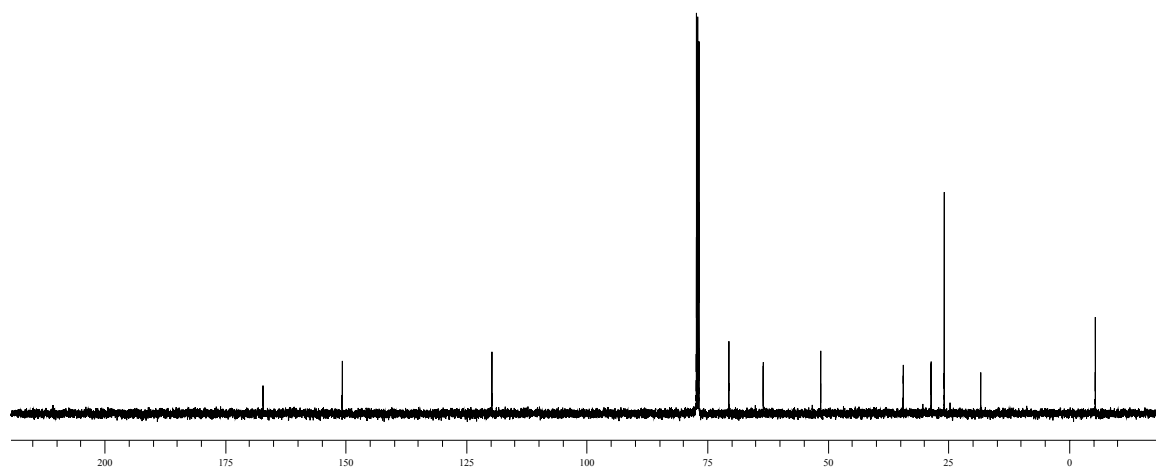
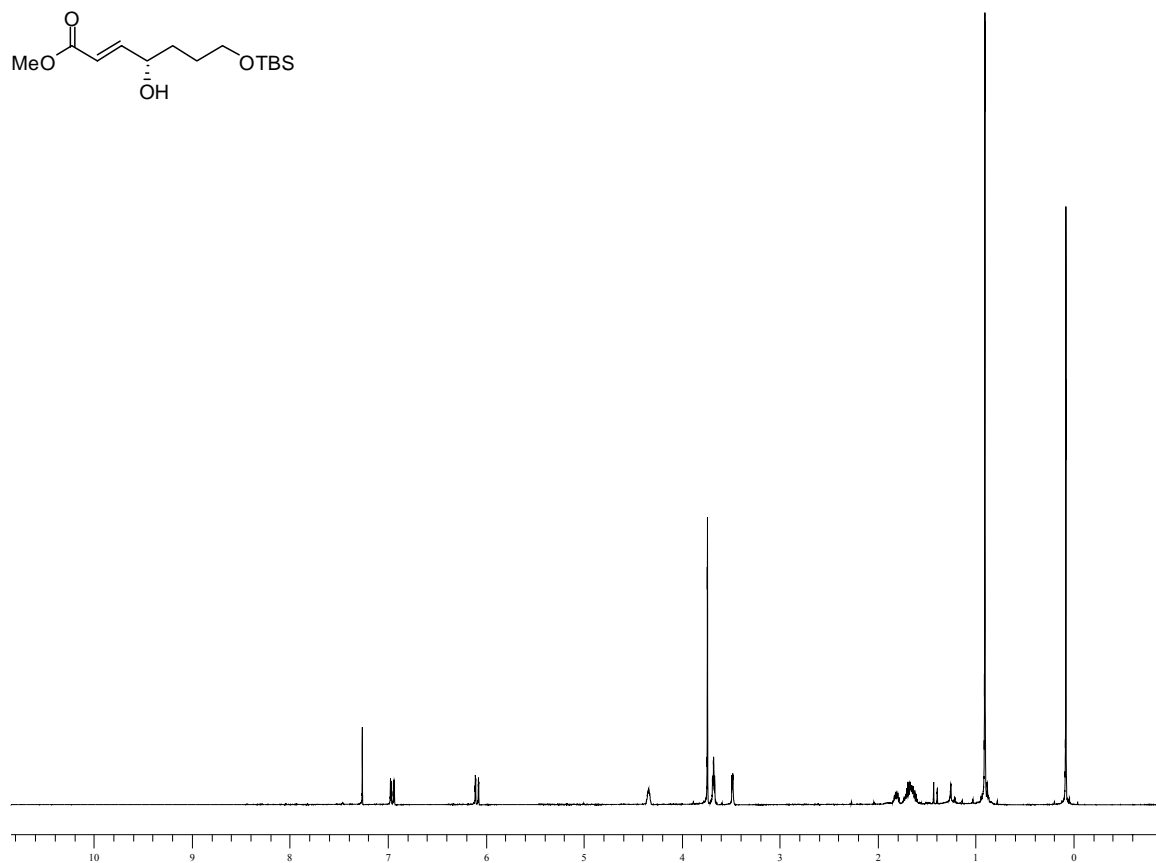
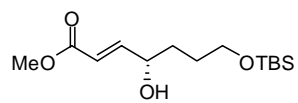
Compound 19.



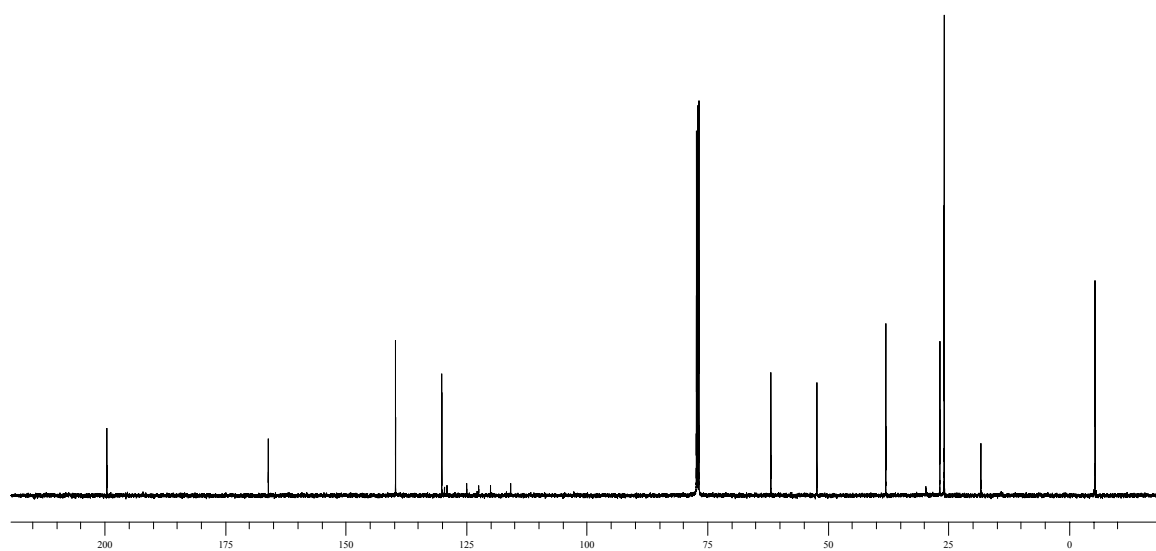
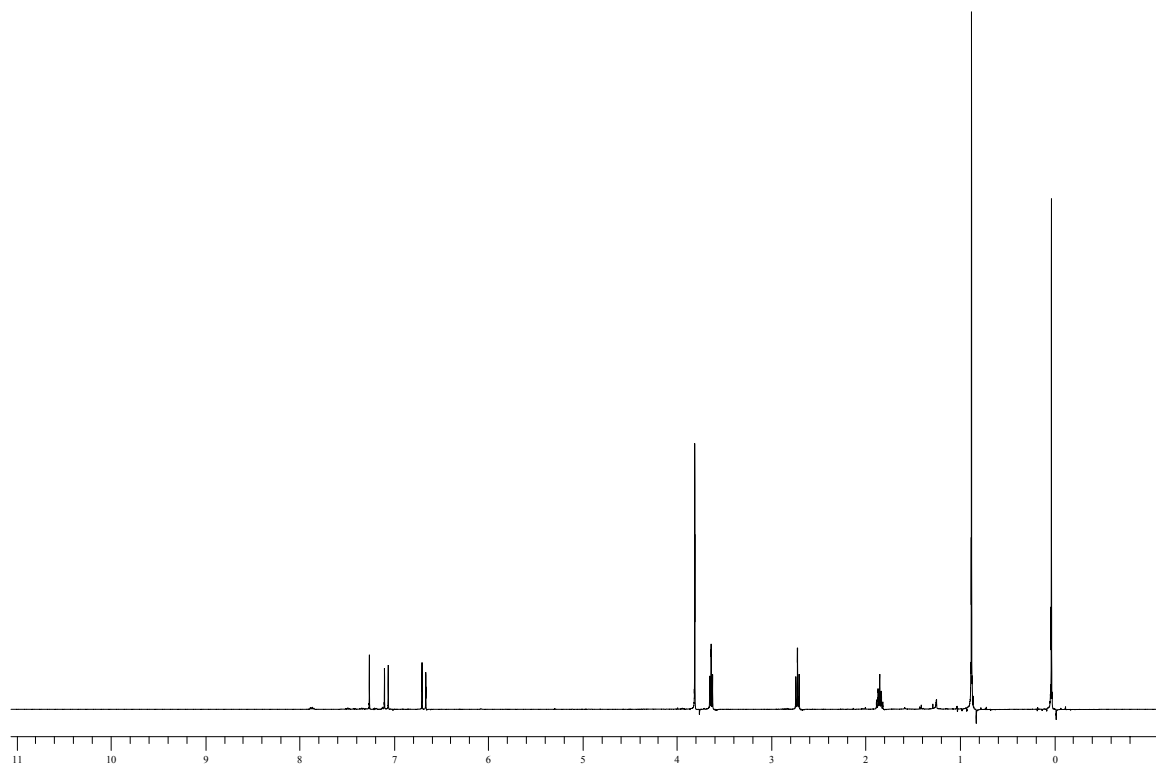
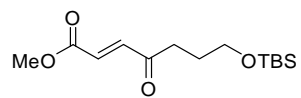
Compound 22.



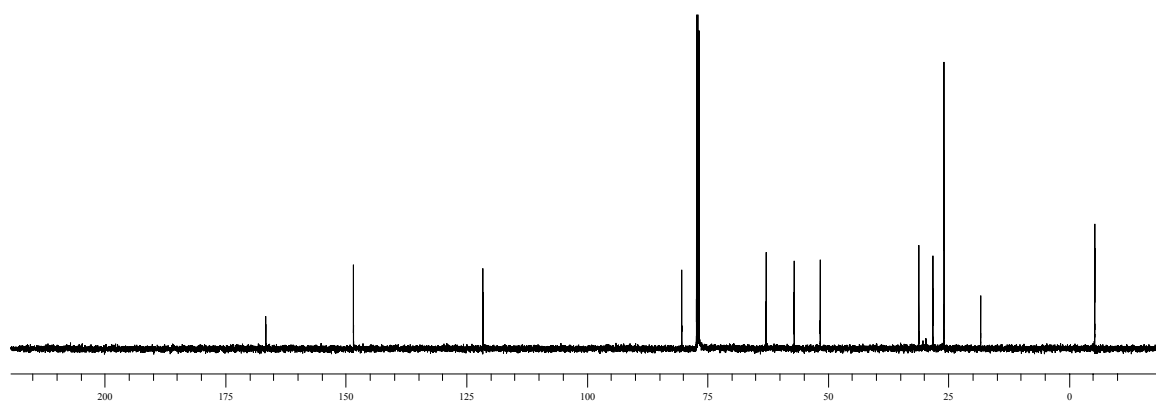
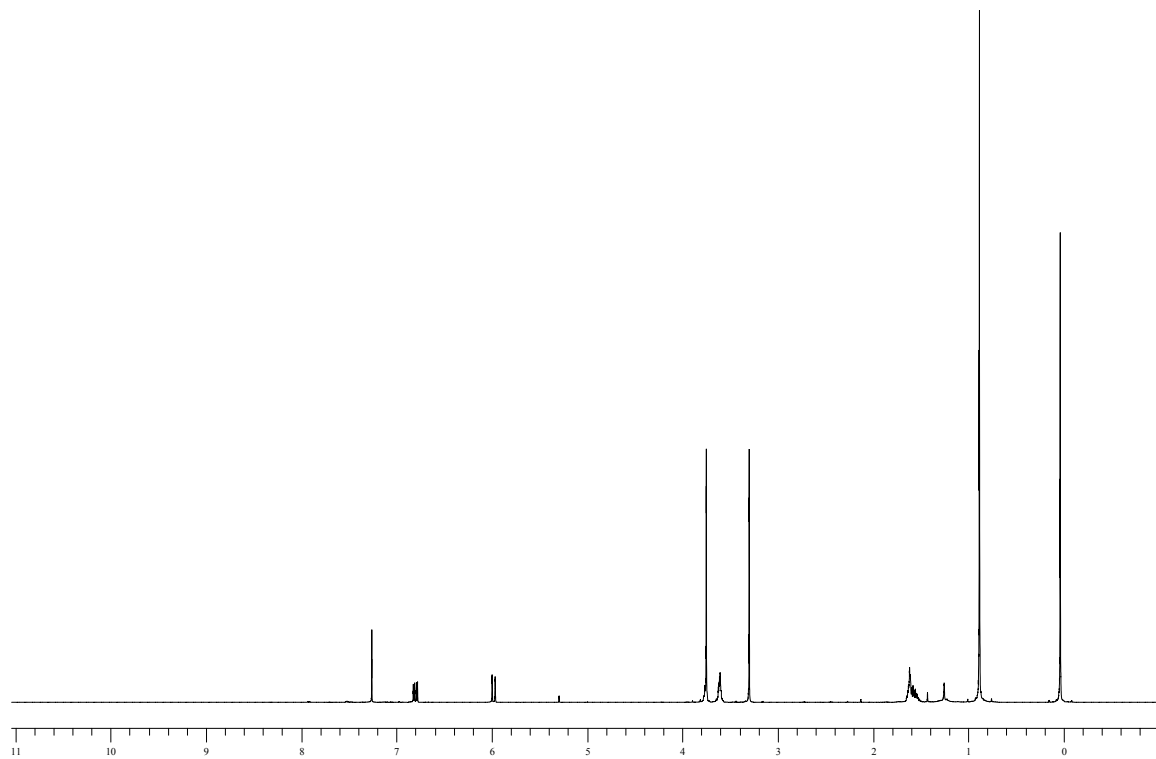
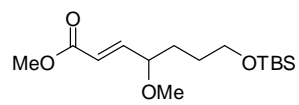
Compound 20.



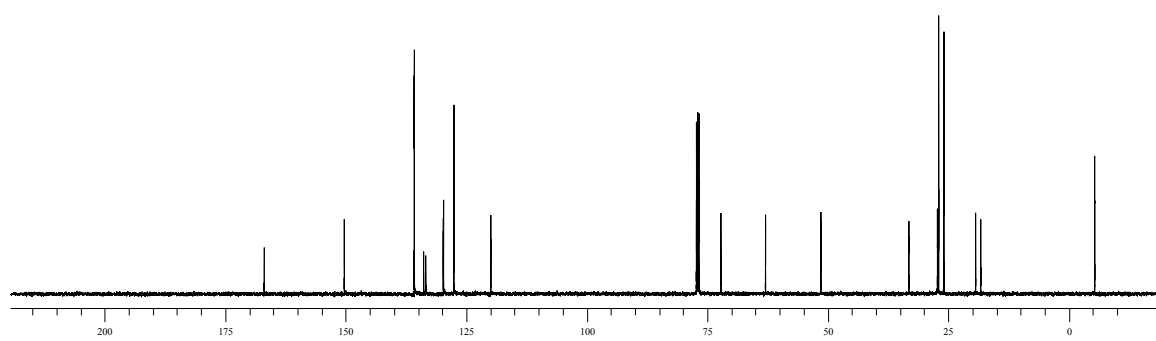
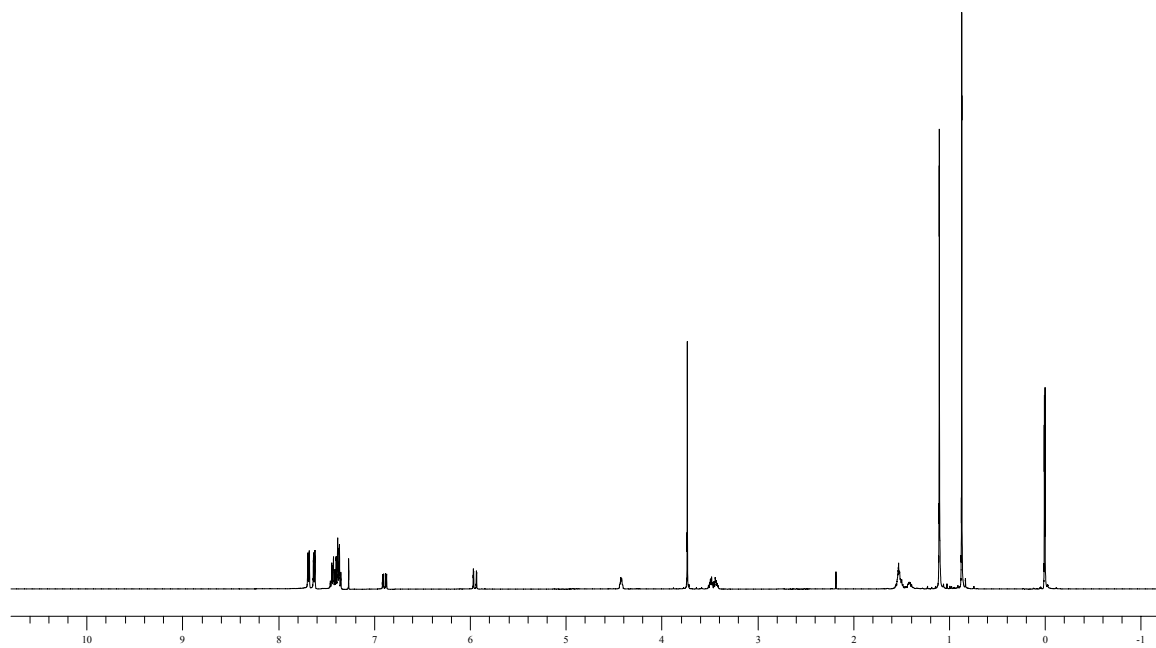
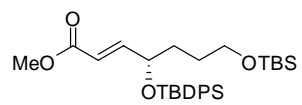
Compound 23.



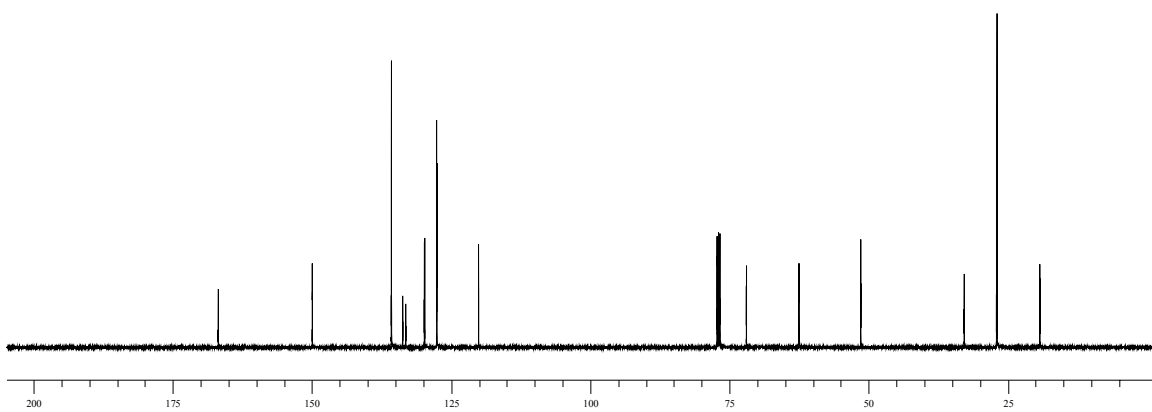
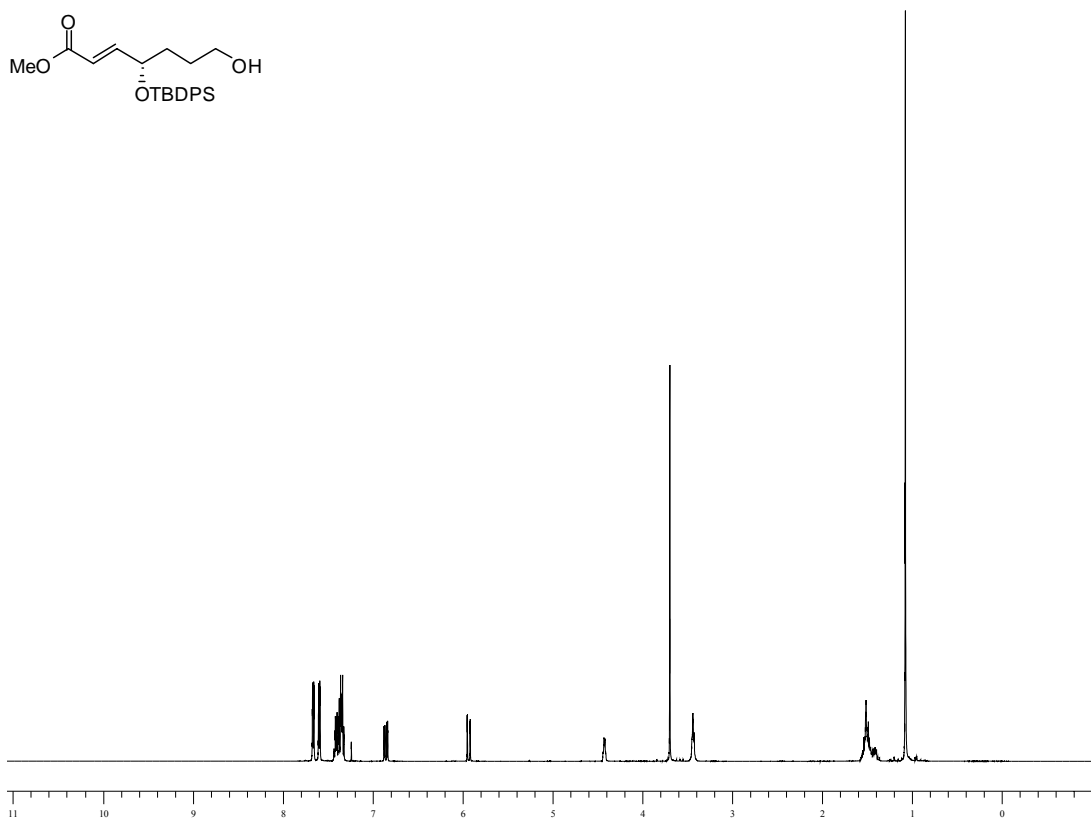
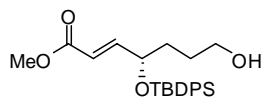
Compound 24.



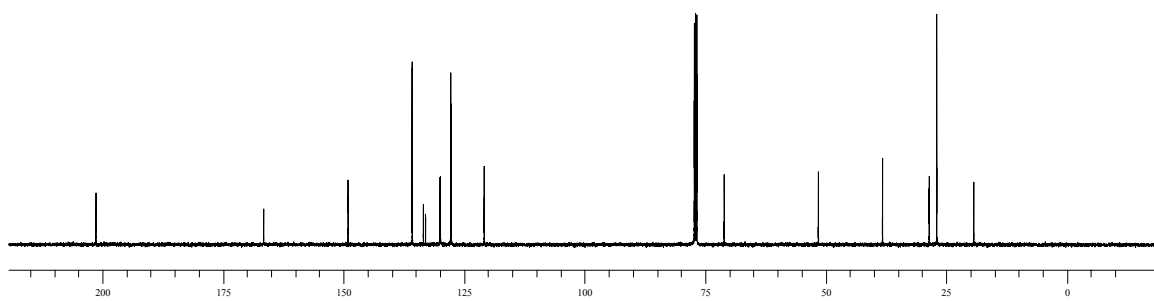
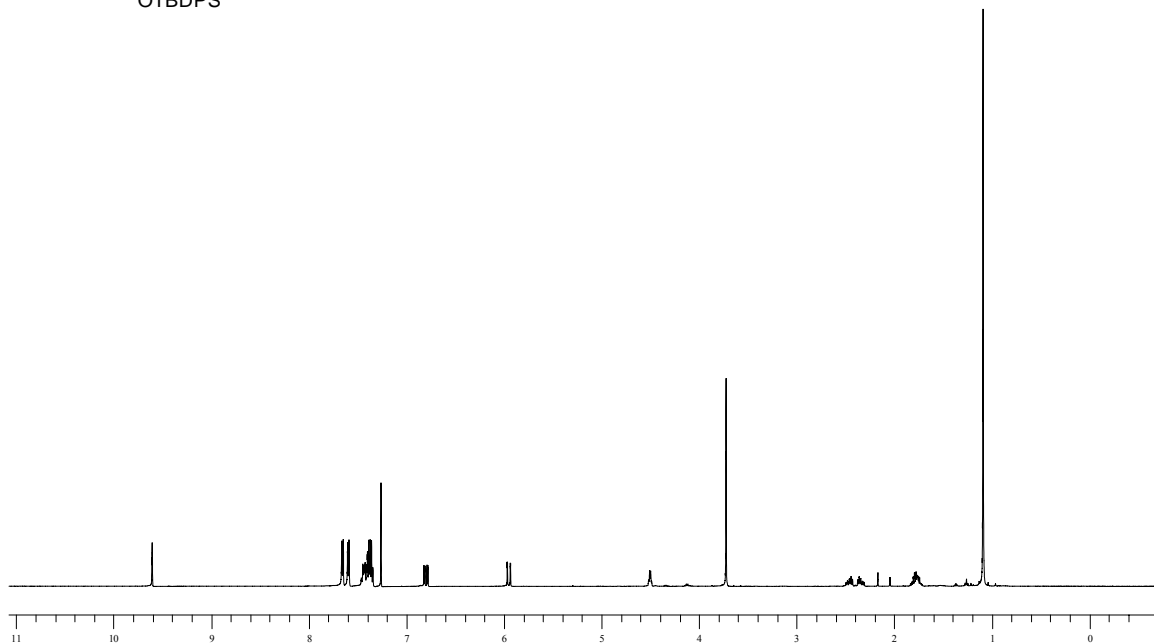
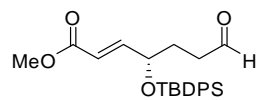
Compound 20b.



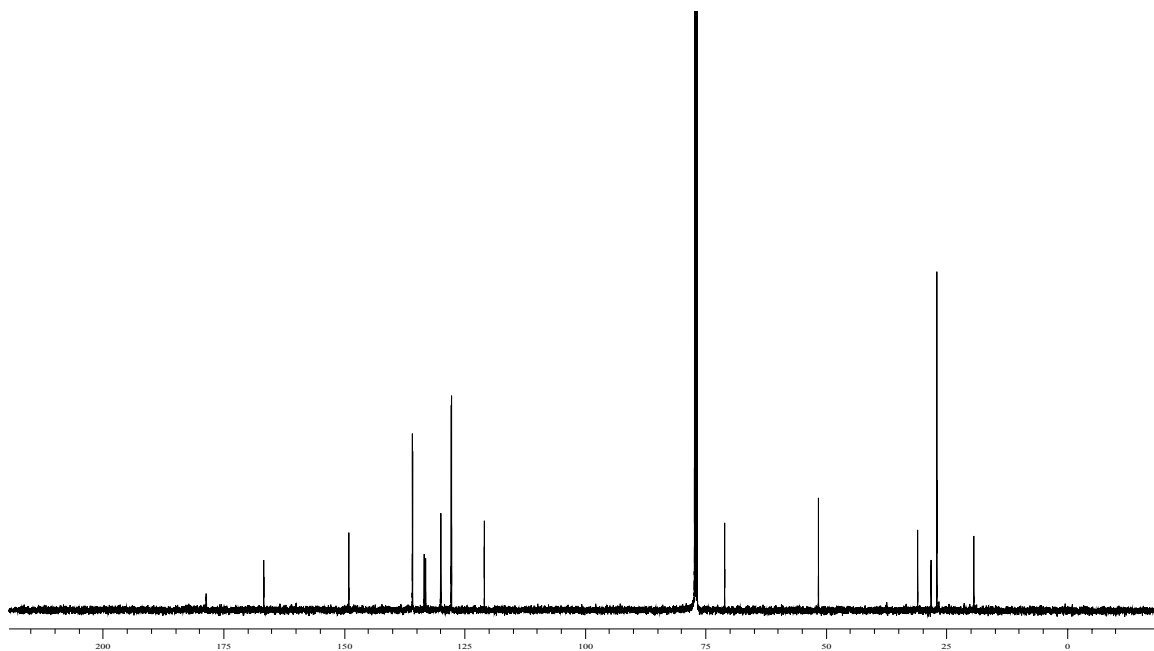
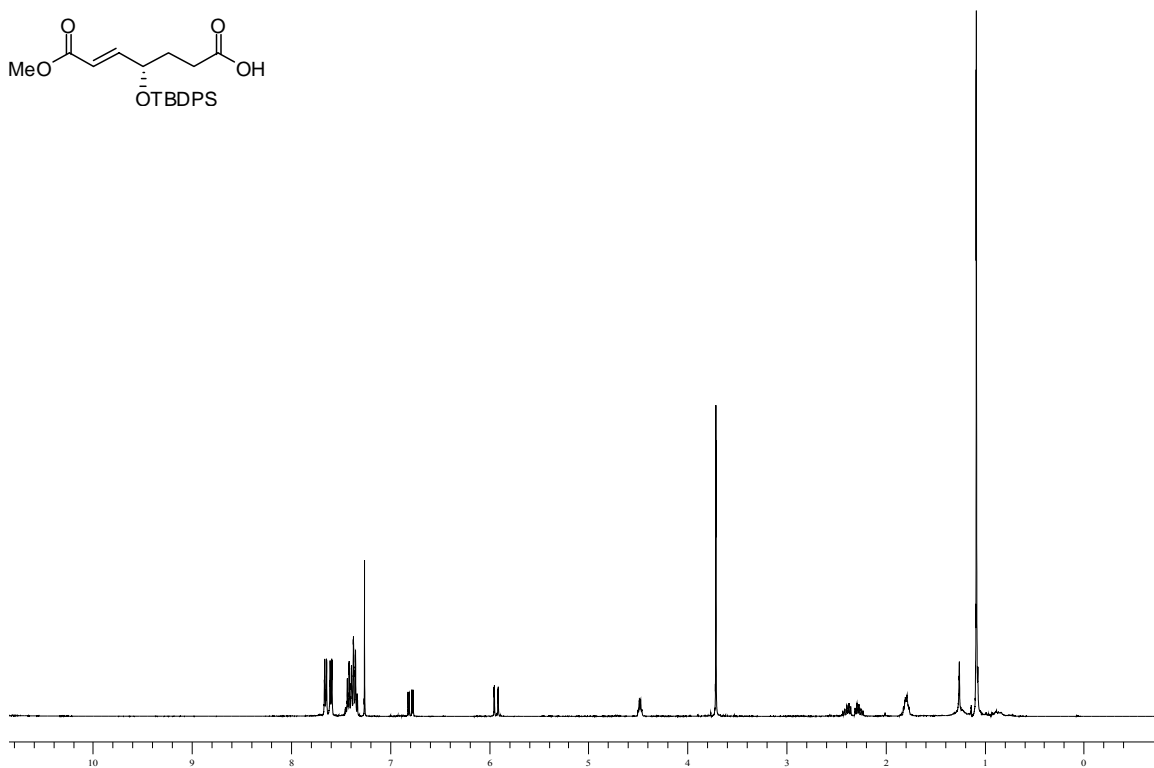
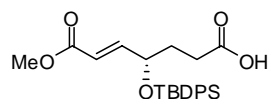
Compound 27.



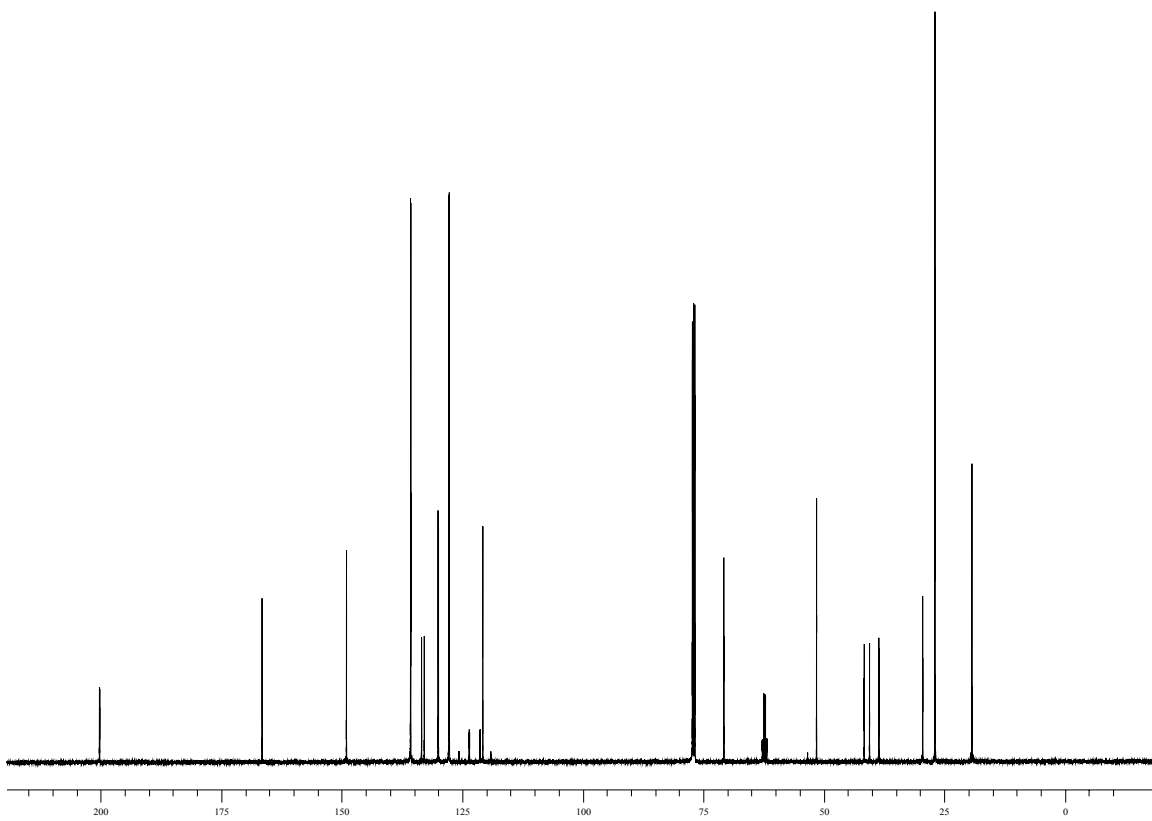
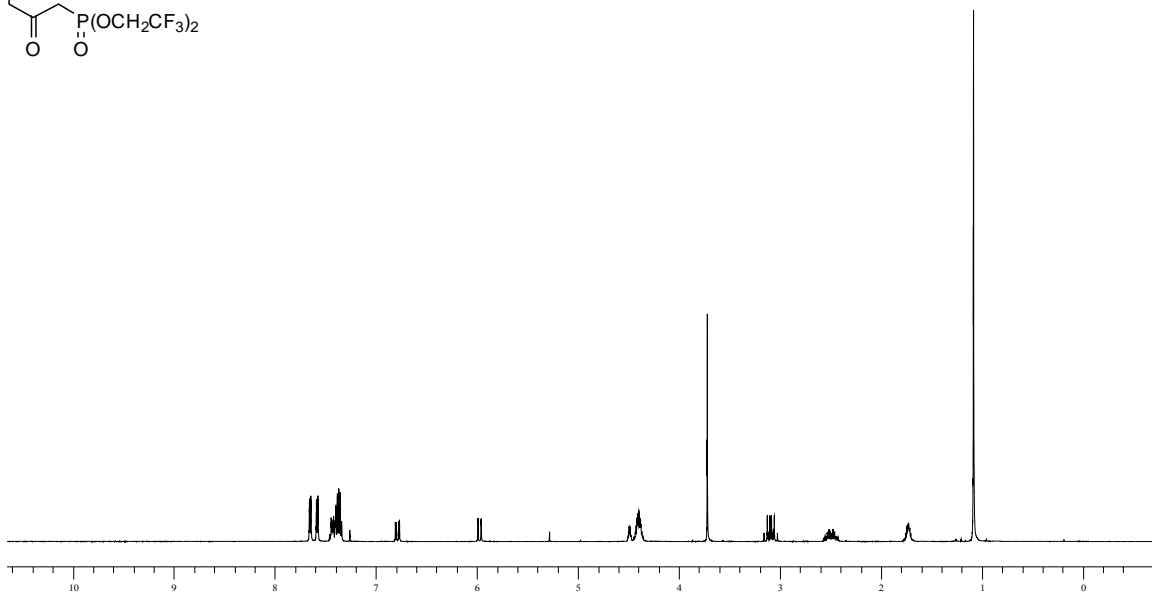
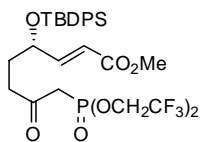
Compound 27b.



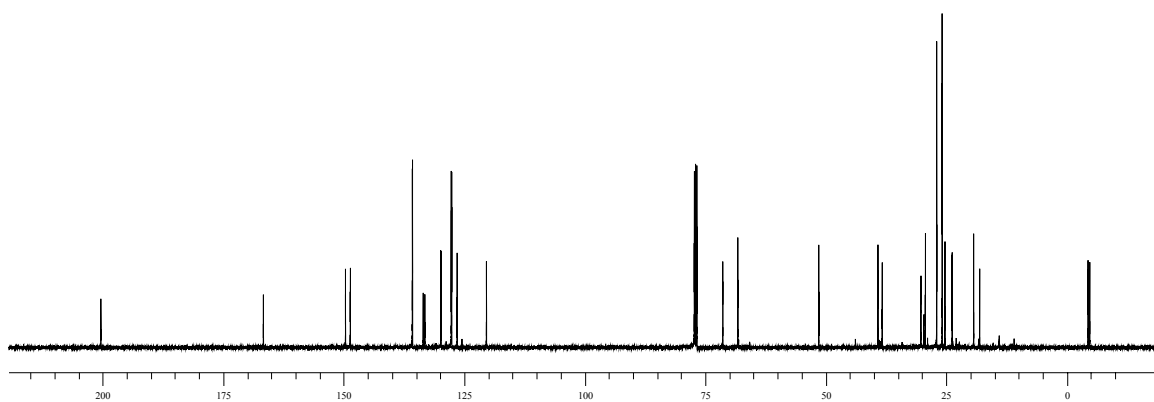
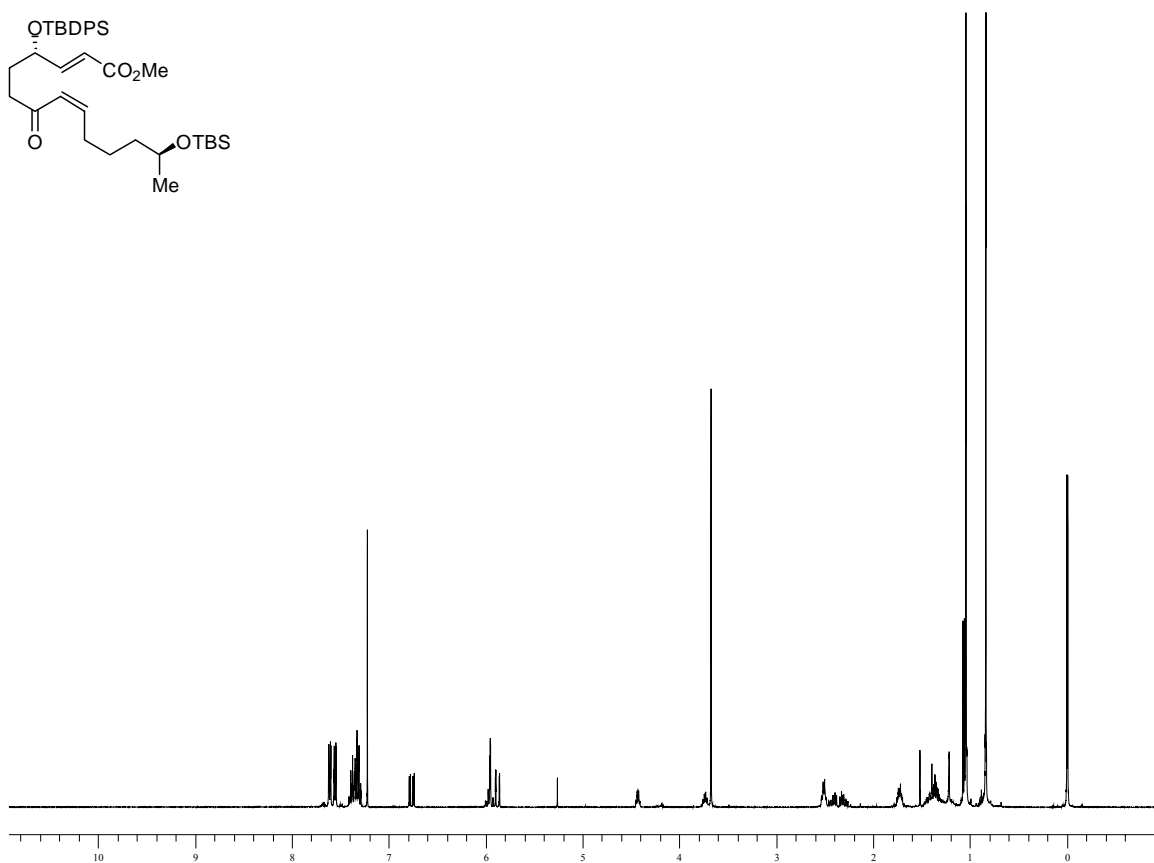
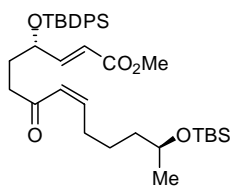
Compound 26.



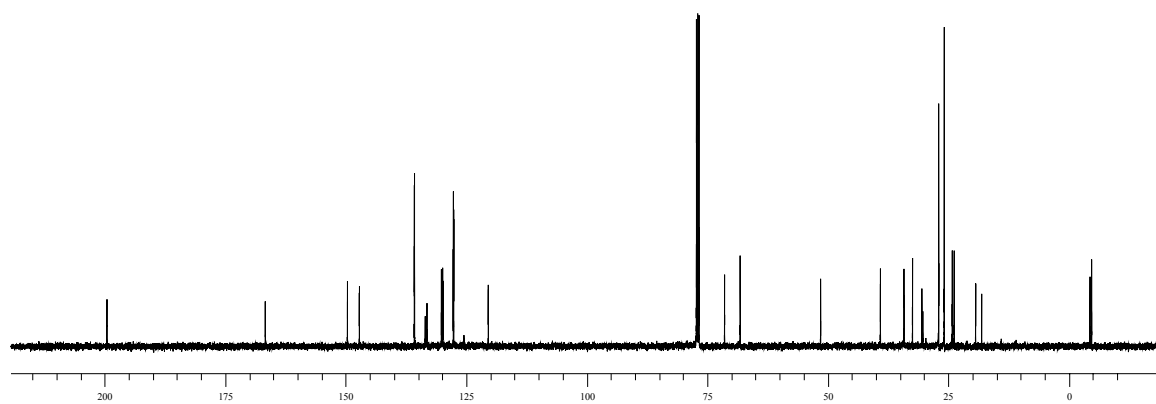
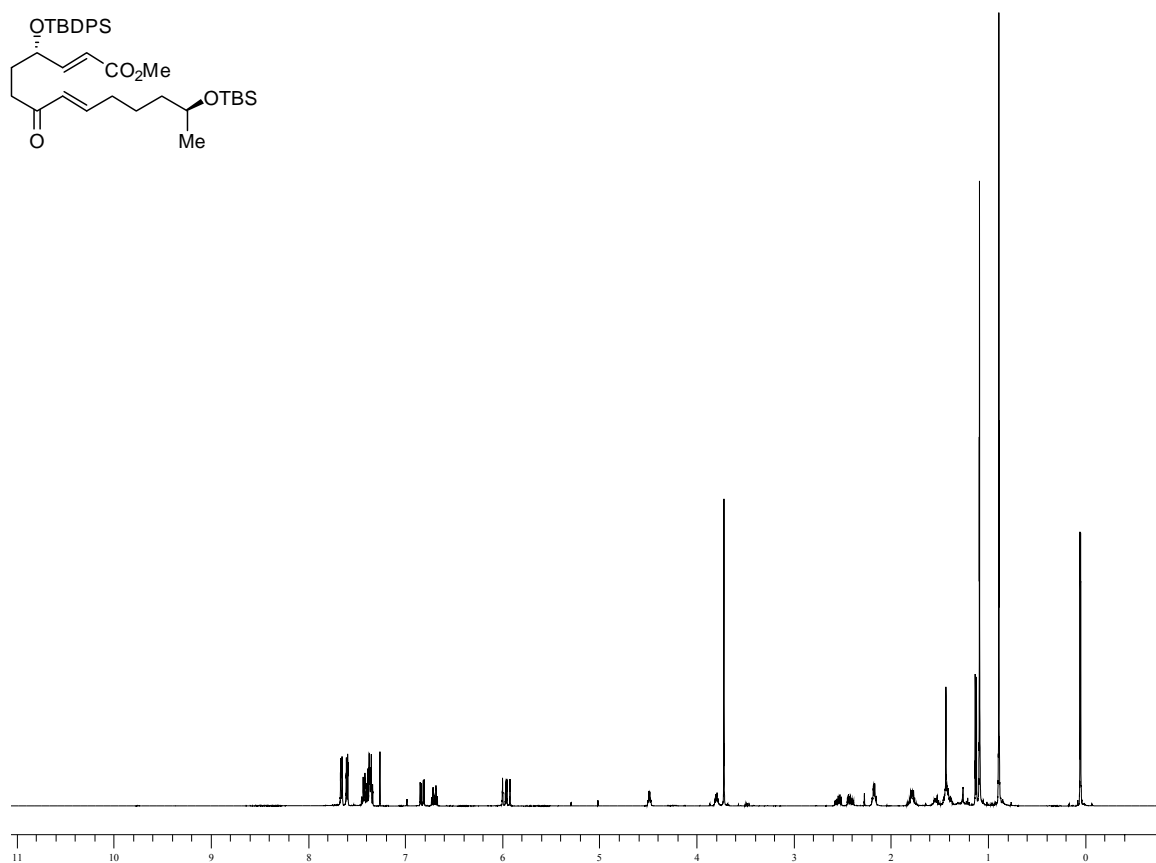
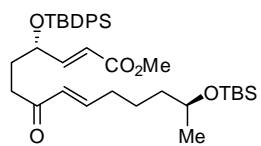
Compound 15.



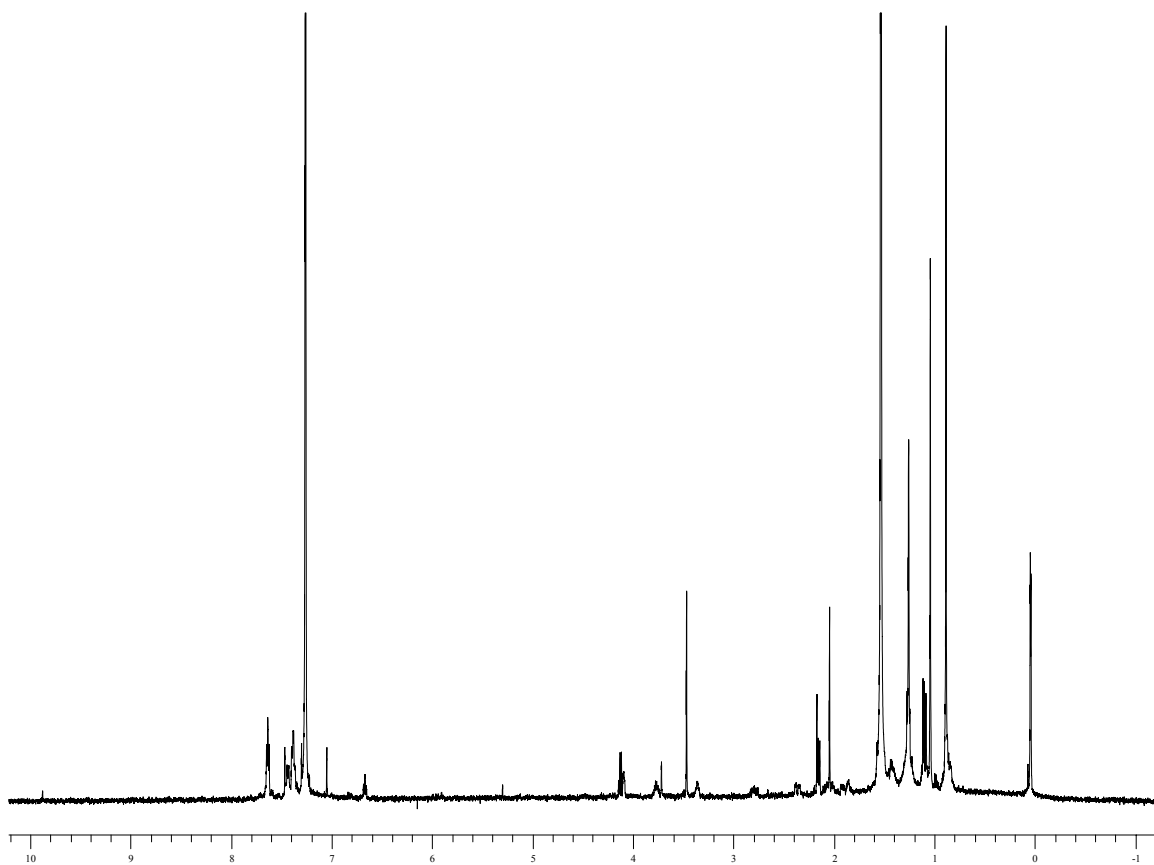
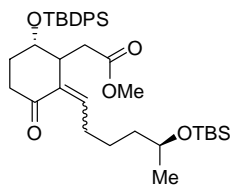
Compound 11-cis.



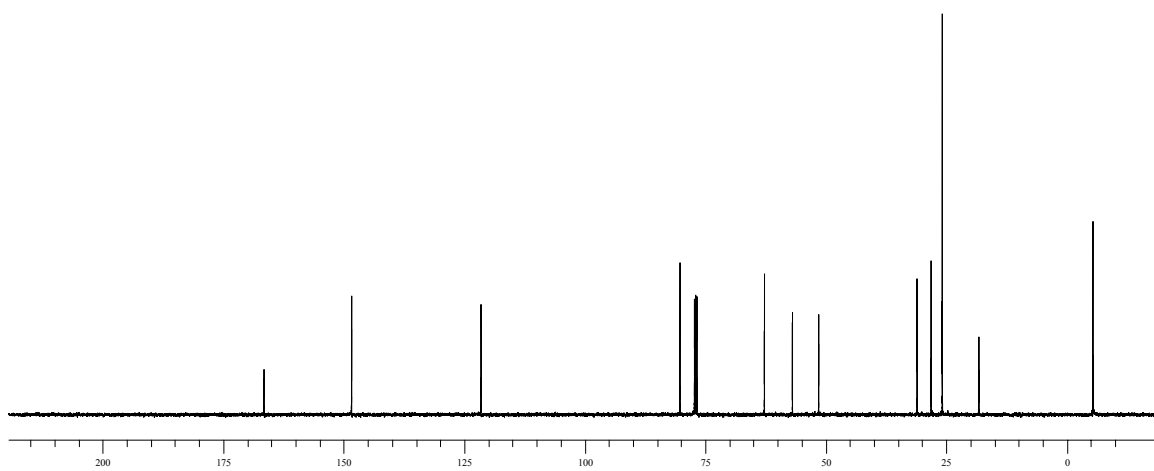
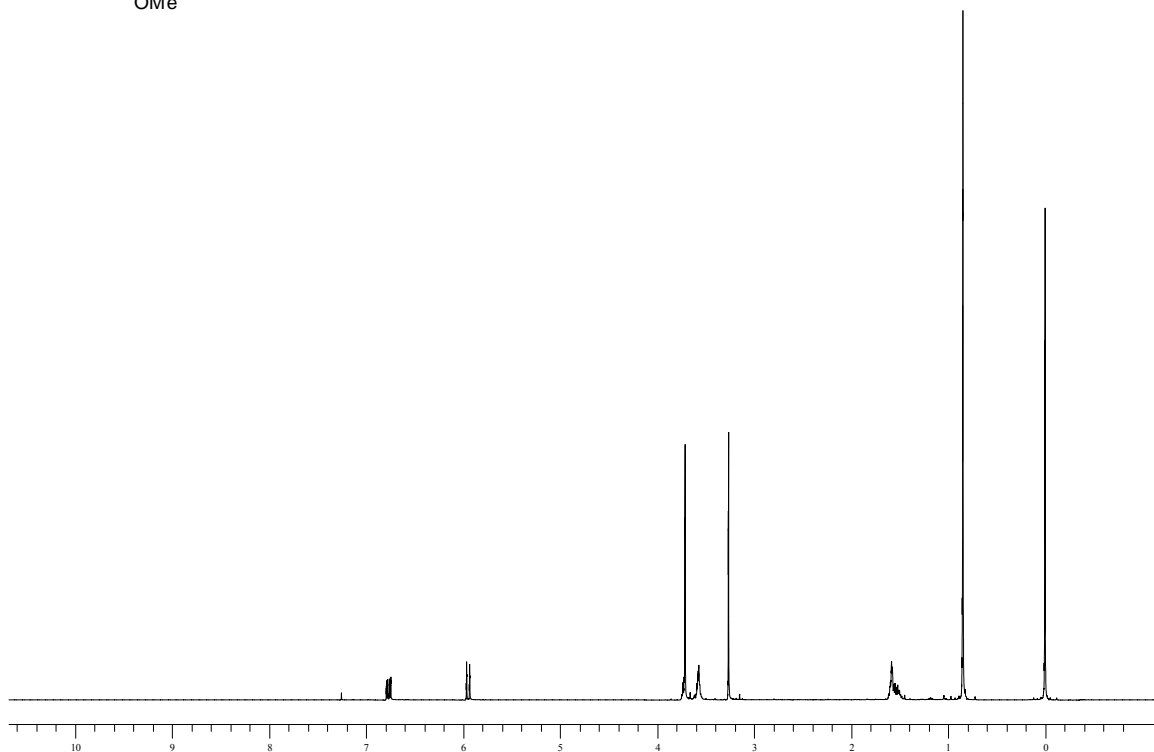
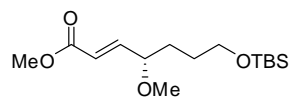
Compound 11-*trans*.



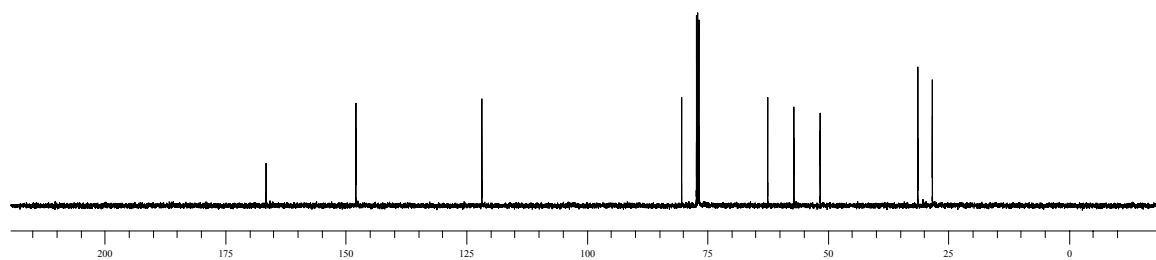
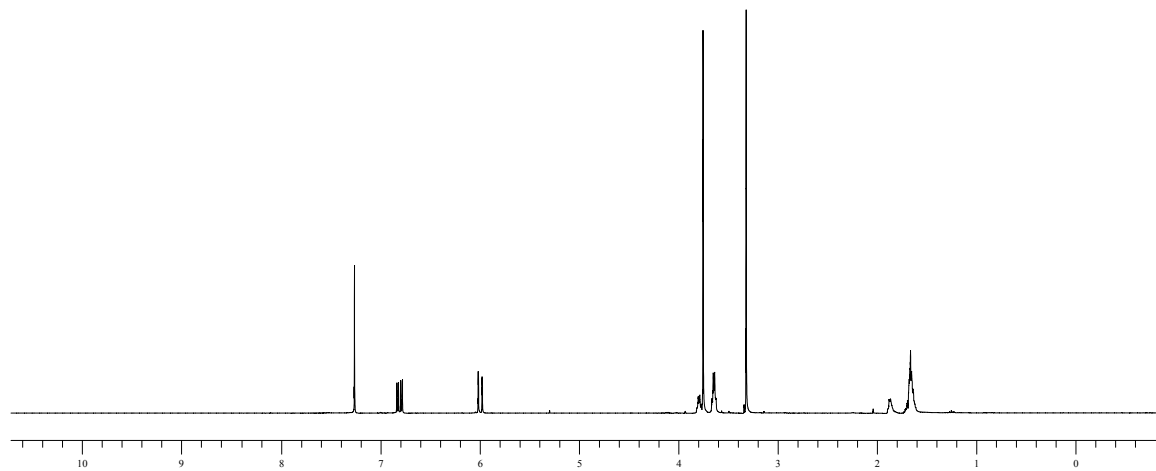
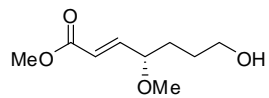
Compound 12.



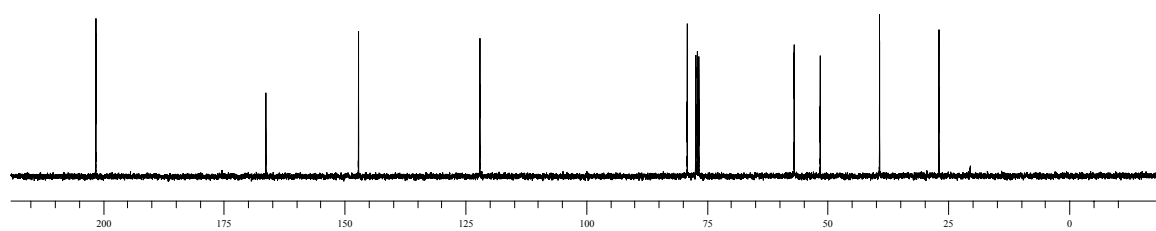
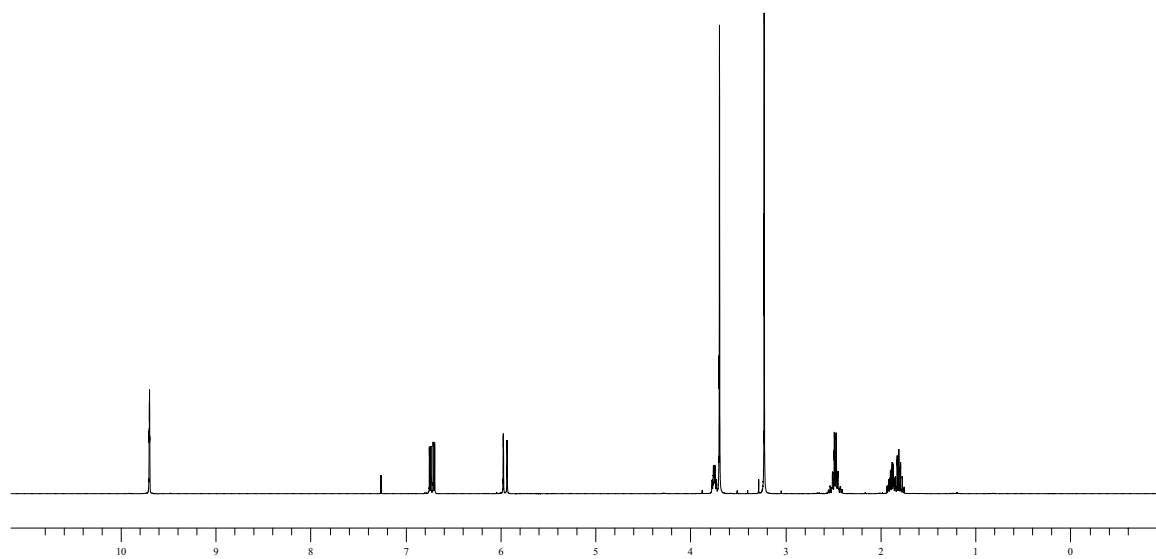
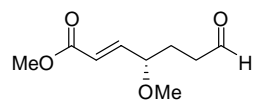
Compound 20c.



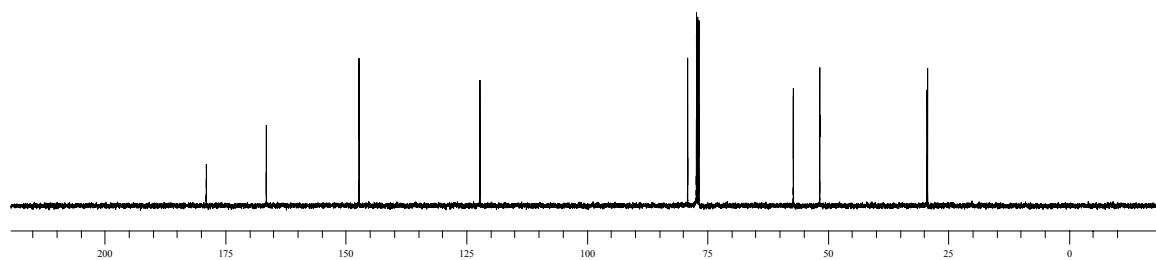
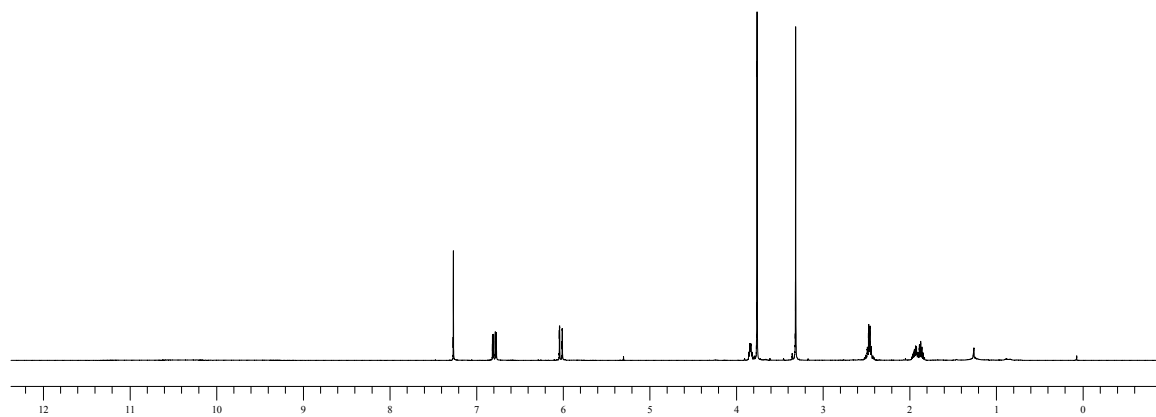
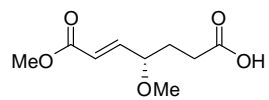
Compound 43.



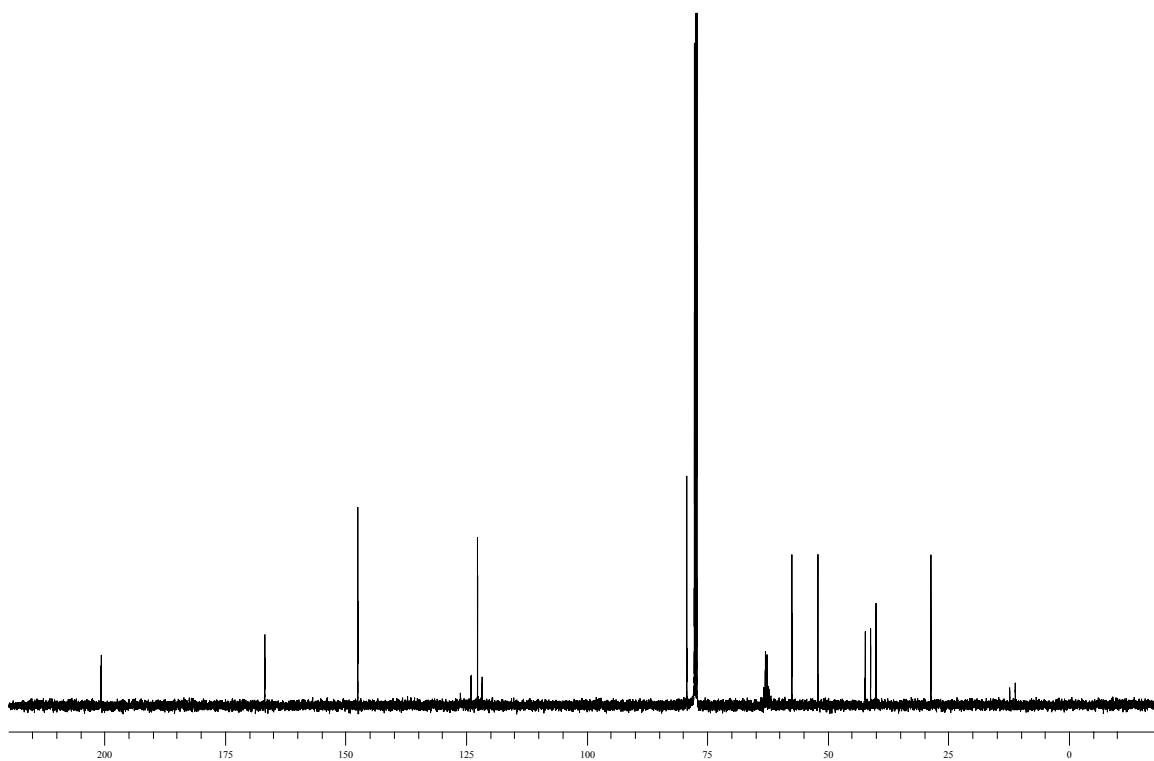
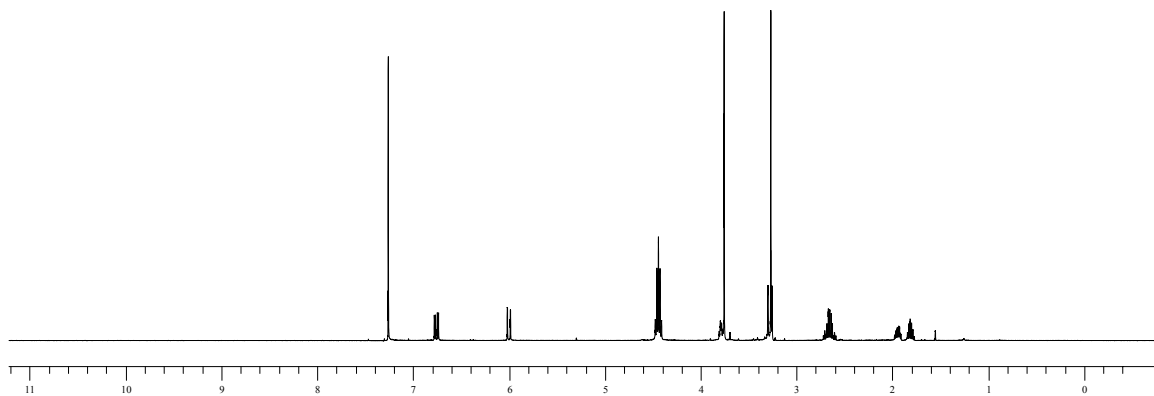
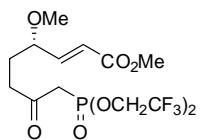
Compound 43b.



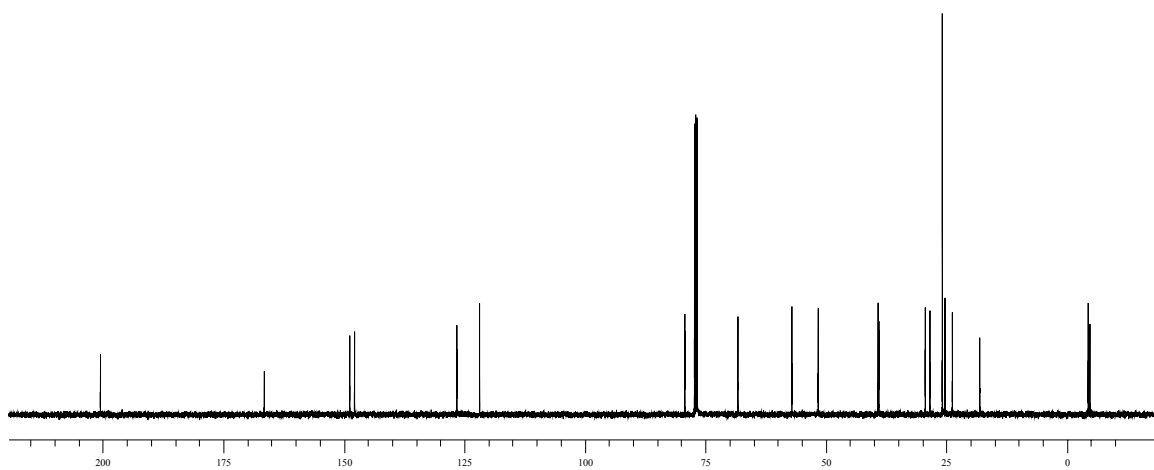
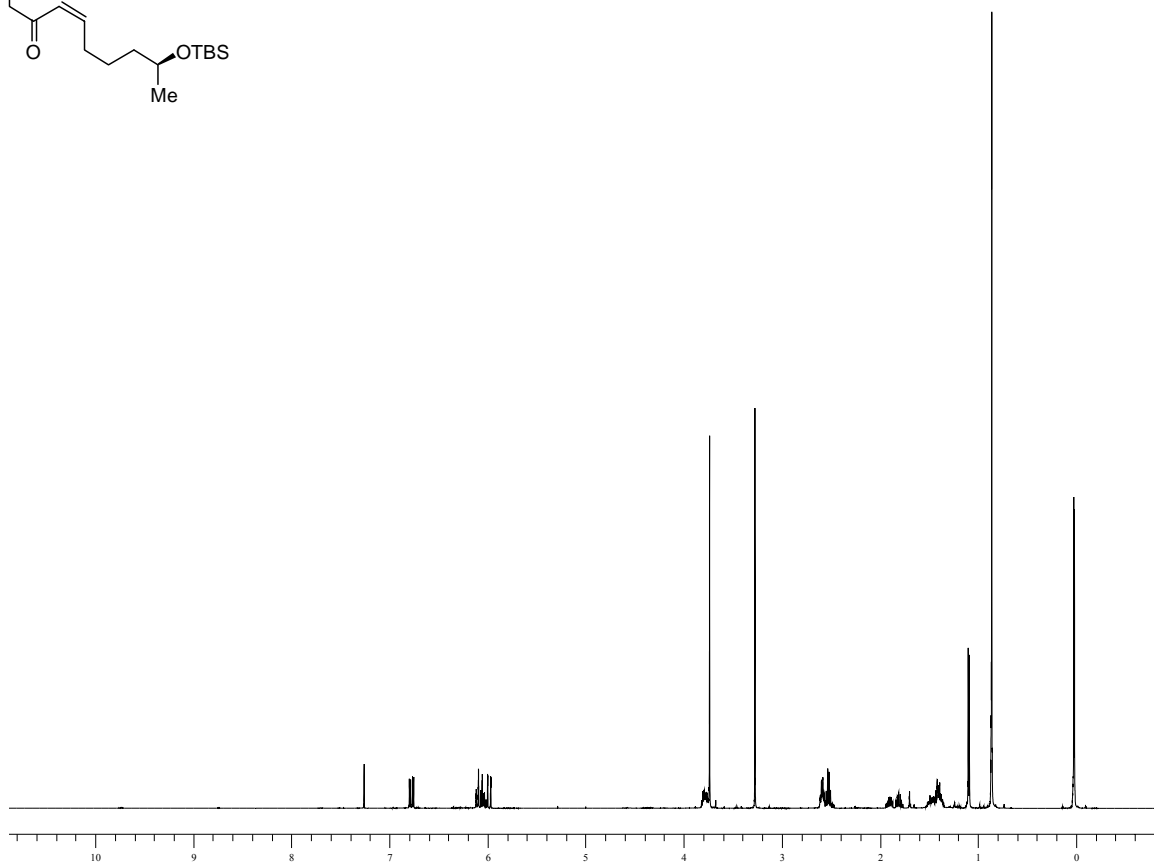
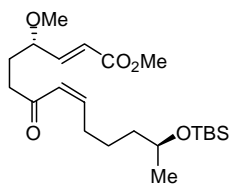
Compound 44.



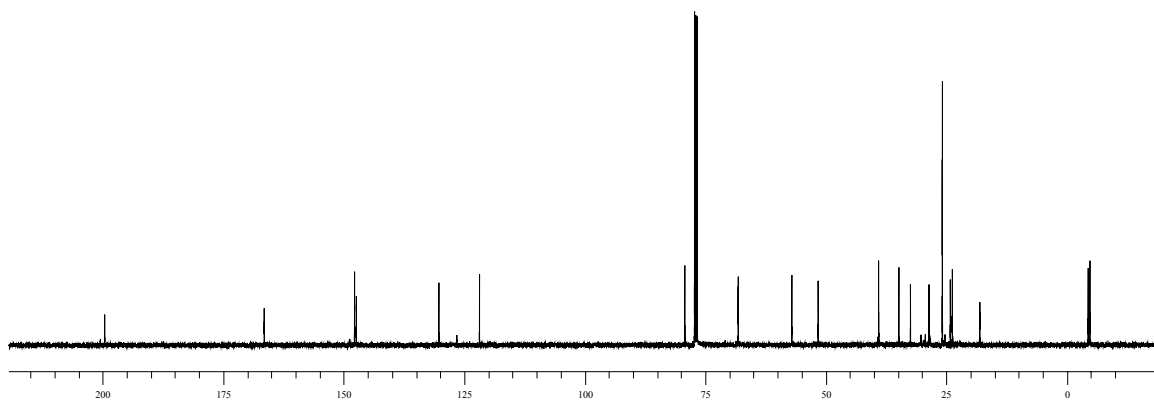
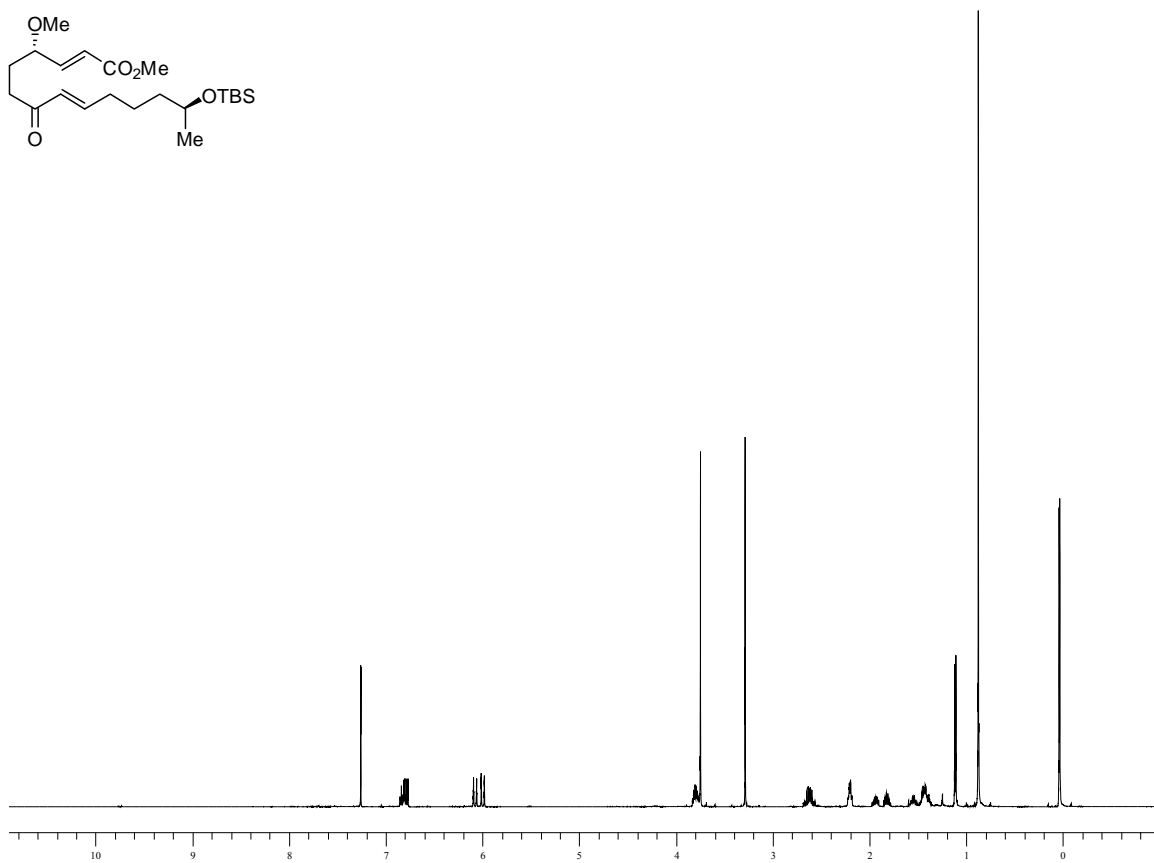
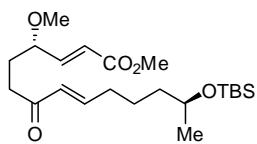
Compound 45.



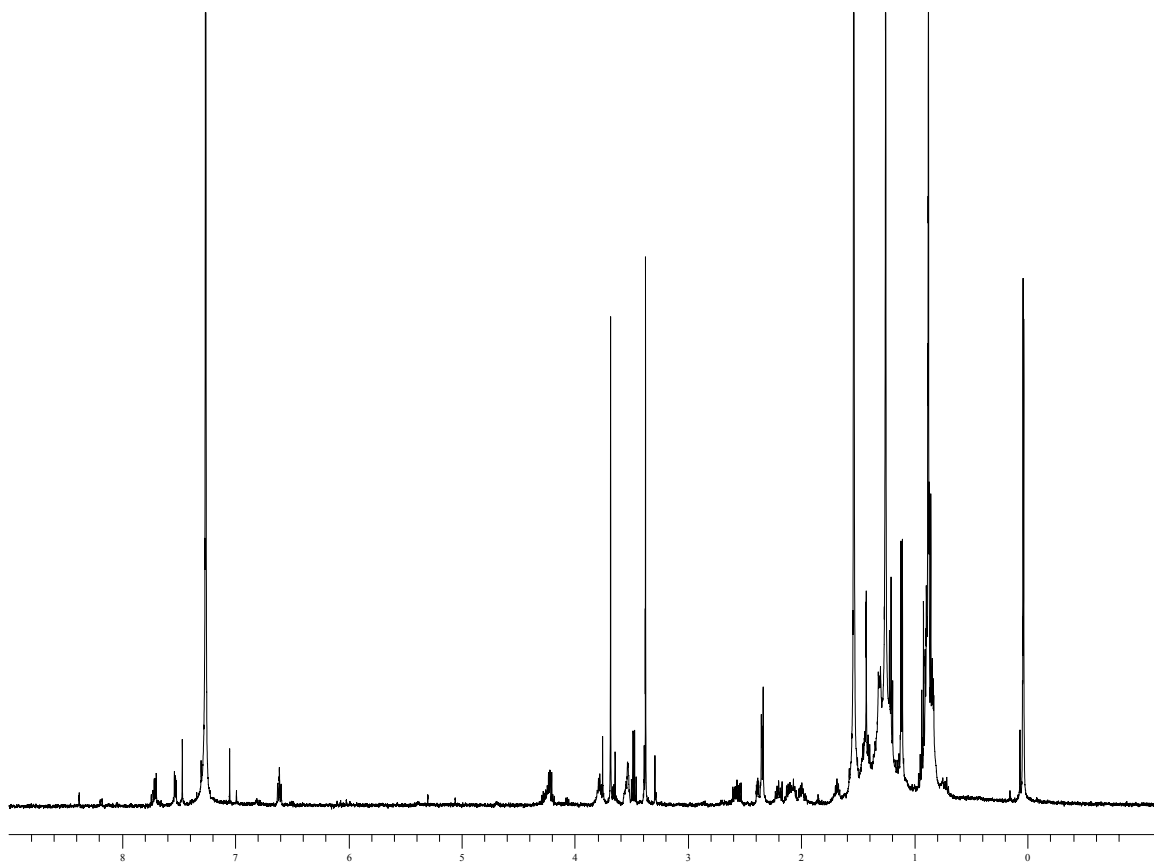
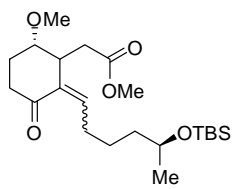
Compound 11-OMe *cis*.



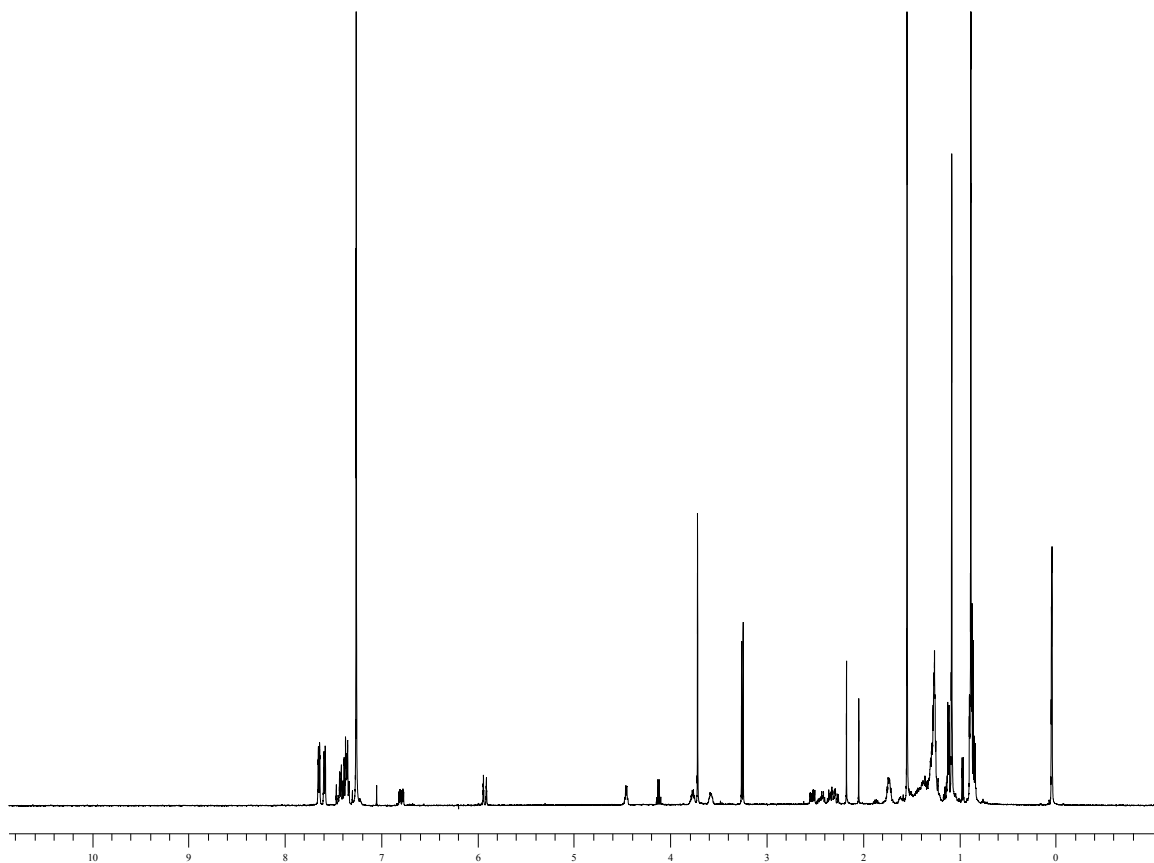
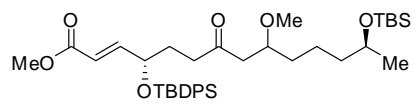
Compound 11-OMe *trans*.



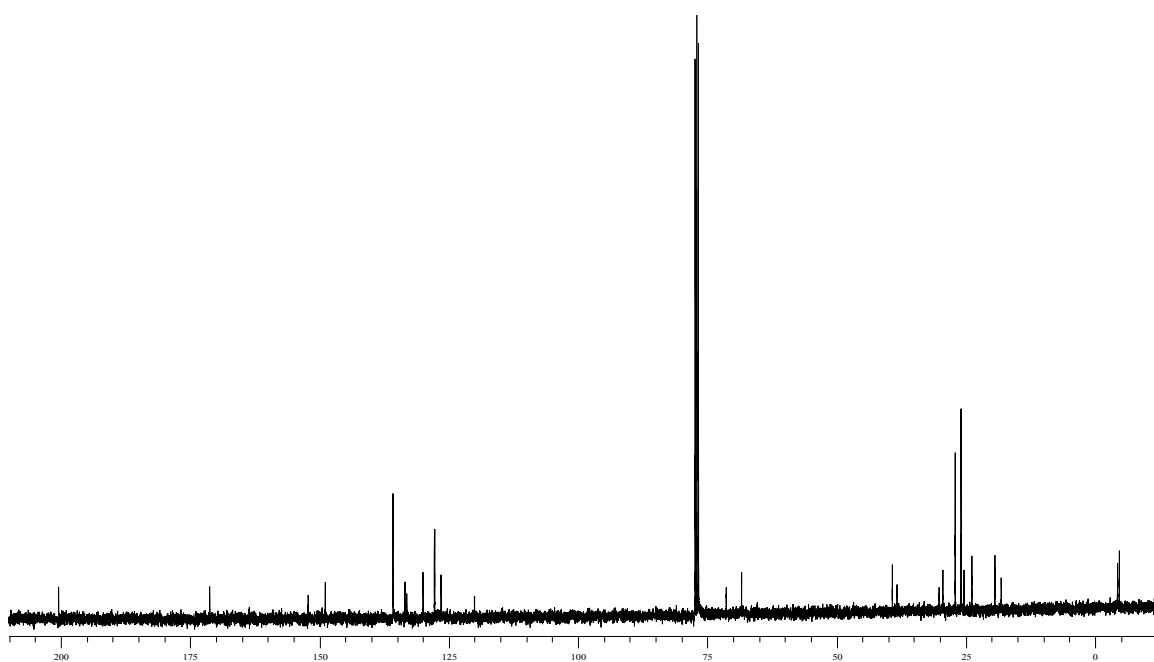
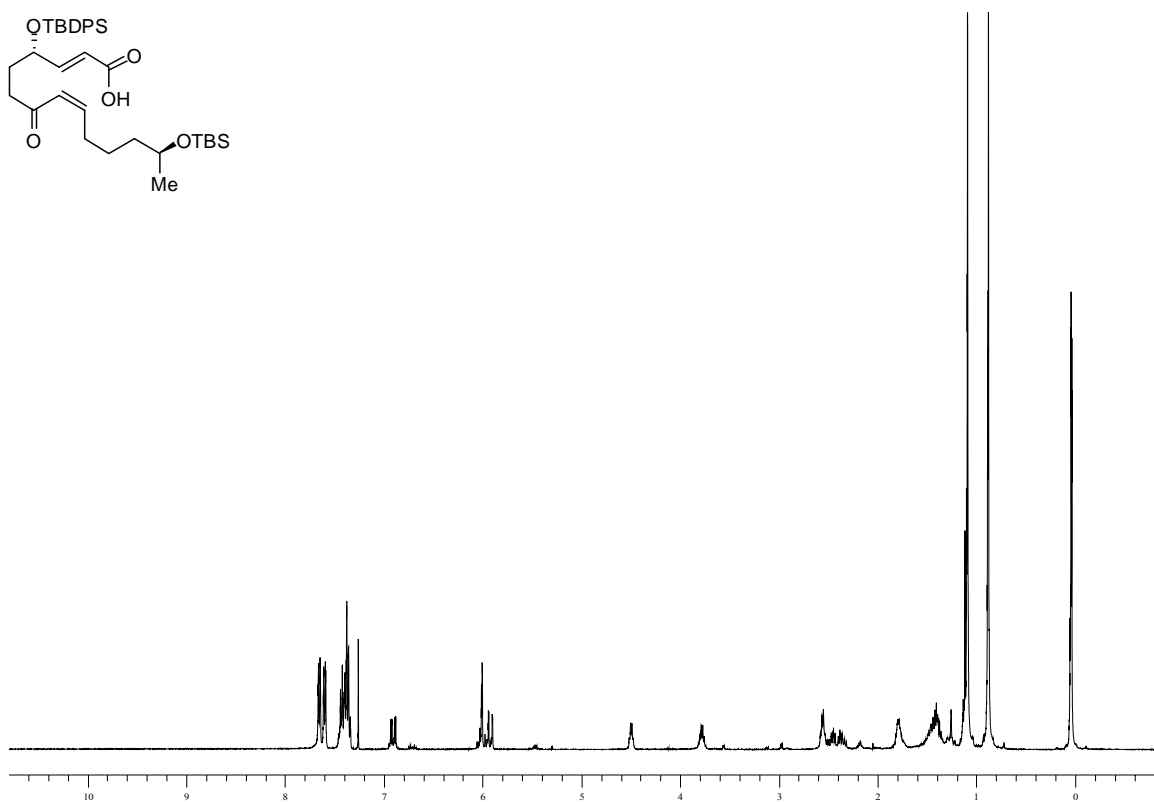
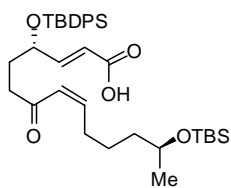
Compound 46.



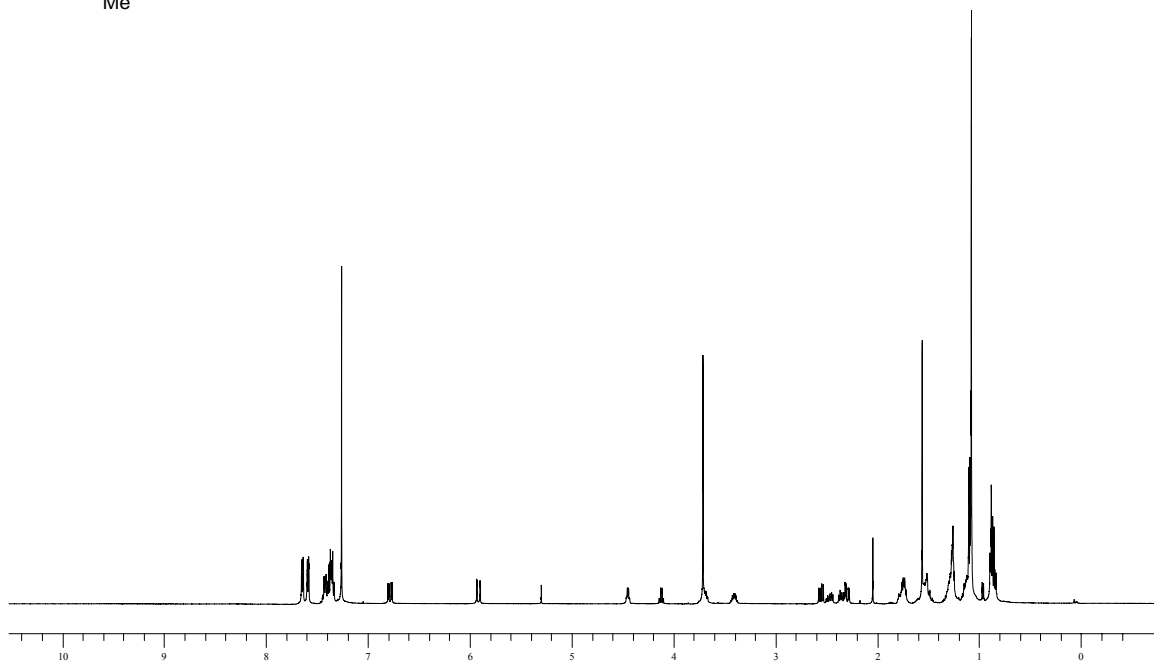
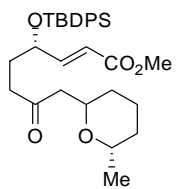
Compound 55.



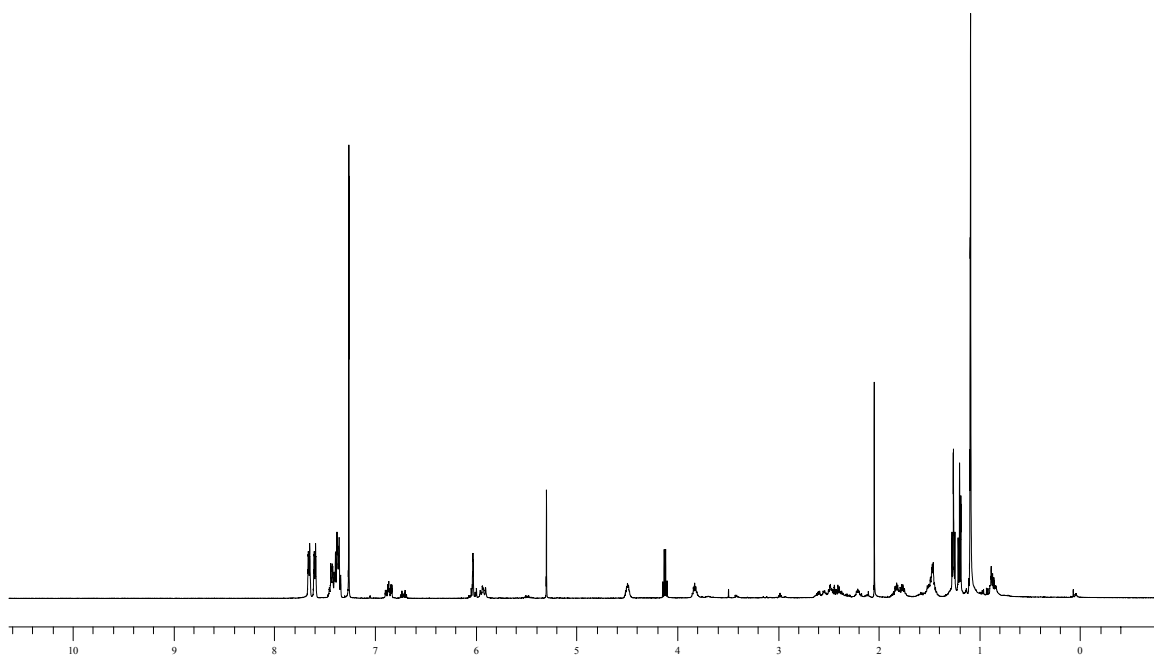
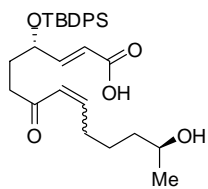
Compound 52-*cis*.



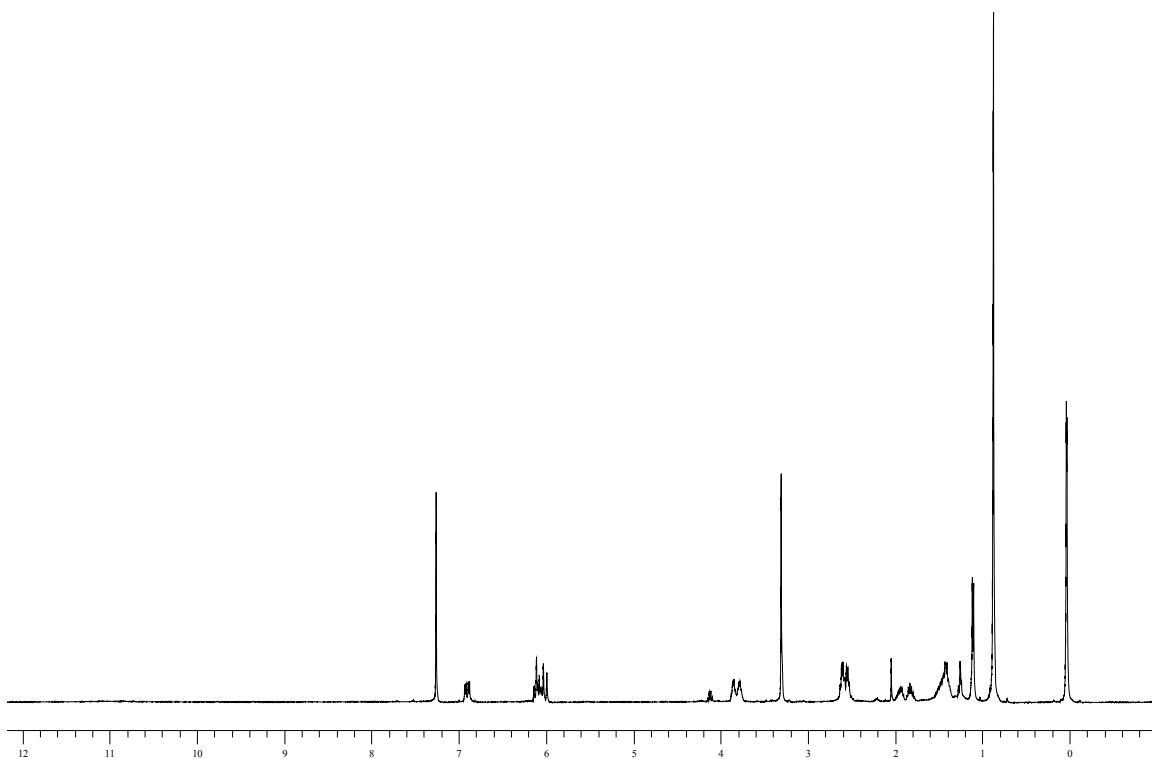
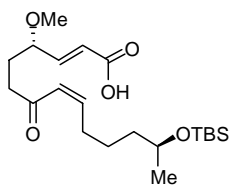
Compound 56.



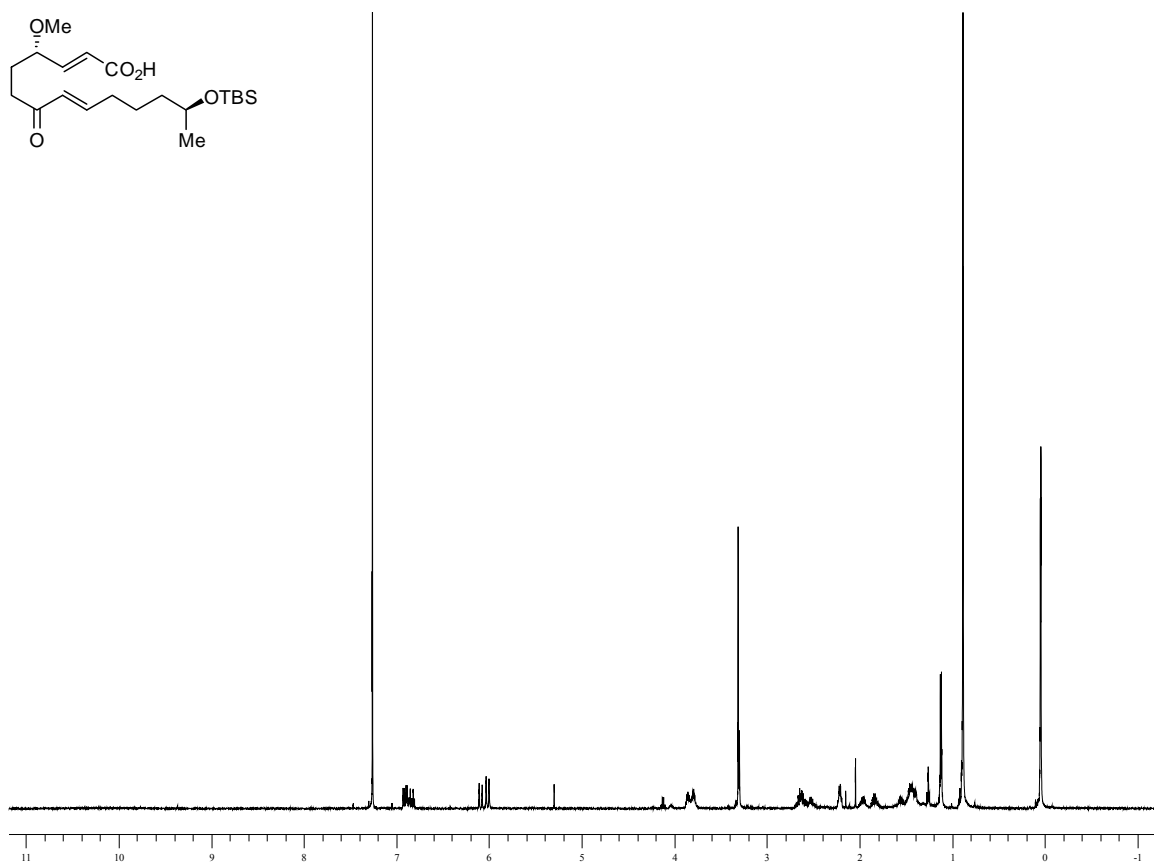
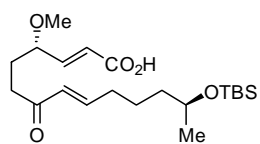
Compound 53-*cis/trans*.



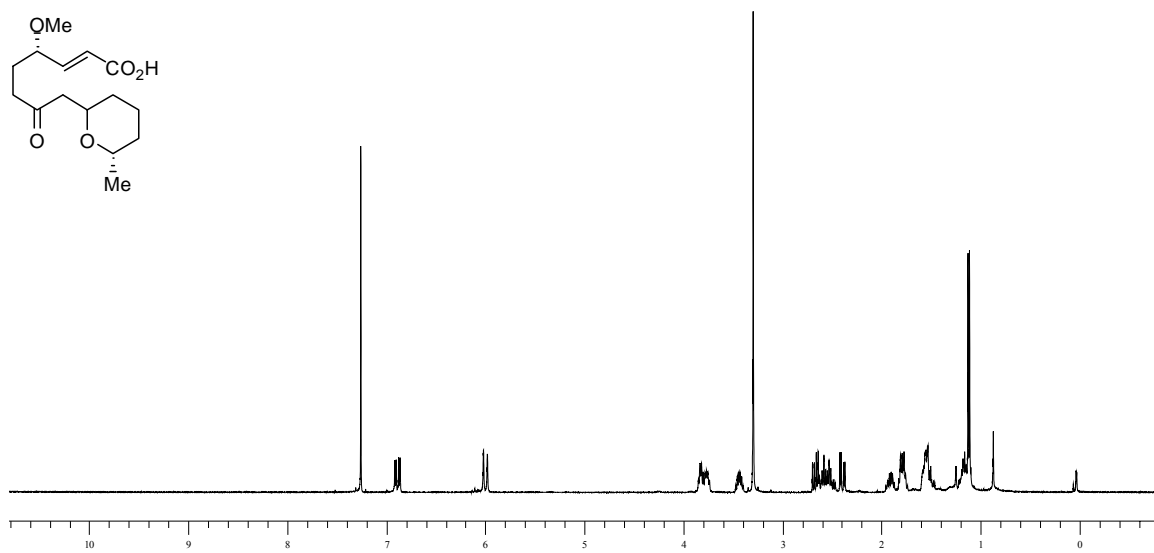
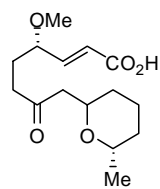
Compound 58-*cis*.



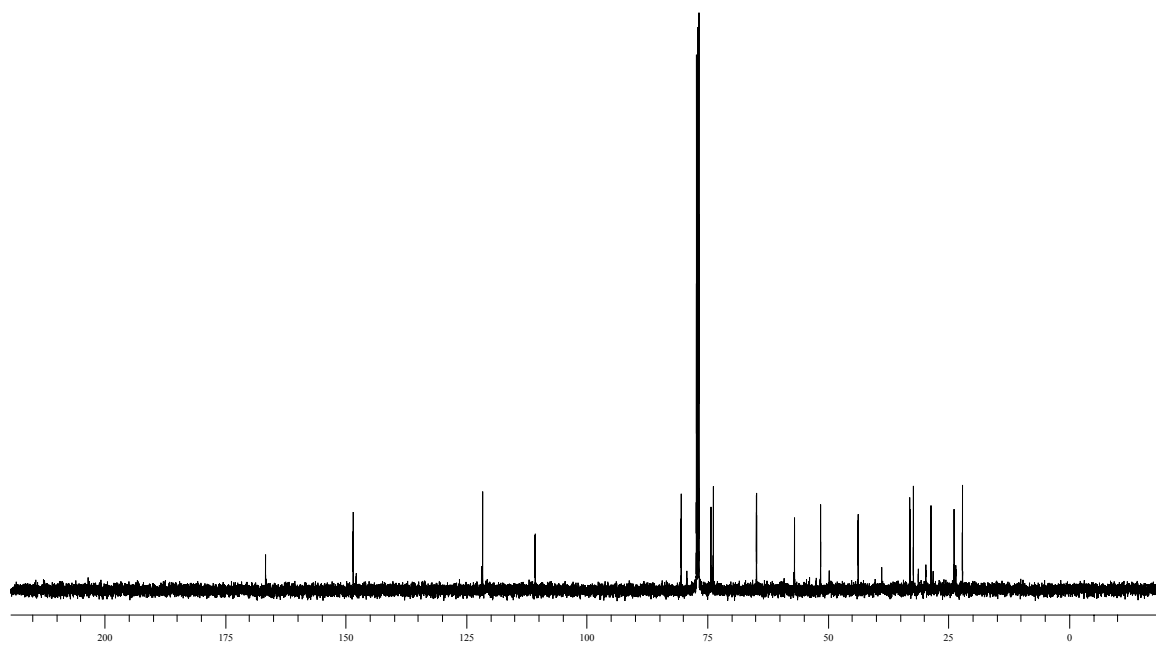
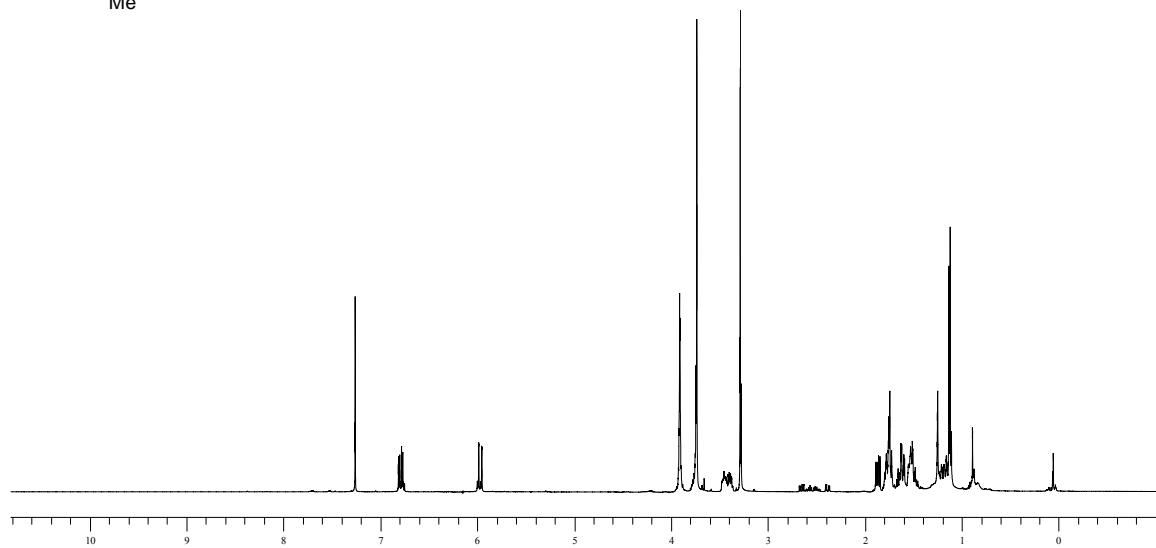
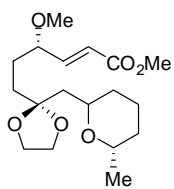
Compound 58-trans.



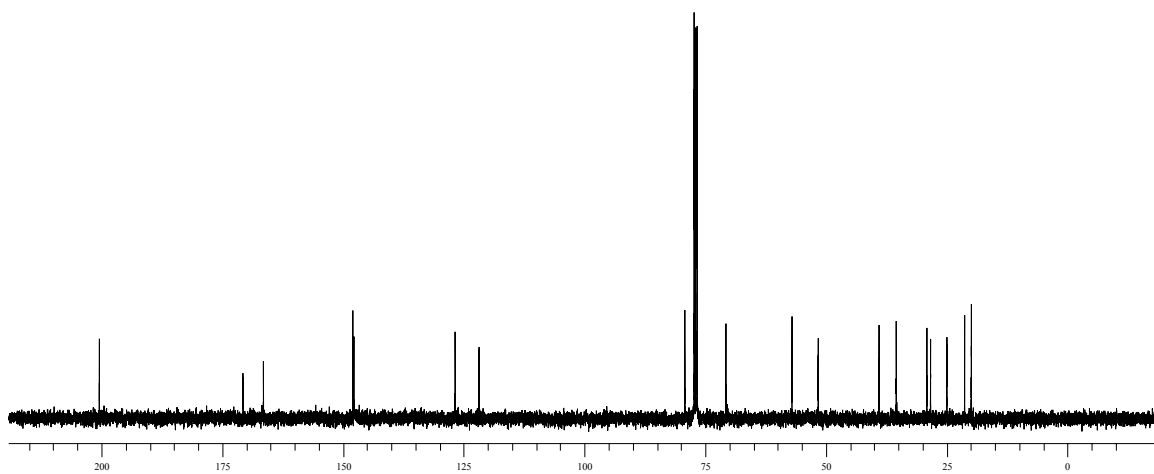
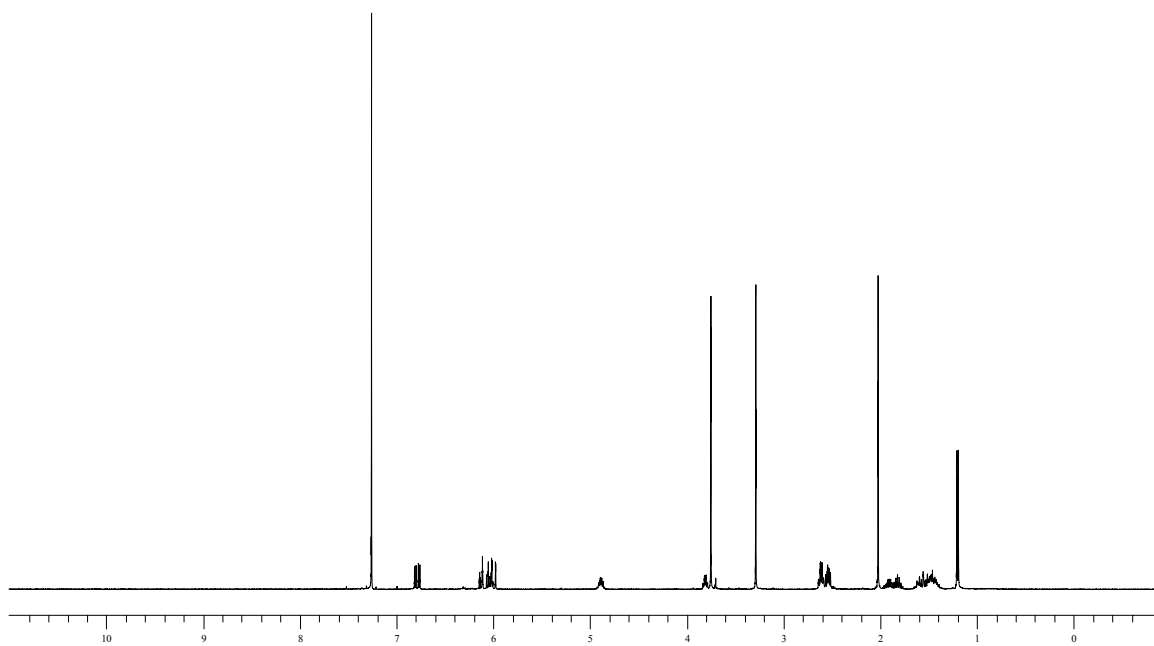
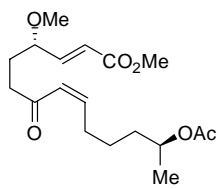
Compound 59.



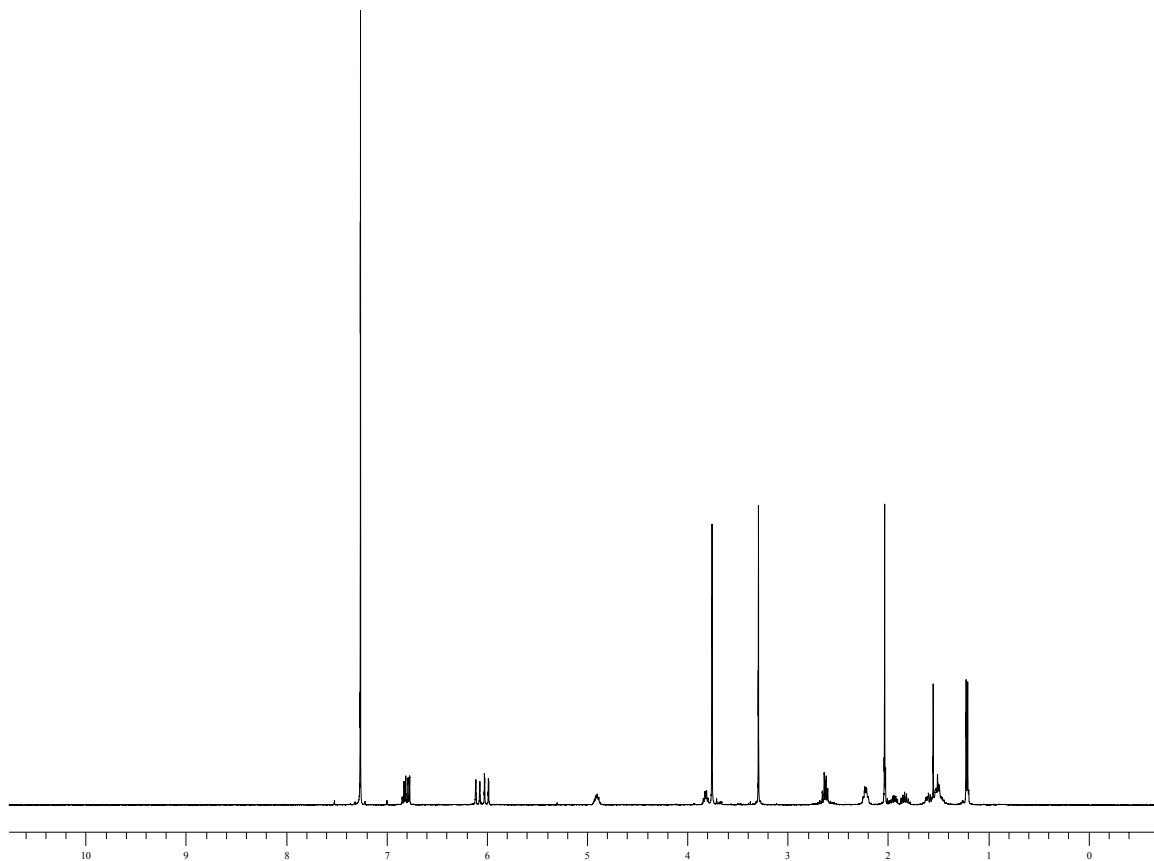
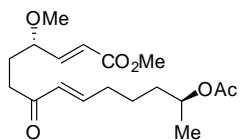
Compound 61.



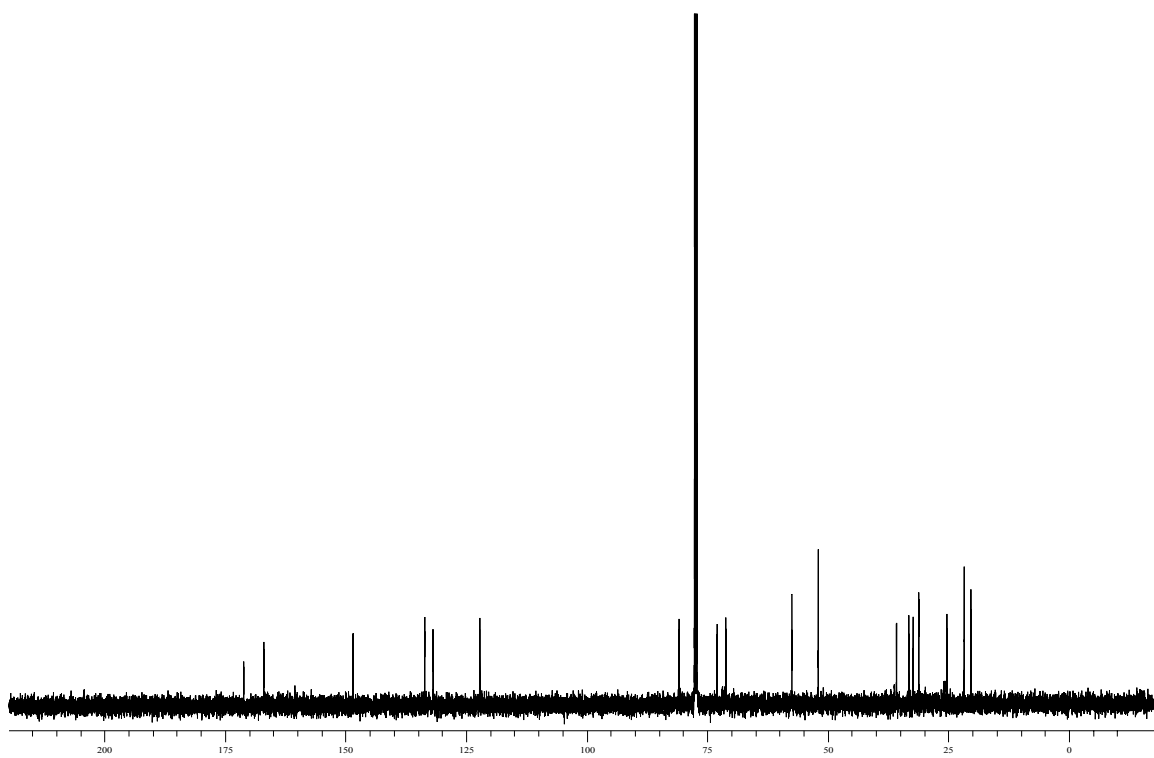
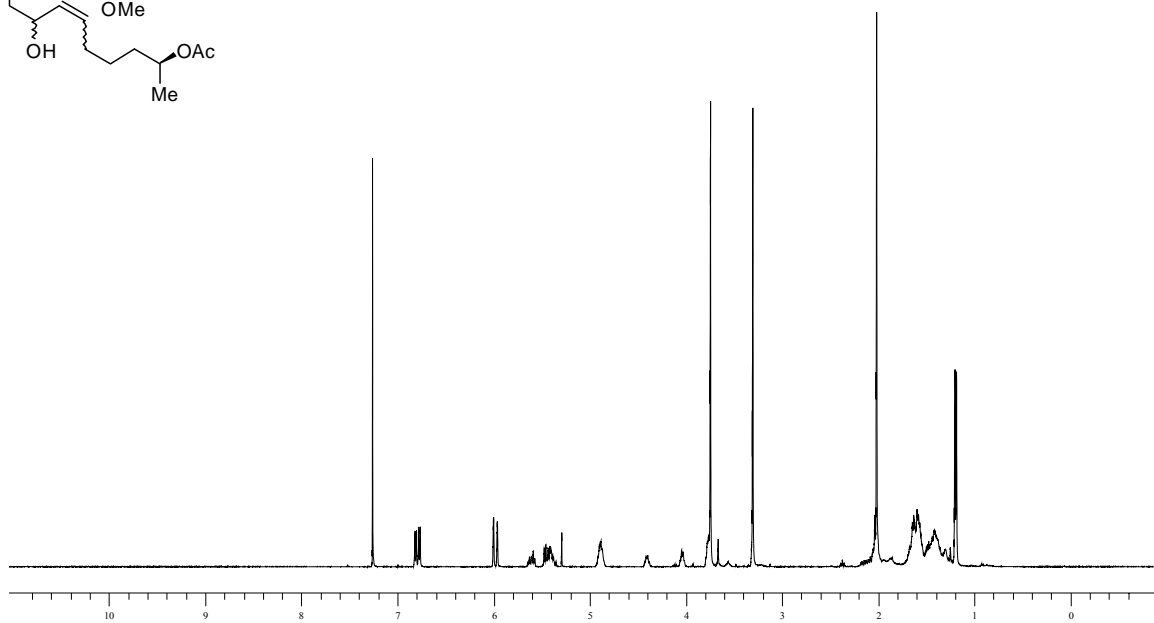
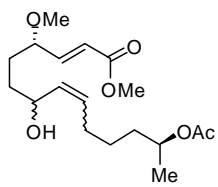
Compound 64-*cis*.



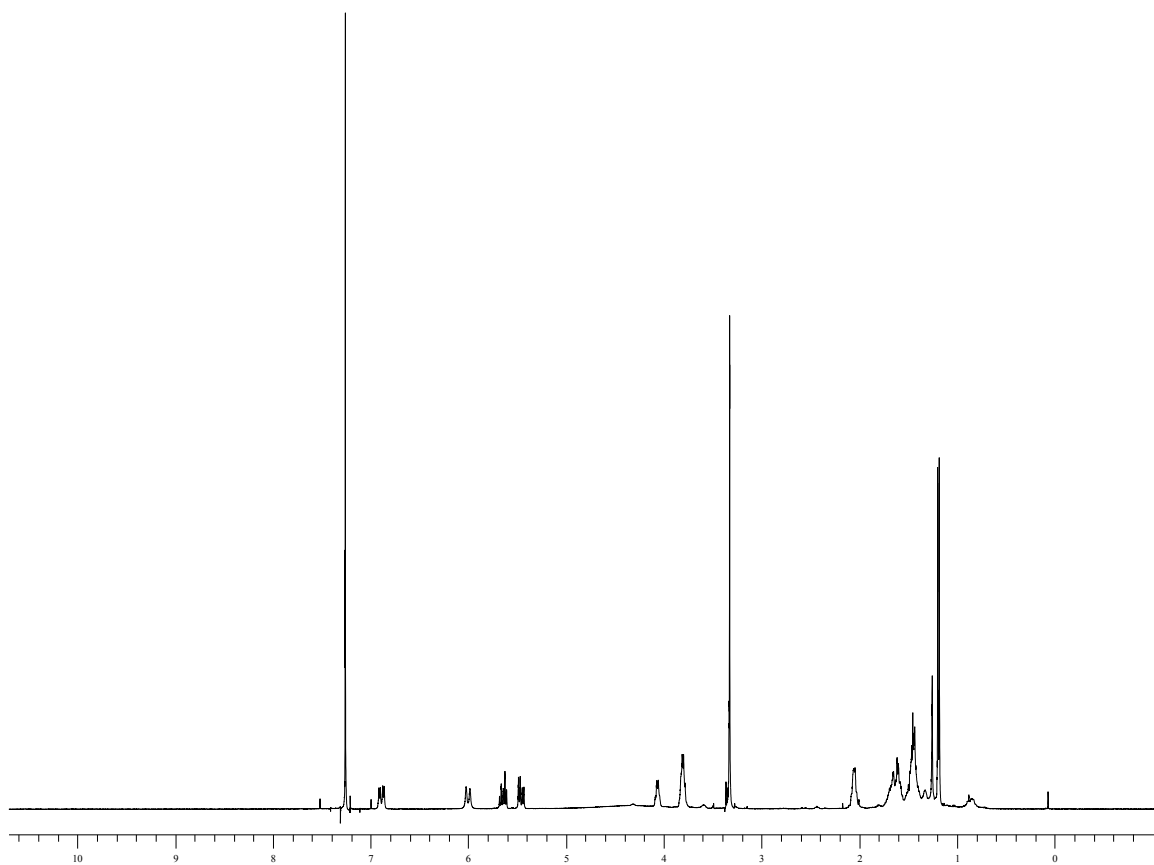
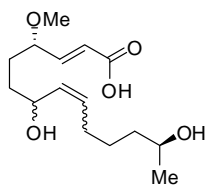
Compound 64-trans.



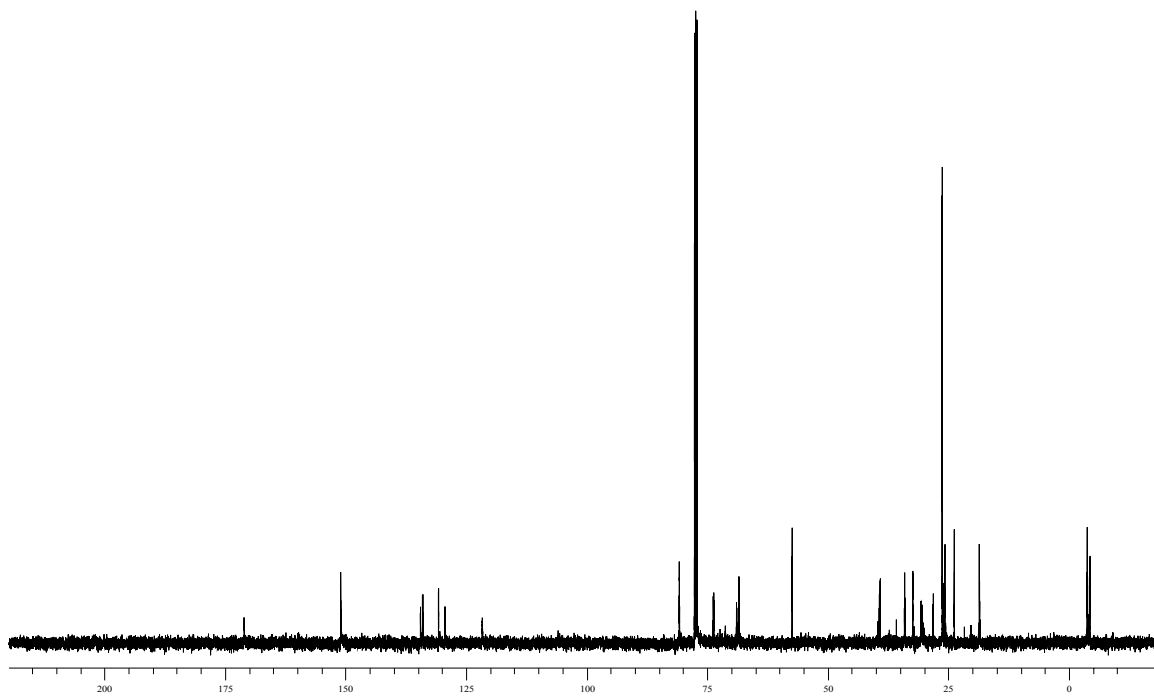
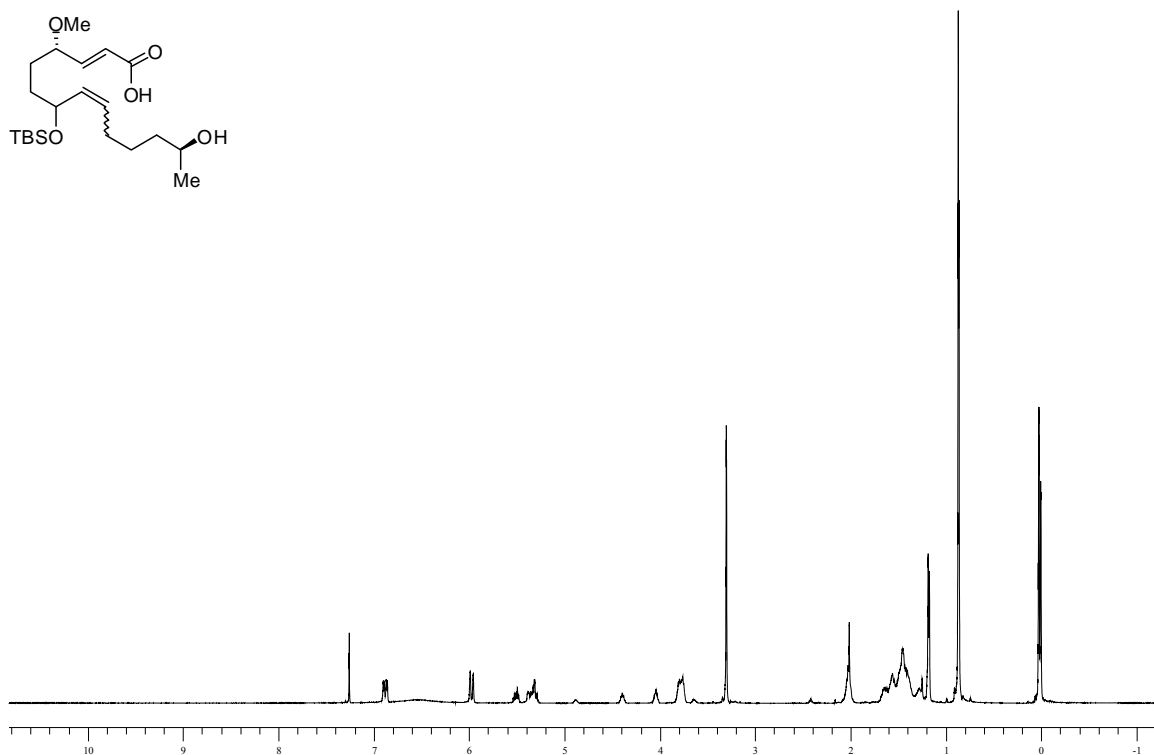
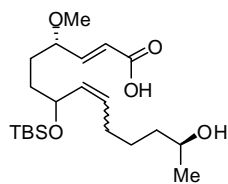
Compound 74.



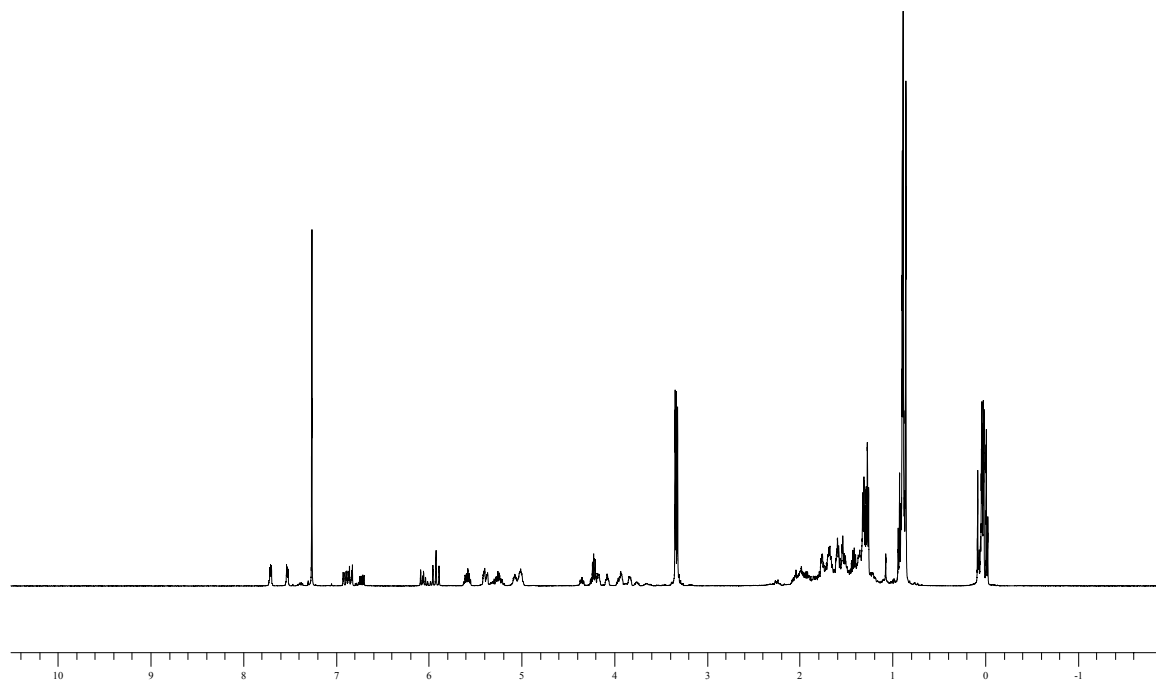
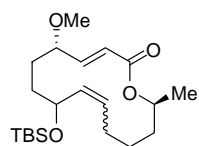
Compound 75.



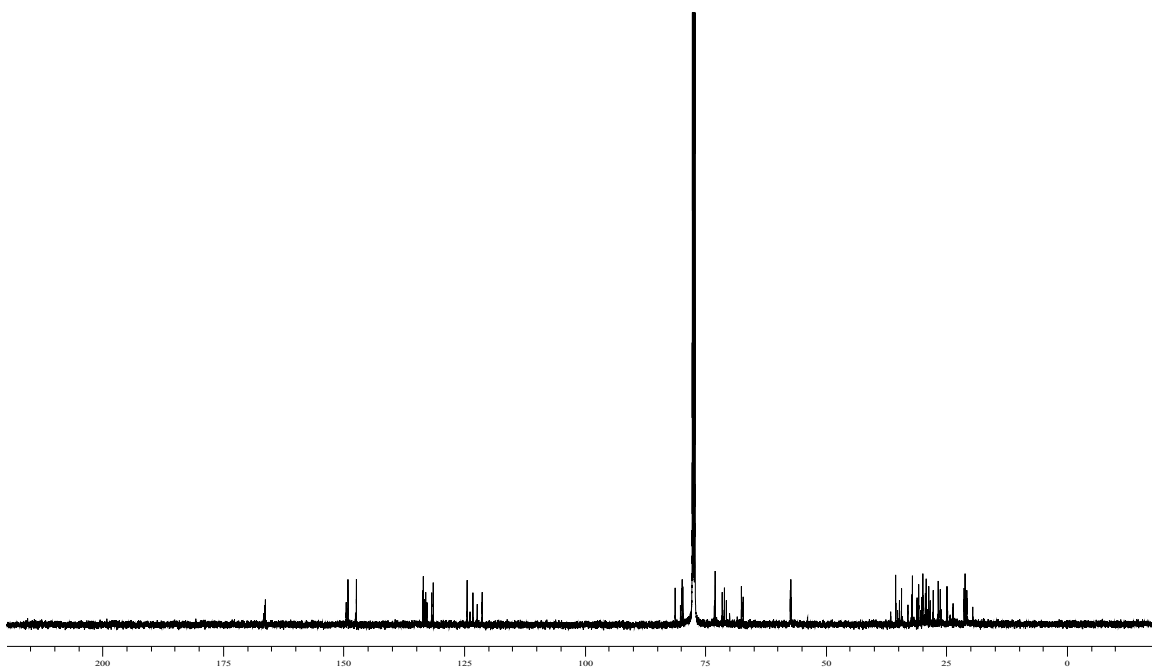
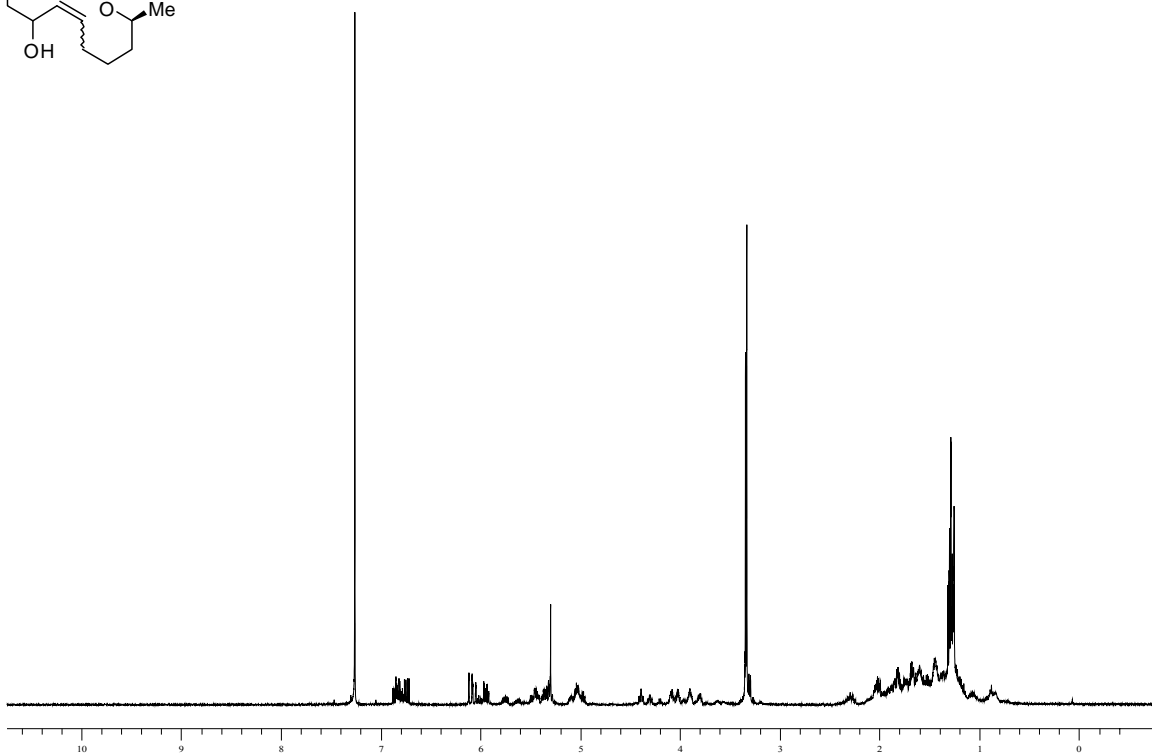
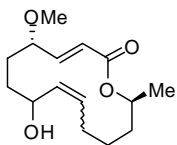
Compound 80.



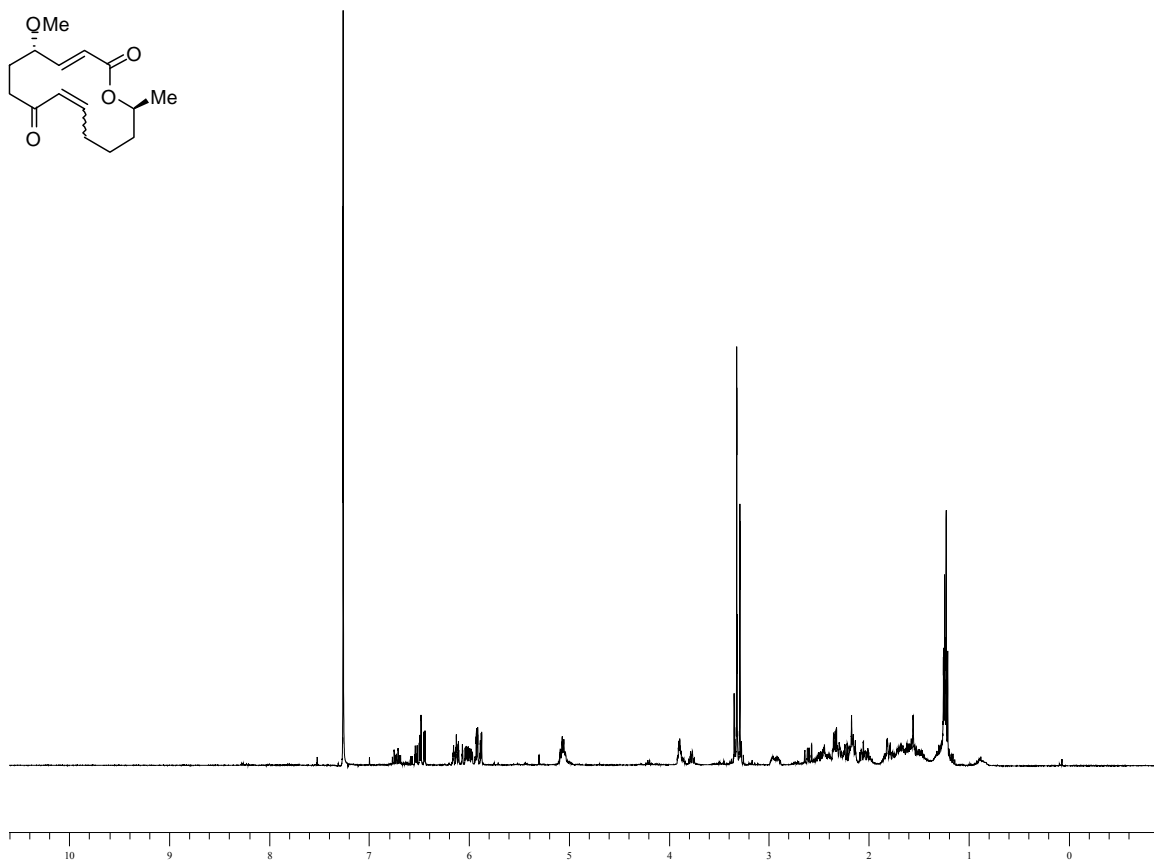
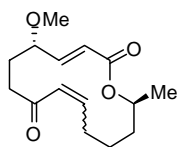
Compound 81.



Compound 81b.



Compound 68-*cis/trans*.



Compound 68-trans.

